GEOLOGY, PETROLOGY, AND METAMORPHIC HISTORY OF WESTERN ALGONQUIN PARK: IMPLICATIONS FOR THE TECTONIC EVOLUTION OF THE WESTERN GRENVILLE OROGEN

Duncan F. McLeish

Submitted in Partial Fulfillment of the Requirements
for the Degree of Bachelor of Sciences, Honours
Department of Earth Sciences
Dalhousie University, Halifax, Nova Scotia
April 2008

DALHOUSIE UNIVERSITY
Inspiring Minds

Department of Earth Sciences
Halifax, Nova Scotia
Canada B3H 4J1
(902) 494-2358
FAX (902) 494-6889

DATE: APRIL 25, 2008

AUTHOR: DUNCAN F. MCLEISH

TITLE: GEOLOGY, PETROLOGY, AND METAMORPHIC HISTORY OF WESTERN ALGONQUIN PARK: IMPLICATIONS FOR THE TECTONIC EVOLUTION OF THE WESTERN GRENVILLE OROGEN

Degree: B.Sc. Honours Convocation: MAY Year: 2008

TABLE OF CONTENTS

TABLE OF FIGURES

Chapter 4

Chapter 5

TABLE OF TABLES

Chapter 3

ACKNOWLEDGEMENTS

I would like to express my sincere thanks to my supervisors, Dr. Nick Culshaw and Dr. Becky Jamieson, for their patient guidance, enthusiastic encouragement, and constructive criticism, generously provided throughout the course of this project. I am especially indebted to Nick for enthusiastically introducing me to the rocks of the Grenville Province and inspiring me to tackle the challenge of understanding their complex history. Nick, beyond your supervision, thank you for your good company and personal support during a challenging field season in Algonquin Park.

In addition to my supervisors, I would like to thank Gordon Brown for thin-section preparation, Patricia Stoffyn-Egli for assistance with microprobe work, and fellow students Jared Butler and Chris Yakymchuk for devoting some of their precious time to helping me understand the often complex concepts and techniques of thermobarometry. Additionally, I owe many thanks to Dr. Patrick Ryall and Dr. Djordje Grujic for their constructive reviews of earlier versions of this thesis; their input has resulted in significant improvements.

A special thanks to Caroline for having faith in me throughout the project and for help with labeling BSE images.

This research was funded, in part, by a Natural Sciences and Engineering Research Council of Canada (NSERC) grant to Dr. Nick Culshaw.

CHAPTER 1: INTRODUCTION

1.1 Introduction to the problem

The Grenville Province (Gill 1949) of eastern Canada, extending almost 2000km from Labrador to southeastern Ontario, represents the intermediate to deep levels of the Grenville orogen. The Grenvillian orogeny resulted from the Late Mesoproterozoic collision of the Laurentian craton with a continental/magmatic arc consisting of preassembled terranes of different genetic affinities (Carr et al. 2000). Orogenesis was generally characterized by crustal thickening produced by northwest directed emplacement of thrust nappes propagating from southeast to northwest (Jamieson et al. 1995). The extent of the orogeny (Fig. 1.1) can be traced from Mexico and the continental interior of the United States, where rocks of Grenvillian age are found in subsurface basement rocks, through the Grenville Province of eastern Canada, and across the Atlantic Ocean to northern Europe where Grenvillian aged rocks are found in the reworked basement of Scandinavia. The deeply eroded nature of Grenvillian rocks presents a unique opportunity to examine the structural and metamorphic evolution of a mountain belt at a deep crustal level presently inaccessible in modern orogenic belts.

The focus of this study is on the Central Gneiss Belt (Wynne-Edwards 1972) of the southwestern Grenville Province (hereafter referred to as the CGB; only the Ontario portion is considered herein), the Kiosk domain (Davidson and Morgan 1981) in particular (Fig. 1.2). Historically, the CGB has challenged many workers who have poorly understood and subsequently misinterpreted its complex and often chaotic structure (e.g. Quirke 1924; Lumbers 1975). The challenge of the CGB is that the tectono-stratigraphic position of this "sea of gneiss" is somewhat of an anomaly; the belt is overlain and

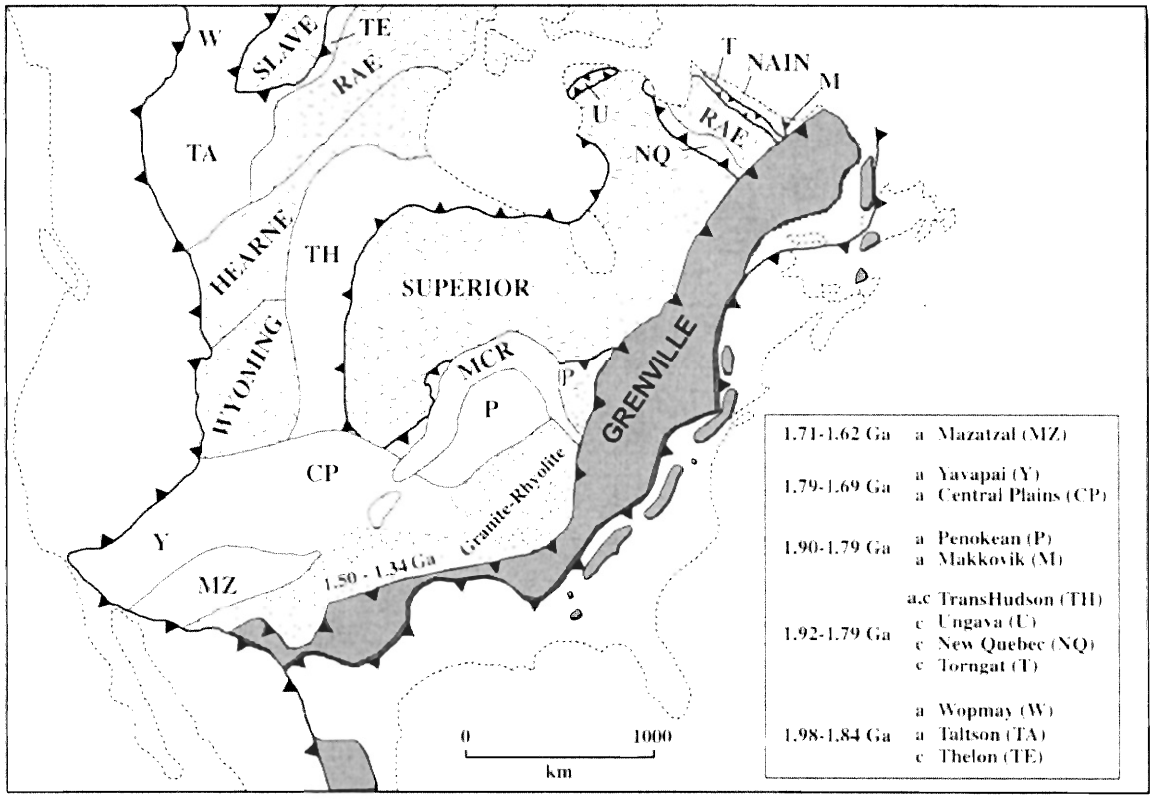

Figure 1.1: Location of the Grenville Province (highlighted in grey) relative to the lithotectonic components of Late Mesoproterozoic Laurentia. Names and ages of principal orogenic events (a = accretionary; c = collisional) listed in legend on lower right. Orogenic fronts shown as thrust symbols. Archean = random dashed patter; Paleoproterozoic = unpatterned. Present day coast line of North American outlined by fine dashes. Modified after Rivers et al. (1997).

underlain by supracrustal rocks, both metasedimentary and metavolcanic, which are somewhat similar in terms of their lithologies and their relatively lower metamorphic grade (Fig. 1.3). Naturally, workers tried to correlate these two packages, the Huronian and the Grenville supracrustal rocks, and trace them through the CGB (e.g. Quirke 1926; Quirke and Collins 1930). Workers were therefore inclined to identify CGB rocks as of supercrustal, sedimentary origin, an assumption which was encouraged by the straight layered nature of the gneiss.

The modern interpretation of the Ontario CGB has developed from a major mapping and remapping project commenced by Davidson in 1980 (Davidson and Morgan 1981). This work established the complex, layered gneisses of the CGB as primarily of igneous origin, representing the deep orogenic core of the Grenvillian orogen. In addition, Davidson and other workers subdivided the CGB into a number of cell-like domains bounded by what appeared to be shear zones, based on structure, lithology, metamorphic grade, geochronology, and, in some cases, geophysical properties (Davidson et al. 1982; Culshaw et al. 1983).

The Kiosk domain was identified very early on in the mapping efforts and was one of the original five, first order divisions of the CGB proposed by Davidson and Morgan (1981). Aeromagnetic data demonstrates that the Kiosk domain is structurally anomalous with respect to surrounding domains; the domain preserves a regionally straight trending, WSW-ENE deformation fabric not seen at such a scale elsewhere in the CGB. Neighbouring domains, in contrast, preserve contorted flow fabrics.

While it was clear from the outset of modern mapping of the CGB that the Kiosk domain is a unique structural entity, it remains relatively poorly explored, more than 25

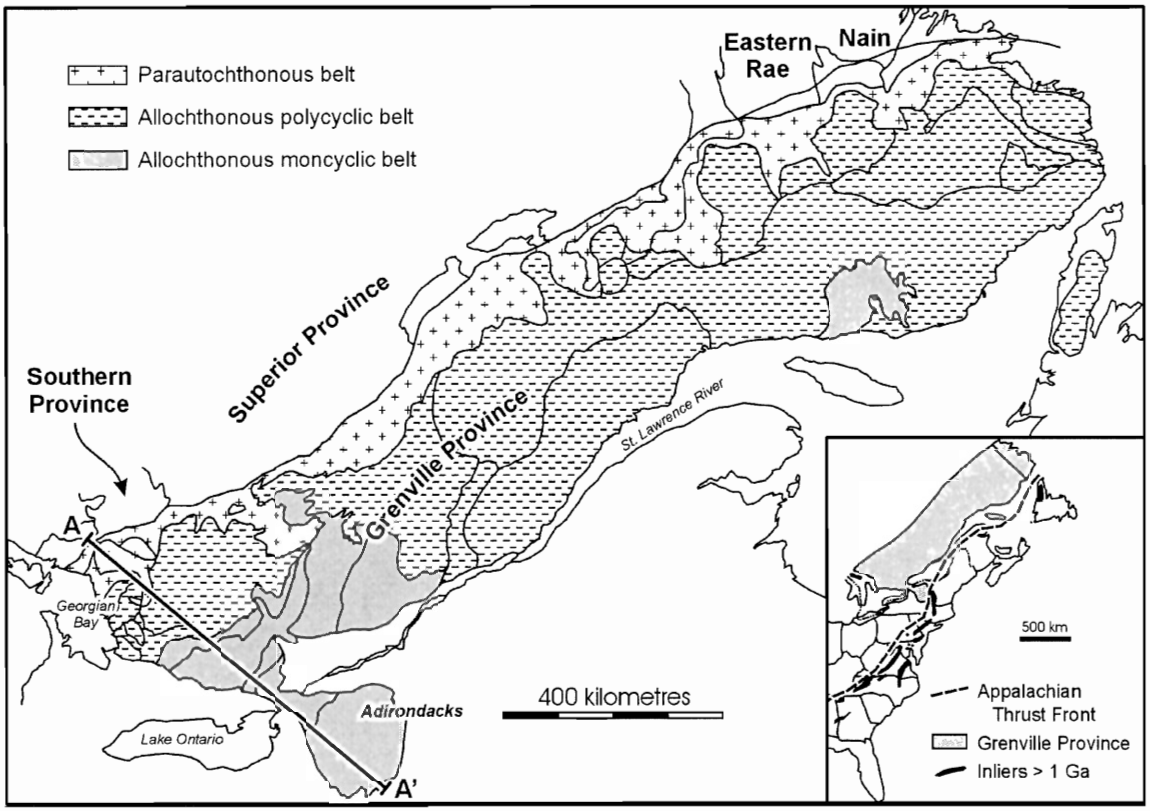

Figure 1.2: Map of the Grenville Province of eastern Canada and New England showing the tectonic divisions of Rivers (1989). The location of figure 1.3 (next page) is outlined by the barred line (A-A'). Figure from Carr et al. (2000).

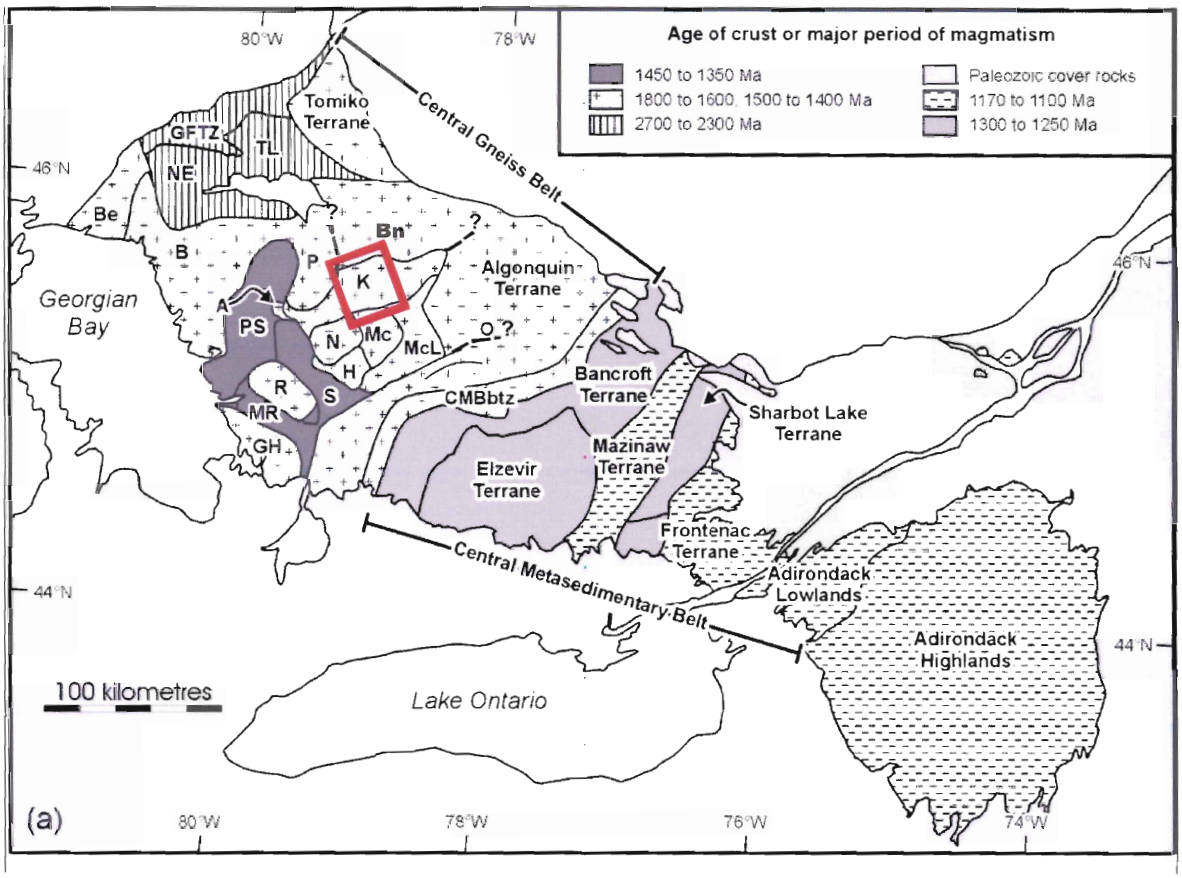

Figure 1.3: Map of the southwestern Grenville province with lithotectonic units shown. Study area is outlined in red. Adirondack Highland and Lowland domains comprise the Central Granulite Terrain (not labelled) of Wynne-Edwards (1972). See text for further discussion. Abbreviations used: A, Ahmic domain; B, Britt domain; Be, Beaverstone domain; Bn, Bonfield terrain; CMBbtz, Central Metasedimentary Belt boundary thrust zone; GFTZ, Grenville Front Tectonic Zone; GH, Go Home domain; H, Huntsville subdomain; K, Kiosk domain; Mc, McCraney subdomain; McL, Mclintock subdomain; MR, Moon River domain; N, Novar subdomain; O, Opeongo domain; P, Powassan domain,; PS, Parry Sound domain; R, Rosseau domain; S, Seguin domain; SD, Shawanaga domain. Note that the Novar, Huntsville, McCraney and McLintock subdomain comprise the Algonquin domain (Ad; not labelled). Figure modified after Carr et al. (2000).

years after its original identification. During this period, workers primarily focused their studies on the neighbouring domains to the immediate west and south of the Kiosk domain; in particular, those which outcrop in and along the Georgian Bay shoreline have been extensively studied (e.g. Bussy et al. 1994; Corrigan et al. 1994; Culshaw et al. 1983, 1988, 1989, 1990, 1994, 1997; Davidson 1984*a*, 1986, 1990; Davidson and Bethune 1988; Jamieson et al. 1992, 1995; Ketchum 1995; Ketchum et al. 1994; Nadeau 1990; van Breeman and Davidson 1990, Wodicka 1994; Wodicka et al. 2000). This is hardly surprising given the fact that exposure along the picturesque Georgian Bay shore is second to none and access to the area is facilitated by major highways and waterways. In contrast, the Kiosk domain spans the remote northwestern portions of Algonquin Provincial Park, an area mostly devoid of roads and heavily forested with dense, old growth of white pine and maple. Traditionally, mappers have resolved accessibility issues in remote areas by use of helicopter or float plane. However, in case of the Kiosk domain, provincial park regulations governing the use of park lands prohibit the use of such methods; aircraft are generally not allowed to land in the park. Much of the Kiosk domain has therefore been left unexplored and poorly understood.

1.2 Geological setting

The Grenville Province is one of the seven first-order divisions of the Canadian Shield; it represents the youngest of orogenic belts found in shield (Stockwell 1964). To its northwest, the Laurentian craton (>1.4 Ga in age with younger supracrustal rocks deposited on its margin) underlies the Grenville Province encompassing the other six, first-order divisions of the Canadian Shield: Bear, Slave, Churchill, Superior, Nain, and Southern Provinces. To the southeast, the Appalachian Structural Province, which has been found to

contain isolated, reworked basement rocks of Grenvillian age, overlies the Grenville Province (Fig. 1.1). In addition, undeformed lower Palaeozoic sedimentary rocks of the St. Lawrence platform overlie the Grenville Province in areas of southern Ontario and parts of eastern Quebec.

Wynne-Edwards (1972) subdivided the Ontario Grenville Province into four zones based on structural and metamorphic style: the Grenville Front Tectonic Zone, the Central Gneiss Belt, the Central Metasedimentary Belt, and the Central Granulite Terrain (Fig. 1.3). To the far west, the Grenville Front Tectonic Zone (GFTZ) is characterized by a very strong, northeast trending foliation which dips moderately to the southeast; seismic data suggests that it may extend through the lower crust (Carr et al. 2000). The Grenville Front (GF) marks the western extent of Grenvillian deformation and truncates east-west trending structures of the neighbouring Southern Province. Lithologically, the GFTZ is composed of Archean crust, generally migmatitic orthogneisses and paragneisses, Mesoproterozoic plutons, and 1.45 Ga granulites (Culshaw et al. 1997). The grade of Grenvillian metamorphic overprint decreases from upper amphibolite facies towards the front, where it only reaches lower amphibolite facies (Haggart et al. 1993). The chemically distinctive Sudbury diabase dyke swarm can be traced across the front into the GFTZ. The dykes, undeformed in the Southern Province, are found highly deformed by Grenvillian orogenesis in the GFTZ (Bethune 1997).

The Central Gneiss Belt (CGB) extends from the GFTZ in the west to the Central Metasedimentary Belt in the east (Fig. 1.3); it is interpreted to represent the deep levels of the Grenvillian orogeny (Carr et al. 2000). As a whole, the straight, northeast trending, homogeneous fabric of the GFTZ is lost in the CGB, where foliation orientation becomes

complex. Rock types are largely quartzofelspathic gneiss, of both plutonic and supracrustal origin, and Mesoproterozoic granitoids ~1.7Ga, ~1.4Ga, and ~1.2Ga in age. Rivers et al. (1989) subdivided the CGB into two genetically different belts: the Parautochthonous Belt and the Allochthonous Polycyclic Belt (Fig. 1.2). The former is interpreted to be of Laurentian origin; the latter is interpreted to be allochthonous in the sense that it originated on the distal margin of Laurentia and polycyclic in the sense that it records pre-Grenvillian deformational events (Rivers et al. 1989). Separating the two belts is the Allochthon Boundary Thrust (ABT); the exact position of this boundary is subject to debate (Davidson, 1996; Ketchum and Davidson 2000; Dickin and Guo 2001). As mentioned above, the CGB has also been subdivided into various domains based on structure, lithology, metamorphic grade, geochronology, and geophysical properties.

The Central Metasedimentary Belt (CMB) extends from the CGB in the west to the Central Granulite terrane in the east (Fig. 1.3). The Central Metasedimentary Belt Boundary Thrust Zone (CMBbtz) separates the CGB from the CMB and represents a major tectonic break in the Grenville province where supracrustal rocks of the CMB, metasediments and metavolcanics, are juxtaposed against rocks of the CGB. The supracrustal rocks of the CMB are a series of metamorphic carbonates, siliclastic, and mafic and felsic volcanics. A variety of younger plutonic rocks, representing multiple episodes of intrusion, cut the supracrustal sequences. Deposition of the sediments and carbonates was coeval with the mafic and felsic volcanism and is believed to have occurred no latter than 1.3 Ga (Carr et al. 2000). Rivers et al. (1989) grouped the CMB with the Central Granulite Terrane to the southeast in a subdivision of the Grenville Province termed the Allochthonous Monocyclic Belt; Carr et al. (2000) applied the term Composite

Arc Belt to the CMB. The CMB is allochthonous in the sense that it is detached from its original basement and monocyclic in the sense that it records only Grenvillian deformation. Structural trends are also variable in the CMB; however, a southwest-northeast foliation with steep southeast plunging lineation is most common in the CMB.

To the southeast of the CMB lies the Central Granulite Terrain (CGT), a structurally complex terrain composed of supracrustal rocks, large massifs of anorthosite, and anorthosite-mangerite-charnockite-granite (AMCG) suites (Figure 1.3). The CGT comprises two distinct lithotectonic domains: the Adirondack Lowlands domain, and the Adirondack Highlands domain; the former contains metasedimentary rocks (mainly marble and quartzite) and the latter contains largely anorthositic plutonic rocks. Both the Adirondack Highland and Lowland domains share a similar metamorphic history which records three main metamorphic events during the ca. 1350-1000 Ma extent of Grenvillian orogenesis (McLelland et al. 1996). Carr et al. (2000) included the Frontenac terrain of southeastern Ontario with the CGT and relabelled it the Frontenac-Adirondack belt, pointing out that this area is unique in the fact that it has a different plutonic history than the neighbouring CGB prior to ~1160 Ga.

1.3 Grenvillian nomenclature

Several primary lithotectonic divisions of the Grenville Province have been suggested by various workers (e.g. Wynne-Edwards 1972; Rivers et al. 1989; Carr et al. 2000) since the development and application of the first modern orogenic models to the Grenville in the early 1970s; many of these lithotectonic divisions employ vastly different terminology and nomenclature. Over the past 35 years, workers have often used the various divisions interchangeably when studying the Grenville province. As a result, an

inconsistency in nomenclature has developed in Grenvillian literature, which has led to some confusion in the discussion of the Grenville Province.

The classic synthesis of Wynne-Edwards (1972) proposes fundamental subdivisions which have direct applicability to the Ontario portion of the Grenville Province. Subdivisions proposed by Rivers et. al (1989) reflect many advances in the understanding of the tectonic assembly and evolution of the Grenville orogen; however, their subdivisions have been difficult to apply to the Ontario portion of the Grenville Province. In particular, several workers have disputed the positioning of several key subdivision boundaries of the Rivers et al. interpretation (e.g. the Allochthon Boundary Thrust). This study therefore employs the classic and widely quoted subdivisions of Wynne-Edwards.

1.4 Previous work

1.4.1 Historical perspective

The physiographic entity which is now know as the Grenville Province was recognized by workers as early as the mid 19th century when it was identified as the "Laurentian System" (Logan 1847). A thick band of marble which runs north from the town of Grenville on the Ottawa River, termed the "Grenville band" (Logan 1863), is responsible for the application of the name Grenville to the southeasternmost series of supracrustal Canadian Shield rocks.

By the early 20th century significant advances had been made in understanding the geology of the southern Canadian Shield. Studies of the supracrustal rocks of the Grenville series and supracurstal rocks to the west of the Timiskaming-Killarney region (e.g. Huronian sediments) conducted by Wilson (1918, 1925) revealed that fundamental lithologic differences existed between these two predominantly metasedimentary portions

of the southern shield. Furthermore, Collins (1925) recognized a major and laterally extensive southeast dipping fault zone (later termed the Grenville Front Tectonic Zone) trending northeast from the Killarney region, separating Grenville rocks from those to the west. These findings led Wilson (1925) to classify the Grenville series and the supracrustal rocks to the west as separate, lithologically distinct "subprovinces" which he termed Grenville and Timiskaming respectively. Additionally, Wilson (1918) was among the first to recognize that a laterally extensive and distinct belt of highly strained, banded metaplutonic gneiss separated these two supracrustal packages; he did not, however, include this belt in either of his Grenville or Timiskaming subprovinces and only briefly speculated about the belt's significance (Wilson, 1925). Nonetheless, Wilson's identification of this banded gneiss belt is significant in the context of this study, because it is among the first to document and discuss what would become known as the Central Gniess Belt (CGB).

Throughout the ensuing 1920s and 1930s much discussion took place as to whether this belt of banded gneiss represented a fundamental geologic break in the Canadian Shield, or whether Huronian sediments and other rock units of the southwestern shield could be traced through the gneiss belt and correlated with supracrustal rocks of the Grenville series. Several workers (e.g. Quirke, 1924 and references therein; Quirke 1926; Quirke and Collins 1930) strongly advocated the latter theory and went to great lengths to try and trace Huronian sediments through the banded gneiss. Although attempts to do so were largely unsuccessful, several isolated pockets of crystalline sediments, quartzite and marble in particular, were identified in the French River and Parry Sound areas of the banded gneiss belt (Quirke, 1924). These findings led to the interpretation that: (1) the banded gneiss

represented Huronian sediments which were metamorphosed by granite intrusions into "paragneiss of igneous aspects" (Quirke 1924, p.321), and (2) the pockets of marble and quartzite included within the banded gneiss represented the preserved protolith of the banded gneiss or, "stuff out of which have been made rocks of Grenville type" (Quirke 1924, p. 321). Many workers in the first half of the 20th century thus believed that, despite being completely separated by the banded gneiss belt, the Grenville subprovince was genetically related and similar in age to the Timiskaming subprovince; Quirke (1924) ultimately concluded that the Grenville and Huronian rocks were identical.

Although workers such as Wilson (1918,1925) noted major lithologic differences between the Grenville and Timiskaming subprovinces, and Collins (1925) identified a major geologic break in the southern Shield rocks, it was not until the middle of the 20th century, with improving knowledge of the structure of the Canadian Shield and the availability of absolute isotopic age dates, was the Grenville physiographic entity widely accepted as a genetically distinct, 1st order division of the Canadian Shield. In his divisions of the Canadian Shield, Gill (1949) identified the Grenville as a 1st order structural province and included in it the banded gneiss belt, which was left unassigned in the divisions of Wilson (1925). K-Ar age determinations of Shield rocks by Stockwell (1964) confirmed Gill's divisions and served to better constrain the boundaries of the structural provinces. Furthermore, this age data on the Shield ended speculation that supracrustal Grenville rocks could be correlated with the Hurronian sediments. In particular, the finding that the sediments of Grenville series were at least 700 million years younger than the Huronian sediments rendered the theory of a Huronian Grenville genetic relationship untenable (Stockwell 1964).

1.4.2 Modern Context

With the advent and application of modern plate tectonic theories to Grenville geology in 1970s, great advances were made in understanding the Grenville province as representing a major orogenic event in Earth's history (e.g. Wynne-Edwards 1972). Although much work was conducted on the GFTZ and the CMB in the 1970s, the large area of banded gneiss which earlier workers had grappled with, the CGB, received little attention. In light of poorly studied nature of the CGB, Davidson and Morgan (1981) initiated extensive reconnaissance work in the CGB and identified the Kiosk domain in their tentative subdivision of the CGB. Culshaw et al. (1983) confirmed the existence of the Kiosk domain as a structurally distinct lithotectonic entity and subdivided the neighbouring Algonquin domain, in a more detailed study of the area.

Davidson (1986) conducted reconnaissance work in the Kiosk and Algonquin domains. To date, this remains the only dedicated study of northwestern and central Algonquin Park geology. Davidson's (1986) study was the first to document and report the anomalous, straight trending and strongly lineated structure of the Kiosk domain gneiss. Additionally, Davidson (1986) summarized the lithology of the Kiosk domain to a much greater extent than the brief paragraph provided in his 1981 report with Morgan.

From the ensuing 1980s to present, despite the proliferation of work on the western Grenville Province (cf. Carr et al. 2000, for a comprehensive review), documentation of any further work on the northwestern Algonquin park region is absent from the literature. Davidson and van Breemen (2001) worked the geochronology of granitoid bodies to the immediate north and west of the park (e.g. Powassan and Mulock batholiths); this work may have indirect implications for Kiosk domain investigations, as granitoid bodies

present in the Kiosk may be related to those studied to the north and west. Other than Dickin and McNutt's (1991) Sm-Nd model age data for samples from the far western Kiosk domain, there is, to date, no record of any geochronologic, geochemical, thermobarometric, or other geological analyses outside of field reconnaissance for the Kiosk domain.

1.5 Physiography and accessibility

The Algonquin Highlands, having a maximum elevation of approximately 600 metres (1920 feet) and substantial relief, are a physiographic anomaly relative to the surrounding flat and low lying terrain of southern Ontario where elevations generally do not exceed 200 metres (640 feet) (Fig. 1.4). The highlands thus serve as a major drainage divide between waters that run east and south into the St. Lawrence Basin and waters that run west into Georgian Bay and Lake Huron. The transition in the east and south, from the surrounding flat lying lowlands to the steeply rolling highlands, is abrupt and is generally marked by the sudden appearance of strongly deformed Mesoproterozoic gneiss and disappearance of the undeformed Devonian carbonate rocks which dominate the plains of the St. Laurence Basin and southern Ontario.

Occupying the western portion of the highlands, northwestern Algonquin Park is characterized by a series of steep, narrow (>1km wide), WSW-ENE oriented ridges and valleys which have a remarkably straight trend over the 100 km^2 + area (Fig. 1.5). In many cases individual ridges are asymmetrical, with the north slope having a higher gradient than the south slope. Field reconnaissance has shown that the morphology of these ridges is an accurate expression of the ENE striking, shallow SSE dipping foliation of the Kiosk domain. Such a finding explains the asymmetrical nature of the ridges; the shallow

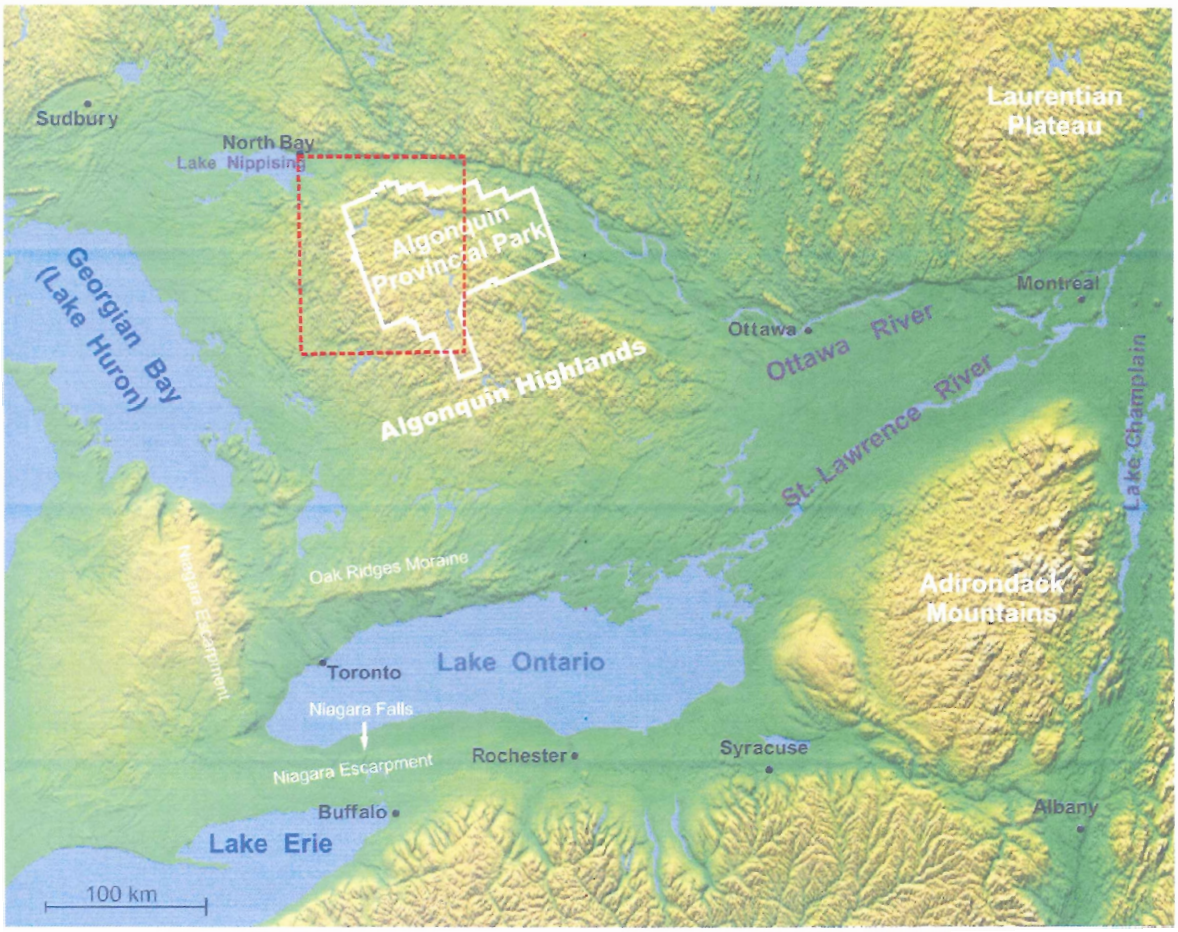

Figure 1.4: Digital elevation model of south and eastern Ontario showing the location of Algonquin Provincial Park relative to major cities. The dark green colour corresponds to an elevation of approximately 80 metres (300 ft); the pale yellow corresponds to an elevation of approximately 600 metres (~2000 ft). The red box indicates the approximate area of Figure 1.5 (next page). Figure modified from Ahern (2006).

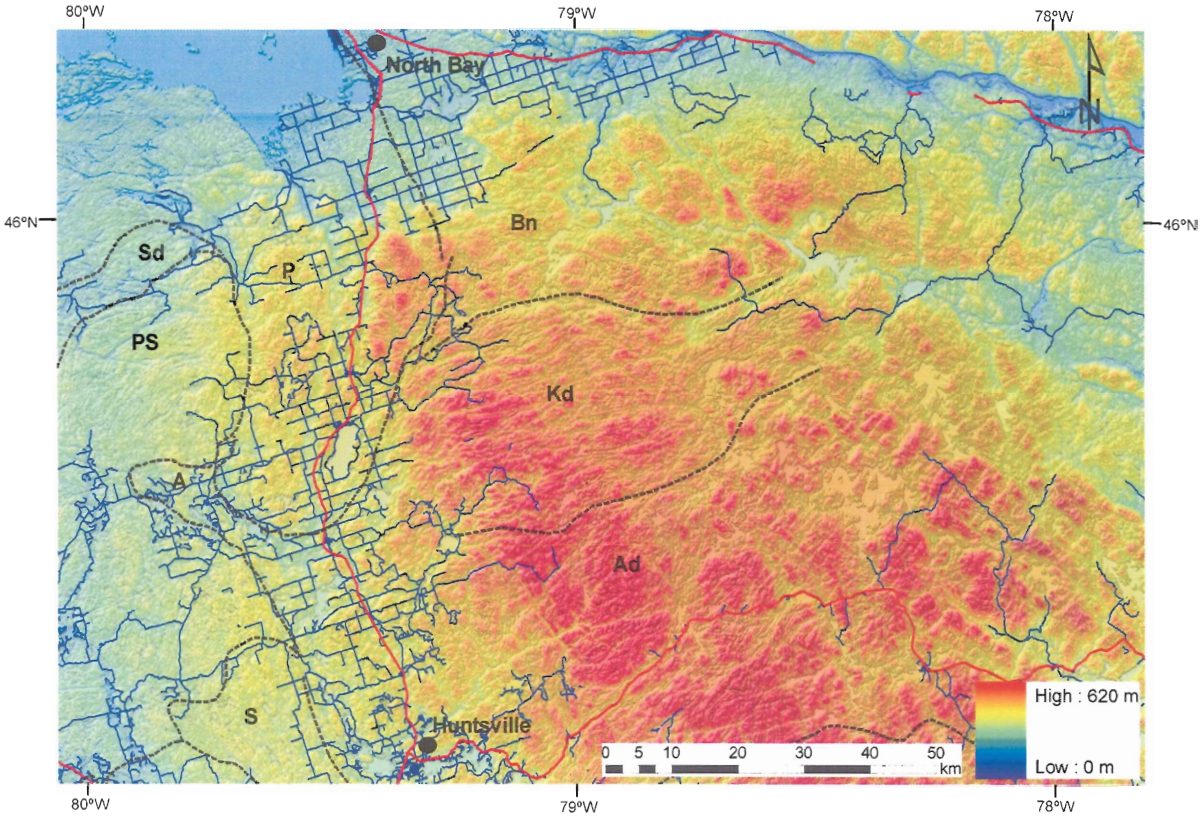

Figure 1.5: Digital elevation model of the northwest Algonquin region with lithotectonic units (black), major roads (red), and minor roads (dark blue) shown. Note how N-S trending ridges found in the Algonquin domain and Bonfield terrain contrast with the E-W trending ridges of the Kiosk domain. The red colour corresponds to an elevation of approximately 600 metres (~2000 ft); the blue colour corresponds to an elevation of approximately 600 metres (~2000 ft). Abbreviations used: A, Ahmic domain; Ad, Algonquin domain; Bn, Bonfield terrain; Kd, Kiosk domain; P, Powassan domain; PS, Parry Sound domain; Sd, Shawanaga domain. Source data obtained from the Canada Geodetic Information System (2008).

south side represents the foliation surface, whereas the steep north side represents a truncation of the foliation plane. Relief in the area is moderate to high relative to the surrounding area with a maximum vertical difference of 150 metres (480 feet) between topographic highs and lows. Bedrock exposure is best along the shorelines of lakes and in streams where it is reasonably abundant and, aside from minor lichen cover, is of good quality. Elsewhere within in the area, bedrock exposure is of poor quality and generally consists off moss covered outcrops found on the steep sides of ridges and sporadically on the forest floor.

The vast majority of the northwestern Algonquin Park interior is accessible only by canoe. A number of seasonal, loose surface, logging roads, originating from the town of South River, provide limited access to the westernmost park boundary. Once in the park, however, most of these roads deteriorate into unmaintained cart tracks overgrown with vegetation. A select few receive limited maintenance from the park staff for selective logging and access purposes and are suitable for use by four wheel drive vehicles during dry weather conditions. Air access is limited by provincial regulations which prohibit aircraft from landing within the park. The dense vegetation, challenging topography, and widespread occurrence of swamps and marshes make travel by foot in the area very difficult over long distances.

1.6 Objectives and methods of investigation

The purpose of this study is to attempt to elucidate the structurally anomalous Kiosk domain and to better understand the lithological, structural, and metamorphic properties of the domain as they relate to the development and assembly of the Grenvillian orogen. In particular, the specific objectives of this study are: (1) identify the different lithologies

present in the Kiosk domain and document their respective mineralogy; (2) assess the anomalous structure of the Kiosk domain and evaluate the contact relationship with neighbouring domains; and (3) unravel the metamorphic history of the Kiosk domain through an estimation of P-T conditions. A combination of field and laboratory study achieved these objectives.

Fieldwork was completed by canoe in August of 2007 during two separate 10 day reconnaissance expeditions (Fig. 1.6). A network of canoe routes established and maintained by park personnel provided access to the northwestern park interior and to the numerous lake and stream outcrops contained therein. Outcrops on ridge sides were reached by hiking cart trails, where available, or by bushwhacking. Fieldwork involved sampling, structural measurements, and description of lithologies present within the study area.

Laboratory work, focused on petrological study, was completed in the ensuing months of 2007 and early 2008. Petrographic assessment of representative samples from the study area provided constrains on the relative timing of mineral formation and allowed various deformation fabrics to be correlated throughout the area. Electron microprobe (EMP) analyses determined mineral chemistry of selected lithologies and provided the data for calculating P-T phase diagrams.

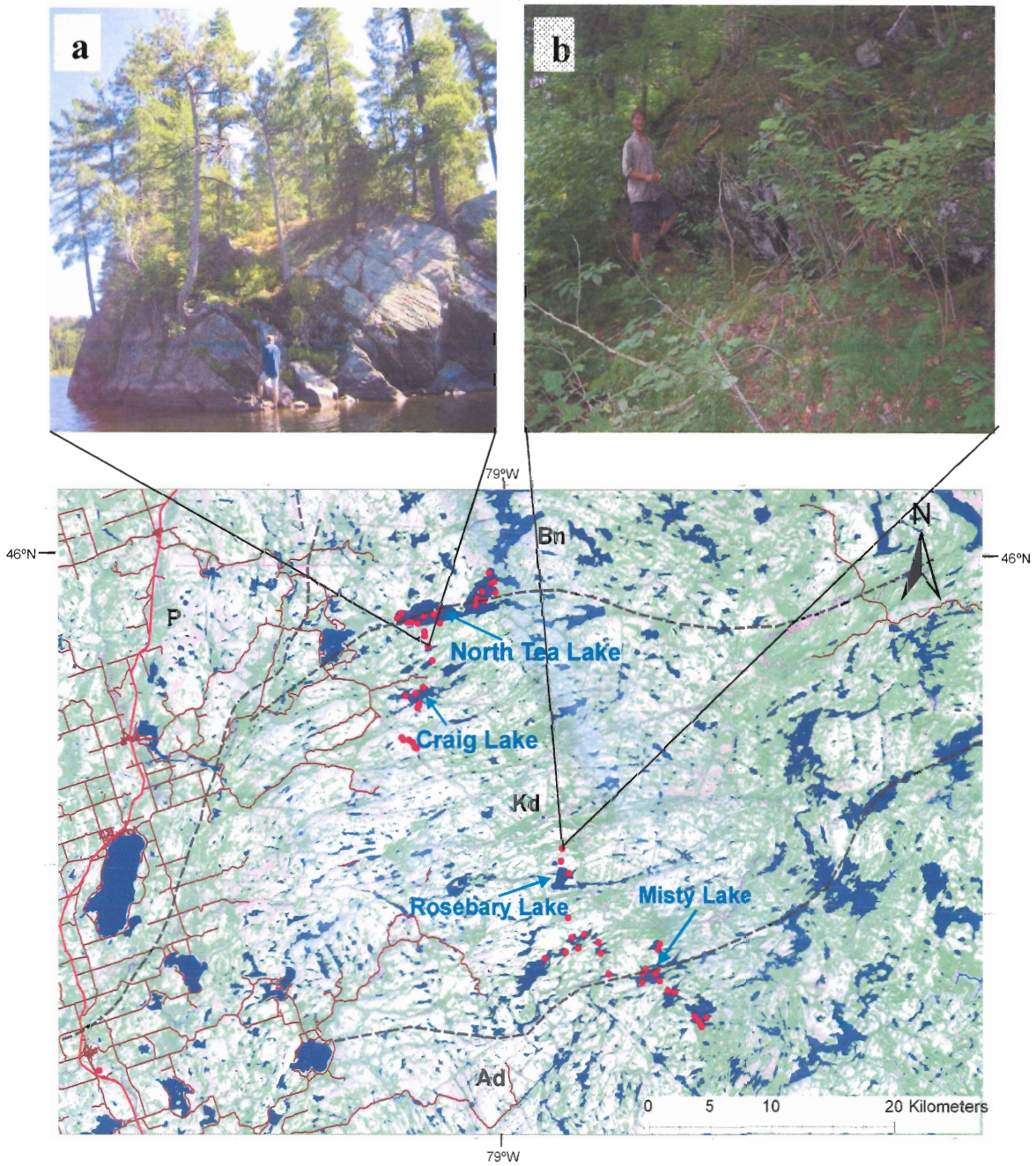

Figure 1.6: Map of the study area showing field stations (red dots; coordinates listed in Appendix B) relative to Kiosk domain, Algonquin domain, and Bonfield terrane. Accompanying field photographs illustrate the average quality of **(a)** shoreline outcrops and **(b)** ridge side outcrops. Notable lakes (North Tea, Craig, Rosebary, and Misty) referred to by this study are also shown.

1.7 Structural Terminology

The tectonic fabrics documented by this study are herein described in terms of their lineation/foliation (L/S) relationship; it is thus important to understand the meaning of this relationship. Flinn (1962) analyzes deformation experienced by a rock in terms of how the shape of an imaginary ellipsoid within the rock, originally spherical in the unformed state, evolves during progressive deformation. Flinn (1962) terms this ellipsoid, "the strain ellipsoid". The shape of the strain ellipsoid is expressed by three orthogonal principal axes, ε_1-ε_2-ε_3, oriented in space parallel to the X-Y-Z axes of the reference coordinate frame (Fig 1.7a). The parameter k ($k = [R_{xy}-1]/[R_{yz}-1]$, where $R_{xy} = \varepsilon_1/\varepsilon_2$ and $R_{yz} = \varepsilon_2/\varepsilon_3$) is used to quantitatively describe shape of the ellipsoid with three major k states being recognized: k>1, k<1, and k=1 (Fig 1.7b). When k>1 prolate (i.e. constriction) strain is produced; when k<1 oblate (i.e. flattened) strain is produced; and when K=1 plane strain is produced. In a rock, k>1, k<1, and k=1 states are manifested by L>S, S>L, and L=S fabrics respectively. Figure 1.8 displays the relationship between k, S, and L.

The L/S relationship has important tectonic implications. In particular, if the L/S relationship in a rock can be identified than the style of finite strain experienced by a rock may be elucidated. In the context of the Grenville geology, L/S fabrics have been associated with early thickening (L=S) fabrics and late flow (S>L) fabrics (e.g. Jamieson et al 2007). See sections 5.4 and 5.5 for discussion of the tectonic implication of L/S fabrics in the northwest Algonquin region.

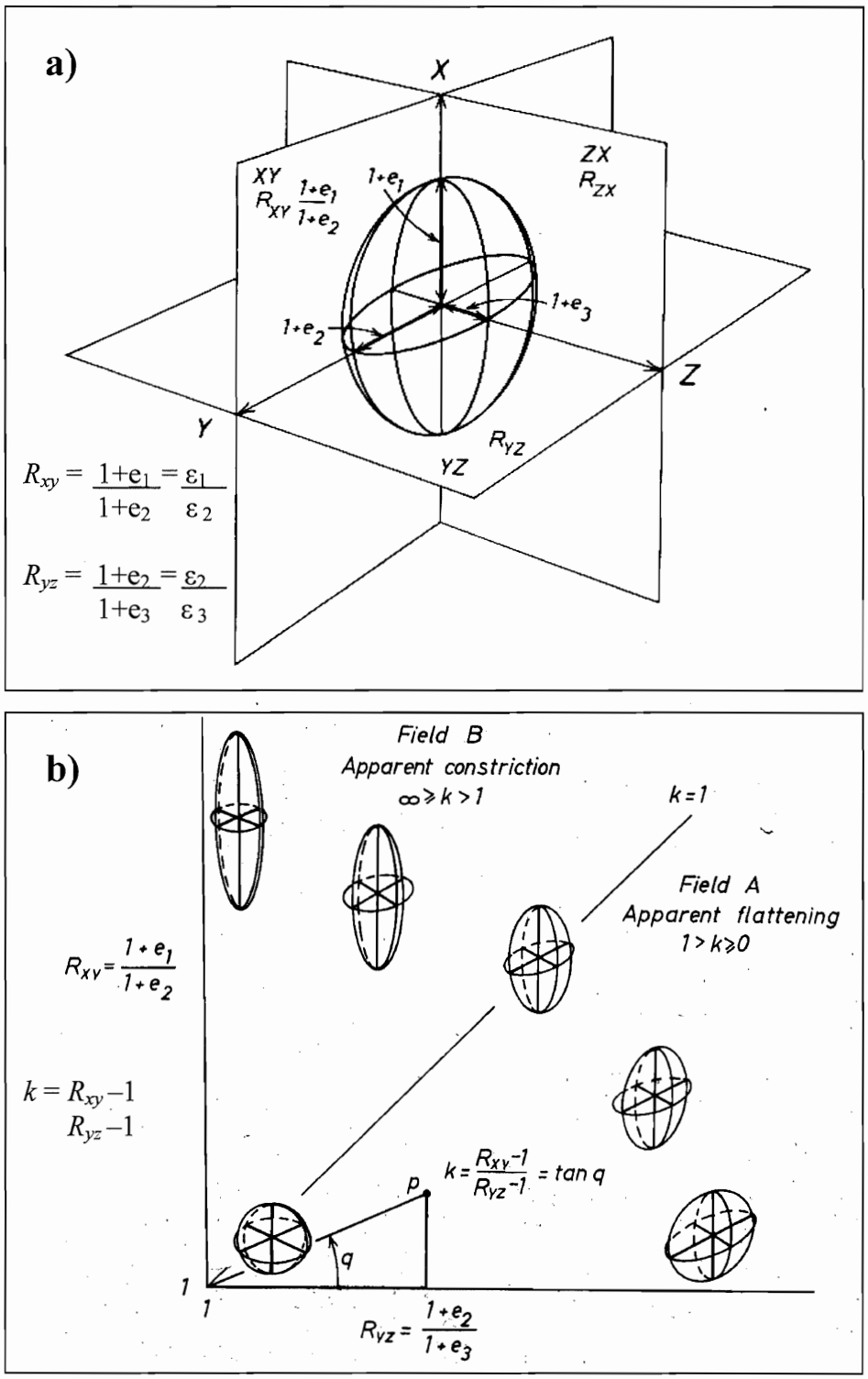

Figure 1.7: a) The strain ellipsoid. Principal strains (e_1, e_2, and e_3) and the strain axes (ε_1, ε_2, and ε_3) are referenced to the coordinate system X-Y-Z. The parameter *R* defines ellipticity. **b)** Flinn diagram showing ellipsoid morphology as a function of prolate ($\infty \geq k > 1$), plane ($k=1$), and oblate ($1 > k \geq 0$) strain styles. Figure modified from Ramsay and Huber (1983).

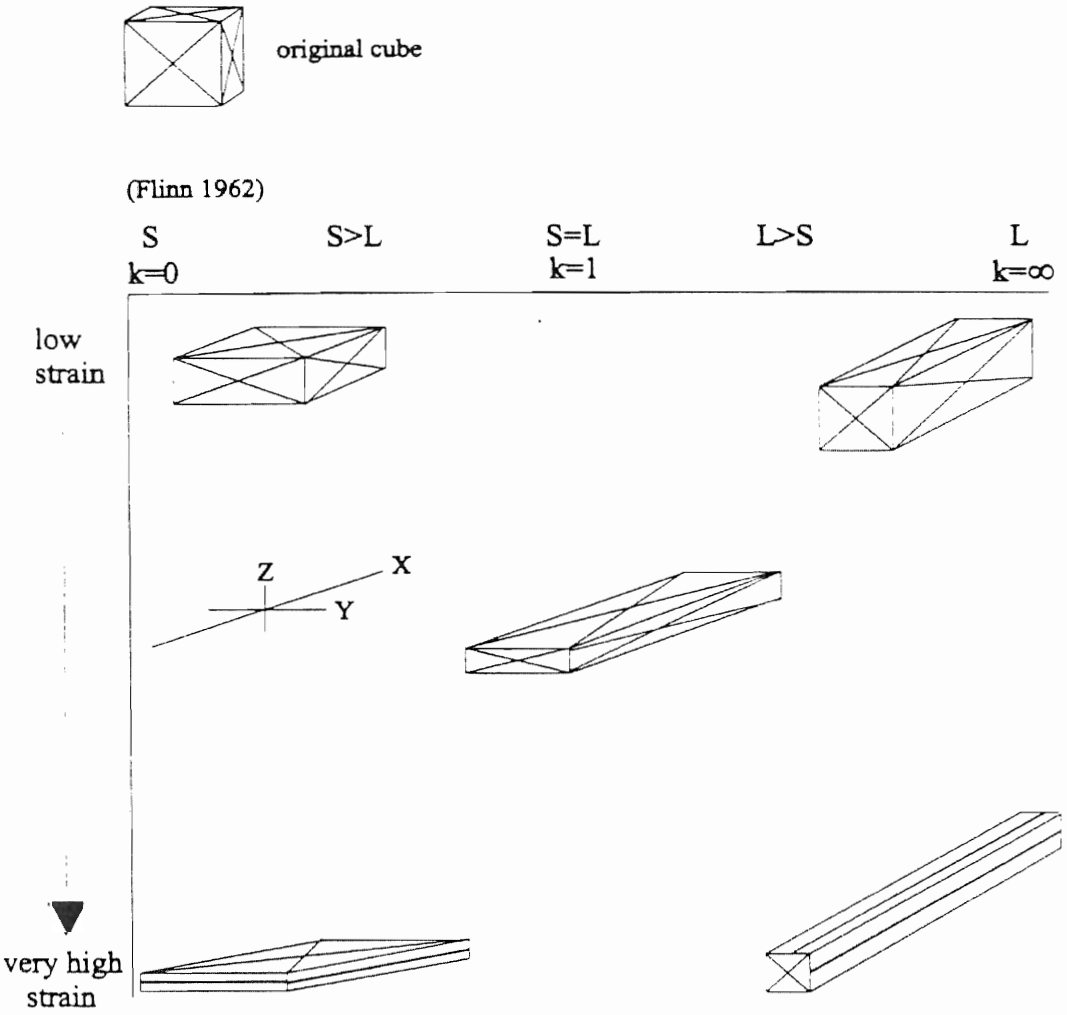

Figure 1.8: Schematic illustration of how strain style, described by *k*, is manifested by L/S fabrics in gneissic rocks. The original cube, representing an undeformed rock, is progressively flatted and/or lengthened (i.e. constricted) depending of the type of strain experienced. See text for further discussion. Figure modified from Timmerman (1998).

CHAPTER 2: GEOLOGY OF NORTHWESTERN ALGONQUIN PARK

2.1 General Statement

Northwestern Algonquin Park is situated within the CGB (Wynne-Edwards 1972) of the Grenville Province. Although this area was originally suggested to be parautochthonous with respect to the pre-Grenvillian Laurentian continent by Rivers et al. (1989), subsequent studies in the CGB belt led workers (e.g. Davidson 1996; Ketchum and Davidson 2000) to conclude that northwestern Algonquin Park and neighbouring regions were allochthonous with respect to the pre-Grenvillian Laurentian continent. The issue of genetic affinity of the northerwestern Algonquin region has led to debate over the position of a key lithotectonic boundary in the Grenville Province, the Allochthon Boundary Thrust (ABT). The positioning of this boundary in the Algonquin/North Bay region is difficult due, in part, to the fact that the area is largely poorly studied compared to regions to the west.

Two primary lithotectonic units of the CGB, the Kiosk domain, the Algonquin domain, comprise northwestern Algonquin Park. Distinct geophysical and structural properties (Figs. 2.1, 2.2) characterize the domains and facilitate their identification in the field. Culshaw et al. (1983) proposed subdivisions for Algonquin domain based on their recognition of cell-like structural units, each demonstrating a unique structural trend and separated by zones of mylonitic gneiss.

To the north of the Kiosk domain lies a terrain of poorly explored granitoid plutons and migmatitic gneiss. To date, this region has not been assigned to any lithotectonic domain, nor has it been recognized as its own distinctive lithotectonic domain. This study applies the informal name, Bonfield terrain, to this region; the

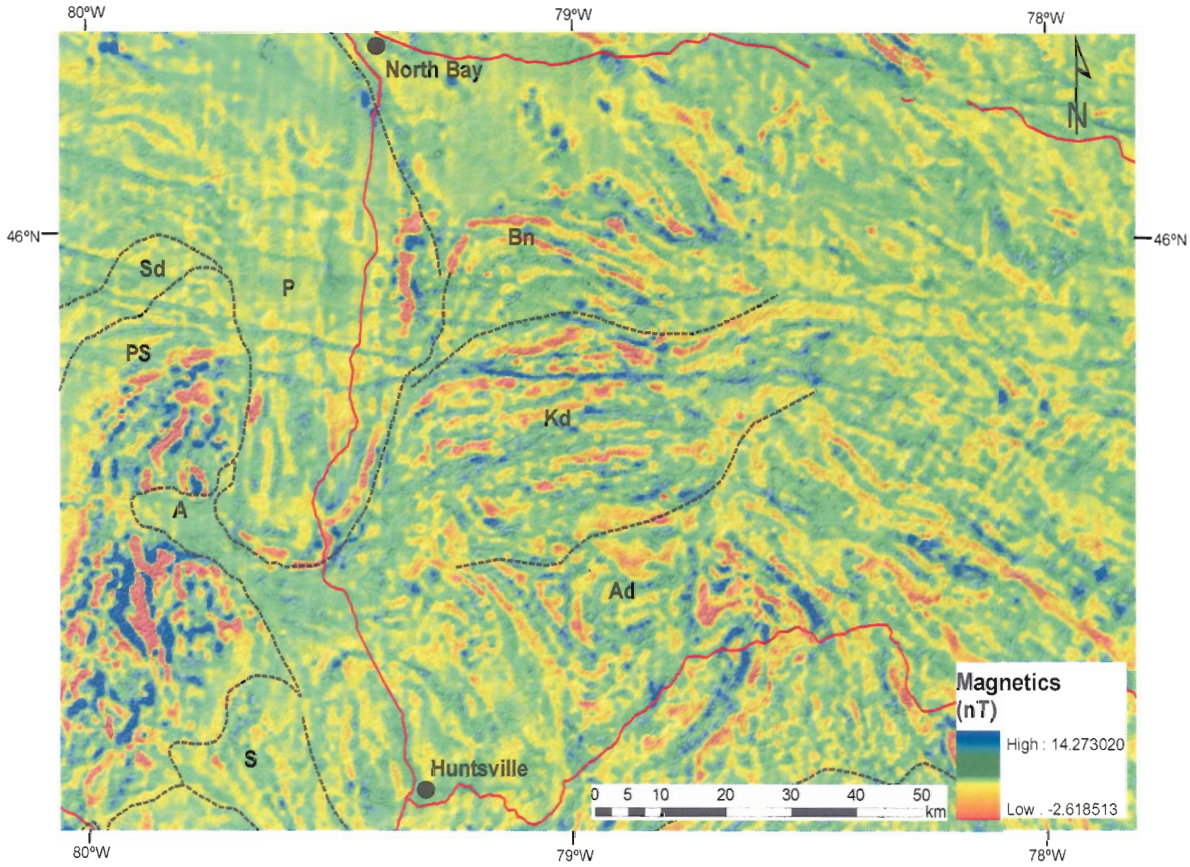

Figure 2.1: Aeromagnetic map of the northwest Algonquin region. The very straight, WSW-ENE trending aeromagnetic pattern of the Kiosk domain is consistent with the orientation of topographic ridges and foliation planes in the Kiosk domain. This pattern is anomalous with respect to neighbouring domains (e.g. the Algonquin domain), which display contorted patterns. See Appendix A for abbreviations. Note that colour scale is inverted in order to better display aeromagnetic pattern. Source data obtained from the Canada Geodetic Information System (2008).

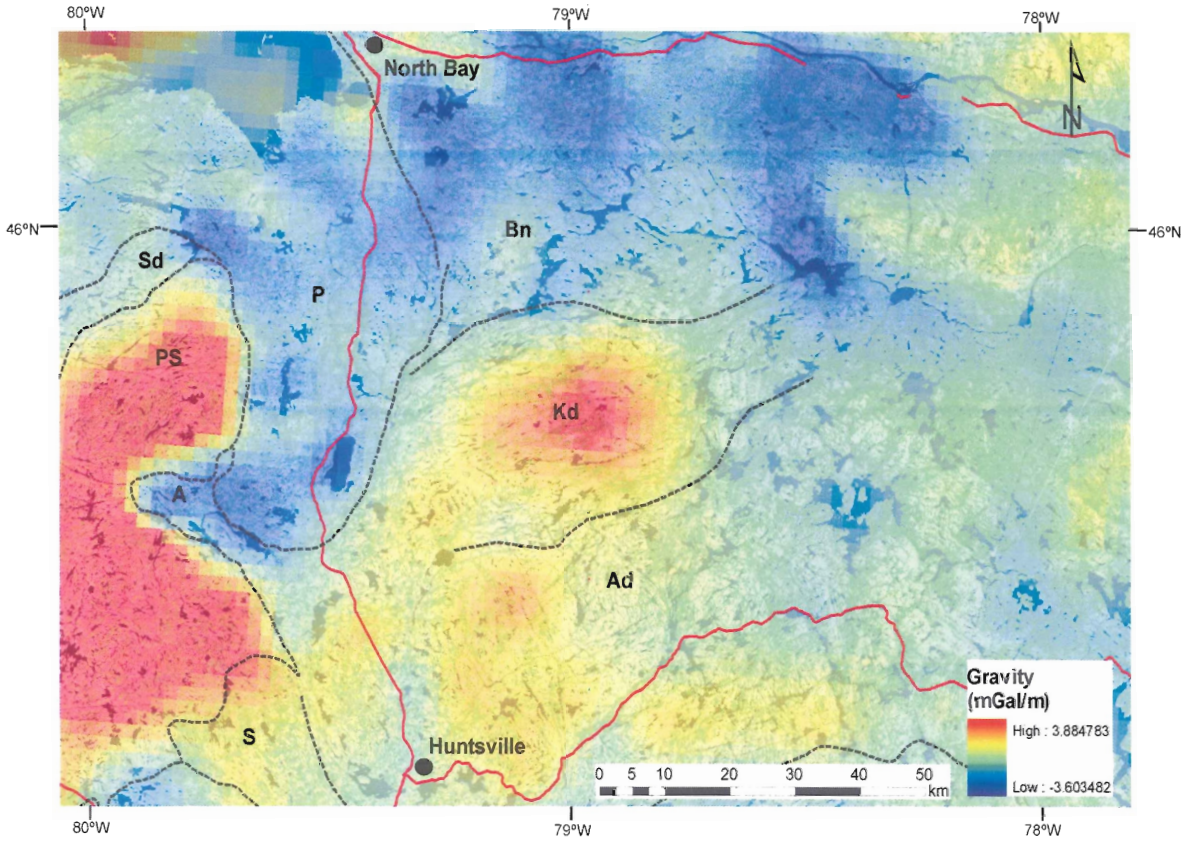

Figure 2.2: Bouguer gravity map (1st vertical derivative) of the northwest Algonquin region. Note the large positive anomaly which is found at the centre of the Kiosk domain. It is possible that this positive anomaly is caused by a granulite facies core in the Kiosk domain, as granulite rocks are known to have high density values. The negative gravity signature of the Bonfield terrain and the Powassan domain is consistent with the large granitoid bodies which intrude these units. Source data obtained from the Canada Geodetic Information System (2008).

name is derived from the Bonfield batholith mapped by Lumbers (1975), which is the dominant geological feature of the area. The reader must note that the term *terrain* is used informally herein; it does not imply that the Bonfied region is a lithotectonic unit within the CGB. As the Bonfield region has not been fully mapped, such a distinction is pending further study. What follows is a summary of the geology of each of these domains, as ascertained from this study and listed in order of their structural level from lowest to highest.

2.2 Bonfield terrain

The Bonfield terrain, extending across the entire northern portion of the study area, is composed of the Bonfield batholith and smaller, unnamed granitoid plutons set in a matrix of variably deformed quartzofeldspathic and migmatitic orthogneiss of upper amphibolite to lower granulite facies metamorphic grade. The host orthogneiss (termed Bonfield gneiss hereafter) likely represents several or many different granitoid bodies stretched out and thinned and into gneissic bands by extreme ductile attenuation (Fig. 2.3). In contrast, recognizable plutons, such as the Bonfield batholith, are much less deformed than the Bonfield gneiss; relict igneous textures are preserved in the Bonfield batholith, whereas they are absent from the highly strained Bonfield gniess. As no clear cross cutting relationships have be observed within the Bonfield terrain, it is difficult to state anything about the relative ages of the plutons and the host orthogneiss. The varying state of deformation observed between the plutons and the Bonfield gneiss does suggest that the latter is older; however, this evidence is not, on its own, sufficient to confidently infer age relationships between the different Bonfield lithologies.

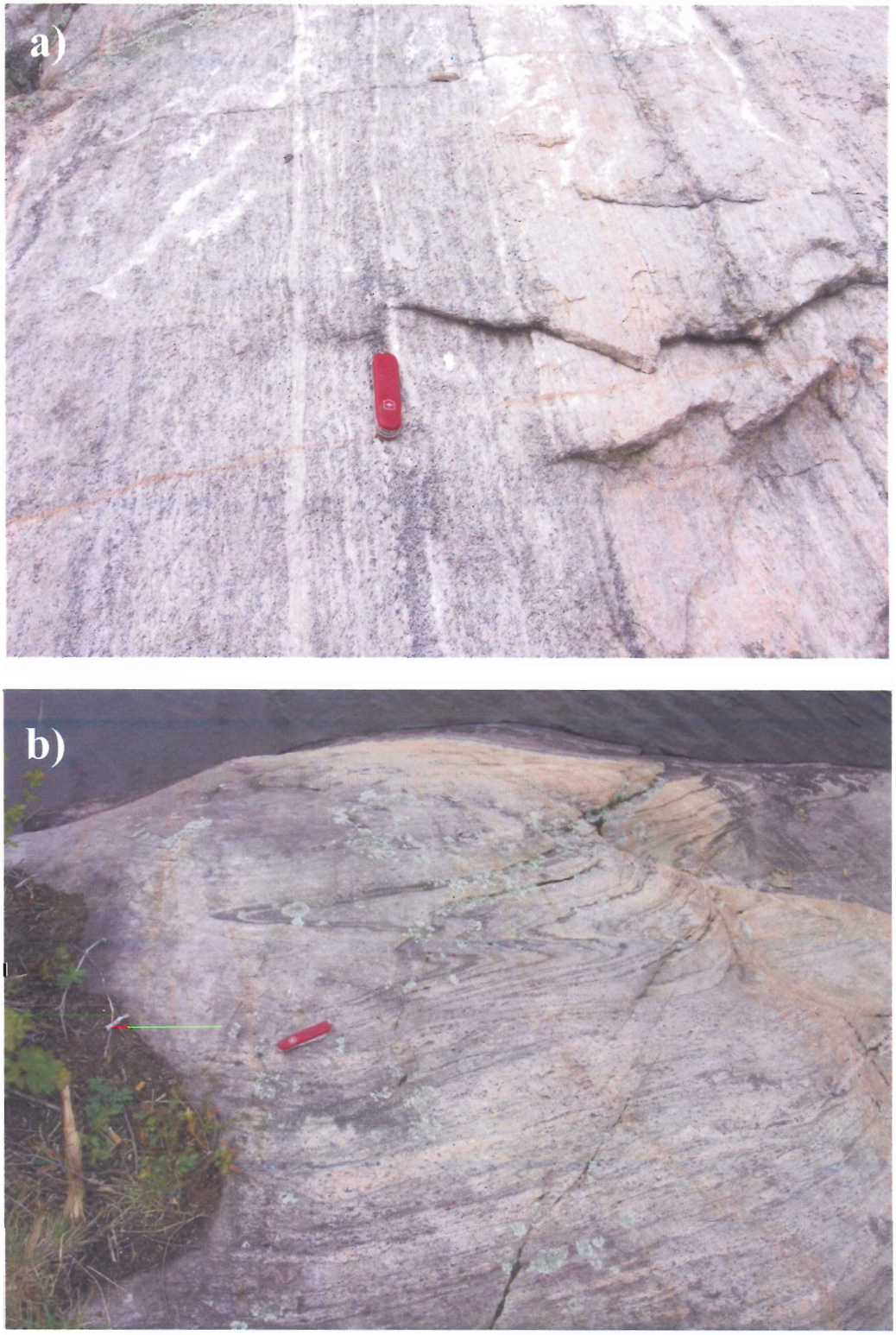

Figure 2.3: (a) Migmatitic Bonfield gneiss at station NA002. Note strongly developed, straight-trending foliation defined by well developed compositional layering. **(b)** Bonfield gneiss at station NA006 showing S>L fabric characteristic of large parts of the southern Bonfield terrain. See Appendix B (Table B1) for station coordinates.

The structural trend of the Bonfield terrain, as defined by metamorphic foliation, is complex compared to the uniformly straight trending structure of the Kiosk domain to the south. Most notably, the variable degree and style of deformation observed in the southernmost Bonfield terrain has produced a variety of fabrics including a widespread S>L fabric (Fig. 2.3), a poorly deformed plutonic fabric, and, less commonly, a L=S fabric very similar to that found in the Kiosk domain (Section 2.4). Structural trend of the Bonfield foliation, where not obscured by plutons, is similar to the WSW-ENE trend of the neighbouring Kiosk domain; however, a second, less common yet consistent, N-S trend was identified.

The observed variability of structural style and orientation may not be a primary feature of the Bonfield terrain, considering this study only examined the southernmost portion of the Bonfield. In particular, the southernmost Bonfield terrain borders a major shear zone which serves as the boundary between the Bonfield terrain and the Kiosk domain to the south. It is entirely possible that the main WSW-ENE foliation trend observed in the southern Bonfield terrain is an overprint of this shear zone which displays a similar trend. In this case, the second N-S foliation trend may represent an earlier structural trend preserved in the Bonfield terrain. A second possibility is that the N-S foliation trend is a product of late pegmatites, observed at several localities in the area, reorienting the fabric in the southern Bonfield terrain. A third possibility is that the N-S foliation trend is also a product of the shear zone and is therefore the same age as the as the WSW-ENE foliation trend.

2.3 Northern Kiosk domain shear zone

Separating the Kiosk domain from the Bonfield terrain is a zone of very high strain characterized by fine grained, highly attenuated, banded gneiss with a pervasive L=S fabric (Figure 2.4). Traversing south across strike, this shear zone is first identified along the southern shores of North Tea lake; it is then found to the south along a portage off North Tea Lake to Cayuga Lake, giving it a width of at least 2 km. Structural trend within the shear zone, defined by strongly developed tectonic foliation, is homogeneous with little deviation from the average WSW-ENE direction. Steeply plunging, NW-SE oriented lineations are found throughout the shear zone. Although the shear zone was not mapped in detail, aeromagnetic data (Fig. 2.1) suggest that it extends the entire length of the northern Kiosk domain boundary.

2.4 Kiosk Domain

The Kiosk domain is characterized by a very straight trending, L=S fabric (Fig. 2.5) which is not found elsewhere in the CGB at such a scale. Structural trend of the Kiosk, as defined by a strong foliation, is mainly WSW-ENE with only minor deviations occurring where foliation appears reoriented by late, cross cutting pegmatite dykes. Stretching lineations, equal to the foliation in strength, plunge moderately to directly down dip and are consistent with a SE-NW tectonic transport direction. Since the extreme degree of ductile deformation observed in the Kiosk domain has obliterated most kinematic indicators, it is difficult to deduce a favoured sense of tectonic transport.

Upper amphibolite to granulite facies orthogneiss, composed of quartzofeldspathic units interlayered with minor mafic bands, represents the principal rock type found in the Kiosk domain (hereafter referred to as the Kiosk gneiss; Fig. 2.6).

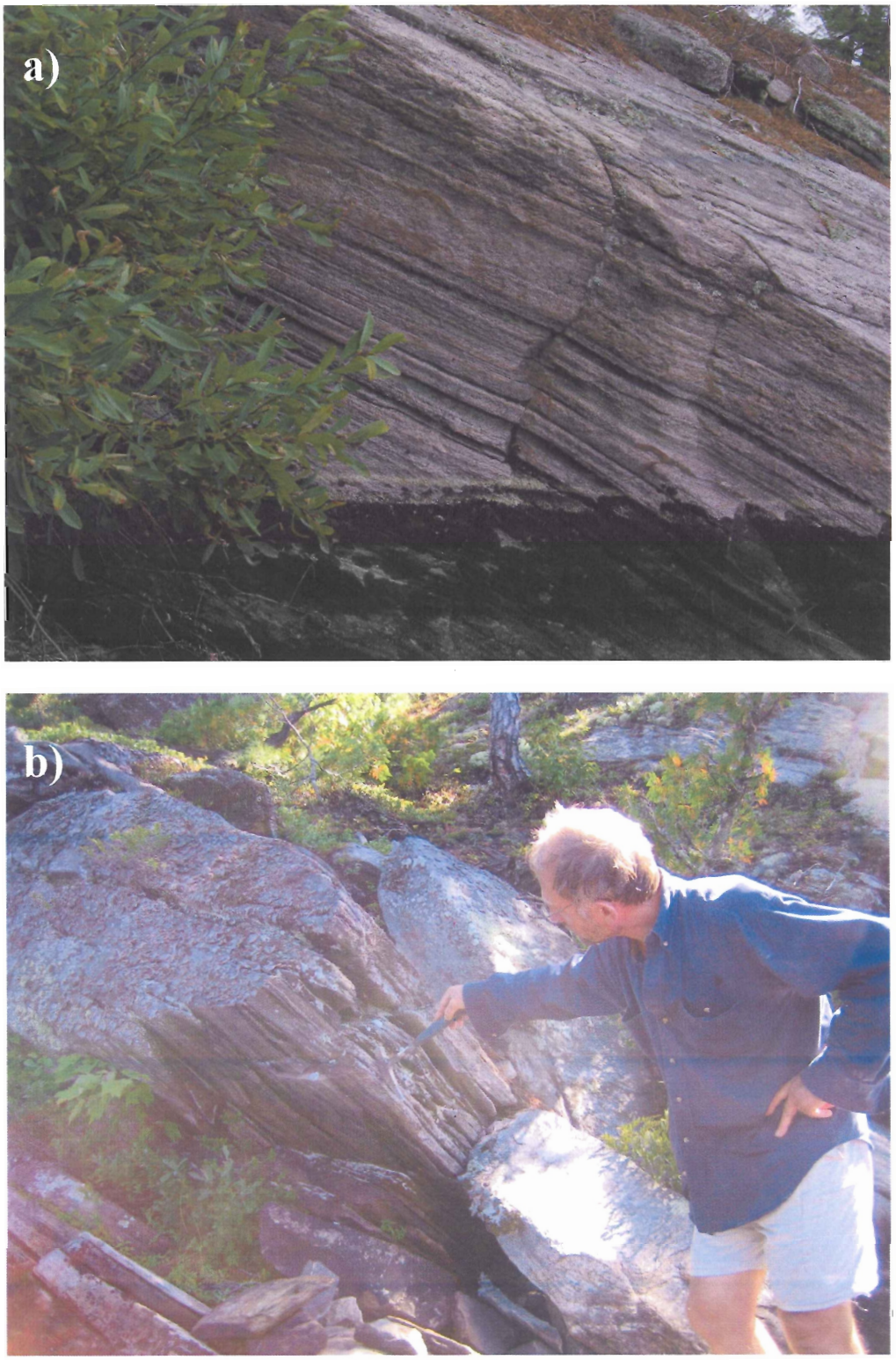

Figure 2.4: Highly strained, sheet-like, L=S fabric of the northern Kiosk domain shear zone. **(a)** South shore of North Tea Lake (NA007). **(b)** Cayuga Lake (NA020).

Figure 2.5: Photo of a foliation plane showing well developed, down-dip lineations in a sample of Kiosk gneiss in the southern Kiosk domain (NA044). This sample demonstrates the typical L=S fabric observed throughout the Kiosk domain.

The fine grained nature, uniformly layered texture, and indistinct grey to pink colour makes the gneiss quite difficult to separate into units in the field. Furthermore, extreme ductile deformation and high grade metamorphism have obliterated most relict primary textures. The recognition of individual plutons or other magmatic bodies, has thus not been possible on the scale of this study. Supracrustal rocks, principally metasediments, are rare and have only been found as thin (>0.5m) layers within larger successions of grey, quartzofeldspathic orthogneiss. These metasedimentary layers occur only on a localized scale and, as reported by Davidson (1986), are difficult to trace due to the great degree of ductile attenuation experienced by the rocks of the Kiosk domain. The only identifying features of the metasediments are the presence of characteristic violet coloured garnet and fine grained aluminous minerals such as corundum. Texturally, they exhibit a highly strained, strongly foliated and strongly lineated, planar fabric, which is identical to that of the surrounding country gneiss.

Mafic enclaves, found interlayered with the Kiosk gneiss, are identified at several localities throughout the Kiosk domain (Fig. 2.6). These enclaves range from less than one metre in diameter to ~2 metres in diameter and are possibly the remnants of mafic dykes boudinaged by ductile shear. They are differentiated from the mafic layers (i.e. melanosomes) of the Kiosk gneiss by the following criteria: (1) they of significantly wider than the mafic bands, (2) they are linearly discontinuous, and (3) they do not form part of the gneissic layering (i.e. gneissic layering may be observed wrapping around the mafic enclaves).

Metamorphic grade is primarily granulite facies throughout the Kiosk domain. Clinopyroxene bearing, creamy brown to biscuit coloured, leucocratic, fine grained

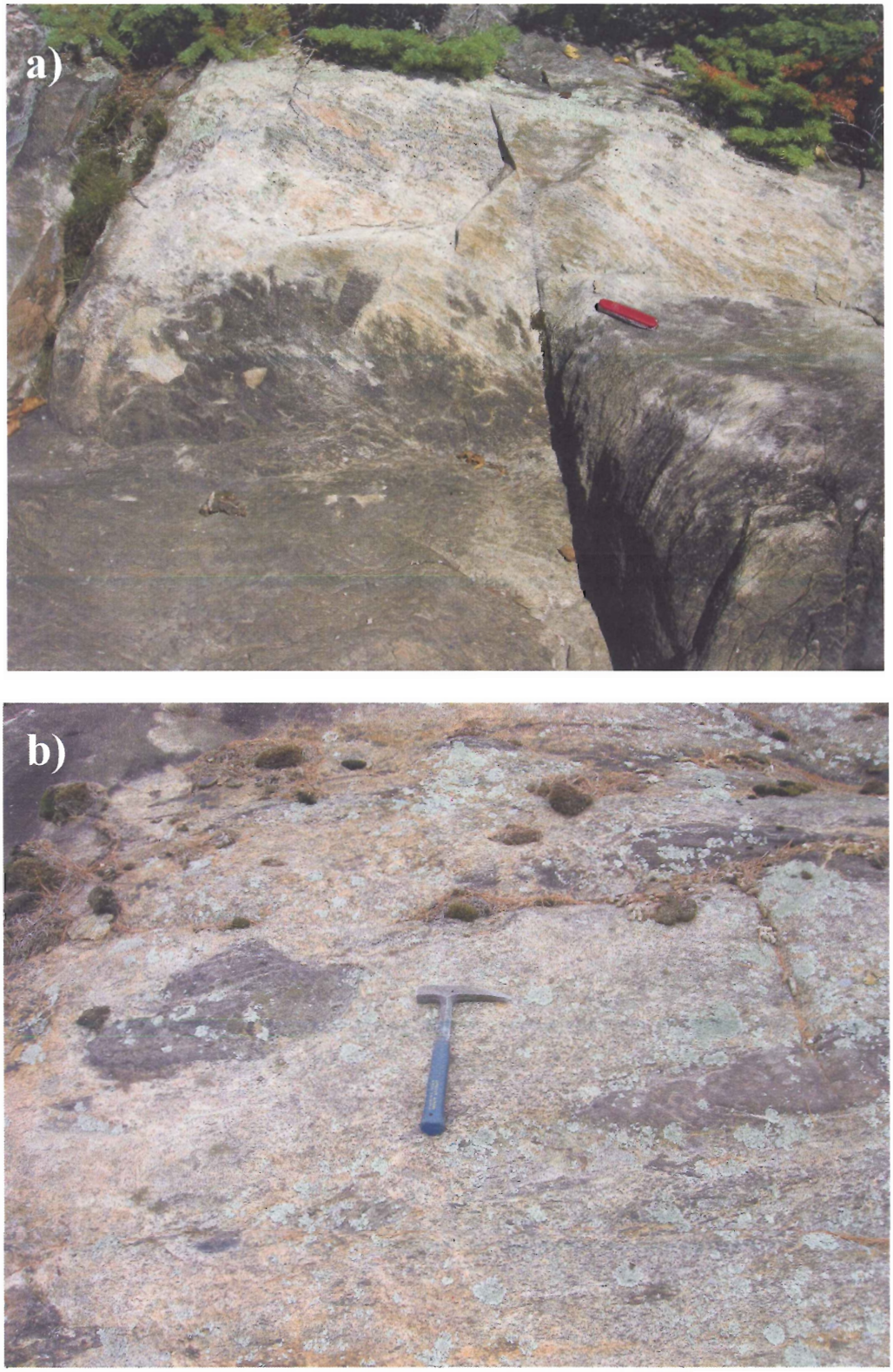

Figure 2.6: Photograph of: **(a)** well-foliated, quartzofeldspathic Kiosk gneiss at NA023 with light-cream brown leucosomes and; **(b)** variably foliated Kiosk gneiss at NA057 with mafic enclaves.

orthogneiss is characteristic of the Kiosk gneiss. Notable retrogression to amphibolite facies, characterized by medium grained, hornblende rich mylonitic gneiss, occurs along the north and south bounding shear zones of the domain.

2.5 Southern Kiosk domain shear zone

The transition from the very straight trending, WSW-ENE, planar fabric of the Kiosk domain to the often complex, variably oriented fabric of the north central Algonquin domain occurs abruptly along the southern Kiosk domain shear zone. Outcropping along the southern shores of Misty Lake, this shear zone contains a strained, amphibolite facies gneiss bearing an L=S fabric. Relative to the Kiosk gneiss, rocks in this shear zone contain a greater proportion of mafic material present in the form of thick (0.5-1m) hornblende rich layers. A significant number of pegmatites were also observed within the shear zone.

2.6 North-central Algonquin domain

Rocks of the north central Algonquin domain generally do not demonstrate the same degree of strain as those of the Kiosk domain. The strongly developed, straight trending L=S fabric of the Kiosk domain gives way to the variably oriented, S>L fabric of the northern Algonquin domain. A medium grained, felspar augen bearing, quartzofeldspathic orthogneiss, with relict igneous texture, contrasts with the highly strained, fine-grained, often mylonitic granulite Kiosk gneiss. Medium-grained orthopyroxene and slightly finer clinopyroxene indicate that metamorphic grade is granulite facies. Certain bands of gneiss within the north-central Algonquin may be of metasedimentary origin, as suggested by their quartz rich composition; however, the lack of distinct metasedimentary mineral assemblages, such the presence of aluminosilicates,

raises doubts about such a conclusion. Mafic layers and pods are also present in the north-central Algonquin domain but are subordinate to the quartzofeldspathic gneiss.

Foliation trend in the northern Algonquin domain is highly variable and reflects the fold-like structures clearly displayed on aeromagnetic maps. Lineation orientations also vary but a SE plunge direction prevails. It is possible that the structural trend observed in the north central Algonquin domain represents folds similar to those observed by Davidson (1986) in the southeastern Algonquin domain; however, more work in the north-central Algonquin domain is required to confirm this hypothesis.

CHAPTER 3: PETROGRAPHY AND MINERAL CHEMISTRY

3.1 General statement

Thin section microscopy was completed on 41 representative samples from the Bonfield terrain and Kiosk and Algonquin domains in order to: (1) document the mineral assemblages present in the study area, (2) evaluate metamorphic textures and overprinting relationships, and (3) identify samples best suited for electron microprobe (EMP) analyses. Thin sections were cut perpendicular to foliation and parallel to lineation. In select samples, sections cut perpendicular to lineation were also prepared. EMP analyses, carried out on selected metabasite and aluminous supracrustal samples from the Kiosk and Algonquin domains, provided the major-element composition data needed for thermobarometric work (Chapter 4). The complete set of EMP analyses and EMP operating conditions are provided in Appendix C. Mineral abbreviations are listed in appendix A.

This chapter presents detailed petrographic descriptions of the principal lithologies identified within the study area (Chapter 2). Table 3.1 presents a summary of the characteristic mineral assemblages of the principal lithologies. Chemical formulas for significant phases (Tables 3.2, 3.3), calculated from EMP analyses, supplement the descriptions where available. The petrographic descriptions are grouped by domain and follow in order of structural level from lowest to highest.

3.2 Bonfield terrain

The Bonfield terrain comprises granitoid bodies set in a matrix of fine grained, compositionally banded Bonfield gneiss (defined in Section 2.2). Within the Bonfield gneiss, lithologically distinct migmatitic and non-migmatitic members have been

Table 3.1: **Mineral assemblages of lithologies identified within the study area. See text for further discussion.**

Unit	Lithology	Assemblage
Bonfield terrain	*granitoid*	Kfs-Qtz-Pl-Cpx±Opx-Grt-Hbl±Bt
	Bonfield gneiss (amphibolite)	Kfs-Qtz-Pl-Hbl-Bt-Scp-Op-Ttn-Zrn-Ap
	Bonfield gneiss (granulite)	Plg-Qtz-Grt-Cpx±Opx-Hbl-Bt-Op-Zrn-Ap
	hornblende porphyroclast mylonite	Ksp-Qtz-Pl-Hbl-Op
Northern Kiosk domain shear zone	*amphibolite-facies banded gneiss*	Pl-Kfs-Qtz-Hbl-Bt-Op-Ttn-Zrn-Ap
	granulite-facies banded gneiss	Pl-Qtz-Hbl-Grt-Cpx-Opx-Scp-Op-Rt-Ttn-Zrn
Kiosk domain	*Kiosk gneiss*	Pl-Qtz-Cpx±Opx-Grt-Hbl±Bt-Scp-Op-Zrn
	mafic enclaves	Pl-Hbl-Grt-Cpx-Opx-Qtz-Bt-Op-Zrn±Ttn±Ap
	supracrustal gneiss	Kfs-Pl-Grt-Crn-Bt-Op-Spl
Southern Kiosk domain shear zone	*mafic amphibolite*	Hbl-Pl-Qtz-Bt-Op-Tnt±Zrn
North-central Algonquin domain	*Algonquin gneiss*	Pl-Qtz-Hbl-Grt-Opx-Cpx-Op-Zrn±Tnt

identified. All three lithologies are exposed in outcrops along the northern and eastern shores of North Tea Lake. Additionally, a hornblende porphyroclast bearing mylonite, exotic with respect to the surrounding Bonfield gneiss, has been identified in outcrops along the southeastern shores of North Tea Lake (NA011).

3.2.1 Granitoid rocks

Leucosome-bearing granitoid rocks of the Bonfield batholith and smaller, unnamed plutonic bodies represent the dominant lithology of the Bonfield terrain. All plutonic bodies display a mineralogy characterized by an equigranular, medium-grained, sub-polygonal Kfs-Qtz-Pl dominated matrix with minor mafic clusters of Cpx±Opx-Grt-Hbl±Bt (Fig 3.1). Mafic clusters typically feature pale pink, poikioblastic garnet porphyroblasts surrounded by olive green hornblende and dark green clinopyroxene, although fine- to medium-grained granular garnet is also contained in some mafic clusters. Brown biotite is a minor component of these samples and may be a late feature, as it grows over and through hornblende. The plagioclase rich felsic matrix contains K-feldspar grains which commonly display well developed Carlsbad twinning and albite exsolution lamellae.

Aside from possible minor replacement of hornblende by biotite, this assemblage appears to be in textural equilibrium; all phases are in mutual contact with no obvious reaction textures between them. The granitoid rocks of the Bonfield terrain are texturally variable with fabrics ranging from strongly foliated to nearly granoblastic. Where foliation is developed, it is defined by a general preferred orientation of matrix minerals and, in contrast to the host country gneiss, is not compositional.

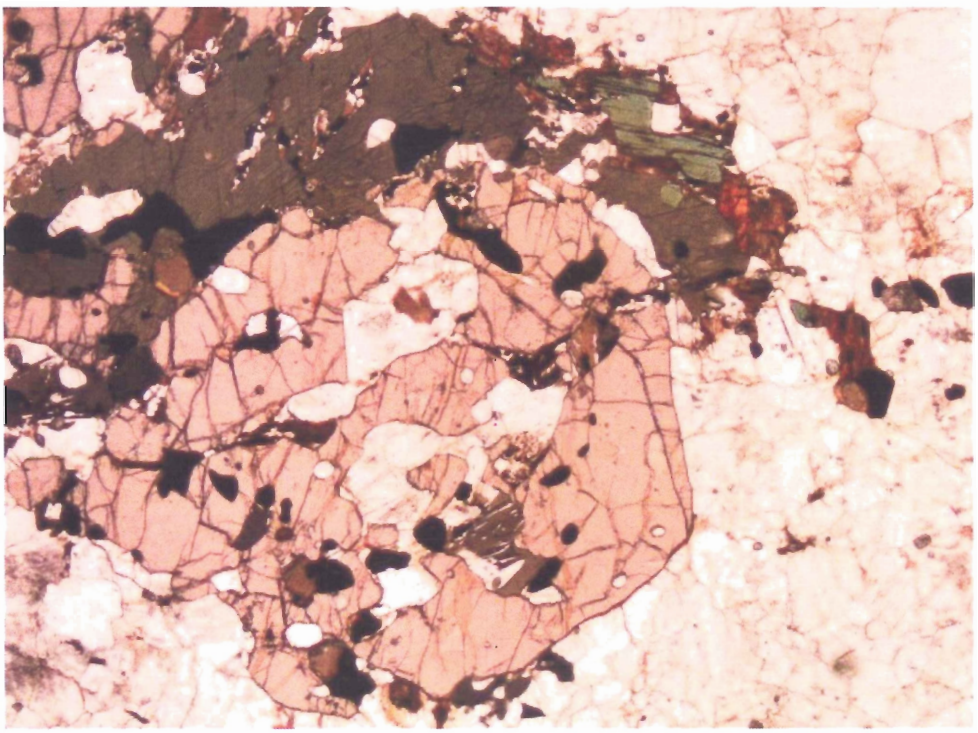

Figure 3.1: Sample NA017A. Mafic cluster in granitoid rock of the Bonfield domain containing pale pink, poikiloblastic garnet porphyroblast surrounded by olive green hornblende and dark green clinopyroxene (5.00x6.25 mm). Felsic matrix primarily contains K-feldspar and quartz with lesser amounts of plagioclase. Sample locations are listed in Appendix B.

3.2.2 Bonfield gneiss

The Bonfield gneiss is characterized by a fine- to medium-grained, pink to grey gneiss which can be classified into two primary divisions: (1) migmatitic, and (2) non-migmatitic. The migmatitic Bonfield gneiss typically exhibits a moderately to strongly developed compositional segregation of distinct, hornblende porphyroblast rich matrix layers alternating with felsic leucosomes containing K-feldspar porphyroblasts. Conversely, the non-migmatitic Bonfield gneiss is generally grey, fine- to very-fine-grained, equigranular, and lacks the distinctive hornblende porphyroblasts and abundant leucosomes of the migmatitic Bonfield gneiss. Despite these compositional and textural variations, all of the Bonfield gneiss exhibits a relatively consistent fabric, defined by a moderate to strongly developed, compositional layering.

The hornblende-porphyroblast-rich, non-leucocratic layers of the migmatitic Bonfield gneiss contain coarse, blue-green hornblende crystals (up to 1cm long axis; Fig 3.2a) set in a fine grained granodioritic matrix composed of Kfs-Qtz-Pl-Hbl-Bt-Op-Ttn-Zrn-Ap. Matrix K-feldspar frequently displays Carlsbad twinning and albite exsolution. Biotite is dark brown and is typically associated with hornblende, growing either along the grain boundaries of the hornblende or through the hornblende crystal itself. Accessory titanite occurs almost exclusively along the grain boundaries of hornblende. Inclusions in the hornblende porphyroblasts include felsic minerals, biotite, opaque minerals, and zircon.

Leucocratic layers of the migmatitic Bonfield gneiss occur at a variable frequency between the non-leucocratic layers but, once averaged over the scale of an outcrop, account for 35% of total rock volume. The leucocratic layers are generally coarser than

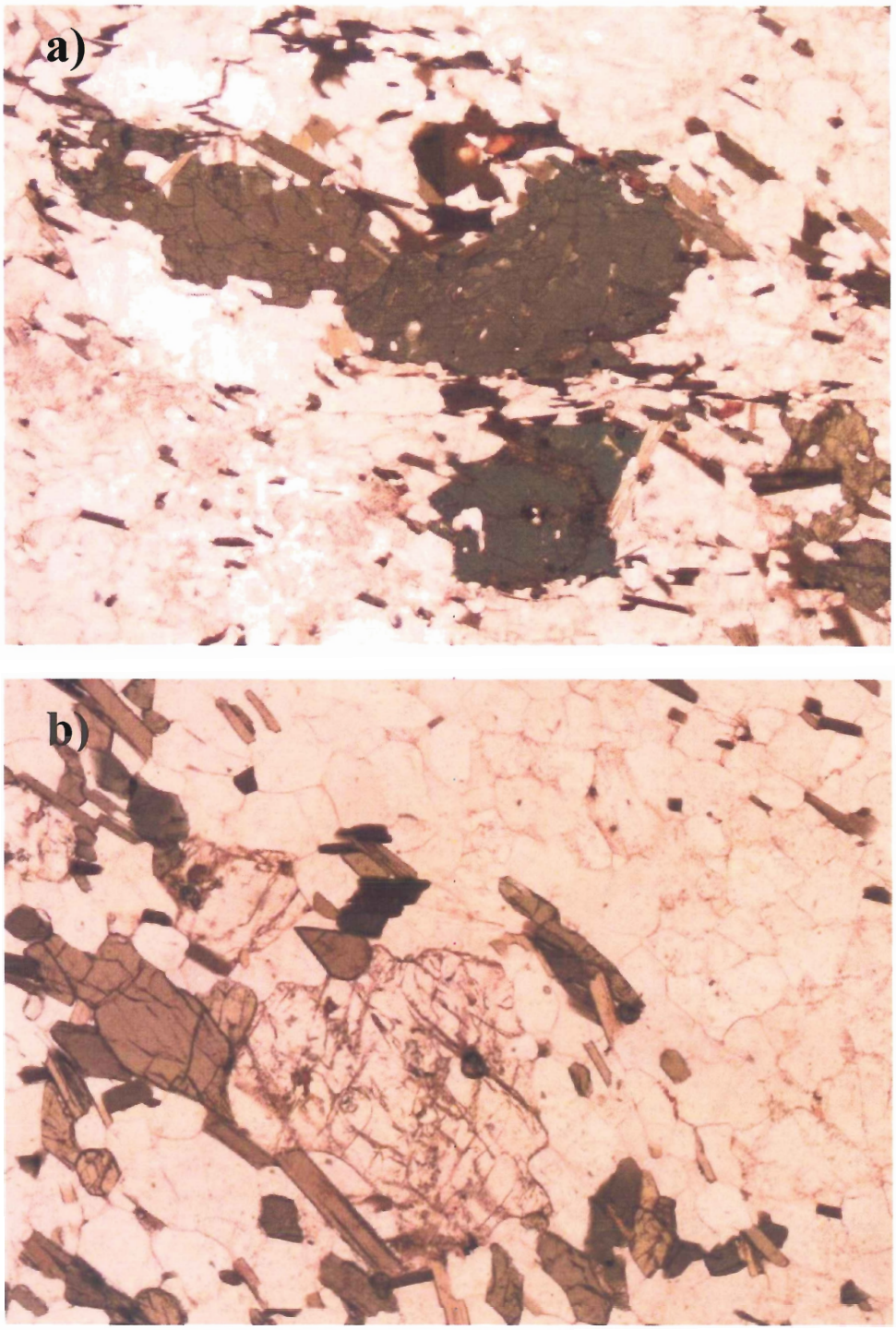

Figure 3.2: **(a)** Migmatitic and **(b)** non-migmatitic Bonfield gneiss. **(a)** Sample NA006B. Blue-turquoise and brown hornblende porphyroblasts set in a fine grained, granodioritic matrix (5.00x6.25 mm). **(b)** Sample NA014A. Well foliated mafic layer containing olive green hornblende and colourless scapolite (high relief mineral) alternating with felsic layer of K-feldspar, quartz, and plagioclase (5.00x6.25 mm).

the matrix layers and are composed of Kfs-Qtz-Pl-Bt-Op-Zrn-Ap; K-feldspar and quartz are by far the dominant minerals, accounting for over 90% of the total leucosome volume. K-feldspar is largely present as medium- to coarse-grained porphyroblasts that typically demonstrate Carlsbad twining and perthitic exsolution; fine grained, recrystallized K-feldspar and quartz are common along the grain boundaries of K-feldspar porphyroblasts.

The non-migmatitic Bonfield gneiss (Fig 3.2b) is typically intermediate in composition, having a matrix composed of Pl-Kfs-Qtz-Hbl-Bt-Op-Scp-Zrn-Ap. Olive-green hornblende and dark beige to brown biotite are the principal mafic minerals and are concentrated in bands which define the foliation. The felsic layers contain near equal proportions of K-feldspar, quartz, and plagioclase and, in contrast to the migmatitic Bonfield gneiss, are uniformly fine-grained. Rare, very pale pink grains of garnet are randomly distributed throughout the felsic and mafic bands of the gneiss. With the exception of biotite growing over/through hornblende, grain boundaries do not display reaction textures and thus suggest equilibrium conditions.

A rare but recurring Plg-Qtz-Grt-Cpx±Opx-Hbl-Bt-Op-Zrn-Ap granulite facies assemblage, observed in non-migmatitic Bonfield samples from NA011 and NA016, suggests that pockets of granulite gneiss are preserved within the Bonfield terrain. Texturally, these rocks are similar to the amphibolite facies version of the non-migmatitic country gneiss in that they are fine grained and equigranular; however, reaction textures are much more abundant and include the overgrowth of clinopyroxene by blue-green hornblende and brown biotite.

3.2.3 Hornblende porphyroclastic mylonite

Distinct hornblende and K-feldspar porphyroclasts set in a very fine grained felsic matrix are characteristic of this mylonite. Coarse K-felspar porphyroclasts (Fig 3.3) are rimmed by fine-grained, recrystallized K-feldspar and frequently have asymmetric tails of quartz and fine grained K-feldspar. Dark green, disaggregating hornblende porphyroclasts display irregular grain boundaries with fine tails of fine grained K-feldspar, quartz, and hornblende. Many porphyroclasts have asymmetric tails which suggest a sinistral shear sense (Fig 3.3); however the shear sense is generally inconsistent with some porphyoclasts suggesting dextral shear. Very fine grained to sub-microscopic K-feldspar and quartz and coarse grained quartz ribbons comprise the felsic matrix.

3.3 Northern Kiosk domain shear zone

Within the northern Kiosk domain shear zone (Section 2.3) two lithologies have been identified: (1) a medium- to fine-grained, intermediate, amphibolites facies banded gneiss, and (2) a very fine-grained granulite facies banded gneiss. The amphibolites facies gneiss has only been identified along the south shore of North Tea Lake where the structurally lowest edge of the shear zone is exposed (NA005, NA008, NA009). The granulite facies gneiss is found further south in the shear zone, several kilometres south of North Tea Lake (NA020).

3.3.1 Amphibolite-facies banded gneiss

The assemblage Pl-Kfs-Qtz-Hbl-Bt-Op-Ttn-Zrn-Ap characterizes the amphibolites facies banded gneiss of the northern Kiosk domain shear zone. Mafic layers are composed primarily of fine- to medium-grained, olive to forest green hornblende and

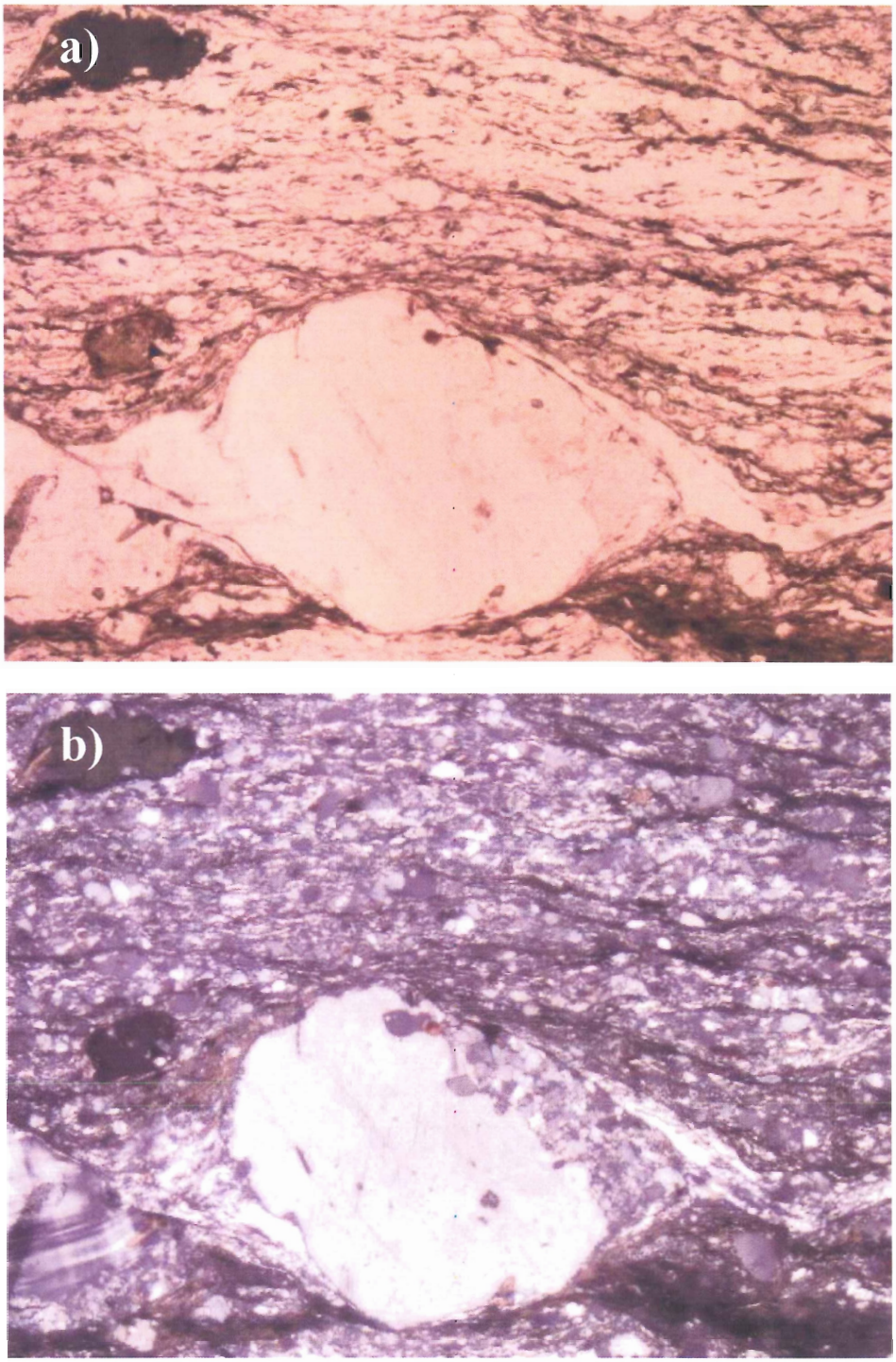

Figure 3.3: Sample NA011A. Hornblende and K-feldspar porphyroclastic mylonite. Asymmetric tails of the K-feldspar porphyroclast suggest sinistral sense of shear. **(a)** Plain polarized light (5.00x6.25 mm). **(b)** Cross polarized light (5.00x6.25 mm).

dark brown biotite (Fig 3.4). They alternate with fine-grained felsic layers composed of near equal proportions of K-feldspar and plagioclase, and lesser amounts of quartz. On average, felsic layers are more voluminous at any given outcrop. This compositional layering, in addition to a strong preferred orientation of biotite and hornblende grains, defines the L=S fabric observed in the shear zone gneiss. Minor replacement of hornblende by biotite is present in these samples; otherwise, all grains are in clean, mutual contact. Aside from a more strongly foliated fabric and the lack of scapolite, this gneiss is very similar to the non-migmatitic Bonfield gneiss.

3.3.2 Granulite facies banded gneiss

The granulite facies banded gneiss of the northern Kiosk domain shear zone is very fine grained (<0.1mm) and contains the mineral assemblage Pl-Qtz-Hbl-Grt-Cpx-Opx-Scp-Op-Rt-Ttn-Zrn (Fig 3.5). Mafic layers, composed primarily of olive to brownish green hornblende, colourless to light pink garnet, clinopyroxene, orthopyroxene, and scapolite alternate with felsic layers composed of plagioclase and quartz. Hornblende can be observed growing over and through pyroxene and garnet grains in the mafic layers. Texturally, this gneiss exhibits the same L=S fabric, notably defined the by preferred orientation of hornblende crystals, as the banded amphibolite; however, the fabric is even stronger than it is in the banded amphibolite. The presence of garnet and pyroxene, very fine grain size, and the intensity of the foliation and lineation clearly differentiates the granulite facies banded gneiss from the amphibolites facies banded gneiss in the northern kiosk domain shear zone.

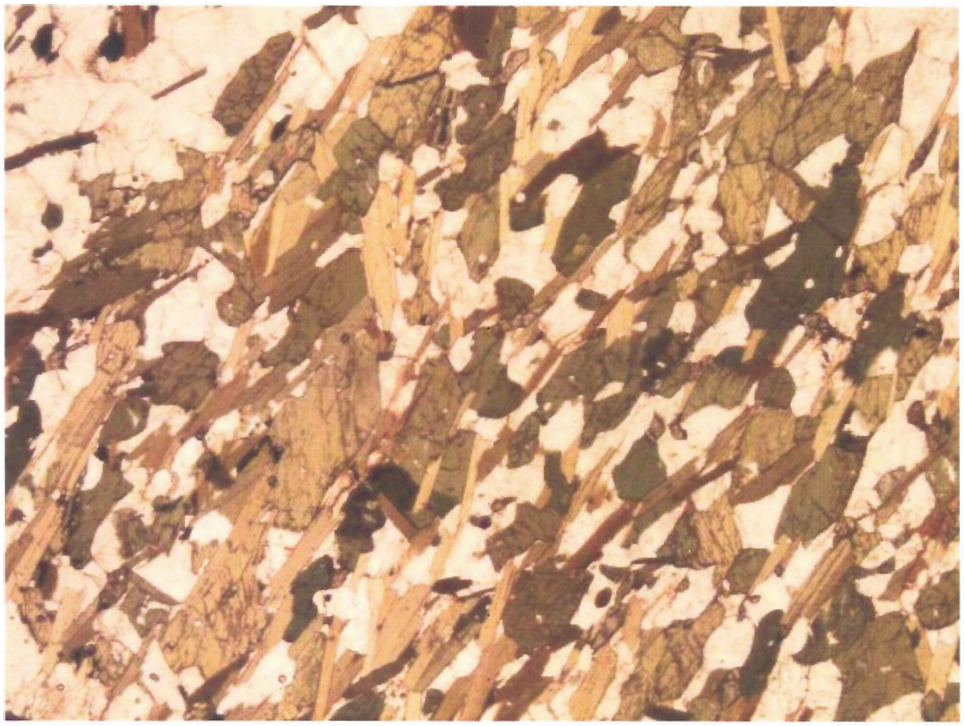

Figure 3.4: Sample NA005B. Mafic layer of northern Kiosk domain shear zone banded amphibolite gneiss containing medium grained olive green to light brown hornblende and dark brown biotite (5.00x6.25 mm). Note the preferred orientation displayed by biotite and hornblende grains.

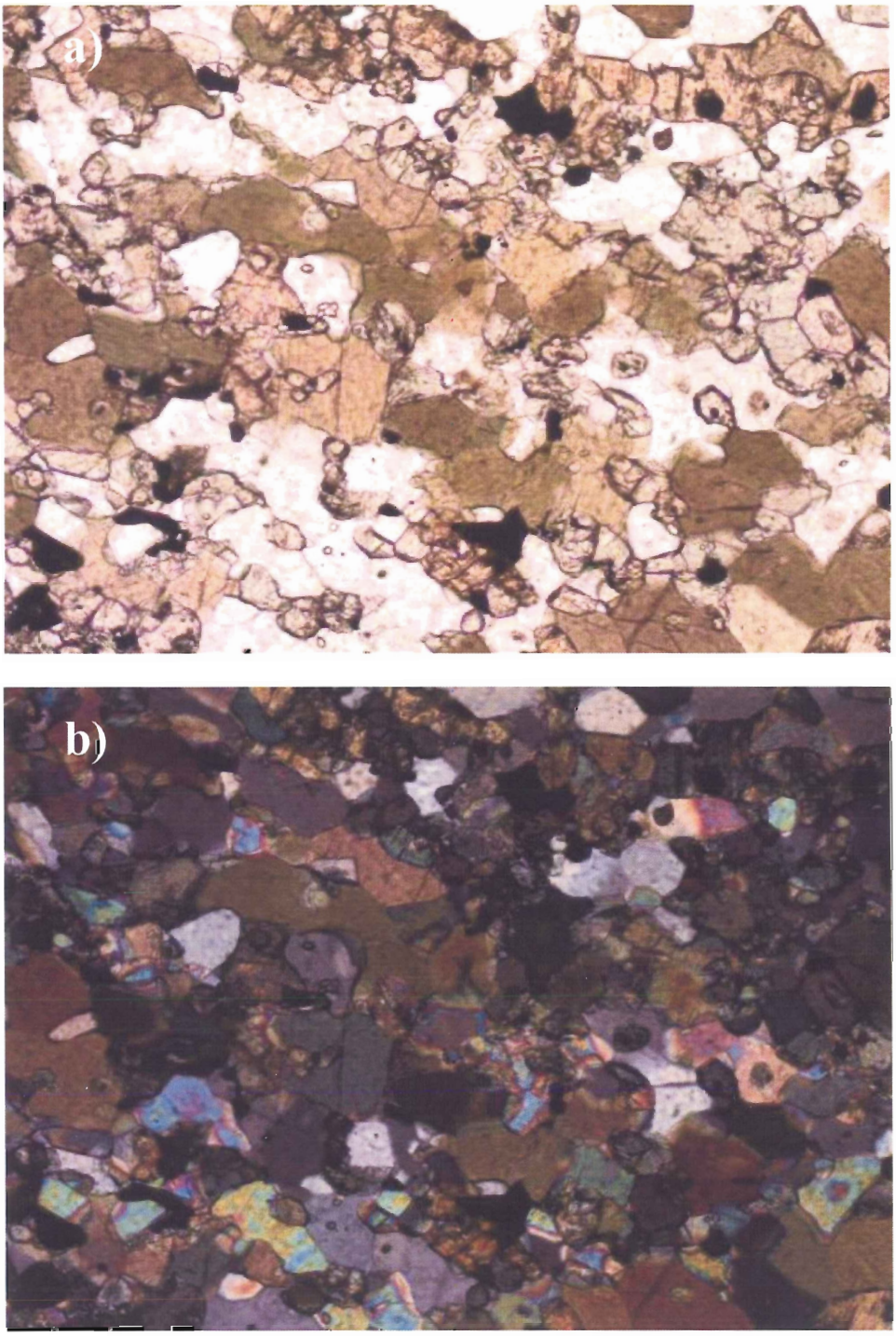

Figure 3.5: Sample NA020B. Northern Kiosk domain shear zone banded granulite gneiss containing hornblende, cpx, garnet, plagioclase, and scapolite (colourless mineral with high birefringence). Note the very fine grain size relative to the amphibolite banded gneiss. **(a)** Plain polarized light (1.25x1.00 mm). **(b)** Cross polarized light (1.25x1.00mm).

3.4 Kiosk domain

The high degree of strain demonstrated by the gneiss of the Kiosk domain complicates the task of identifying and classifying the various lithologies present in the Kiosk domain. At any given outcrop, the various bands of the Kiosk gneiss may represent genetically different protoliths, juxtaposed against each other by the extreme degree of ductile shear experienced by these rocks. For example, at several localities, certain bands of gneiss, which exhibited mineralogy strongly suggestive of a supracrustal origin, were interlayered with bands of unquestionable plutonic origin. Moreover, even when it is clear that a gneissic rock is of plutonic origin, individual bands may suggest genetically different plutonic protoliths (e.g. granitic vs. gabbroic). This lithological variation and complexity on outcrop scale renders the classification of lithology in the Kiosk domain, beyond the general recognition of "Kiosk gneiss" and obvious outliers, difficult on the scale of this study. Therefore, only three simple, first-order divisions of Kiosk domain lithology are recognized and described herein: (1) Kiosk gneiss, (2) mafic enclaves, and (3) supracrustal gneiss. Table 3.2 presents the mineral chemistry of these lithologies.

3.4.1 Kiosk gneiss

A moderate to strongly developed foliation, well developed compositional layering, yellow biscuit to grey colour, and Pl-Qtz-Cpx±Opx±Bt-Grt-Hbl-Sc-Op-Zrn assemblage characterize the granulite facies Kiosk gneiss which is locally migmatitic (Fig 3.6). Felsic layers, composed of medium to fine grained, sub-polygonal plagioclase and quartz, comprise 50-70 vol% of these samples. Mafic minerals, including hornblende, clinopyroxene, orthopyroxene, and garnet, are generally concentrated into subordinate bands which regularly alternate with the felsic layers. In some samples,

Table 3.2: Mineral chemistry of selected Kiosk domain lithologies

Lithology	Mineral	Structural formula*	End-members
Kiosk gneiss	Hornblende	$(Na_{0.37}K_{0.32})(Ca_{1.89}Na_{0.11})(Mg_{2.63}Fe_{1.78}Al_{0.46}Ti_{0.24})(Si_{6.26}Al_{1.74})O_{22}(OH)_2$	N/A
	Garnet	$(Mg_{0.71}Fe_{1.75}Ca_{0.57})Al_{1.96}(Si_{2.98}O_4)$	Grs_{18} Alm_{56} $Prp_{23}Sps_3$
	Orthopyroxene	$(Mg_{1.19}Fe_{0.79})(Si_{1.94}Al_{0.06})O_6$	$En_{60}Fs_{40}$
	Clinopyroxene	$(Ca_{0.90}Na_{0.07})(Mg_{0.71}Fe_{0.29}Al_{0.05})(Si_{1.92}Al_{0.08})O_6$	$Di_{71}Hd_{29}$
	Plagioclase	$Na_{0.64}Ca_{0.32}Al_{1.41}Si_{2.60}O_8$	$Ab_{67}An_{33}$
Mafic enclaves	Hornblende	$(Na_{0.40}K_{0.35})(Ca_{1.91}Na_{0.09})(Mg_{2.76}Fe_{1.48}Al_{0.51}Ti_{0.28})(Si_{6.20}Al_{1.80})O_{22}(OH)_2$	N/A
	Garnet	$(Mg_{0.89}Fe_{1.59}Ca_{0.59})Al_{1.96}(Si_{2.97}O_4)$	Grs_{19} $Alm_{51}Prp_{28}Sps_2$
	Orthopyroxene	$(Mg_{1.25}Fe_{0.71}Al_{0.02})(Si_{1.95}Al_{0.05})O_6$	$En_{64}Fs_{36}$
	Clinopyroxene	$(Ca_{0.90}Na_{0.05})(Mg_{0.75}Fe_{0.25}Al_{0.06})(Si_{1.93}Al_{0.07})O_6$	$Di_{75}Hd_{25}$
	Plagioclase	$Na_{0.59}Ca_{0.37}Al_{1.41}Si_{2.60}O_8$	$Ab_{61}An_{39}$
	Biotite	$(K_{0.91})(Mg_{1.69}Fe_{0.79}Ti_{0.22})(Si_{2.73}Al_{1.30})O_{10}(OH)_2$	$Phl_{68}Ann_{32}$
Corundum bearing supracrustal gneiss	Garnet	$(Mg_{0.68}Fe_{2.19}Ca_{0.18})Al_{1.99}(Si_{2.97}O_4)$	$Grs_6Alm_{71}Prp_{22}Sps_1$
	Plagioclase	$Na_{0.70}Ca_{0.27}Al_{1.31}Si_{2.70}O_8$	$Ab_{72}An_{28}$
	K-feldspar	$K_{0.76}Na_{0.20}Al_{1.06}Si_{2.96}O_8$	$Or_{79}Ab_{21}$
Supracrustal gneiss	Garnet	$(Mg_{0.82}Fe_{1.84}Ca_{0.35})Al_{1.98}(Si_{2.98}O_4)$	$Grs_{11}Alm_{59}Prp_{27}Sps_3$
	Plagioclase	$Na_{0.70}Ca_{0.26}Al_{1.31}Si_{2.70}O_8$	$Ab_{73}An_{27}$
	K-feldspar	$K_{0.81}Na_{0.18}Al_{1.05}Si_{2.95}O_8$	$Or_{81}Ab_{19}$
	Biotite	$(K_{0.90})(Mg_{1.34}Fe_{1.08}Ti_{0.34})(Si_{2.72}Al_{1.33})O_{10}(OH)_2$	$Phl_{56}Ann_{44}$

*Structural formulas after Deer et al. (1996)

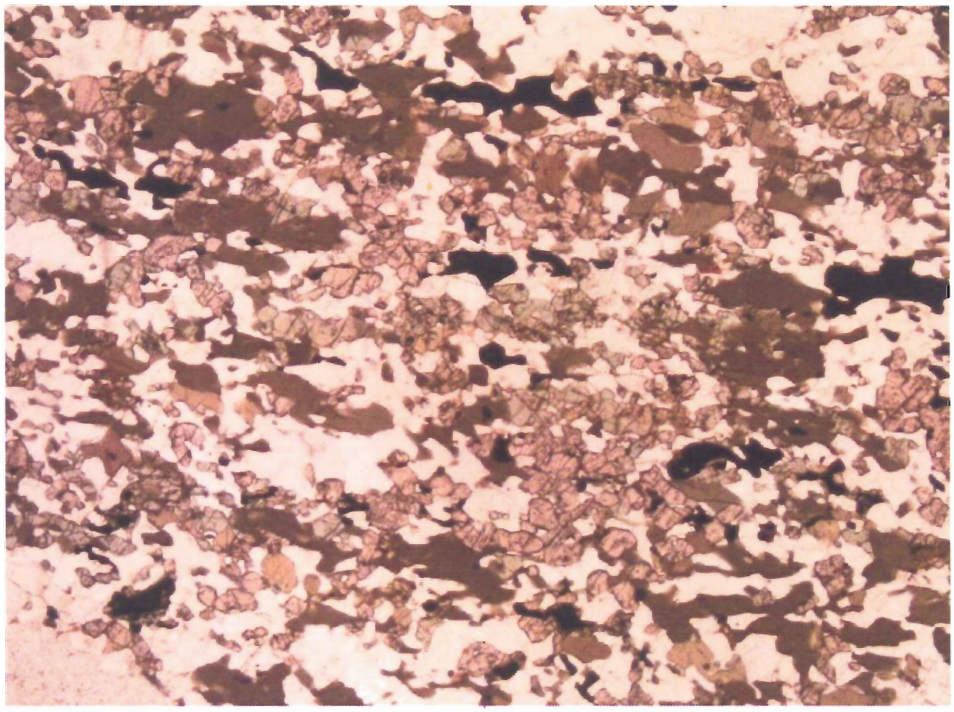

Figure 3.6: Sample NA023A. Kiosk gneiss with a moderately foliated, well equilibrated fine-grained matrix of pink garnet, pale green clinopyroxene, brown to olive green hornblende, plagioclase, and minor quartz (6.25x5.00 mm).

patches of mafic minerals are present in the felsic layers. Olive green hornblende dominates the mafic bands and can rarely be observed being overgrown by pale green clinopyroxene. Biotite is relatively rare in these samples and is likely late; where present, it is typically dark brown in colour and can be found growing through hornblende crystals perpendicular to the foliation direction. In migmatitic samples of the Kiosk gneiss, bands of perthitic K-feldspar-porphyroclast bearing leucosomes, set in a fine to medium subpolygonal matrix of plagioclase and quartz, are present within the gneissic layering.

Textures displayed by these samples are somewhat variable and depend upon the amount of strain experienced by the rock. In particular, some finer grained samples demonstrate a strong L=S fabric (Fig 3.7), defined by the preferred orientation of matrix minerals, akin to that observed along the northern Kiosk shear zone, while others demonstrate a notably weaker version of this fabric. In the highly strained samples, many garnet porphyroblasts appear disaggregated and strung out along the foliation plane with quartz, biotite, and hornblende growing around the garnet grain. These deformed garnets, in many cases, have been reduced to irregular granular masses which bear little resemblance to the six to eight sided, idioblastic structure of the intact garnet porphyroblasts. Samples are generally uniformly fine-grained and, except for minor replacement of hornblende by clinopyroxene, appear to be in textural equilibrium.

3.4.2 Mafic enclaves

Subordinate enclaves of medium- to fine-grained mafic granulite (Pl-Hbl-Grt-Cpx-Opx-Qtz-Bt-Op-Zrn±Ttn±Ap) are found throughout the Kiosk domain as lenses within the Kiosk gneiss. These mafic lenses are commonly garnetiferous with colourless to light pink poikiloblastic garnet porphyroblasts set in a sub-polygonal matrix of

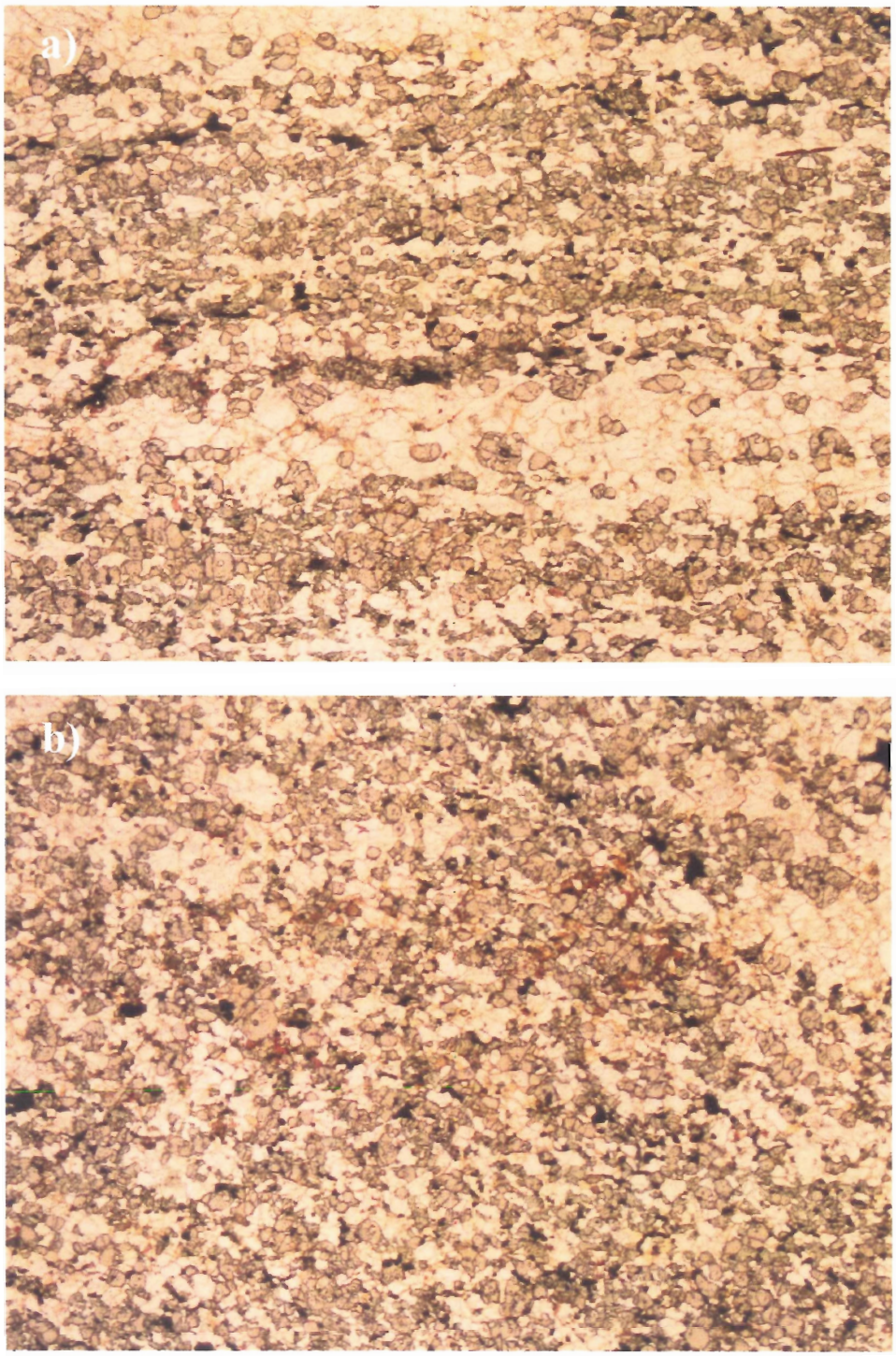

Figure 3.7: Sample NA027B. Kiosk gneiss with well foliated, well lineated L=S fabric. **(a)** Photomicrograph taken perpendicular to foliation (6.25x5.00 mm). **(b)** Photomicrograph taken perpendicular to lineation (6.25x5.00 mm).

medium- to fine-grained plagioclase, olive-green to brown hornblende, dark-brown biotite, and colourless to pale green clinopyroxene (Fig 3.8a). Garnet porphyroblasts have abundant inclusions of plagioclase, quartz, zircon, and, in some samples, clinopyroxene; inclusions show no variation in mineral chemistry compared to matrix counterparts. All grains are in mutual contact with no obvious reaction textures observed along grain boundaries.

Most samples of the mafic enclaves are poorly foliated relative to the Kiosk gneiss. In particular, biotite and hornblende grains, which are strongly aligned in the Kiosk gneiss, display only a moderate preferred orientation. Additionally, garnet porphyroblasts display a relatively intact, subhedral grain structure (Fig 3.8a), in contrast to the strained, disaggregated and recrystallized garnets of the Kiosk gneiss. These mafic enclaves are morphologically diverse; their shape can vary greatly, depending on the degree deformation experienced.

It is important to note that, while most samples of Kiosk mafic enclaves are characterized by the mineralogical and textural properties described above, several mineralogically and texturally anomalous mafic enclaves were identified within the Kiosk domain. Most notably, several enclaves from a locality north of Rosebary Lake (NA061) contain coarse, colourless orthopyroxene porphyroblasts (up to 3cm long axis) rimmed by fine grained, colourless to pale green clinopyroxene (Fig 3.8b). In the CGB, only anorthosites are known to contain orthopyroxene porphyroblasts of this size (R. Jamieson 2008, personal communication). The matrix of these samples contain fine grained, strongly foliated, granular garnet, pale green clinopyroxene, dark-brown mica, and plagioclase layered with K-feldspar and quartz rich leucosomes.

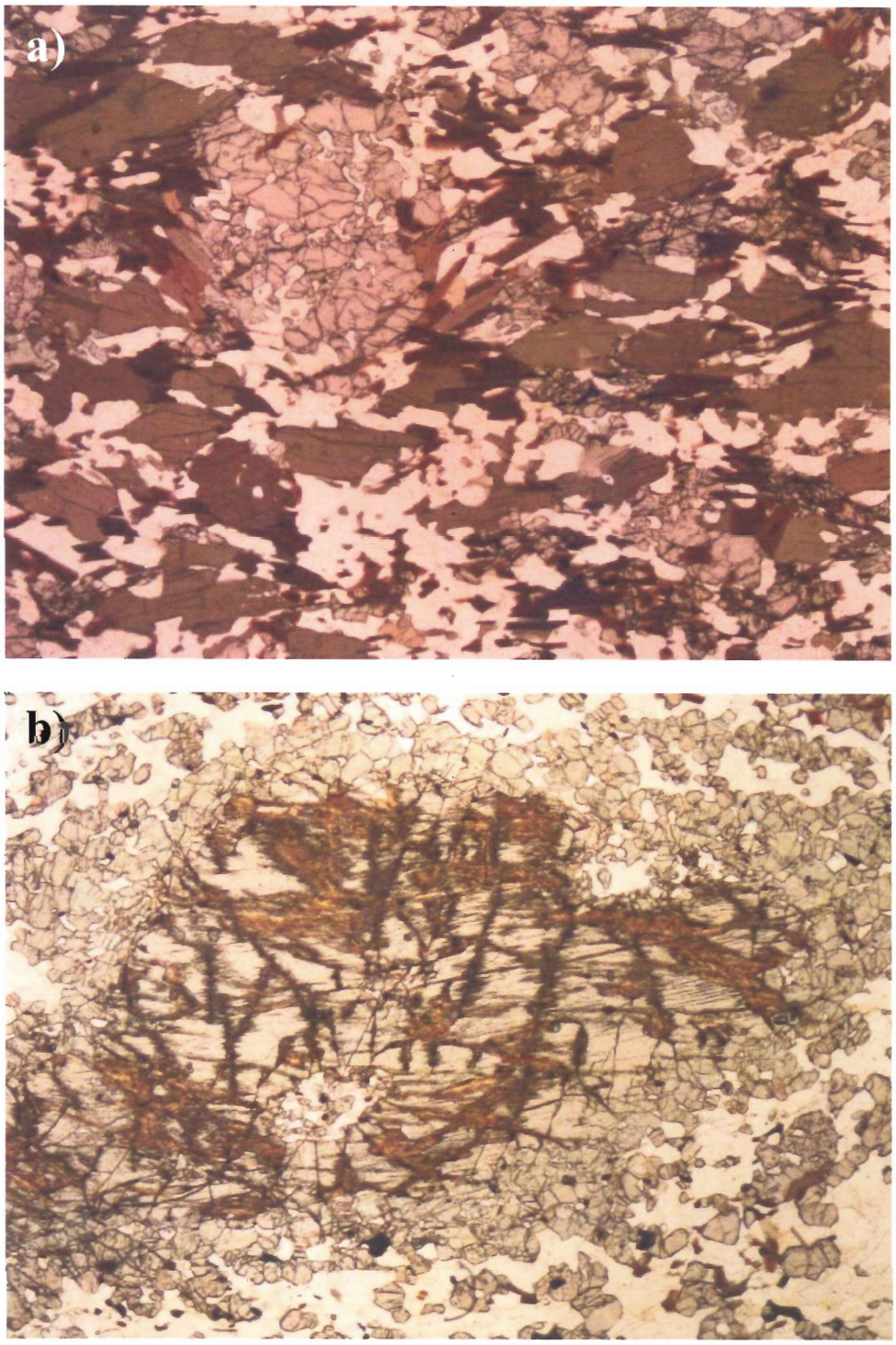

Figure 3.8: (a) Sample NA061E. Garnetiferous mafic enclave containing poikiloblastic garnet porphyroblasts set in a medium-grained matrix of olive-green hornblende and late, brown to red biotite (6.25x5.00 mm). **(b)** Sample NA061A. orthopyroxene porphyroclast bearing mafic enclave containing large Opx porphyroclasts rimmed by fine-grained clinopyroxene and garnet (6.25x5.00 mm).

3.4.3 Supracrustal Gneiss

A number of samples of predominantly quartzofeldspathic Kiosk gneiss, containing aluminous minerals indicative of a supracrustal protolith, were identified north of Rosebary Lake (NA061). Specifically, a pink to grey, fine-grained, leucocratic, strongly foliated gneiss containing corundum porphyroblasts (Fig 3.9a) and the assemblage Kfs-Pl-Grt-Crn-Bt-Op-Spl characterize these samples. Corundum porphyroblasts, ranging from coarse- to fine-grained, are commonly rimmed by garnet and plagioclase. In some samples, the garnet rims are thicker than the corundum grains themselves. Garnet is also found as prophyroblasts (Fig 3.9b) with inclusions of corundum, plagioclase, opaque minerals, and spinel. The matrix of these samples is generally 70-90% felsic and is predominantly composed of medium to fine-grained, polygonal, perthitic K-feldspar and subordinate plagioclase; quartz is either absent or rare in these samples and is usually only found in salmon-pink coloured leucocratic layers. Late, dark ruby-red biotite is usually present in association with garnet rich layers, although some grains are found randomly distributed in the felsic matrix.

Texturally, these samples are similar to the rest of the Kiosk gneiss in that they are generally very strongly foliated and lineated. In particular, garnet porphyroblasts appear fragmented and take on a very unusual elongated banded structure aligned with the foliation plane (Fig 3.9b). Clusters of fine grained, granular corundum and garnet may, in places, represent the fragmented remnants of porphyroblasts. These samples show evidence of grain size reduction in the matrix and dynamic recrystalization of garnet porphyroblasts.

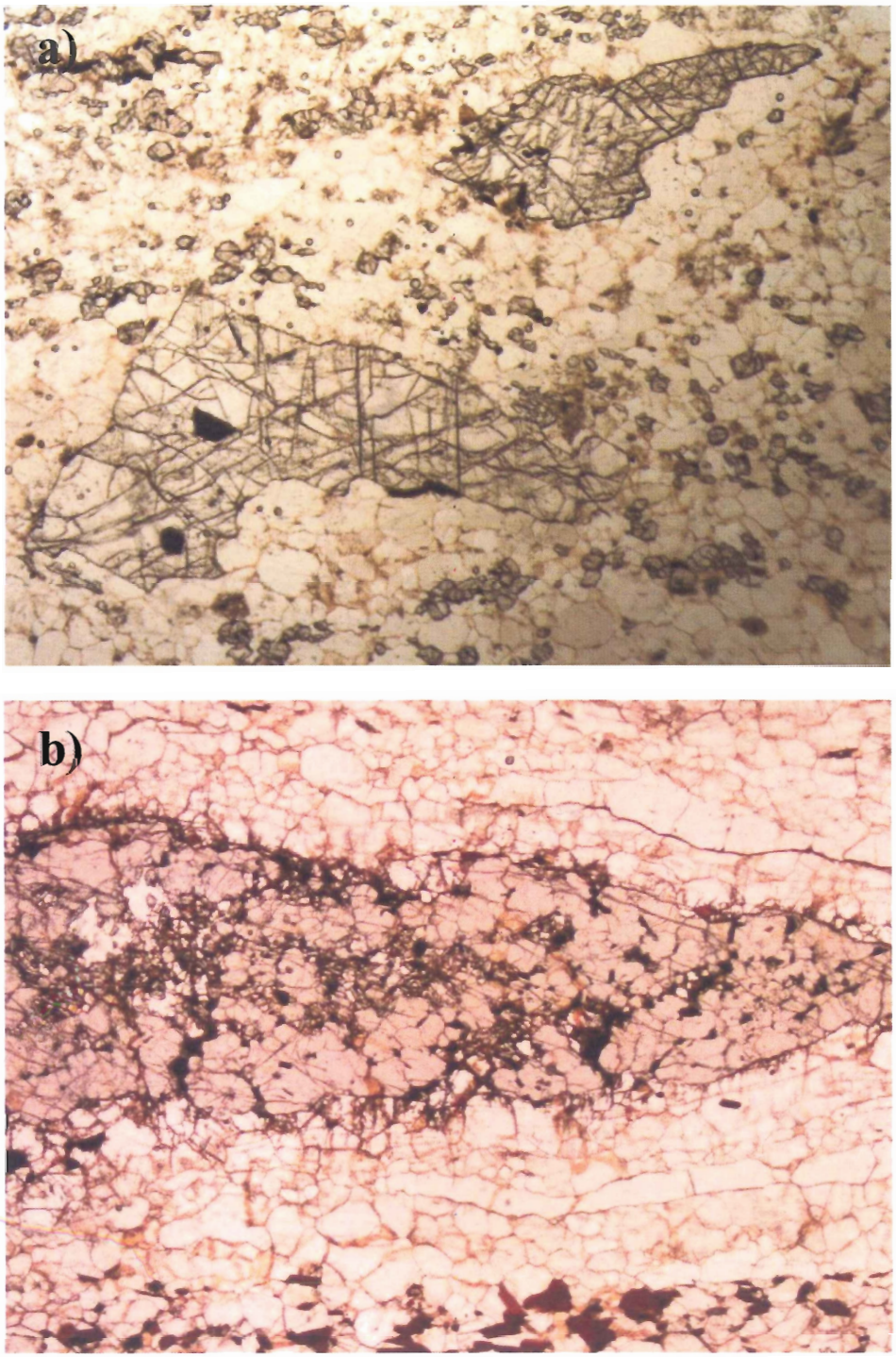

Figure 3.9: Kiosk supracrustal gneiss at NA061. **(a)** Sample NA061C. Corundum porphyroblasts set in a garnetiferous, felsic rich matrix devoid of quartz (6.25x5.00 mm). **(b)** Sample NA061F. Deformed garnet porphyroblast with very fine grained inclusions of spinel, corundum, ilmenite, plagioclase (6.25x5.00 mm).

3.5 Southern Kiosk domain shear zone

A notable change in metamorphic grade and lithology occurs in the southernmost portion of the Kiosk domain in the area of Misty Lake (NA054). Specifically, the Kiosk gneiss, the light-pink to grey, felsic to intermediate granulite, gives way to a mafic rich, banded amphibolite. Another interesting observation is the abundance of pegmatites in this region. Only one distinct lithology identified within this shear zone, the mafic amphibolites, is described herein; however, it should be noted that other lithologies, notably local felsic enclaves, are found along the shear zone.

3.5.1 Mafic amphibolite

The assemblage Hbl-Pl-Qtz-Bt-Op-Tnt±Zn characterises the mafic amphibolite of the southern Kiosk shear zone (Fig 3.10a). Mafic minerals, including blue to turquoise, medium- grained hornblende and pale brown to beige, medium- to fine-grained biotite, comprise 50-60% of these samples and are concentrated into bands alternating with plagioclase rich layers. Texturally, all phases are in mutual contact with each other and display no obvious reaction textures. A strong foliation, notably defined by the preferred orientation of hornblende and biotite grains, is present in these samples; however, the grain size reduction noted at the northern Kiosk shear zone is not present in these samples.

3.6 North-central Algonquin domain

The transition from the southern Kiosk domain shear zone to the Algonquin domain is marked by the return to granulite facies. Lithologically, the north-central Algonquin domain is complex with various small granitoid bodies set in a matrix of intermediate Algonquin gneiss containing mafic enclaves. This study does not attempt to

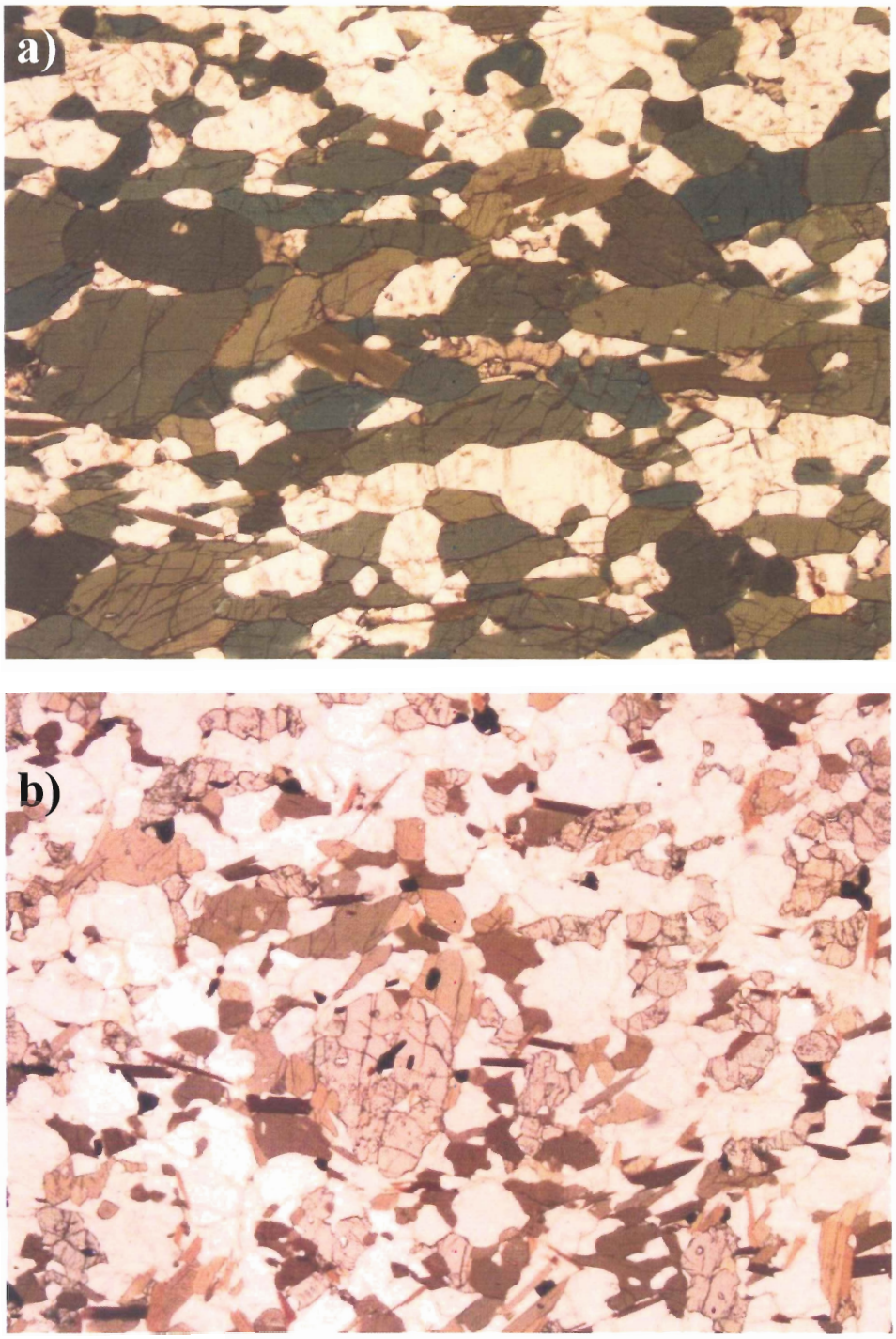

Figure 3.10: Photomicrograph of **(a)** mafic amphibolite of the southern kiosk shear zone (NA054B) and **(b)** north-central Algonquin domain gneiss (NA046). **(a)** Strongly foliated blue-green hornblende and light brown biotite; note difference in hornblende colour and coarseness of grain size compared to northern Kiosk shear zone (Fig. 3.4) (6.25x5.00 mm). **(b)** Pink, poikiloblastic garnet porphyroblasts set in a weakly foliated matrix of biotite, clinopyroxene, and plagioclase; note the strong contrast in foliation strength between this sample and samples from the Kiosk domain (6.25x5.00 mm).

describe or classify the granitoid bodies of the north-central Algonquin domain. Table 3.3 presents mineral chemical data for the Algonquin gneiss.

3.6.1 North-central Algonquin gneiss

Light pink to grey colour, weak foliation, medium grain size, equigranular texture, and a Pl-Qtz-Hbl-Grt-Opx-Cpx-Op-Zn±Tnt assemblage characterize this gneiss. Olive-green to light brown hornblende, colourless to light-pink poikiloblastic garnet, light green clinopyroxene, colourless orthopyroxene and plagioclase dominate the mafic layers of this gneiss (Fig 3.10b); felsic layers contain plagioclase with lesser amounts of dark brown biotite, quartz and minor ganret. All grains, with the exception of minor overgrowth of hornblende by biotite, appear to be in textural equilibrium.

A medium grain size and weakly foliated fabric differentiates this gneiss from the fine- to very fine-grained, highly strained fabric of the Kiosk domain; there is little evidence, either in thin section or in the field, of the L=S fabric which dominates samples of the Kiosk domain. Additionally, these samples are lithologically different from Kiosk domain samples. In particular, the mafic Algonquin gneiss contains orthopyroxene in near equal proportions to clinopyroxene; in contrast, clinopyroxene dominates Kiosk domain granulites, with only a few samples containing significant proportions of orthopyroxene, which suggest a different bulk composition.

Table 3.3: Mineral chemistry of the Algonquin gneiss

Lithology	Mineral	Structural formula*	End-members
Algonquin gneiss	Hornblende	$(Na_{0.42}K_{0.34})Ca_{1.90}(Mg_{2.30}Fe_{1.96}Al_{0.49}Ti_{0.28})(Si_{6.27}Al_{1.73})O_{22}(OH)_2$	N/A
	Garnet	$(Mg_{0.58}Fe_{1.85}Ca_{0.59})Al_{1.96}(Si_{2.97}O_4)$	Grs_{19} $Alm_{60}Prp_{19}Sps_2$
	Orthopyroxene	$(Mg_{1.09}Fe_{0.88})(Si_{1.96}Al_{0.04})O_6$	$En_{55}Fs_{45}$
	Clinopyroxene	$(Ca_{0.91}Na_{0.04})(Mg_{0.70}Fe_{0.33}Al_{0.03})(Si_{1.94}Al_{0.06})O_6$	$Di_{68}Hd_{32}$
	Plagioclase	$Na_{0.59}Ca_{0.38}Al_{1.41}Si_{2.60}O_8$	$Ab_{60}An_{40}$
	Biotite	$(K_{0.92})(Mg_{1.36}Fe_{1.09}Ti_{0.34})(Si_{2.73}Al_{1.30})O_{10}(OH)_2$	Phl_{55} Ann_{45}

*Structural formulas after Deer et al. (1996)

CHAPTER 4: THERMOBAROMETRY

4.1 General Statement

Elucidating the metamorphic history of the Kiosk domain is paramount to better understanding the tectonic evolution of southwestern Grenville Province and, in particular, the tectonic processes which gave rise to the anomalous structures preserved within the domain. Using a suite of thermodynamically modelled, experimentally calibrated thermobarometers to assess the pressure (P) and temperature (T) conditions represented by specific mineral assemblages, this chapter aims to determine the peak metamorphic conditions experienced by the rocks in the Kiosk domain and, for comparison, the Algonquin domain. The constraint of metamorphic conditions in the study area subsequently allows for the validity of various tectonic models of the western Grenville orogen to be tested in the context of the Kiosk and Algonquin domain geology.

The objectives of this section are: (1) outline the principles and methods used by this study to determine P-T estimates (2) discuss known errors and uncertainties associated with these methods, (3) present peak P-T estimates for the Kiosk and Algonquin domains, and (4) examine similarities and differences between the estimated peak P-T conditions of the Kiosk and Algonquin domains and different assemblages contained therein.

4.2 Principles

Metabasite and metapelite rocks commonly contain minerals which are only stable within a limited range of P-T conditions (Spear 1995). Petrographic analysis of these rocks can therefore be used to qualitatively assess the metamorphic history of the area in which they are contained. However, large uncertainties associated with qualitative

thermobarometric methods can limit their ability to yield geologically useful information. For example, the presence of metamorphic pyroxenes in a mineral assemblage indicates that the assemblage equilibrated at P-T conditions at or above granulite facies but does not provide further constraint within this broad P-T range; one has no way on knowing whether the mineral assemblage equilibrated at 800 °C or 1000 °C. Thus, if thermobarometric analysis is to be effectively applied to understanding the tectonometamorphic evolution of a package of uniformly high grade rocks (e.g. the CGB), a quantitative method of analysis is needed.

Given that the composition of minerals in an equilibrated assemblage is thermodynamically governed by the equilibrium P-T conditions, it is possible to calculate the P-T conditions under which a certain assemblage reached chemical equilibrium. This calculation requires several variables, including the chemical compositions of all solid solution phases and thermodynamic data (e.g. entropy, enthalpy, volume) for all phases of interest, to be known. With these variables precisely constrained, a variety of experimentally calibrated, net-transfer, P dependant reactions (termed barometers herein; e.g. Ghent 1976) and T dependent exchange reactions (termed thermometers herein; e.g. Ferry and Spear 1978) can be used to solve for P and T respectively, assuming the required phases are present in the assemblage in question.

4.3 Methods

This study employs the TWEEQU (Thermobarometry With Estimation of EQUuilibrium state) method of Berman (1991) to calculate P-T conditions under which specific mineral assemblages equilibrated. TWEEQU calculates reactions using the TWQ computer program which uses the internally consistent thermodynamic dataset of

Berman (1988). The greatest advantage of this method is that, by employing a thermodynamically consistent dataset, errors associated with using separately calibrated thermobarometers are eliminated. For example, if the commonly used garnet-Al_2SiO_5-plagioclase-quartz barometer calibration of Ghent (1976) is combined with the equally prevalent garnet-biotite thermometer calibration of Ferry and Spear (1978) to determine P-T conditions, the resulting P-T calculation will be inaccurate because the calibrations rely on inconsistent thermodynamic data. Conversely, using the TWEEQU method, all reactions are calculated using the single, internally consistent, thermodynamically calibrated database; the resulting P-T calculations are free of intercalibration errors.

TWQ plots equilibrium reactions as lines on P vs. T diagrams (e.g. Fig. 4.2). As it is inferred that reaction lines represent equilibrium between reactant and products, the intersection of these lines can be interpreted as defining the P-T conditions of equilibrium. If the assemblage in question is well equilibrated, multiple reaction lines should yield one, precise intersection; conversely, a poorly equilibrated assemblage will yield a set of non-coincident intersections. Thus, not only can TWQ be used to calculate the P-T conditions under which an assemblage equilibrated, it can also evaluate the degree of equilibration in the mineral composition from which the reactions are calculated.

Several updated versions of TWQ have been developed since the program's 1992 debut (TWQ v. 1) to include new and revised activity models for solid solutions and thermodynamic data. Most notably, major updates to the database were released in 1996 (TWQ v. 2.02) and 2006 (TWQ v. 2.32). Although the new versions of TWQ incorporate new experimental data produced since the release of the original (TWQ v. 1), the newer

versions do not include thermodynamic properties of amphibolites. Therefore, if thermobarometry calculations are to be carried on equilibria involving amphibole, the database from TWQ v.1 must be used.

Depending on the lithology in question, this study employs different versions of the TWQ database in thermobarometric analysis. In particular, the presence of hornblende in the equilibrium assemblage of both the Kiosk and Algonquin gneiss requires the use of the TWQ v.1 database. Conversely, the amphibole-free assemblage of the Kiosk supracrustal gneiss permits the use of the most recent TWQ v. 2.32 database.

4.4 Potential error sources and uncertainties

Although the thermobarometric methods employed here are quantitative, it is important to note that, as with all thermobarometric methods, the resulting P-T estimates are subject to considerable uncertainties. These uncertainties stem from: (1) inaccuracies in the thermodynamic database, notably including inaccuracies in mineral thermodynamic properties and mineral activity models; (2) extrapolation of experimental thermometer/barometer calibrations to the P-T range of interest; (3) errors related to microprobe analysis (standard errors listed in Appendix C); and (4) geological errors involving heterogeneities in mineral composition and unrecognized disequilibrium in an assemblage. All of these uncertainties affect the precision and accuracy of a P-T estimate.

A quantitative assessment of uncertainties is beyond the scope of this study (cf. Essene, 1989, for review and discussion); nonetheless, it is important to recognize their influence on P-T calculations. In particular, the accuracy of activity-composition (a-X) relationships is of concern in this study because P-T calculations are carried out on assemblages that contain phases for which the activity model is not agreed upon (e.g.

amphibole) or the activity of the phase is unclear (e.g. H_2O). The issue of the activity of H_2O is addressed in Section 4.8.

It should be noted that error ranges reported in TWQ calculations (Fig. 4.1) only account for the imprecision of reaction intersections in P-T space; TWQ does not quantify errors resulting from inaccuracies in the thermodynamic database and thus the error ranges reported here are underestimated. It is possible to quantify, through rigorous statistical methods, the propagation of errors arising from such inaccuracies (e.g. Hodges and McKenna 1987). Such an undertaking, however, is beyond the scope of this study and therefore the standard errors of ± 50 °C and ± 1 kbar are assumed. The interested reader is referred to the studies of Powell and Holland (1988, 1994), Holland and Powell (1998), and Worley and Powell (2000) for further discussion.

4.5 Peak P-T conditions in the Kiosk domain

The peak P-T conditions recorded by the Kiosk gneiss, mafic enclaves, and supracrustal gneiss of the Kiosk domain are reported in Figure 4.1. These lithologies were chosen for P-T analysis because they contain mineral assemblages well suited to thermobarometry. Furthermore, given that these lithologies contain contrasting mineral assemblages, they provide independent records of the metamorphic history of the Kiosk domain. The following subsections briefly explain how the reported P-T estimates were obtained from the three lithologies.

4.5.1 Kiosk gneiss

A sample of Kiosk gneiss from Craig Lake (NA023), containing the equilibrium assemblage of Pl-Cpx-Opx-Hbl-Grt, was selected for P-T analysis based on its homogenously fine-grained, sub-polygonal, recrystallized texture, which is strongly

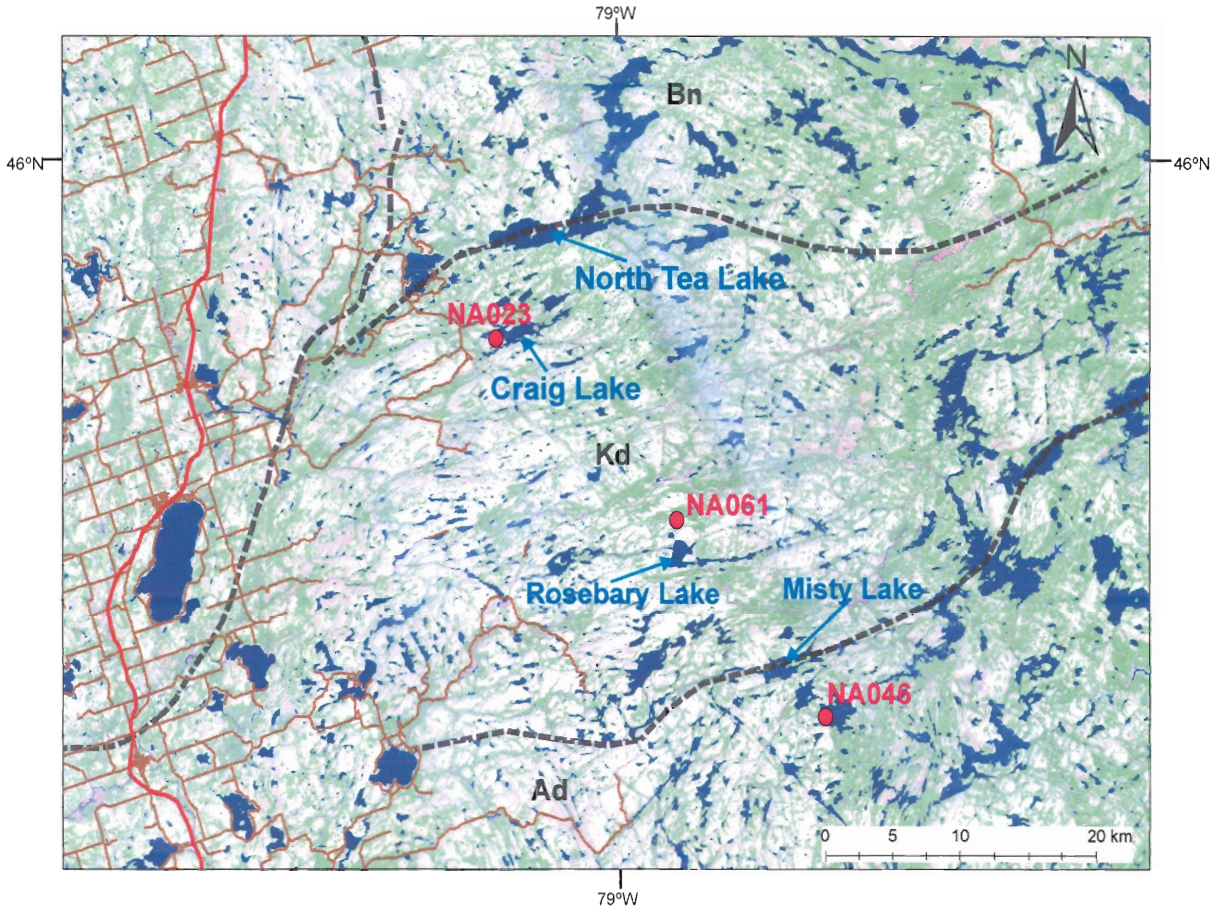

Domain	Rock type	Sample number	Equilibrium assemblage*	P-T result
Kiosk domain	Kiosk gneiss	NA023A	Pl-Cpx-Opx-Hbl-Grt	14.0 ± 0.04 kbar 813 ± 2 °C
	Mafic enclave	NA061E	Pl-Grt-Cpx-Opx-Hbl	14.2 ± 0.3 kbar 823 ± 21 °C
	Supracrustal gneiss	NA061F	Pl-(Kfs)-Crn-Grt-Spl	14.1 kbar 1000 °C
Algonquin domain	Algonquin gneiss	NA046	Pl-Grt-Opx-Cpx-Hbl	12.4 ± 0.2 kbar 805 ± 17 °C

* Parentheses indicate that phase was not used in TWQ calculations

Figure 4.1: Thermobarometry results from the Kiosk domain (KD) and Algonquin domain (AD). Sample numbers correspond to station locations shown on map. Station coordinates are listed in Appendix B. Mineral abbreviations listed in Appendix A. Dashed black lines are domain boundaries. Major roads are shown in red and minor roads in brown. See text for further discussion.

indicative of equilibration during Grenvillian metamorphism. No systematic variation in mineral composition was observed within this sample; therefore, the average composition of each phase in the equilibrium assemblage was used in TWQ calculations. The resulting TWQ estimate of equilibrium P-T conditions is 14.0 ± 0.04 kbar and 813 ± 2 °C based on a well defined intersection of three independent reactions (Fig. 4.2).

4.5.2 Mafic enclaves

A garnetiferous mafic enclave from a locality north of Rosebary Lake (NA061) with the equilibrium assemblage Pl-Grt-Cpx-Opx-Hbl provided a second P-T estimate for the Kiosk domain. This sample shows no significant variation in mineral composition and, with the exception of late biotite, displays equilibrium textures. TWQ calculations of equilibrium P-T conditions, employing average compositions of each phase in the equilibrium assemblage, yields an estimate of 14.2 ± 0.3 kbar and 823 ± 21 °C based on a moderately well defined intersection of three independent reactions (Fig. 4.3).

4.5.3 Supracrustal gneiss

A sample of supracrustal gneiss from NA061, bearing the equilibrium assemblage Pl-Kfs-Crn-Grt-Spl, provided a third, questionable, P-T estimate for the Kiosk domain. This peculiar, anhydrous, Al_2SiO_5-absent aluminous assemblage yields a TWQ estimate of approximately 14.1 kbar and 1000 °C (Fig. 4.4). An error estimation was not obtainable in TWQ for this sample because, having only 2 independent reactions, the resulting intersection is infinitely precise.

In addition to having only 2 independent reactions, other uncertainties are involved with this estimate. For example, when ilmenite and rutile, which are present in

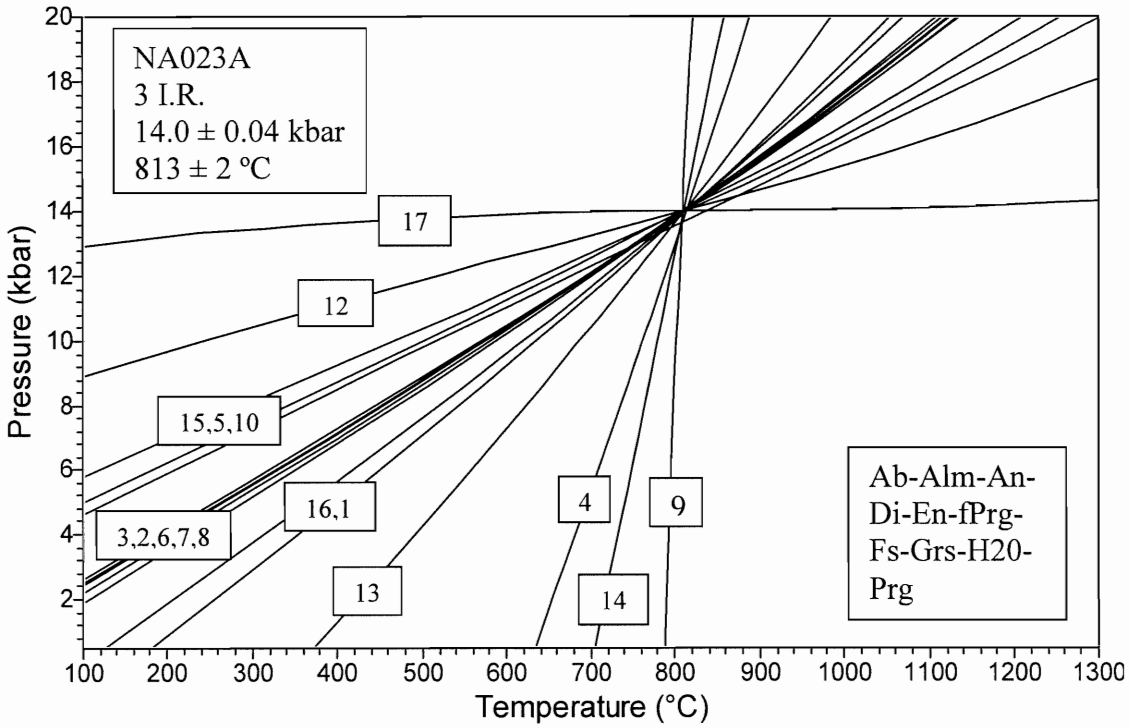

Number	Reaction
1	2Ab+8Alm+10Di+2H2O=2fPrg+8Fs+5En+6An
2	6Ab+14Alm+10Grs+6H2O=6fPrg+9Fs+18An
3	fPrg+20Di+16Alm+4Ab+4H2O=12An+26Fs+5Prg
4	2Alm+6Di=2Grs+3Fs+3En
5	6Ab+8Alm+9En+16Grs+6H2O=6fPrg+18Di+18An
6	9Prg+52Grs+44Alm+24Ab+24H2O=72An+36Di+33fPrg
7	4Ab+22Fs+16Grs+7Prg+4H2O=11fPrg+28Di+12An
8	2Ab+8Alm+10Di+2H2O=2Prg+12Fs+En+6An
9	Prg+2Fs=2En+fPrg
10	3fPrg+12Di+4Alm=12Fs+4Grs+3Prg
11	2Grs+24Di+22Alm+6Ab+6H2O=18An+33Fs+6Prg
12	8Grs+4Fs+7En+2Ab+2H2O=6An+14Di+2fPrg
13	4Prg+10Di+8Alm+2Ab+2H20=6An+13En+6fPrg
14	4Alm+12Di+3Prg=3fPrg+4Grs+12En
15	10Grs+12En+14Alm+6Ab+6H2O=18An+21Fs+6Prg
16	9Prg+20Grs+28Alm+12Ab+12H2O=36An+18Di+21fPrg
17	2Ab+11En+8Grs+2H2O=2Prg+14Di+6An

Figure 4.2: TWQ equilibrium diagram of Kiosk gneiss (calculated using TWQ version 1 database). Box in lower right of diagram lists components included in the diagram calculation. See text for further discussion of component selection. Mineral abbreviations are listed in Appendix A. I.R. stands for Independent Reactions.

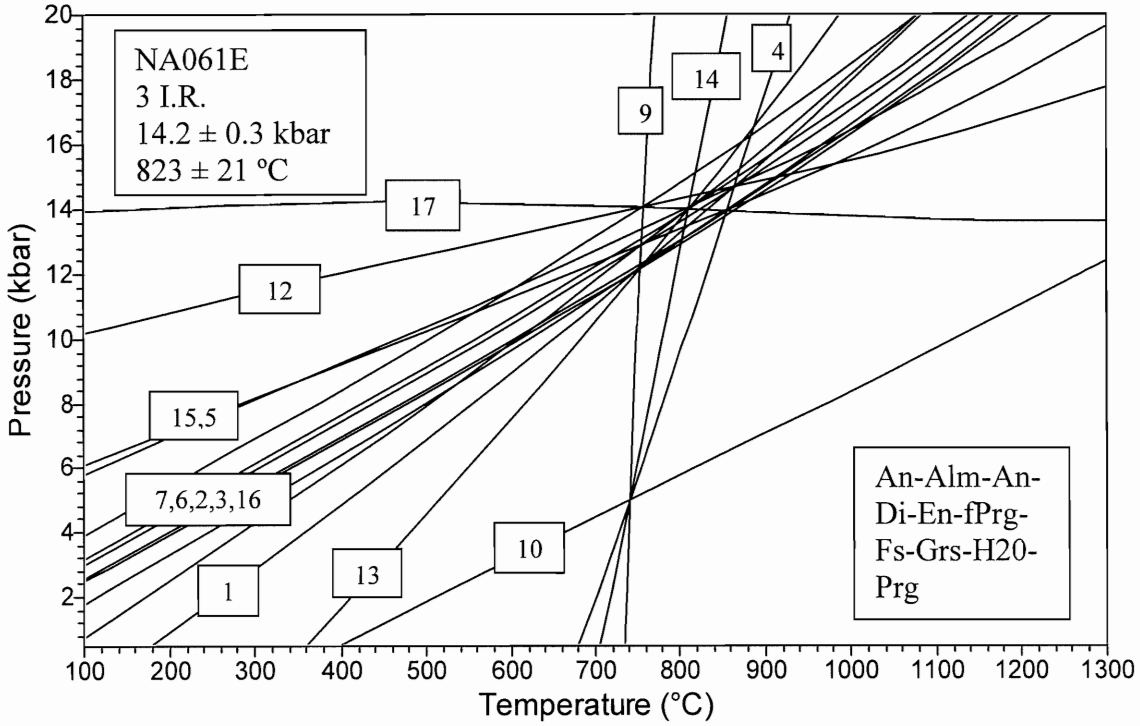

Number	Reaction
1	2Ab+8Alm+10Di+2H2O=2fPrg+8Fs+5En+6An
2	6Ab+14Alm+10Grs+6H2O=6fPrg+9Fs+18An
3	fPrg+20Di+16Alm+4Ab+4H2O=12An+26Fs+5Prg
4	2Alm+6Di=2Grs+3Fs+3En
5	6Ab+8Alm+9En+16Grs+6H2O=6fPrg+18Di+18An
6	9Prg+52Grs+44Alm+24Ab+24H2O=72An+36Di+33fPrg
7	4Ab+22Fs+16Grs+7Prg+4H2O=11fPrg+28Di+12An
8	2Ab+8Alm+10Di+2H2O=2Prg+12Fs+En+6An
9	Prg+2Fs=2En+fPrg
10	3fPrg+12Di+4Alm=12Fs+4Grs+3Prg
11	2Grs+24Di+22Alm+6Ab+6H2O=18An+33Fs+6Prg
12	8Grs+4Fs+7En+2Ab+2H2O=6An+14Di+2fPrg
13	4Prg+10Di+8Alm+2Ab+2H20=6An+13En+6fPrg
14	4Alm+12Di+3Prg=3fPrg+4Grs+12En
15	10Grs+12En+14Alm+6Ab+6H2O=18An+21Fs+6Prg
16	9Prg+20Grs+28Alm+12Ab+12H2O=36An+18Di+21fPrg
17	2Ab+11En+8Grs+2H2O=2Prg+14Di+6An

Figure 4.3: TWQ equilibrium diagram of Kiosk mafic enclaves (calculated using TWQ version 1 database). Box in lower right of diagram lists components included in the diagram calculation. See text for further discussion of component selection. Mineral abbreviations are listed in Appendix A. I.R. stands for Independent Reactions.

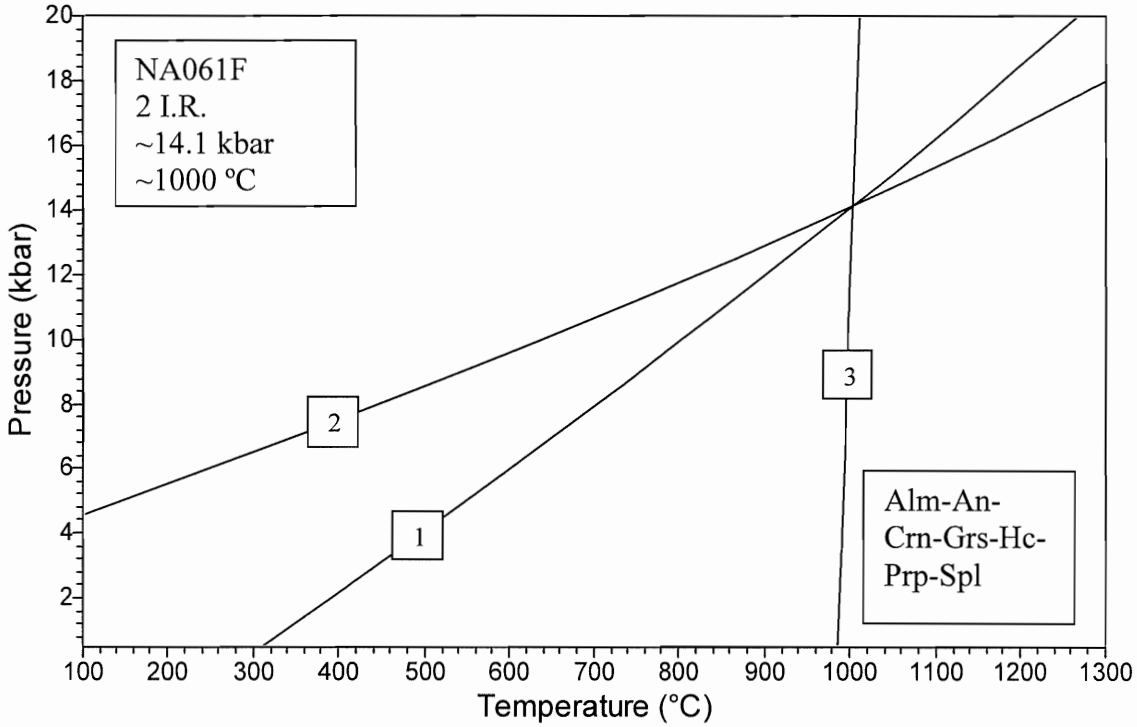

Number	Reaction
1	Grs+4Crn+Alm=3An+3Hc
2	3Spl+Alm+10Grs=3Hc+9Prp
3	Prp+Grs+4Crn=3An+3Spl

Figure 4.4: TWQ equilibrium diagram of Kiosk supracrustal gneiss (calculated using TWQ version 2.32 database). Box in lower right of diagram lists components included in the diagram calculation. See text for further discussion of component selection. Mineral abbreviations are listed in Appendix A. I.R. stands for Independent Reactions.

small quantities and texturally appear to be part of the equilibrium assemblage, are included in TWQ calculations several anomalously high P-T intersections (e.g. 16 kbar, 1200 °C; 20 kbar, 1300 °C) are obtained. Furthermore, when biotite, which is present as a texturally late phase in this sample, is included in the TWQ calculations several anomalously high P (~18 kbar; 20 kbar) intersections are obtained. Thus, the addition a third independent reaction, either by including ilmenite/rutile or biotite in the assemblage, does not support the 14.1 kbar and 1000 °C estimate. However, the 14.1 kbar and 1000 °C estimate is geologically reasonable and consistent with those obtained from Kiosk domain metabasite rocks; thus, the TWQ results suggest that these other phases are not in equilibrium with the Pl-Kfs-Crn-Grt-Spl assemblage.

4.6 Peak P-T conditions in the north-central Algonquin domain

The tectonometamorphic history of the Algonquin domain is better constrained than that of the Kiosk domain. In particular, several workers (e.g. Timmermann 1998; Anovitz and Essene 1990) presented P-T estimates for the Algonquin domain based on thermobarometric work completed on rocks in the southern portion of the domain. This study conducts P-T analysis on a sample of country gneiss from the north-central Algonquin domain in order to compare P-T conditions within the two domains and compare P-T results produced by this study with those of previous workers.

4.6.1 North-central Algonquin domain country gneiss

A sample of north-central Algonquin domain gneiss bearing the equilibrium assemblage Pl-Grt-Opx-Cpx-Hbl was selected for P-T analysis based on its equilibrium textures and homogenous mineral compositions. Using average mineral compositions,

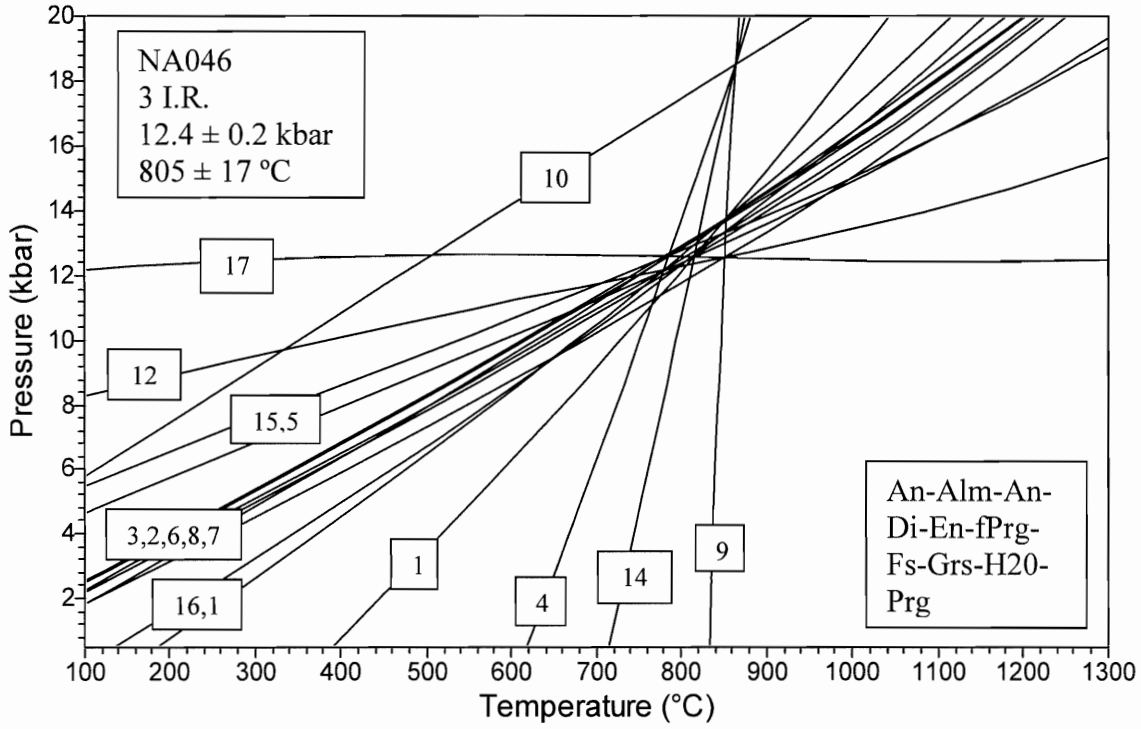

Number	Reaction
1	2Ab+8Alm+10Di+2H2O=2fPrg+8Fs+5En+6An
2	6Ab+14Alm+10Grs+6H2O=6fPrg+9Fs+18An
3	fPrg+20Di+16Alm+4Ab+4H2O=12An+26Fs+5Prg
4	2Alm+6Di=2Grs+3Fs+3En
5	6Ab+8Alm+9En+16Grs+6H2O=6fPrg+18Di+18An
6	9Prg+52Grs+44Alm+24Ab+24H2O=72An+36Di+33fPrg
7	4Ab+22Fs+16Grs+7Prg+4H2O=11fPrg+28Di+12An
8	2Ab+8Alm+10Di+2H2O=2Prg+12Fs+En+6An
9	Prg+2Fs=2En+fPrg
10	3fPrg+12Di+4Alm=12Fs+4Grs+3Prg
11	2Grs+24Di+22Alm+6Ab+6H2O=18An+33Fs+6Prg
12	8Grs+4Fs+7En+2Ab+2H2O=6An+14Di+2fPrg
13	4Prg+10Di+8Alm+2Ab+2H20=6An+13En+6fPrg
14	4Alm+12Di+3Prg=3fPrg+4Grs+12En
15	10Grs+12En+14Alm+6Ab+6H2O=18An+21Fs+6Prg
16	9Prg+20Grs+28Alm+12Ab+12H2O=36An+18Di+21fPrg
17	2Ab+11En+8Grs+2H2O=2Prg+14Di+6An

Figure 4.5: TWQ equilibrium diagram of Algonquin gneiss (calculated using TWQ version 1 database). Box in lower right of diagram lists components included in the diagram calculation. See text for further discussion of component selection. Mineral abbreviations are listed in Appendix A. I.R. stands for Independent Reactions.

TWQ calculations produce a P-T result of 12.4 ± 0.2 kbar and 805 ± 17 ºC based on a moderately well defined intersection of three independent reactions (Fig. 4.5).

4.7 Selection of components in P-T calculations

Obtaining reliable P-T estimations in TWQ is greatly dependant upon proper selection of end-members to be considered in the calculation of a P-T diagram. Ideally, all end-members of the equilibrium assemblage in question would be considered in order to describe the chemical system present at equilibrium. Moreover, including all end-members in reaction calculations ensures that all potential independent reactions are plotted in P-T space, thereby increasing confidence in the resulting P-T estimate. Inaccuracies in the thermodynamic properties of certain end-members, however, can result in the erroneous positioning of reactions in P-T space and ultimately reduce the precision and accuracy of the P-T estimate. Additionally, other factors, such as retrograde Fe-Mg exchange, can also have a significant influence on the positioning of a reaction curve in P-T space. Certain end-members of an assemblage, which can be shown to regularly produce anomalous, outlying reaction curves in P-T space, may therefore be omitted from P-T calculations on the grounds that they do not accurately represent equilibrium P-T conditions.

In this study, Fe end-members of most phases are excluded from TWQ calculations because the thermodynamic data for Fe end-members are generally not as well constrained as Mg end-members. Furthermore, ambiguities exist in the Fe^{3+}/Fe^{2+} ratio of Fe end-members because microprobe analysis does not distinguish between the oxidation states; all iron is considered to be Fe^{2+}. For reactions that depend on Fe^{2+}/Mg exchange, this can result in the incorrect positioning of a reaction in P-T place and thus

influence the accuracy of a P-T estimate (Spear 1995). Although TWQ can calculate Fe^{3+}/Fe^{2+}using stoichiometric normalization, a variety of uncertainties, discussed by Finger (1972), are associated which this calculation; the resulting Fe^{3+} estimates can therefore be inaccurate. Despite these uncertainties, certain Fe end-members (e.g. Fs, Alm) are herein included in the P-T calculations in order to obtain a sufficient number of independent reactions for a P-T estimate.

Pyrope is omitted from the calculation of P-T diagrams because it consistently produces outlying reactions when included in any of the completed TWQ calculations (Fig. 4.6). The considerable number of lower T and P intersections produced by including Pyrope in the calculations is not likely a result of retrograde Fe-Mg exchange as no non-coincidental reactions are produced when Fe end-members (notably Fs and Alm) are included in the calculations. It is possible that anomalous intersections produced by including Pyrope are a result of the mischaracterization of pyrope, potentially caused by a systematic probe calibration error during microprobe analysis.

TWQ P-T calculations that consider quartz as part of the equilibrium assemblage generate a large number of outlying reactions (Fig. 4.7). The addition of these reactions to the P-T diagram produces a large number of invariant points that yield geologically unrealistic P-T estimates. Quartz is therefore excluded form the equilibrium reaction calculations.

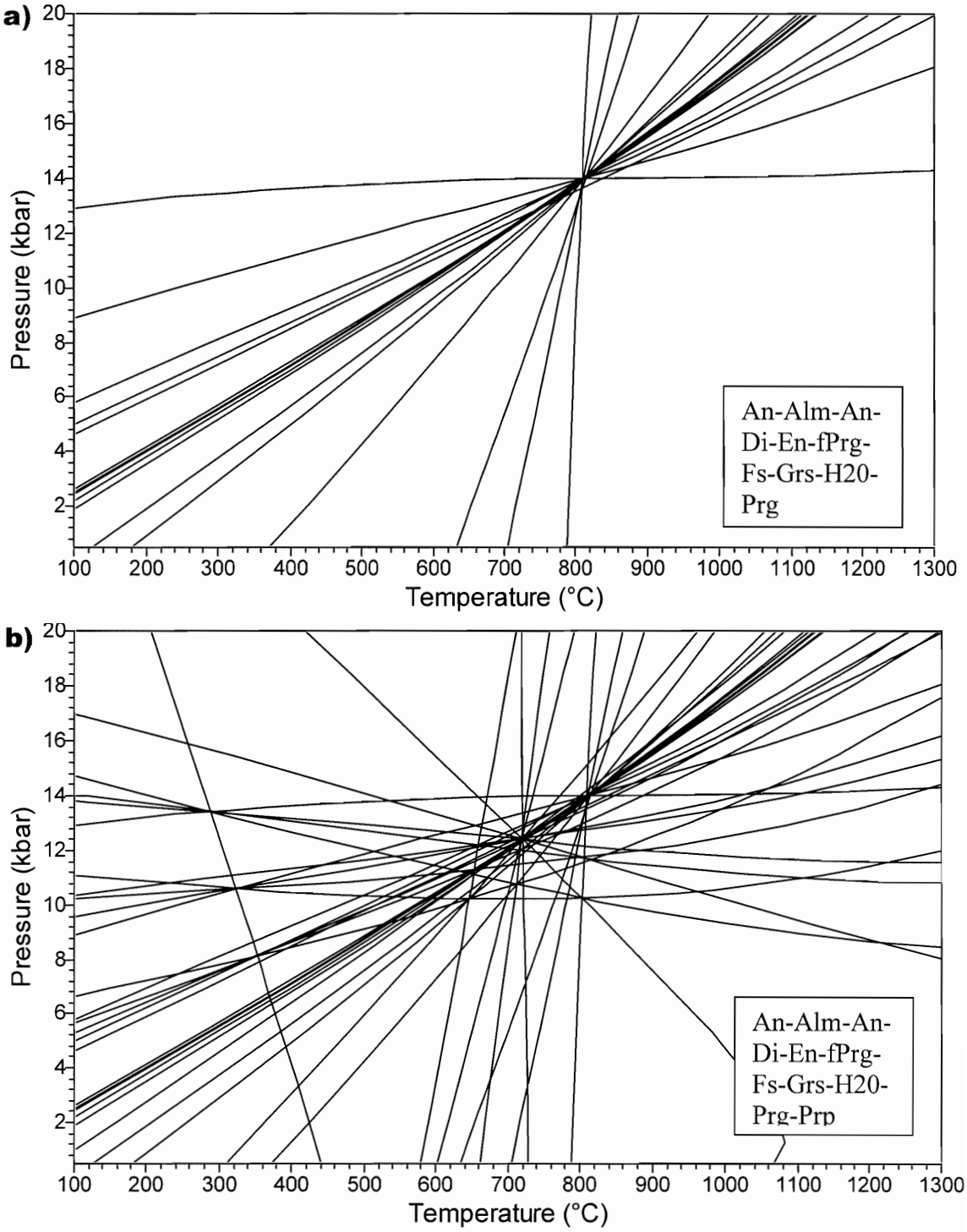

Figure 4.6: TWQ equilibrium diagrams of Kiosk gneiss (NA023) showing the large number of outlying reactions and geologically unrealistic intersections (i.e. anomalously low P&T) generated when pyrope is included in the equilibrium assemblage. **a)** without pyrope. **b)** with pyrope.

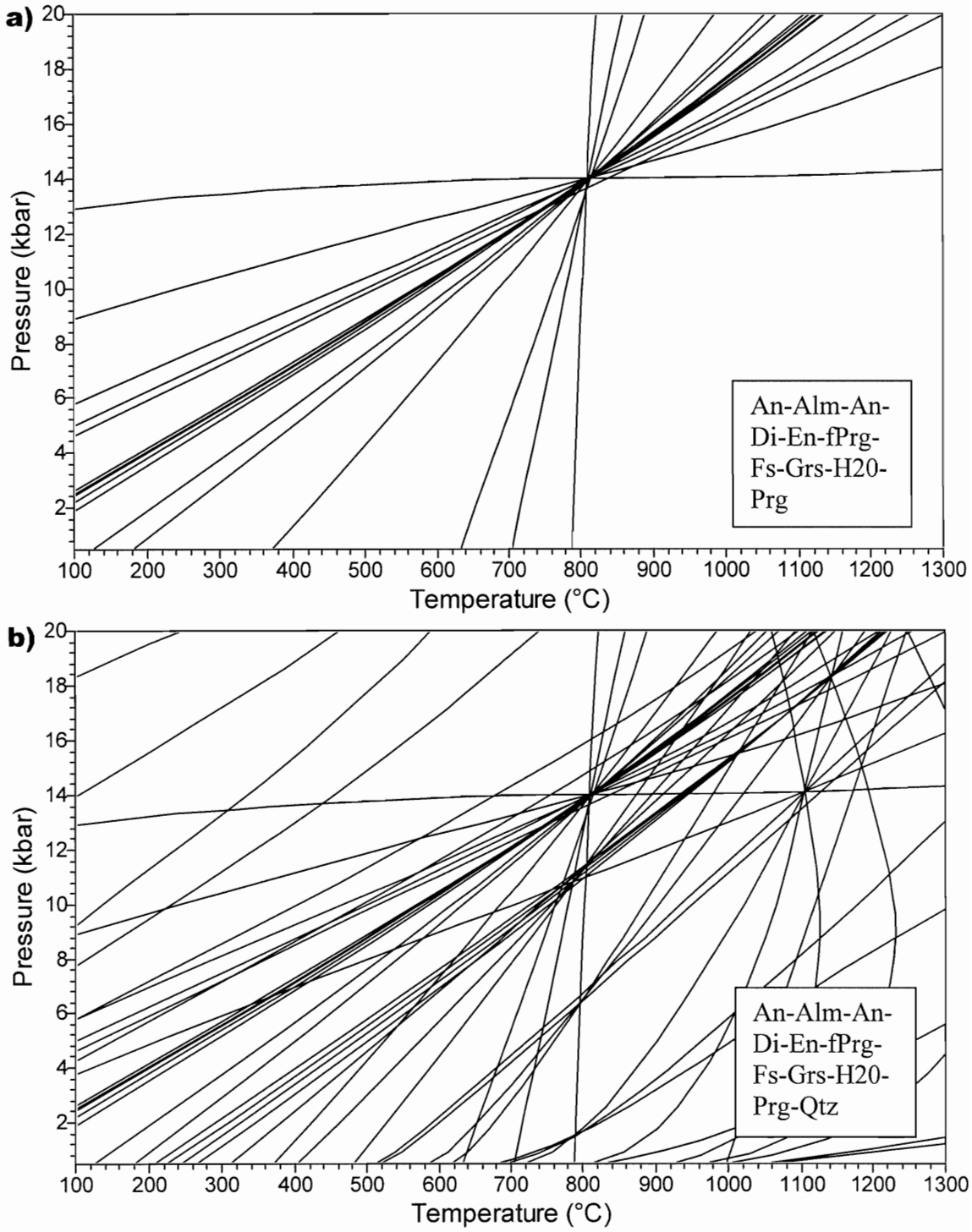

Figure 4.7: TWQ equilibrium diagrams of Kiosk gneiss (NA023) showing the large number of outlying reactions and geologically unrealistic intersections (i.e. anomalously high P&T) generated when quartz is included in the equilibrium assemblage. **a)** without quartz. **b)** with quartz.

4.8 Fugacity of water in P-T calculations

When considering a hydrous mineral assemblage that has equilibrated under granulite facies metamorphic conditions, it is often unreasonable to assume that a continuous hydrous fluid phase is present at equilibrium (i.e. $f_{H_2O} = 1$). Progressive fluid loss of a rock during prograde metamorphism significantly reduces the fluid content of a rock, thereby limiting the distribution of free fluids to isolated areas of a rock or eliminating free fluids altogether (Spear, 1995). Thus, for reactions involving H_2O in granulite rocks, it may not be accurate to assume that the fugacity (i.e. activity) value of H_2O (f_{H_2O}) is 1 because water may only be present as a component of a crystalline phase. This study addresses the added uncertainty of f_{H_2O} in granulite rocks by using geological observations to constrain f_{H_2O} within a certain range of reasonable values.

In their discussion of water barometry, Bohlen et al. (1980) indicated that dilution of the hydrous fluid phase by other volatiles, notably CO_2, is a major mechanism by which low f_{H_2O} values (e.g. $f_{H_2O} < 0.7$) are achieved. Given that no source of CO_2, such as carbonate rocks, has been identified in Kiosk or Algonquin domain, and that no carbonate is observed in the samples examined by this study, it is likely that f_{H_2O} is in the range of 0.7-1. The effect that f_{H_2O} uncertainty has on P-T estimates for the Kiosk and Algonquin domains is considered in Figure 4.8. It is clear that, by performing a sensitivity analysis to test the effect of f_{H_2O} on calculated reactions, the affect that f_{H_2O} uncertainty has on the accuracy of the P-T estimates presented herein is minimal.

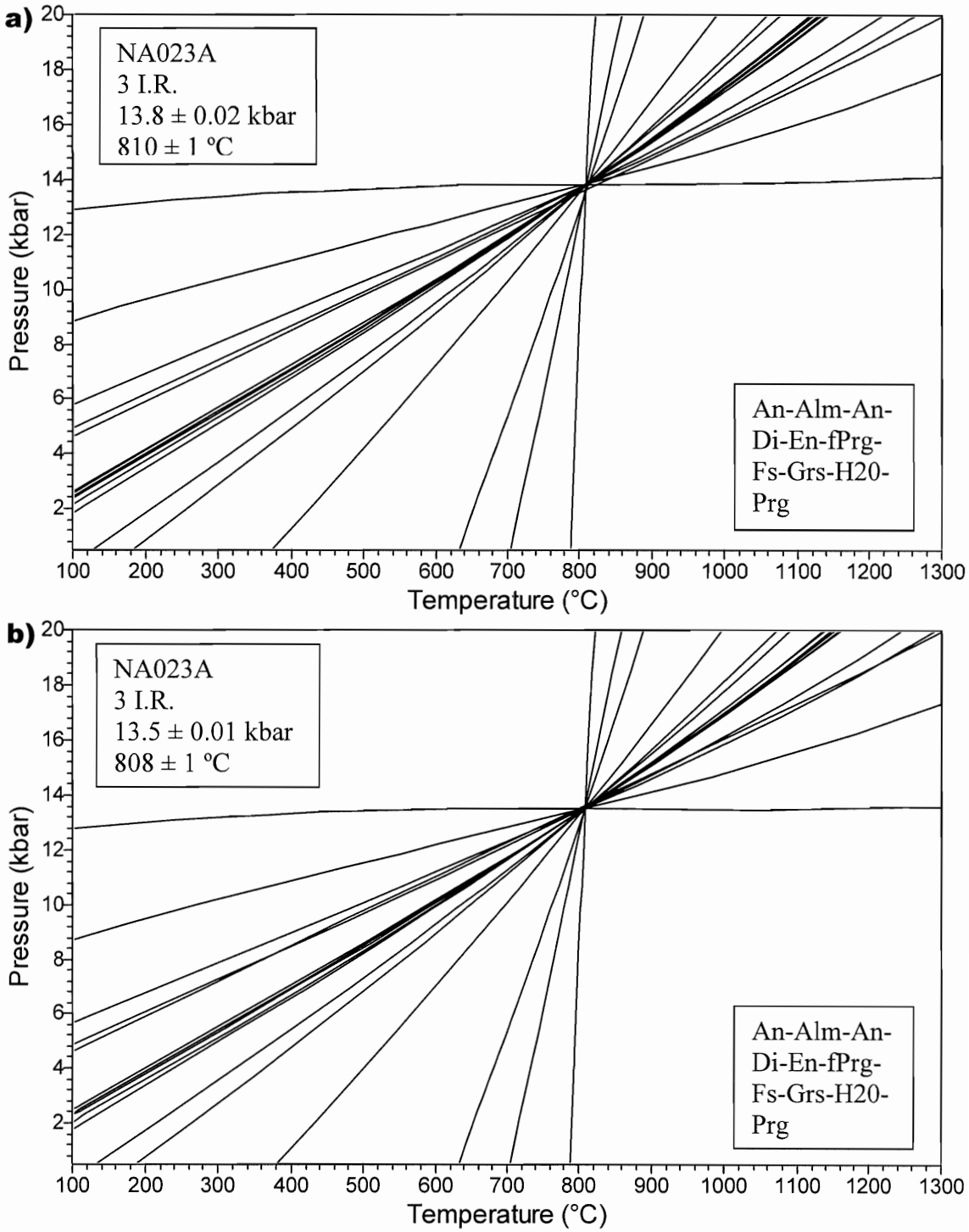

Figure 4.8: TWQ equilibrium diagrams of Kiosk gneiss (NA023) showing the nominal affect of varying water fugacity values in P-T calculations. a) assuming $f_{H_2O} = 0.9$. b) assuming $f_{H_2O} = 0.7$. All other lithologies examined herein react similarly to such variations of f_{H_2O}.

CHAPTER 5: DISCUSSION

5.1 General statement

This study presents new lithological, structural, and metamorphic findings from northwestern Algonquin Park which have significant implications for the tectonic evolution of the Grenville orogen. This chapter will: (1) discuss how the Kiosk domain and its boundary regions fit into the established tectonometamorphic framework of the CGB; (2) examine how the new findings shed light upon existing problems in Grenville geology; and (3) evaluate previously proposed tectonic models of the western Grenville orogen in the context of northwestern Algonquin geology.

5.2 Crustal architecture

Deciphering the complex crustal architecture of the CGB, through the identification of lithologically distinct tectonometamorphic domains, has been the subject of extensive study since the onset of modern mapping in the CGB (e.g. Culshaw et al. 1983, 1988, 1989, 1990, 1994, 1997; Davidson et al. 1982; Davidson 1984*b*; Dickin and McNutt 1990; Dickin and Guo 2001; Jamieson et al. 1992, 1995, 2007; Ketchum and Davidson 2000). These works have, however, generally focused on the Parry Sound and Georgian Bay region to the south and west of the northwestern Algonquin Park. With the exception two of small scale, regional reconnaissance studies (Davidson and Morgan, 1981; Davidson, 1986) little attention has been devoted to the examination of the Kiosk domain and its boundary regions. Thus, the incorporation and positioning of the Kiosk domain and its boundary regions within the tectonometamorphic framework of CGB, as most recently proposed by the regional synthesis of Carr et al. (2000), is somewhat uncertain. What follows is a discussion of how this study's findings yield a better

understanding of crustal architecture of the northwestern Algonquin region as it relates to the well studied Georgian Bay region to the west.

Several findings presented herein suggest that the Kiosk domain and Bonfield terrain are similar to the Parry Sound and Shawanaga domains respectively, in terms of their strain history, metamorphic history, and geophysical properties. Foremost, the Parry Sound domain contains strongly developed L=S fabrics similar in trend to those found in the Kiosk domain. Although these fabrics are not as widespread as they are in the Kiosk domain, their occurrence in the CGB is restricted outside of Kiosk domain. Second, the P-T signature of ~14 kbar and 800-1000 °C reported herein for the Kiosk domain is similar to that reported by Wodicka et al. (2000) for the interior of the western Parry Sound Domain. This P-T signature is relatively uncommon within the CGB; the majority of P-T estimates from the CGB have a nominal deviation from the average of 10 kbar and 800 °C due to thorough equilibration. Third, migmatitic gneiss of the Bonfield terrain bears strong resemblance to the migmatite of the Shawanaga domain. In particular, both of these rocks contain the distinct coarse-grained hornblende porphyroblasts set in a matrix of cream pink leucosomes and grey mesosomes which are a distinctive feature of the Shawanaga domain. Fourth, the Kiosk domain and Parry Sound domain both contain large positive gravity anomalies (Fig. 2.1). However, Archibald (2008) performed an in-depth examination of the geophysical properties of these two domains and found that the Kiosk domain penetrates much deeper into the crust than the Parry Sound domain.

It is important to note that these similarities do not necessarily imply that the Kiosk domain is correlative with the Parry Sound and domain. Major lithological differences exist between these two entities which suggest that they are genetically

unrelated. However, as the Kiosk and Parry sound domains contain similar tectonic fabrics and P-T signatures rarely found in the CGB, they likely experienced a similar tectonometamorphic evolution during the Grenville orogen.

5.3 Allochthon Boundary Thrust

The positioning of the Allochthon Boundary Thrust (ABT) within the northwestern Algonquin region is subject to considerable debate with alternative positions being proposed by different workers (Fig. 5.1). Observations from the northern Kiosk shear zone presented herein agree with the positioning of the ABT along the northern Kiosk domain, as originally postulated by Davidson (1996) and later supported, with some modification, by Dicken and Guo (2001) on the bases of Sm-Nd model age data.

First, the northern Kiosk shear zone is a boundary which places high grade rocks (i.e. Kiosk granulites) on top of lower grade rocks (i.e. Bonfield granitoids and the amphibolite facies Bonfield gneiss). Such a boundary is consistent with being a major thrust, which is a requirement of the ABT.

Second, the degree of strain and ductile attenuation, demonstrated by the strongly developed L=S fabrics of the northern Kiosk shear zone, suggests that this boundary is a fundamental tectonic break along which potentially significant displacement occurred. In contrast, the eastern margin of the Powassan Batholith (PB), the alternative position proposed by Ketchum and Davidson (2000), does not display such characteristics of being a major ductile tectonite zone. Unless it is admitted that tectonism along the eastern margin of the PB is cryptic, it is difficult envisage this position as being a superior alternative to the northern Kiosk shear zone.

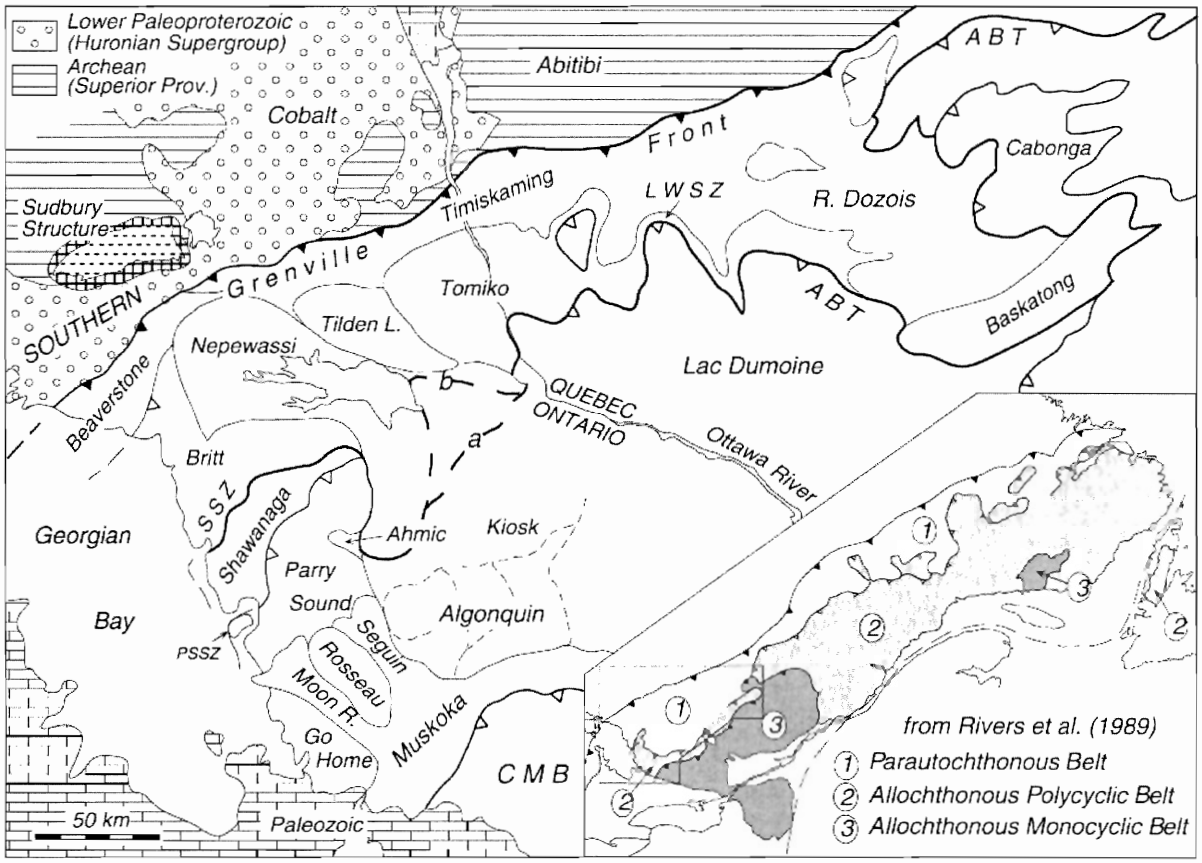

Figure 5.1: Lithotectonic subdivisions of the western CGB. The location of the ABT is shown (bolded black line). The disputed course of the ABT is shown with bolded dashed lines. Course (b) is that of Ketchum and Davidson (2000); Course (a) is suggested by Davidson (1996), Dickin and Guo (2001), and this study. See text for further discussion. Figure from Ketchum and Davidson (2000).

5.4 Implications for tectonic models of the Grenville orogen

Two species of tectonic models have been proposed for the western Grenville orogen: (1) orogen evolution through a convergence driven sequence of crustal thickening, thermal relaxation, and lower crustal extensional flow (e.g. Jamieson et al. 2007); and (2) orogen evolution by thrust-stacking only (e.g. Rivers et al. 1989). This section will examine how the Kiosk domain, as an uncommon record of the early crustal thickening phase of orogenesis, stands to substantiate the model of Jamieson et al. (2007).

Outside of the Grenville Front Tectonic Zone (GFTZ), there is generally little record of thickening fabrics of the Grenville orogen; the Kiosk domain, however, likely contains these early fabrics. Boundary relationships demonstrate that the anomalous, very straight trending, L=S fabric of the Kiosk domain predates the contorted S>L flow fabric of the north-central Algonquin domain and Bonfield terrain. Furthermore, in the western Kiosk domain, the Kiosk L=S fabric can be observed being reoriented in a manner similar to the late, flow related, Seguin and Moon River domains (N. Culshaw 2008, personal communication). It is therefore most probable that this anomalous fabric represents an early, relict crustal thickening fabric developed prior to crustal flow. The uncommon P-T signature of the Kiosk domain may also be relict record of the thermobarometric conditions which gave rise to such a fabric. Further study of the Kiosk domain, dating of the metamorphism in particular, has the potential to yield additional information that may confirm this hypothesis.

The Kiosk domain provides further geological evidence to support the claim made by both of these models that the Grenville orogeny propagated in a northwesterly

direction. In particular, strongly developed, steeply dipping, NNW-SSE oriented lineations are consistent with a northwest directed thrusting direction.

5.5 Similarities between the Kiosk domain and GFTZ

Although the GFTZ and Kiosk domain are separated by more than 150km and contain rocks of different metamorphic and lithologic character, it is interesting to note that the structures present in these two regions are strikingly similar. Most notably, the majority of the CGB is characterized by complex, heterogeneous, folded, S>L fabrics which greatly contrast with the very straight trending, homogenous, L=S fabric found in the GFTZ and Kiosk domains. In fact, nowhere else in the CGB are strongly developed, L=S fabrics found that continue, largely uninterrupted for large distances (>50km) along strike. Furthermore, both the GFTZ and northern Kiosk domain shear zone contain feldspar porphyroclastic mylonites indicative of deformation under P-T conditions significantly lower than average for the CGB.

The tectonic model of Jamieson et al. (2007) predicts the existence of such rocks along the GFTZ, as material is exhumed along the lower crustal ramp. However, the Kiosk domain is located outboard of this ramp by over 150km. Thus the development of the Kiosk fabric cannot be accounted for by such a model unless it is admitted that the fabric is relict from when the northwestern Algonquin region was the inboard edge of the orogen. However, if this is the case, the tectonic model predicts that such a relict of crustal thickening would not be preserved, as rocks from the Algonquin region are shown to flow during inboard propagation of the orogen. Therefore, although the Kiosk domain can be used to support the general orogenic mechanisms proposed by this model (Section

5.4), the presence of a thickening fabric in the Kiosk domain raises questions about the predicted evolution of specific lithotectonic units during the Grenville orogeny.

CHAPTER 6: CONCLUSIONS

6.1 Conclusions

1. Northwestern Algonquin comprises two distinct lithotectonic domains, the Kiosk domain and the Algonquin domain. A poorly studied region to the north of the Kiosk domain, herein termed the Bonfield terrain, encompasses the remainder of the study area. The Kiosk and Algonquin domains are generally characterized by small, variably deformed metapluntonic bodies set in a matrix of fine-grained quartzofeldspathic orthogneiss rarely interlayered with thin bands of paragneiss. Metamorphic grade throughout these domains is largely granulite facies, with notable regression to amphibolite facies occurring along the bounding shear zones of the Kiosk domain. In contrast, the Bonfield terrain contains large, poorly deformed granitoid plutons set in a matrix of amphibolite facies gneiss.

2. Several lithologies, exotic with respect to the CGB, have been identified within Kiosk domain. An anhydrous, Ai_2SiO_5-free corundum-garnet-spinel-plagioclase-K-feldspar bearing rock, believed to be of supracrustal origin, was identified in the central Kiosk domain. At the same locality, a metabasite rock with orthopyroxene porphyroblasts over 3cm in length was identified. Along the Kiosk domain – Bonfield terrain boundary zone, a feldspar porphyroclastic mylonite, characteristic of P-T conditions much lower than those observed in the Kiosk domain, has been identified.

3. The Kiosk domain contains a well developed, widespread L=S thickening fabric not found elsewhere at such a scale in the CGB. Field relations show this fabric to be early relative to neighbouring domains which preserve S>L flow fabrics.

4. Pressure and temperature estimates from metamorphic mineral assemblages in metabasite and supracrustal rocks indicate that peak conditions of $P \geq 14$ kbar and $T \geq 800$ °C were achieved in the Kiosk domain. In contrast, the metabasite rocks in the Algonquin domains record lower P conditions of ~12 kbar and T conditions of ~800 °C.

5. The finding of an L=S thickening fabric in the Kiosk domain that predates S>L flow fabrics of neighbouring domains is consistent with previously proposed tectonic models which show orogen development by continental thickening flowed by lower crustal extensional flow. The uncommon P-T signature of the Kiosk domain may be a relict record of the thermobarometric conditions which gave rise to the thickening fabric. Finally, the finding of strong NW-SE oriented lineations in the Kiosk domain is consistent with the NW directed emplacement of thrust sheets shown by these models.

7.2 Recommendations for further study

Dating of the metamorphism in the Kiosk domain is essential to confirming the early fabric hypothesis of the Kiosk domain. Further petrographic and thermobarometric study of the exotic Kiosk supracrustal gneiss may reveal information about its petrogenesis. Field reconnaissance must be completed throughout Bonfield terrain in order to: (1) elucidate its tectonostratigraphy by mapping lithotectonic domains within

the terrain and identifying their position within the CGB; (2) confirm the position of the ABT within this region; and (3) better understand the tectonic significance of the anomalous feldspar porphyroclastic mylonite.

References Cited:

Ahern, F. 2006. Algonquin Park through time and space. Warick Publishing, Toronto.

Archibald, H. B. 2008. Geological interpretation of gravity anomalies in the southwestern Grenville Province, Ontario. Honours thesis, Dalhousie University, Halifax, Nova Scotia, Canada.

Anovitz, L.M., and Essene, E.J. 1990. Thermobarometry and pressure-temperature time paths in the Grenville Province, Ontario. Journal of Petrology, **31**: 197-241.

Berman, R.G. 1988. Internally consistent thermodynamic data for minerals in the system Na_2O–K_2O–CaO–MgO–FeO–Fe_2O_3–Al_2O_3–SiO_2–TiO_2–H_2O–CO_2. Journal of Petrology, **29**: 445–522.

Berman, R. 1991. Thermobarometry using multiequilibrium calculations: a new technique with petrologic applications. Canadian Mineralogist, **29**: 833-855.

Bethune, K.M. 1997. The Sudbury dyke swarm and its bearing on the tectonic development of the Grenville Front, Ontario, Canada. Precambrian Research, **85**: 117–146.

Bohlen, S.R., Peacor, D.R., and Essene, E.J. 1980. Crystal chemistry of a metamorphic biotite and its significance in water barometry. American Mineralogist, **65**: 55-62.

Bussy, F., Krogh, T.E., Klemens, W.P., and Schwerdtner, W.M.1995. Tectonic and metamorphic events in the westernmost Grenville Province, central Ontario: New results from high precision U-Pb zircon geochronology. Canadian Journal of Earth Sciences, **32**: 660–671.

Canada Geodetic Information System. 2008. Geoscience data repository, Geological Survey of Canada, Earth science sector, Natural Resources Canada, Government of Canada.

Carr, S.D., Easton, R.M., Jameison, R.A., and Culshaw, N.G. 2000. Geological transect across the Grenville orogen of Ontario and New York. Canadian Journal of Earth Sciences, **37**: 193-216.

Collins, W.H. 1925. North Shore of Lake Huron. Geological Survey of Canada Memoir 143, 160 p.

Corrigan, D., Culshaw, N.G., and Mortensen, J.K. 1994. Pre-Grenvillian evolution and Grenvillian overprinting of the Parautochthonous Belt in the Key Harbour area, Ontario: U-Pb constraints. Canadian Journal of Earth Sciences, **31**: 583–596.

Culshaw, N.G., Davidson, A., and Nadeau, L. 1983. Structural subdivisionsof the Grenville Province in the Parry Sound-Algonquin region, Ontario. *In* Current research, part B. Geological Survey of Canada, Paper 83-1B, pp. 243–252.

Culshaw, N.G., Corrigan, D., Drage, J., and Wallace, P. 1988. Georgian Bay geological synthesis: Key Harbour to Dillon, Grenville Province of Ontario. *In* Current research, part C. Geological Survey of Canada, Paper 88-1C, pp. 129–133.

Culshaw, N.G., Check, G., Corrigan, D., Drage, J., Gower, R., Maggart, M.J., Wallace, P., and Wodicka, N. 1989. Georgian Bay geological synthesis: Dillon to Twelve Mile Bay, Grenville Province of Ontario. *In* Current research, part C. Geological Survey of Canada, Paper 89-1C, pp. 157–163.

Culshaw, N.G., Jamieson, R.A., Corrigan, D., Ketchum, J.W.F., Reynolds, P.H., Wodicka, N., Heaman, L., and Krogh, T.E. 1990. History of the Central Gneiss Belt, Grenville Province, along Georgian Bay, Ontario. Lithoprobe Abitibi-Grenville Project, Workshop Report, **3**:73-76.

Culshaw, N.G., Ketchum, J.W.F., Wodicka, N., and Wallace, P.1994. Ductile extension following thrusting in the deep crust: Evidence from the southern Britt Domain, southwest Grenville Province, Georgian Bay, Ontario. Canadian Journal of Earth Sciences, **31**: 160–175.

Culshaw, N.G., Jamieson, R.A., Ketchum, J.W.F., Wodicka, N., Corrigan, D., and Reynolds, P.H. 1997. Transect across the northwestern Grenville orogen, Georgian Bay, Ontario: Polystage convergence and extension in the lower orogenic crust. Tectonics, **16**: 966–982.

Davidson, A. 1984*a*. Identification of ductile shear zones in the southwestern Grenville Province of the Canadian Shield. *In* Precambrian tectonics illustrated. *Edited by* A. Kroner and R. Greiling. E. Schweizerbart'sche Verlagsbuchhandlung, Stuttgart, pp. 263–279.

Davidson, A. 1984*b*. Tectonic boundaries within the Grenville Province of the Canadian shield. Journal of Geodynamics, **1**: 433-444.

Davidson, A. 1986. New interpretations in the southwestern Grenville province. *In* The Grenville Province. *Edited by* J.M.Moore, A. Davidson, and A.J. Baer. Geological Association ofCanada, Special Paper 31, pp. 61–74.

Davidson, A. 1990. Evidence for eclogite metamorphism in the southwestern Grenville Province. *In* Current Research, Part 1C.Geological Survey of Canada, Paper **90-1C**, pp. 113–118.

Davidson, A. 1996. Geology of Grenville Province. Geological Survey of Canada, Open File 3346, scale 1:2,000,000.

Davidson, A., and Morgan, W.C. 1981. Preliminary notes on the geology east of Georgina Bay, Grenville Structural Province. *In* Current research, part A. Geological Survey of Canada, Paper 81-1A, pp. 291–298.

Davidson, A., Culshaw, N.G., and Nadeau, L. 1982. A tectonometamorphic framework for part of the Grenville Province, Parry Sound region, Ontario. *In* Current research, part A. Geological Survey of Canada, Paper 82-1A, pp. 175–190.

Davidson, A., and Bethune, K.M. 1988. Geology on the north shore of Georgian Bay, Grenville Province of Ontario. *In* Current research, part C. Geological Survey of Canada, Paper 88-1C, pp. 135–144.

Davidson, A., and van Breemen, O. 2001. Mid-Mesproterozoic granitoid rocks in the North Bay area, Grenville Province, Ontario. *In* Current research, part F. Geological Survey of Canada, Paper 2001-F8, 15 p.

Deer, W.A., Howie, R.A., and Zussman, J. 1996. An introduction to the rock-forming minerals. Prentice Hall.

Dickin, A.P., and McNutt, R.H. 1990. Nd model-age mapping of Grenville lithotectonic domains: mid-Proterozoic crustal evolution in Ontario. *In* Mid-Proterozoic Laurentia–Baltica. *Edited by* C.F. Gower, T. Rivers, and A.B. Ryan. Geological Association of Canada, Special Paper 38: 79–94.

Dickin, A.P., and Guo, A. 2001. The location of the Allochthon Boundary Thrust and the Archean–Proterozoic suture in the Mattawa area of the Grenville Province: Nd isotope evidence. Precambrian Research, **107**: 31–43.

Essene, E.J., 1982. Geological thermometry and barometry. Reviews in Mineralogy, **10**:153-206.

Essene, E. J., 1989. The current status of thermobarometry in metamorphic rocks. *In* Evolution of Metamorphic Belts. *Edited by* J.S. Daly, R.A. Cliff, and B.W. Yardley. Special Publication of the Geological Society 43: 1-44.

Ferry, J.M, and Spear, F.S. 1978. Experimental calibration of the partitioning of Fe and Mg between biotite and garnet, Contributions to Mineralogy and Petrology, **66**:113–117

Finger, L.W. 1972. The uncertainty in the calculated ferric iron content of a microprobe analysis. Carnegie Institution of Washington Year Book, **71**: 600-603.

Flinn, D. 1962. On folding in three-dimensional progressive deformation. Quarterly Journal of the Geological Society of London, **114**:107-136.

Ghent, E.D. 1976. Plagioclase-garnet-Al_2SiO_5-quartz: a potential geobarometer-geothermometer. American Mineralogist, **61**:710–714.

Gill, J.E. 1948. Mountain building in the Canadian Precambrian Shield: XVIII International Geological Conference, pt. **13**: 97-104.

Gill, J.E. 1949. Natural Division of the Canadian Shield. Royal Society of Canada Transactions, **43**: 61-69.

Haggart, M.J., Jamieson, R.A., Reynolds, P.H., Krogh, T.E., Beaumont, C., and Culshaw, N.G. 1993. Last gasp of the Grenville orogeny — thermochronology of the Grenville Front Tectonic Zone near Killarney, Ontario. The Journal of Geology, **101**: 575–589.

Hodges, K.V., and McKenna, L.W. 1987. Realistic propagation of uncertainties in geologic thermobarometry. American Mineralogist, **72**: 671-680.

Holland, T. J. B., and Powell, R. 1998. An internally consistent thermodynamic data set for phases of petrological interest. Journal of Metamorphic Geology, **16:** 309-343.

Jamieson, R.A., Culshaw, N.G., Wodicka, N., Corrigan, D., and Ketchum, J.W.F. 1992. Timing and tectonic setting of Grenvillian metamorphism –constraints from a transect along Georgian Bay, southwestern Ontario. Journal of Metamorphic Geology, **10**:321-332.

Jamieson, R.A., Culshaw, N.G., and Corrigan, D. 1995. North-west propagation of the Grenville orogen: Grenvillian structure and metamorphism near Key Harbour, Georgian Bay, Ontario, Canada. Journal of Metamorphic Geology, **13**: 185–207.

Jamieson, R.A., Beaumont, C., Nguyen, M.H., and Culshaw, N.G. 2007. Synconvergent ductile flow in variable-strength continental crust: Numerical Models with application to the western Grenville orogen. Tectonics, **26**.

Ketchum, J.W.F. 1995. Extensional shear zones and lithotectonic domains in the southwest Grenville orogen: Structure, metamorphism, and U-PB geochronology of the central Gneiss Belt near Point-au-Baril, Ontario. Ph.D. Thesis, Dalhousie University, Halifax, Nova Scotia, Canada.

Ketchum, J.W.F., Jamieson, R.A., Heaman, L.M., Culshaw, N.G., and Krogh, T.E. 1994. 1.45 Ga granulites in the southwestern Grenville Province: geologic setting, *P–T* conditions, and U–Pb geochronology. Geology, **22**: 215–218.

Ketchum, J.W.F and Davidson, A. 2000. Crustal Architecture and tectonic assembly of the Central Gneiss Belt, southwestern Grenville Province, Canada — a new interpretation. Canadian Journal of Earth Sciences, **37**: 217–234.

Kretz, R. 1983. Symbols for rock forming minerals. American Mineralogist, **68**: 277-279

Logan, W.E. 1847. Report of progress for the year 1845-6. Geological Survey of Canada, pp. 1-98.

Logan, W.E. 1863. Report on the Geology of Canada. Geological Survey of Canada, Report of Progress from Its commencement to 1863, 983 p.

Lumbers, S.B. 1975. Geology of the Burwash Area, Districts of Nipissing, Parry Sound, and Sudbury. Ontario Division of Mines Geological Report 116, 158 pp. + map 2271.

McLelland, J.M., Daly, J.S., and McLelland, J.M. 1996. The Grenville orogenic cycle (ca. 1350–1000 Ma): An Adirondack perspective. Tectonophysics, **265**: 1–28.

Nadeau, L. 1990. Tectonic, thermal and magmatic evolution of the Central Gneiss Belt, Huntsville region, southwestern Grenville orogen. Ph.D. thesis, Carleton University, Ottawa, Ontario, Canada.

Powell, R., and Holland, T. J. B. 1988. An internally consistent thermodynamic dataset with uncertainties and correlations: 3. Application methods, worked examples and a computer program. Journal of Metamorphic Geology, **6**: 173–204.

Powell, R., and Holland, T.J.B. 1994. Optimal geothermometry and geobarometry. American Mineralogist, **79**: 120-133.

Quirke, T.T. 1924. Correlation of Huronian and Grenville rocks: Journal of Geology, **32**: 316-335.

Quirke, T.T. 1926. Huronian-Grenville relations. American Journal of Science, **11**: 195-173.

Quirke, T.T., and Collins, W.H. 1930. The Disappearance of the Huronian. Geological Survey of Canada Memoir 160, 129 p.

Ramsey, J.G., and Martin, I.H. 1983. The techniques of modern structural geology, volume 1: strain analysis. Academic Press, London.

Rivers, T. 1997. Lithotectonic elements of the Grenville Province: review and tectonic implications. Precambrian Research, **86**: 117–154.

Rivers, T., Martignole, J., Gower, C.F., and Davidson, A. 1989. New tectonic subdivisions of the Grenville Province, southeast Canadian Shield. Tectonics, **8**: 63–84.

Spear, F.S. 1995. Metamorphic phase equilibria and pressure-temperature-time paths. Mineralogy Society of America, Monograph, Washington, D.C.: 799 p.

Stockwell, C.H., 1964. Fourth report on structural provinces, orogenies and time-classification of rocks of the Canadian Precambrian shield. *In* Age Determinations and Geological Studies, Part II. Geological Survey of Canada Paper 64-17, pp. 1-21.

Timmermann, H. 1998. Geology, metamorphism, and U–Pb geochronology in the Central Gneiss Belt between Huntsville and Haliburton, southwestern Grenville Province, Ontario. Ph.D. thesis, Dalhousie University, Halifax, Nova Scotia, Canada.

van Breemen, O., and Davidson, A. 1990. U–Pb zircon and baddeleyite ages from the Central Gneiss Belt, Ontario. *In* Radiogenic age and isotopic studies: report 3. Geological Survey of Canada, Paper 89-2, pp. 85–92.

Wilson, M. E. 1918. The subprovincial limitations of pre-Cambrian nomenclature in the St. Lawrence Basin. Journal of Geology, **26**: 325-333.

Wilson, M. E. 1925. The Grenville pre-Cambrian subprovince. Journal of Geology, **33**: 389-407.

Wodicka, N. 1994. Middle Proterozoic evolution of the Parry Sound domain, southwestern Grenville orogen, Ontario, Structural, metamorphic, U/Pb and 40Ar/39Ar constraints. Ph.D. thesis, Dalhousie University, Halifax, N.S.

Wodicka, N., Ketchum, J.W.F., and Jamieson, R.A. 2000. Grenvillian metamorphism of monocyclic rocks, Georgian Bay, Ontario: implications for convergence history. Canadian Mineralogist **38**.

Worley, B., and Powell, R. 2000. High-precision relative thermobarometry; theory and a worked example. Journal of Metamorphic Geology, **18**: 91-101.

Wynne-Edwards, H.R. 1972. The Grenville Province. *In* Variations in tectonic styles in Canada. *Edited by* R.A. Price and R.J.W. Douglas. Geological Association of Canada, Special Paper 11, 263–334.

APPENDIX A: ABBREVIATIONS USED IN TEXT AND DIAGRAMS

Table A.1: Mineral abbreviations (after Kretz 1983)

Ab	albite
An	anorthite
Alm	almandine
Ap	apatite
Bt	biotite
Cpx	clinopyroxene
Crn	corundum
Di	diopside
En	enstatite
fPrg	ferropargasite
Fs	ferrosilite
Grs	grossular
Grt	garnet
Hbl	hornblende
Hc	hercynite
Kfs	K-feldspar
Op	opaque minerals
Opx	orthopyroxene
Pl	plagioclase
Prg	pargastie
Prp	pyrope
Rt	rutile
Qtz	quartz
Scp	scapolite
Spl	spinel
Ttn	titanite
Zrn	zircon

Table A.2: Other abbreviations

A	Ahmic domain
Ad	Algonquin domain
B	Britt domain
Be	Beaverstone domain
Bn	Bonfield terrain
CMBbtz	Central Metasedimentary Belt boundary thrust zone
GFTZ	Grenville Front Tectonic Zone
GH	Go Home domain
H	Huntsville domain
Kd	Kiosk domain
Mc	McCraney Subdomain
McL	McLintock subdomain
MR	Moon River domain
N	Novar subdomain
O	Opeongo subdomain
P	Powassan domain
PS	Parry Sound domain
R	Rosseau domain
S	Seguin domain
Sd	Shawanaga domain

APPENDIX B: STATION AND SAMPLE INFORMATION

Table B.1 presents geographic and structural information for the field stations of this study. Station coordinates apply to UTM Zone 17T (WGS 84 datum). Structural measurements were taken using Right Hand Rule. The sample column identifies samples taken at corresponding station locations. Letters postfixed to the end of a sample number differentiate between multiple samples taken at the corresponding station (e.g. NA005A,B = NA005A, NA005B). NT = None Taken.

Table B.1 Station coordinates and structural measurements

Station ID	Easting	Northing	Foliation	Lineation	Sample
NA001	646743	5088699	NT	NT	NT
NA002	647067	5089111	085/65	NT	NT
NA003	650086	5089659	075/55	170-50	NA005A,B
NA004	648892	5089063	170/55	NT	NA006A,B
NA005	647589	5088458	070/15	NT	NA008A,B
NA006	647934	5088485	075/35	NT	NT
NA007	648464	5088436	060/27	NT	NT
NA008	649028	5087822	060/40	125-25	NT
NA009	650231	5088590	070/30	NT	NA009
NA010	649694	5089200	005/85	NT	NT
NA011	653687	5090633	060/40	NT	NA011A,B,C
NA012	652993	5090253	070/74	160-26	NT
NA013	652994	5090311	040/36	NT	NT
NA014	653084	5090742	075/53	NT	NA014A,B,C
NA015	653465	5091335	075/25	NT	NT
NA016	654535	5091310	065/43	NT	NA016A
NA017	654158	5092006	085/38	NT	NA017A,B
NA018	654366	5092162	150/35	NT	NT
NA019	653897	5092791	100/32	NT	NT
NA020	649074	5087507	065/40	140-40	NA020A,B
NA021	649401	5086725	110/50	NT	NT
NA022	649843	5085623	020/15	NT	NT
NA023	647885	5082747	090/60	120-25	NA023A,B,C
NA024	648670	5082981	088/55	NT	NA024A,B,C
NA025	649278	5083479	115/70	NT	NT
NA026	649033	5082192	080/45	125-30	NA026A
NA027	649019	5082080	070/45	130-43	NA027A,B
NA028	648924	5081873	080/40	NT	NT
NA029	649111	5078777	060/43	NT	NA029
NA030	648956	5078780	067/37	135-37	NA030
NA031	648767	5079092	065/40	NT	NA031A,B
NA032	648431	5079323	050/43	120-35	NA032A,B,C
NA033	647936	5079313	059/47	NT	NT
NA034	647810	5079454	070/65	NT	NA034
NA035	669881	5062995	020/25	120-25	NA035
NA036	662329	5063807	050/40	NT	NT
NA037	663743	5065312	045/33	126-33	NT
NA038	662743	5064969	043/32	114-26	NA038

Station ID	Easting	Northing	Foliation	Lineation	Sample
NA039	663313	5064168	050/35	115-35	NT
NA040	660694	5063184	040/30	135-21	NT
NA041	664951	5064756	080/58	125-53	NT
NA042	665184	5063912	080/48	NT	NT
NA043	665953	5062337	055/26	120-24	NT
NA044	669716	5062661	065/23	115-15	NT
NA045	673142	5059608	285/50	290-05	NT
NA046	673465	5059294	305/20	NT	NA046
NA047	673580	5059161	020/15	110-15	NT
NA048	673712	5058946	120/55	NT	NT
NA049	673787	5058825	280/70	NT	NA049
NA050	674136	5059584	090/20	NT	NA050
NA051	671460	5061370	110/20	NT	NA051
NA052	671367	5061361	NT	NT	NT
NA053	670837	5061426	030/23	120-23	NT
NA054	670115	5062131	067/27	NT	NA054A,B
NA055	668731	5061897	094/30	134-20	NA055
NA056	668660	5062597	105/33	145-18	NA056
NA057	668912	5062974	195/65	NT	NT
NA058	669934	5065003	77/68	100-10	NT
NA059	669837	5064537	275/35	NT	NA059
NA060	661422	5070835	060/50	NT	NA060
NA061	661452	5071852	075/50	095-25	NA061A,B,C,D,E,F
NA062	662150	5069925	055/35	NT	NT

APPENDIX C: MICROPROBE ANALYSES

Microprobe analyses were completed at the Dalhousie University Regional Electron Microprobe and Image Analysis Facility using the JEOL JXA-8200 electron microprobe. The standard operation conditions of 15 kV acceleration voltage, 5μm beam diameter, and 20 nA beam current were employed. The accuracy of major elements analysis is ± 1.5-2.0% (Patricia Stoffyn 2008, Dalhousie microprobe technician, personal communication). The following tables present the complete set of analyses obtained for amphibole, biotite, clinopyroxene, feldspar, garnet, ilmenite, and orthopyroxene minerals. The "No." row in the tables refers to the microprobe images presented in Appendix D. The number preceding the underscore indicates the image number. The number following the underscore refers to the analysis point.

Table B.1: Amphibole analyses

Sample No.	NA23A 05_4	NA23A 05_6	NA23A 05_33	NA23A 05_46	NA23A 05_50	NA23A 05_54	NA23A 05_61	NA23A 05_72	NA46 02_1	NA46 02_11	NA46 02_14	NA46 02_18
Wt.%												
SiO2	42.2488	42.5368	42.5666	41.7244	41.8061	42.59	42.9548	42.0321	42.4167	42.3175	42.293	42.1684
TiO2	2.2433	2.1906	1.9494	2.0699	2.0322	2.2098	1.9508	2.3336	2.7574	2.5328	2.7341	2.4699
Al2O3	12.6713	12.6626	12.6676	12.5538	12.6018	12.7805	12.7915	12.3179	12.7175	12.8043	12.6911	12.8328
Cr2O3	0.0185	0	0.0132	0.034	0	0.0045	0.0795	0.084	0.0347	0.028	0.0478	0.0844
FeO	14.9295	14.9282	14.7851	14.2865	14.5519	14.2421	13.8944	13.4869	15.8955	15.9621	15.8289	16.2401
MnO	0.0692	0.0675	0.0442	0.0516	0.0613	0.0687	0.0983	0.1142	0.0449	0.062	0.0552	0.0643
MgO	11.3041	11.5731	12.0356	11.8802	11.8826	11.9492	12.1698	12.6034	10.2014	10.1756	10.2738	9.8071
CaO	11.8898	12.0806	11.8852	12.0453	11.9817	11.7135	11.914	11.7843	11.8868	11.8535	12.1038	12.0664
Na2O	1.5623	1.6675	1.6798	1.6001	1.6927	1.6455	1.6979	1.8284	1.462	1.5222	1.3679	1.4179
K2O	1.7532	1.6508	1.625	1.7848	1.6437	1.6757	1.6542	1.6379	1.8369	1.799	1.7927	1.8224
Total	98.69	99.3577	99.2518	98.0306	98.2541	98.8796	99.2053	98.2228	99.2539	99.0571	99.1884	98.9737
Cations	(calculated on the basis of 23 O)											
Si	6.2675	6.2652	6.2675	6.2284	6.2261	6.2744	6.2974	6.2353	6.279	6.279	6.2652	6.2744
Ti	0.2507	0.2415	0.2162	0.2323	0.2277	0.2438	0.2162	0.2599	0.3059	0.2829	0.3036	0.276
Al	2.2149	2.1988	2.1988	2.208	2.2126	2.2195	2.2103	2.1528	2.2195	2.2402	2.2172	2.2517
Cr	0.0023	0	0.0023	0.0046	0	0	0.0092	0.0092	0.0046	0.0023	0.0046	0.0092
Fe	1.8515	1.8377	1.8216	1.7825	1.8124	1.7549	1.7043	1.6721	1.9688	1.9803	1.9619	2.0217
Mn	0.0092	0.0092	0.0046	0.0069	0.0069	0.0092	0.0115	0.0138	0.0046	0.0069	0.0069	0.0092
Mg	2.5001	2.5415	2.6404	2.6427	2.6381	2.6243	2.6588	2.7876	2.2517	2.2517	2.2701	2.1758
Ca	1.8906	1.9067	1.8745	1.9274	1.9113	1.8492	1.8722	1.8722	1.886	1.8837	1.9205	1.9251
Na	0.4485	0.4761	0.4784	0.4623	0.4899	0.4692	0.483	0.5267	0.4186	0.437	0.3933	0.4094
K	0.3312	0.3105	0.3059	0.3404	0.3128	0.3151	0.3105	0.3105	0.3473	0.3404	0.3381	0.345
Total	15.7688	15.7895	15.8102	15.8355	15.8401	15.7619	15.7757	15.8424	15.6883	15.7067	15.6837	15.6975

Table B.2: Amphibole analyses (cont.)

Sample	NA46	NA46	NA46	NA46	NA46	NA46	NA46	NA46	NA46	NA46	NA46	NA46
No.	02_20	02_23	02_24	02_25	02_28	02_37	02_7	03_38	03_52	03_58	03_61	03_64
Wt.%												
SiO2	42.6624	41.9576	41.6572	42.4541	42.4372	42.5683	41.9322	42.3582	42.4947	42.3471	42.2486	42.4939
TiO2	2.7148	2.6162	2.7839	2.4182	2.5777	2.3542	2.6185	2.6606	2.3607	2.2906	2.3405	2.331
Al2O3	12.6062	12.6875	12.9018	13.1291	12.3415	12.4092	12.5424	12.8053	12.5768	12.6478	12.9252	12.8044
Cr2O3	0.0352	0.0453	0.0294	0	0.0116	0.0198	0.0342	0.0675	0.0409	0.0554	0.0414	0.0521
FeO	15.9417	16.3504	16.162	15.2357	15.0156	14.8357	16.5888	15.7979	15.7043	16.0935	15.6493	15.8126
MnO	0.0648	0.0739	0.033	0.0279	0.0604	0.0587	0.0631	0.091	0.0779	0.0938	0.0922	0.0683
MgO	10.3746	9.8229	9.9226	10.5687	11.1518	11.3026	10.3198	10.3749	10.5922	10.596	10.6024	10.376
CaO	11.9501	11.8533	11.8765	12.0124	12.1945	12.0468	11.6013	11.9137	11.9491	12.0624	12.176	12.0227
Na2O	1.4755	1.4841	1.5825	1.4466	1.4593	1.4632	1.4834	1.5441	1.4134	1.4714	1.3859	1.4866
K2O	1.849	1.8267	1.9396	1.8295	1.7762	1.8036	1.7423	1.782	1.745	1.7613	1.7531	1.7667
Total	99.6744	98.718	98.8886	99.1223	99.0258	98.8622	98.9261	99.3953	98.9551	99.4194	99.2146	99.2144
Cations	(calculated on the basis of 23 O)											
Si	6.2905	6.2652	6.2146	6.2698	6.279	6.2997	6.2491	6.2606	6.302	6.2675	6.2537	6.2905
Ti	0.3013	0.2944	0.3128	0.2691	0.2875	0.2622	0.2944	0.2967	0.2622	0.2553	0.2599	0.2599
Al	2.1896	2.2333	2.2678	2.2862	2.1528	2.1643	2.2034	2.231	2.1988	2.2057	2.254	2.2333
Cr	0.0046	0.0046	0.0046	0	0.0023	0.0023	0.0046	0.0069	0.0046	0.0069	0.0046	0.0069
Fe	1.9665	2.0424	2.0171	1.8814	1.8584	1.8354	2.0677	1.9527	1.9481	1.9918	1.9366	1.9573
Mn	0.0092	0.0092	0.0046	0.0046	0.0069	0.0069	0.0069	0.0115	0.0092	0.0115	0.0115	0.0092
Mg	2.2793	2.1873	2.2057	2.3276	2.461	2.4932	2.2931	2.2862	2.3414	2.3391	2.3391	2.2885
Ca	1.8883	1.8975	1.8975	1.9021	1.9343	1.9113	1.8538	1.886	1.8975	1.9136	1.932	1.9067
Na	0.4209	0.4301	0.4577	0.414	0.4186	0.4209	0.4278	0.4416	0.4071	0.4232	0.3979	0.4255
K	0.3473	0.3473	0.368	0.345	0.3358	0.3404	0.3312	0.3358	0.3312	0.3335	0.3312	0.3335
Total	15.6998	15.7136	15.7527	15.7021	15.7366	15.7389	15.7343	15.709	15.7044	15.7504	15.7228	15.7136

Table B.3: Amphibole analyses (cont.)

Sample No.	NA46 03_69	NA61E 02_15	NA61E 03_12	NA61E 03_15	NA61E 03_16	NA61E 03_8	NA61E 04_27	NA61E 04_31	NA61E 04_33	NA61E 04_36	NA61E 05_28	NA61E 05_29
Wt.%												
SiO2	42.3941	40.7014	42.2203	42.5981	42.1809	41.2171	42.3303	42.7238	42.7708	42.3481	42.0599	42.7041
TiO2	2.3524	2.5784	2.0048	2.4415	2.472	2.4057	2.9703	2.3305	2.1598	2.3185	2.3961	2.1393
Al2O3	13.0198	13.8843	12.4028	13.315	13.5389	13.4488	13.0867	13.1043	13.3903	13.6048	13.2158	13.044
Cr2O3	0.0482	0.014	0.0348	0.0725	0.0924	0.0271	0.0617	0.0476	0.0572	0.0578	0.0203	0
FeO	15.8462	12.0569	11.9558	10.8316	11.2179	12.0817	11.8707	11.6544	12.0415	11.4341	12.029	11.8642
MnO	0.0478	0.0323	0.0606	0.0521	0.0618	0.0617	0.0708	0.0555	0.0809	0.0413	0.0533	0.0578
MgO	10.4659	12.3655	13.2623	13.4902	13.2328	12.4717	12.4914	13.0367	12.7567	12.8127	12.7595	13.0402
CaO	11.9926	12.1718	12.0885	12.0894	11.8794	12.1929	12.0882	11.8949	11.9387	12.1211	12.0892	11.9188
Na2O	1.4501	1.707	1.7365	1.7576	1.6665	1.7636	1.7391	1.7605	1.7921	1.6745	1.7351	1.7064
K2O	1.8453	2.0521	1.5255	1.9044	2.0322	1.8768	1.9634	1.9565	1.7772	2.0405	1.8827	1.7587
Total	99.4624	97.5638	97.292	98.5525	98.3749	97.5472	98.6727	98.5648	98.7653	98.4535	98.241	98.2336
Cations	(calculated on the basis of 23 O)											
Si	6.2606	6.0628	6.2698	6.2169	6.1824	6.1318	6.2077	6.2537	6.2514	6.2077	6.1985	6.2698
Ti	0.2622	0.2898	0.2231	0.2691	0.2714	0.2691	0.3266	0.2576	0.2369	0.2553	0.2645	0.2369
Al	2.2655	2.438	2.1712	2.2908	2.3391	2.3575	2.2632	2.2609	2.3069	2.3506	2.2954	2.2586
Cr	0.0046	0.0023	0.0046	0.0092	0.0115	0.0023	0.0069	0.0046	0.0069	0.0069	0.0023	0
Fe	1.9573	1.5019	1.4858	1.3225	1.3754	1.5042	1.4559	1.426	1.472	1.4007	1.4835	1.4559
Mn	0.0069	0.0046	0.0069	0.0069	0.0069	0.0069	0.0092	0.0069	0.0092	0.0046	0.0069	0.0069
Mg	2.3046	2.7462	2.9371	2.9348	2.8911	2.7669	2.7301	2.8451	2.7807	2.7991	2.8037	2.8543
Ca	1.8975	1.9435	1.9228	1.8906	1.8653	1.9435	1.8998	1.8653	1.8699	1.9044	1.909	1.8745
Na	0.4163	0.4922	0.4991	0.4968	0.4738	0.5083	0.4945	0.4991	0.5083	0.4761	0.4968	0.4853
K	0.3473	0.391	0.2898	0.3542	0.3795	0.3565	0.368	0.3657	0.3312	0.3818	0.3542	0.3289
Total	15.7251	15.8723	15.8102	15.7918	15.7987	15.8493	15.7642	15.7849	15.7757	15.7872	15.8148	15.7734

Table B.4: Amphibole analyses (cont.)

Sample No.	NA61E 07_14	NA61E 07_16	NA61E 07_17	NA61E 09_18	NA61E 09_21	NA61 19_10	NA61 19_11	NA61 19_15	NA61 20_43	NA610 20_44
Wt.%										
SiO2	42.2829	42.2574	42.4761	42.4444	42.2822	41.8199	41.2596	41.4552	42.1929	41.3264
TiO2	2.3884	2.4924	2.3942	2.5359	2.4993	2.8346	2.617	2.8273	2.5618	3.3886
Al2O3	13.7448	13.7349	13.4154	13.4248	13.4565	12.8744	13.0811	13.3614	12.9216	12.8981
Cr2O3	0.035	0.0113	0.036	0.0205	0	0.0269	0.0215	0.0278	0.0152	0.0404
FeO	12.3625	12.2826	12.0573	12.3366	12.612	11.9638	12.4603	12.4319	12.1233	12.5685
MnO	0.056	0.0424	0.0232	0.0769	0.0593	0.0386	0.0568	0.0585	0.0534	0.0426
MgO	12.348	12.3793	12.4003	12.3126	12.0668	12.4532	12.11	11.9277	12.175	11.7409
CaO	12.2058	11.9226	12.0845	12.1243	12.1706	12.1539	11.9791	12.071	12.1664	11.938
Na2O	1.6466	1.7293	1.6401	1.7069	1.743	1.6613	1.8115	1.6669	1.6645	1.6412
K2O	1.9231	1.9082	1.9324	1.9374	1.9897	1.701	1.5332	1.7183	1.6721	1.7797
Total	98.9932	98.7605	98.4595	98.9204	98.8794	97.5276	96.9302	97.5461	97.5462	97.3644
Cations	(calculated on the basis of 23 O)									
Si	6.187	6.1916	6.2353	6.2146	6.2054	6.2054	6.1732	6.164	6.2537	6.1663
Ti	0.2622	0.2737	0.2645	0.2783	0.276	0.3174	0.2944	0.3151	0.2852	0.3795
Al	2.3713	2.3713	2.3207	2.3161	2.3276	2.2517	2.3069	2.3414	2.2586	2.2678
Cr	0.0046	0.0023	0.0046	0.0023	0	0.0023	0.0023	0.0023	0.0023	0.0046
Fe	1.5134	1.5042	1.4812	1.5111	1.5479	1.4835	1.5594	1.5456	1.5019	1.5686
Mn	0.0069	0.0046	0.0023	0.0092	0.0069	0.0046	0.0069	0.0069	0.0069	0.0046
Mg	2.6933	2.7025	2.714	2.6864	2.6404	2.7554	2.7025	2.6427	2.691	2.6105
Ca	1.9136	1.8722	1.8998	1.9021	1.9136	1.932	1.9205	1.9228	1.932	1.909
Na	0.4669	0.4922	0.4669	0.4853	0.4968	0.4784	0.5267	0.4807	0.4784	0.4738
K	0.3588	0.3565	0.3611	0.3611	0.3726	0.322	0.2921	0.3266	0.3151	0.3381
Total	15.778	15.7734	15.7527	15.7688	15.7895	15.7527	15.7849	15.7504	15.7251	15.7228

Table B.5: Biotite analyses

Sample No.	NA046 02_10	NA046 02_6	NA046 03_2	NA046 03_37	NA046 03_4	NA046 03_54	NA046 03_62	NA046 03_7	NA046 03_72	NA61E 02_17	NA61E 02_18	NA61E 03_6
Wt.%												
SiO2	36.1745	36.0939	36.9933	36.7235	37.1752	36.6469	36.4991	36.9288	36.203	35.7374	36.5601	36.5284
TiO2	6.2258	5.7964	5.7089	6.2025	5.5919	5.8575	6.156	6.5066	5.9847	5.3247	5.0435	5.6264
Al2O3	14.6643	14.5047	14.8732	14.8417	14.7054	15.0022	14.9155	14.8881	14.5259	15.3224	14.9204	15.0051
Cr2O3	0.0481	0.0534	0.0587	0.0549	0.0583	0.0381	0.0673	0.0537	0.0732	0.0086	0.0153	0.0196
FeO	18.3637	18.0889	17.3528	17.5666	17.2891	17.5809	17.917	16.4049	17.2051	12.9465	13.0248	13.0326
MnO	0.052	0.0378	0.0277	0.0537	0.0401	0.0435	0.0565	0.043	0.0141	0	0.0175	0.0062
MgO	11.5646	11.7577	12.4046	12.0494	12.7673	12.3409	12.0009	12.7929	12.109	15.2797	15.5936	15.2141
CaO	0	0.1297	0.0275	0.0102	0.0299	0	0.0217	0.04	0.0424	0.0091	0.0306	0.0196
Na2O	0.0513	0.0633	0.0208	0.0229	0.0249	0.0183	0.0209	0.0247	0.0411	0.0857	0.0861	0.0898
K2O	9.656	8.8285	9.737	10.0027	10.0215	9.8535	9.7091	10.0754	9.5486	9.966	9.8692	10.1535
Total	96.8004	95.3543	97.2046	97.5282	97.7037	97.3819	97.3641	97.7581	95.7472	94.6802	95.1612	95.6954
Cations	(calculated on the basis of 11 O)											
Si	2.7148	2.7357	2.7456	2.7258	2.7478	2.7214	2.7148	2.7203	2.7313	2.6807	2.7236	2.7104
Ti	0.3509	0.33	0.319	0.3465	0.3113	0.3267	0.3443	0.3608	0.3399	0.3003	0.2827	0.3135
Al	1.2969	1.2958	1.3013	1.298	1.2815	1.3134	1.3079	1.2925	1.2914	1.3552	1.3101	1.3123
Cr	0.0033	0.0033	0.0033	0.0033	0.0033	0.0022	0.0044	0.0033	0.0044	0	0.0011	0.0011
Fe	1.1528	1.1462	1.0769	1.0901	1.0692	1.0923	1.1143	1.0109	1.0857	0.8118	0.8118	0.8085
Mn	0.0033	0.0022	0.0022	0.0033	0.0022	0.0022	0.0033	0.0022	0.0011	0	0.0011	0
Mg	1.2936	1.3288	1.3728	1.3332	1.4069	1.3662	1.331	1.4047	1.3618	1.7083	1.7314	1.683
Ca	0	0.011	0.0022	0.0011	0.0022	0	0.0022	0.0033	0.0033	0.0011	0.0022	0.0011
Na	0.0077	0.0088	0.0033	0.0033	0.0033	0.0022	0.0033	0.0033	0.0055	0.0121	0.0121	0.0132
K	0.9251	0.8536	0.9218	0.9471	0.9449	0.9339	0.9218	0.9471	0.9196	0.9537	0.9383	0.9614
Total	7.7495	7.7165	7.7484	7.7528	7.7737	7.7616	7.7484	7.7495	7.7451	7.8243	7.8144	7.8056
Mol. % end-members												
Ann	47.1223	46.31111	43.96048	44.98411	43.18081	44.42953	45.56905	41.84882	44.35955	32.213007	31.920415	32.450331
Phl	52.8777	53.68889	56.03952	55.01589	56.81919	55.57047	54.43095	58.15118	55.64045	67.786993	68.079585	67.549669

Table B.6: Biotite analyses (cont.)

Sample No.	NA61E 03_7	NA61E 03_19	NA61E 04_18	NA61E 04_19	NA61E 04_32	NA61E 04_34	NA61E 04_37	NA61E 07_8	NA61E 07_9	NA61E 07_10	NA61E 07_11	NA61E 07_12
Wt.%												
SiO2	36.2208	37.0254	37.4342	37.4893	37.4516	37.9762	37.8174	37.5472	37.1656	37.5164	37.521	37.6304
TiO2	5.6269	5.3106	5.7151	5.682	5.4832	5.6434	5.4314	5.555	5.6428	5.5778	5.4765	5.3676
Al2O3	15.0849	15.4058	15.065	15.0467	15.0988	14.7193	15.2879	15.1774	14.9745	14.9061	15.1898	15.1122
Cr2O3	0.0047	0.0704	0.0763	0.0739	0.0314	0.0594	0.0473	0.0419	0.005	0	0.0122	0.0204
FeO	13.4819	12.4034	12.1473	11.9328	13.0183	12.2461	12.4743	13.1173	12.9238	12.9341	12.8657	12.7878
MnO	0.0146	0.0338	0.0598	0.0389	0.0389	0.0327	0.0344	0.0456	0.0141	0.0225	0.0141	0.0169
MgO	15.2037	15.9596	15.768	15.8027	15.4681	16.103	15.9729	15.2394	15.2045	15.2979	15.4963	15.5944
CaO	0.0153	0.0182	0.0373	0.0445	0.0449	0.054	0.0344	0.0292	0.0136	0.0298	0.0088	0.0035
Na2O	0.087	0.0472	0.089	0.061	0.078	0.1082	0.0902	0.0527	0.0495	0.0354	0.0595	0.0388
K2O	10.0608	10.1671	10.2252	10.1325	10.0577	9.8628	10.0895	10.3014	10.092	9.9776	9.8163	9.9817
Total	95.8007	96.4416	96.6172	96.3044	96.771	96.8052	97.2798	97.1072	96.0854	96.2977	96.4603	96.5537
Cations	(calculated on the basis of 11 O)											
Si	2.6906	2.7137	2.7346	2.7423	2.739	2.7621	2.7423	2.7401	2.739	2.7544	2.7456	2.7511
Ti	0.3146	0.2926	0.3135	0.3124	0.3014	0.3091	0.2959	0.3047	0.3124	0.308	0.3014	0.2948
Al	1.3211	1.331	1.2969	1.298	1.3013	1.2617	1.3068	1.3057	1.3002	1.2892	1.3101	1.3024
Cr	0	0.0044	0.0044	0.0044	0.0022	0.0033	0.0022	0.0022	0	0	0.0011	0.0011
Fe	0.8382	0.7601	0.7425	0.7304	0.7964	0.7447	0.7568	0.8008	0.7964	0.7942	0.7876	0.7821
Mn	0.0011	0.0022	0.0033	0.0022	0.0022	0.0022	0.0022	0.0033	0.0011	0.0011	0.0011	0.0011
Mg	1.6841	1.7435	1.7171	1.7237	1.6863	1.7457	1.7259	1.6577	1.6698	1.6742	1.6896	1.6995
Ca	0.0011	0.0011	0.0033	0.0033	0.0033	0.0044	0.0022	0.0022	0.0011	0.0022	0.0011	0
Na	0.0121	0.0066	0.0121	0.0088	0.011	0.0154	0.0132	0.0077	0.0066	0.0055	0.0088	0.0055
K	0.9537	0.9504	0.9526	0.946	0.9383	0.9152	0.9328	0.9592	0.9482	0.9339	0.9163	0.9306
Total	7.8177	7.8067	7.7814	7.7726	7.7825	7.7649	7.7814	7.7847	7.7748	7.7627	7.7638	7.7693
Mol. % end-members												
Ann	33.231574	30.360281	30.187835	29.762438	32.07798	29.902827	30.482942	32.572707	32.292596	32.174688	31.793961	31.515957
Phl	66.768426	69.639719	69.812165	70.237562	67.92202	70.097173	69.517058	67.427293	67.707404	67.825312	68.206039	68.484043

Table B.7: Biotite analyses (cont.)

Sample No.	NA61E 09_13	NA61E 09_14	NA61E 09_15	NA61E 09_16	NA61E 12_33	NA61E 12_37	NA61E 12_40	NA61E 12_44	NA61E 12_47	NA61E 12_48	NA61E 12_50	NA61E 20_22
Wt.%												
SiO2	37.0805	36.7214	37.2449	37.355	36.978	37.7136	37.9815	37.7897	37.9596	37.8999	38.0082	36.8096
TiO2	5.5386	5.3732	5.5106	5.5226	5.4894	5.6115	5.4954	5.4143	5.8875	5.506	5.3188	6.0747
Al2O3	14.9594	15.1274	15.2034	15.4569	14.8594	14.9079	15.0511	15.496	15.4283	15.7488	14.6596	14.6485
Cr2O3	0.0362	0.0232	0.0174	0.0299	0	0.012	0	0	0	0	0	0.0257
FeO	13.1609	12.8551	13.2346	13.3455	12.6529	13.2375	11.5782	10.094	11.0297	10.2727	12.8945	13.2188
MnO	0.0101	0.0169	0.0315	0.0332	0.0191	0.0107	0.0321	0.0282	0.0231	0.0147	0.0293	0.0318
MgO	14.9501	14.9301	15.1131	15.1461	14.9979	15.2358	16.1865	17.5955	16.6956	17.5278	15.5497	14.9861
CaO	0	0.0245	0.0093	0	0	0.0194	0.0318	0.0532	0	0.0345	0.043	0.0565
Na2O	0.0559	0.0896	0.0671	0.0789	0.0834	0.0853	0.0867	0.2354	0.0718	0.309	0.0609	0.0205
K2O	10.0366	9.6095	10.0011	10.0736	10.12	10.0199	10.079	9.9573	10.2776	9.9911	9.7149	10.0853
Total	95.8284	94.771	96.4331	97.0417	95.2001	96.8537	96.5224	96.6636	97.3733	97.3046	96.279	95.9576
Cations	(calculated on the basis of 11 O)											
Si	2.7423	2.7379	2.7357	2.728	2.7489	2.7555	2.7632	2.7269	2.7324	2.7181	2.783	2.7247
Ti	0.308	0.3014	0.3047	0.3036	0.3069	0.308	0.3003	0.2937	0.319	0.297	0.2926	0.3377
Al	1.3035	1.3288	1.3167	1.3299	1.3024	1.2837	1.2903	1.3178	1.309	1.331	1.265	1.2782
Cr	0.0022	0.0011	0.0011	0.0022	0	0.0011	0	0	0	0	0	0.0011
Fe	0.814	0.8019	0.8129	0.8151	0.7865	0.8085	0.704	0.6094	0.6644	0.616	0.7898	0.8184
Mn	0.0011	0.0011	0.0022	0.0022	0.0011	0.0011	0.0022	0.0022	0.0011	0.0011	0.0022	0.0022
Mg	1.6478	1.6588	1.6544	1.6489	1.6621	1.6599	1.7556	1.8931	1.7919	1.8744	1.6973	1.6533
Ca	0	0.0022	0.0011	0	0	0.0011	0.0022	0.0044	0	0.0022	0.0033	0.0044
Na	0.0077	0.0132	0.0099	0.011	0.0121	0.0121	0.0121	0.033	0.0099	0.0429	0.0088	0.0033
K	0.9471	0.9141	0.9372	0.9383	0.9603	0.9339	0.935	0.9163	0.9438	0.9141	0.9075	0.9526
Total	7.7748	7.7616	7.777	7.7803	7.7814	7.766	7.7649	7.7979	7.7726	7.7968	7.7495	7.777
Mol. % end-members												
Ann	33.065237	32.588288	32.946946	33.080357	32.120395	32.754011	28.62254	24.351648	27.048813	24.734982	31.75586	33.110814
Phl	66.934763	67.411712	67.053054	66.919643	67.879605	67.245989	71.37746	75.648352	72.951187	75.265018	68.24414	66.889186

Table B.8: Biotite analyses (cont.)

Sample No.	NA61E 20_36	NA61E 20_37	NA61E 20_38	NA61E 20_39	NA61E 20_40	NA61E 20_41	NA61E 20_42	NA61E 19_8	NA61E 19_9	NA61E 19_12	NA61E 19_14	NA61F 03_15
Wt.%												
SiO2	36.7181	36.7239	36.8976	37.1042	36.9558	36.8703	36.8548	36.7589	37.0614	36.6694	36.747	36.6737
TiO2	6.0868	6.1023	6.0585	6.1256	6.1929	6.2241	5.9411	6.025	5.8967	6.0222	6.0674	6.3426
Al2O3	14.6647	14.76	14.7821	14.945	14.6419	14.5093	14.7361	14.86	14.7079	14.7372	14.8572	15.2856
Cr2O3	0.0141	0.0435	0.0401	0.0199	0.0367	0.0233	0.0285	0.0319	0.057	0.0536	0	0.0105
FeO	13.2496	13.0857	13.4365	13.4073	13.3438	13.3624	13.3202	13.5261	13.3607	13.2246	13.3645	15.9342
MnO	0.0232	0.0164	0.0243	0.0328	0.022	0.0373	0.0299	0.0079	0.0051	0.0175	0.004	0.0478
MgO	14.8599	14.7397	14.8442	14.7469	14.665	14.6725	14.7046	14.7561	14.7266	14.9949	14.7065	12.32
CaO	0.0064	0.047	0.004	0.0021	0.0054	0.0178	0.0374	0.0068	0	0.0259	0.0312	0.0205
Na2O	0.0479	0.0412	0.0196	0.0326	0.0207	0.0243	0.0487	0.037	0.0219	0.0353	0.0472	0.0967
K2O	8.8602	8.8837	9.0244	9.0021	9.0288	9.0261	8.8942	9.0549	9.0008	8.8233	9.1493	9.3924
Total	94.531	94.4435	95.1313	95.4186	94.913	94.7674	94.5956	95.0647	94.8382	94.604	94.9744	96.124
Cations	(calculated on the basis of 11 O)											
Si	2.7379	2.739	2.7379	2.7412	2.7467	2.7467	2.7467	2.7313	2.7555	2.7324	2.7324	2.7302
Ti	0.341	0.3421	0.3377	0.3399	0.3465	0.3487	0.3333	0.3366	0.33	0.3377	0.3399	0.3553
Al	1.2892	1.298	1.2925	1.3013	1.2826	1.2738	1.2947	1.3013	1.2892	1.2947	1.3024	1.3409
Cr	0.0011	0.0022	0.0022	0.0011	0.0022	0.0011	0.0022	0.0022	0.0033	0.0033	0	0.0011
Fe	0.8261	0.8162	0.8338	0.8283	0.8294	0.8327	0.8305	0.8404	0.8305	0.8239	0.8316	0.9922
Mn	0.0011	0.0011	0.0011	0.0022	0.0011	0.0022	0.0022	0	0	0.0011	0	0.0033
Mg	1.6522	1.639	1.6423	1.6247	1.6247	1.6291	1.6335	1.6346	1.6324	1.6654	1.6302	1.3673
Ca	0	0.0033	0	0	0	0.0011	0.0033	0	0	0.0022	0.0022	0.0011
Na	0.0066	0.0055	0.0033	0.0044	0.0033	0.0033	0.0066	0.0055	0.0033	0.0055	0.0066	0.0143
K	0.8426	0.8459	0.8547	0.8481	0.8558	0.858	0.8459	0.858	0.8536	0.8382	0.8679	0.8921
Total	7.6989	7.6923	7.7055	7.6912	7.6923	7.6978	7.7	7.7099	7.6989	7.7055	7.7143	7.6989
Mol. % end-members												
Ann	33.333333	33.243728	33.673923	33.766816	33.796504	33.824844	33.705357	33.955556	33.720411	33.097658	33.780161	42.051282
Phl	66.666667	66.756272	66.326077	66.233184	66.203496	66.175156	66.294643	66.044444	66.279589	66.902342	66.219839	57.948718

Table B.9: Biotite analyses (cont.)

Sample No.	NA61F 13_1	NA61F 13_2	NA61F 13_3	NA61F 13_4	NA61F 13_5	NA61F 13_8	NA61F 13_10
Wt.%							
SiO2	34.9506	36.3392	36.6071	36.5274	35.1576	37.0257	35.6577
TiO2	5.2937	6.1752	6.0531	6.2278	5.908	6.496	5.8013
Al2O3	14.7102	15.149	15.1942	15.1234	14.8069	15.1917	14.7309
Cr2O3	0.047	0.0009	0.031	0.0381	0.0412	0.0998	0.0711
FeO	19.9472	16.0596	16.0639	16.4046	18.1248	16.1688	18.2576
MnO	0.0202	0.0506	0.031	0.0326	0.0601	0.0017	0.0258
MgO	11.1539	12.2907	12.5229	12.3505	11.3523	12.2416	11.6377
CaO	0.0446	0.0229	0.0248	0	0.0452	0	0.0334
Na2O	0.0986	0.1021	0.0918	0.1028	0.1187	0.1026	0.1232
K2O	8.085	9.6276	9.5579	9.9308	9.3999	9.8686	8.9856
Total	94.3511	95.8178	96.1778	96.7381	95.0148	97.1965	95.3243
Cations	(calculated on the basis of 11 O)						
Si	2.6972	2.7225	2.7291	2.7181	2.6906	2.7335	2.7104
Ti	0.3069	0.3476	0.3399	0.3487	0.3399	0.3608	0.3322
Al	1.3376	1.3376	1.3354	1.3266	1.3354	1.3222	1.32
Cr	0.0033	0	0.0022	0.0022	0.0022	0.0055	0.0044
Fe	1.287	1.0065	1.001	1.0208	1.1605	0.9988	1.1605
Mn	0.0011	0.0033	0.0022	0.0022	0.0044	0	0.0022
Mg	1.2826	1.3728	1.3915	1.3706	1.2947	1.3475	1.3189
Ca	0.0033	0.0022	0.0022	0	0.0033	0	0.0022
Na	0.0143	0.0143	0.0132	0.0143	0.0176	0.0143	0.0187
K	0.7964	0.9207	0.9086	0.9427	0.9174	0.9295	0.8712
Total	7.7297	7.7275	7.7264	7.7473	7.766	7.7132	7.7418
Mol. % end-members							
Ann	50.085616	42.302358	41.83908	42.686293	47.267025	42.569151	46.805679
Phl	49.914384	57.697642	58.16092	57.313707	52.732975	57.430849	53.194321

Table B.10: Clinopyroxene analyses

Sample No.	NA23A 05_60	NA23A 05_38	NA23A 05_5	NA23A 05_30	NA23A 05_34	NA23A 05_66	NA23A 05_31	NA23A 05_70	NA46 02_4	NA46 03_74	NA46 02_3	NA46 03_43
Wt.%												
SiO2	51.5798	50.9317	52.2011	51.9346	51.9003	52.1932	52.4462	51.6293	51.5802	52.0819	51.8969	51.9646
TiO2	0.2924	0.3636	0.2198	0.1816	0.2083	0.271	0.1814	0.2263	0.2922	0.1482	0.2332	0.2421
Al2O3	3.6999	4.031	2.9144	2.8254	3.0281	2.9285	2.4142	2.6765	2.4579	1.6654	2.3258	2.2426
Cr2O3	0.0653	0	0	0.0046	0	0.0545	0.0056	0.0867	0.0132	0	0.0113	0.0295
FeO	9.7967	9.9141	9.6857	9.6167	8.9918	9.718	8.3167	9.1144	11.4308	10.1555	10.8913	10.9011
MnO	0.1792	0.17	0.1444	0.174	0.1306	0.2018	0.1055	0.1766	0.175	0.1109	0.1597	0.1654
MgO	12.3901	11.9912	12.7928	12.9449	13.0207	13.0192	13.5518	13.4579	11.8631	13.2896	12.1544	12.4265
CaO	22.1582	22.168	22.4574	22.6531	22.7041	22.7435	22.9419	23.0676	22.3087	22.4063	22.5049	22.5722
Na2O	0.9735	1.0387	0.9267	0.9357	0.9128	0.886	0.8273	0.8904	0.5659	0.4841	0.5484	0.5644
K2O	0.0363	0.0441	0.0271	0.0214	0.034	0.0371	0.0157	0.0406	0.0214	0.0259	0.035	0.0359
Total	101.1713	100.6523	101.3693	101.2919	100.9306	102.0527	100.8063	101.3662	100.7084	100.3678	100.7608	101.1442
Cations	(calculated on the basis of 6 O)											
Si	1.9134	1.9026	1.9314	1.9254	1.9254	1.9212	1.9416	1.9134	1.9362	1.9506	1.9422	1.9386
Ti	0.0084	0.0102	0.006	0.0048	0.006	0.0078	0.0048	0.0066	0.0084	0.0042	0.0066	0.0066
Al	0.162	0.1776	0.1272	0.1236	0.1326	0.1272	0.1056	0.117	0.1086	0.0738	0.1026	0.0984
Cr	0.0018	0	0	0	0	0.0018	0	0.0024	0.0006	0	0.0006	0.0006
Fe	0.3042	0.3096	0.3	0.2982	0.279	0.2994	0.2574	0.2826	0.3588	0.318	0.3408	0.3402
Mn	0.0054	0.0054	0.0048	0.0054	0.0042	0.006	0.0036	0.0054	0.0054	0.0036	0.0048	0.0054
Mg	0.6852	0.6678	0.7056	0.7152	0.72	0.7146	0.7476	0.7434	0.6642	0.7416	0.678	0.6912
Ca	0.8808	0.8874	0.8904	0.9	0.9024	0.897	0.9102	0.9162	0.8976	0.8988	0.9024	0.9024
Na	0.0702	0.075	0.0666	0.0672	0.0654	0.063	0.0594	0.0642	0.0414	0.0354	0.0396	0.0408
K	0.0018	0.0024	0.0012	0.0012	0.0018	0.0018	0.0006	0.0018	0.0012	0.0012	0.0018	0.0018
Total	4.0338	4.038	4.0338	4.0416	4.0374	4.0398	4.0314	4.053	4.023	4.0272	4.02	4.0266
Mol. % end-members												
Di	69.254093	68.324125	70.167064	70.574304	72.072072	70.473373	74.38806	72.45614	64.926686	69.988675	66.548881	67.015707
Hd	30.745907	31.675875	29.832936	29.425696	27.927928	29.526627	25.61194	27.54386	35.073314	30.011325	33.451119	32.984293

Table B.11: Clinopyroxene analyses (cont.)

Sample	NA46	NA46	NA46	NA46	NA46	NA46	NA61E	NA61E	NA61E	NA61E	NA61E	NA61E
No.	03_43	03_71	02_5	02_33	02_30	02_32	12_29	05_26	12_41	05_25	03_18	04_26
Wt.%												
SiO2	51.9646	52.1189	52.4767	51.9166	52.5099	52.0677	52.4699	51.6302	51.4782	51.5741	51.7149	51.0332
TiO2	0.2421	0.2298	0.1674	0.2018	0.1334	0.1169	0.1569	0.2508	0.3872	0.2613	0.1866	0.4788
Al2O3	2.2426	2.5892	2.0081	1.782	1.4827	1.7035	2.5628	3.2369	4.4321	3.1518	2.7271	5.5173
Cr2O3	0.0295	0.0068	0.0301	0	0	0.0005	0	0	0	0	0.0642	0.0775
FeO	10.9011	11.0138	9.9411	9.6969	9.7456	10.0772	9.1865	9.038	8.5803	8.3398	8.2183	8.2414
MnO	0.1654	0.1608	0.1219	0.0978	0.0892	0.1231	0.1566	0.1347	0.1521	0.1353	0.1422	0.1335
MgO	12.4265	11.9403	12.6489	13.1927	13.353	13.197	14.0049	13.7891	12.777	13.7101	14.0353	12.2669
CaO	22.5722	22.7497	23.0926	23.166	23.3535	23.5324	21.5204	21.75	22.1299	22.2313	22.3062	22.3174
Na2O	0.5644	0.5989	0.5671	0.5286	0.5034	0.5125	0.6427	0.7678	0.8404	0.7603	0.6774	0.9543
K2O	0.0359	0.0236	0.0254	0.0298	0.0399	0.0254	0.0205	0.0218	0.0274	0.017	0.0318	0.047
Total	101.1442	101.4317	101.0792	100.6121	101.2105	101.3561	100.7211	100.6192	100.8046	100.1809	100.1039	101.0672
Cations	(Calculated on the basis of 6 O)											
Si	1.9386	1.9386	1.9512	1.941	1.9506	1.9374	1.9422	1.9164	1.9032	1.9194	1.926	1.881
Ti	0.0066	0.0066	0.0048	0.0054	0.0036	0.003	0.0042	0.0072	0.0108	0.0072	0.0054	0.0132
Al	0.0984	0.1134	0.0882	0.0786	0.0648	0.075	0.1116	0.1416	0.1932	0.138	0.12	0.2394
Cr	0.0006	0	0.0006	0	0	0	0	0	0	0	0.0018	0.0024
Fe	0.3402	0.3426	0.309	0.303	0.303	0.3138	0.2844	0.2808	0.2652	0.2598	0.2562	0.2538
Mn	0.0054	0.0048	0.0036	0.003	0.003	0.0036	0.0048	0.0042	0.0048	0.0042	0.0042	0.0042
Mg	0.6912	0.6624	0.7008	0.735	0.7392	0.732	0.7728	0.7632	0.7044	0.7608	0.7794	0.6738
Ca	0.9024	0.9066	0.9198	0.9282	0.9294	0.9384	0.8538	0.8652	0.8766	0.8868	0.8904	0.8814
Na	0.0408	0.0432	0.0408	0.0384	0.036	0.0372	0.0462	0.0552	0.06	0.0546	0.0492	0.0684
K	0.0018	0.0012	0.0012	0.0012	0.0018	0.0012	0.0012	0.0012	0.0012	0.0006	0.0018	0.0024
Total	4.0266	4.02	4.0206	4.0338	4.0314	4.0416	4.0212	4.0356	4.02	4.0314	4.0344	4.02
Mol. % end-members												
Di	67.015707	65.910448	69.399881	70.809249	70.926885	69.994263	73.098751	73.103448	72.648515	74.544386	75.260718	72.639069
Hd	32.984293	34.089552	30.600119	29.190751	29.073115	30.005737	26.901249	26.896552	27.351485	25.455614	24.739282	27.360931

Table B.12: Clinopyroxene analyses (cont.)

Sample No.	NA61E 07_13	NA61E 03_20	NA61E 04_30	NA61E 12_39	NA61E 09_20	NA61E 02_14	NA61 19_13	NA61E 07_15	NA61E 12_31	NA61E 12_42	NA61E 09_17	NA61E 09_19	NA61E 12_30
Wt.%													
SiO2	52.0865	52.2505	52.3303	52.0326	52.4669	50.9415	51.4284	52.416	52.4317	53.0462	52.7576	52.7316	52.5471
TiO2	0.2637	0.269	0.283	0.265	0.1716	0.1591	0.212	0.1818	0.2395	0.1473	0.1847	0.1868	0.195
Al2O3	3.4188	2.6908	2.7931	3.391	2.6866	3.0134	2.69	2.8276	3.051	2.41	2.7513	2.5401	2.5623
Cr2O3	0.0066	0.0263	0.0455	0.0089	0	0	0.0106	0.01	0	0	0.0091	0	0
FeO	8.1906	7.6152	8.0051	8.3402	7.9613	7.991	7.8943	8.1937	7.7602	7.5761	7.5292	7.3147	7.2897
MnO	0.1203	0.1411	0.1724	0.114	0.1369	0.0915	0.1221	0.1426	0.1443	0.1358	0.109	0.1284	0.0885
MgO	13.6072	14.2209	13.6686	13.2107	13.6727	13.6541	13.6893	13.6185	13.1207	14.3732	13.713	13.8801	13.9531
CaO	22.3851	22.4724	22.4762	22.7424	22.752	22.8281	22.9108	22.9407	23.0265	23.1027	23.2992	23.4054	23.4168
Na2O	0.7508	0.6799	0.7078	0.7944	0.7245	0.7165	0.6795	0.7112	0.7366	0.6385	0.6949	0.6796	0.6328
K2O	0.0196	0.0374	0.0244	0.0148	0.0239	0.0174	0.007	0.0091	0.0213	0	0.023	0.0287	0.0239
Total	100.8491	100.4035	100.5063	100.9139	100.5964	99.4127	99.6441	101.0511	100.5318	101.4297	101.0709	100.8953	100.7091
Cations	(Calculated on the basis of 6 O)												
Si	1.9224	1.9332	1.9374	1.9224	1.941	1.9134	1.9254	1.9332	1.9398	1.9428	1.9404	1.9422	1.9386
Ti	0.0072	0.0072	0.0078	0.0072	0.0048	0.0042	0.006	0.0048	0.0066	0.0042	0.0054	0.0054	0.0054
Al	0.1488	0.1176	0.1218	0.1476	0.117	0.1332	0.1188	0.123	0.1332	0.1038	0.1194	0.1104	0.1116
Cr	0	0.0006	0.0012	0	0	0	0.0006	0	0	0	0	0	0
Fe	0.2526	0.2358	0.2478	0.258	0.2466	0.2508	0.2472	0.2526	0.24	0.2322	0.2316	0.2256	0.225
Mn	0.0036	0.0042	0.0054	0.0036	0.0042	0.003	0.0036	0.0042	0.0048	0.0042	0.0036	0.0042	0.003
Mg	0.7488	0.7842	0.7542	0.7278	0.7542	0.7644	0.7638	0.7488	0.7236	0.7848	0.7518	0.762	0.7674
Ca	0.885	0.891	0.8916	0.9006	0.9018	0.9186	0.9192	0.9066	0.9126	0.9066	0.918	0.9234	0.9258
Na	0.054	0.0486	0.051	0.057	0.0522	0.0522	0.0492	0.051	0.0528	0.0456	0.0498	0.0486	0.045
K	0.0012	0.0018	0.0012	0.0006	0.0012	0.0006	0.0006	0.0006	0.0012	0	0.0012	0.0012	0.0012
Total	4.0242	4.0248	4.02	4.0248	4.0236	4.0404	4.0344	4.0254	4.0152	4.0242	4.0218	4.023	4.0236
Mol. % end-members													
Di	74.775315	76.882353	75.269461	73.828363	75.359712	75.295508	75.548961	74.775315	75.0934	77.168142	76.449054	77.156744	77.32769
Hd	25.224685	23.117647	24.730539	26.171637	24.640288	24.704492	24.451039	25.224685	24.9066	22.831858	23.550946	22.843256	22.67231

Table B.13: Feldspar analyses

Sample No.	NA23A 05_1	NA23A 05_2	NA23A 05_3	NA23A 05_7	NA23A 05_8	NA23A 05_9	NA23A 05_40	NA23A 05_41	NA23A 05_43	NA23A 05_44	NA23A 05_45	NA23A 05_51
Wt.%												
SiO2	62.18	60.6044	60.1568	60.0699	60.0989	60.1413	59.9795	60.1074	59.3784	60.1634	59.5537	60.1622
TiO2	0	0	0	0	0	0	0.0244	0	0	0	0	0
Al2O3	24.6857	26.0122	26.1398	26.4021	26.331	26.2532	26.2192	25.6846	26.3646	25.5372	26.0538	26.3344
Cr2O3	0	0	0	0	0	0	0	0	0	0	0	0
FeO	0.054	0.1284	0.245	0.3641	0.292	0.7035	0.3647	0.2743	0.4729	0.2301	0.3785	0.3827
MnO	0	0	0	0	0	0	0	0	0	0	0	0
MgO	0	0	0	0	0	0.3091	0	0	0	0	0	0
CaO	5.1954	6.6132	6.8708	7.0478	7.1602	6.9852	6.9019	6.5332	7.1278	6.4197	6.9763	7.2791
Na2O	8.1812	7.478	7.4693	7.4127	7.3066	7.293	7.4606	7.5273	7.2416	7.6087	7.401	7.3106
K2O	0.4959	0.3838	0.3467	0.4004	0.3772	0.3622	0.2584	0.3054	0.3083	0.4075	0.3137	0.3412
Total	100.7922	101.2199	101.2283	101.6969	101.5658	102.0474	101.2086	100.4321	100.8935	100.3666	100.6769	101.8101
Cations	(calculated on the basis of 8 O)											
Si	2.7352	2.6656	2.6504	2.6384	2.6416	2.636	2.6448	2.6664	2.6296	2.6712	2.6416	2.64
Ti	0	0	0	0	0	0	0.0008	0	0	0	0	0
Al	1.28	1.3488	1.3576	1.3672	1.364	1.356	1.3624	1.3432	1.3768	1.3368	1.3624	1.3624
Cr	0	0	0	0	0	0	0	0	0	0	0	0
Fe	0.0016	0.0048	0.0088	0.0136	0.0104	0.0256	0.0136	0.0104	0.0176	0.0088	0.0144	0.0144
Mn	0	0	0	0	0	0	0	0	0	0	0	0
Mg	0	0	0	0	0	0.02	0	0	0	0	0	0
Ca	0.2448	0.312	0.324	0.332	0.3376	0.328	0.3264	0.3104	0.3384	0.3056	0.332	0.3424
Na	0.6976	0.6376	0.6384	0.6312	0.6224	0.62	0.6376	0.6472	0.6216	0.6552	0.6368	0.6224
K	0.028	0.0216	0.0192	0.0224	0.0208	0.02	0.0144	0.0176	0.0176	0.0232	0.0176	0.0192
Total	4.9872	4.9904	4.9992	5.0056	4.9968	5.0056	5	4.9952	5.0016	5.0008	5.0048	5.0016
Mol. % end-members												
Or	3.8588754	3.276699	2.919708	3.4271726	3.2338308	3.125	2.208589	2.6474128	2.7534418	3.4198113	2.6894866	2.9925187
Ab	74.023769	67.144061	66.334165	65.531561	64.833333	65.400844	66.141079	67.585631	64.75	68.193172	65.730801	64.510779
An	25.976231	32.855939	33.665835	34.468439	35.166667	34.599156	33.858921	32.414369	35.25	31.806828	34.269199	35.489221

Table B.14: Feldspar analyses (cont.)

Sample No.	NA23A 05_52	NA23A 05_53	NA23A 05_57	NA23A 05_59	NA23A 05_63	NA23A 05_64	NA23A 05_65	NA23A 05_67	NA23A 05_68	NA23A 05_69	NA46 03_1	NA46 03_3
Wt.%												
SiO2	61.3674	60.255	60.0025	60.0879	60.6343	60.6878	60.6806	60.5731	60.9654	60.5827	58.6396	58.7708
TiO2	0	0	0	0	0	0	0	0	0	0	0	0
Al2O3	25.5034	26.1318	26.0222	26.4849	26.4159	26.2327	26.0033	26.0937	26.0941	26.0947	26.7945	27.1022
Cr2O3	0	0	0	0	0	0	0	0.0037	0.0192	0.0037	0	0
FeO	0.1932	0.4078	0.8361	0.2066	0.6752	0.6553	0.6183	0.2929	0.7007	0.9408	0.0381	0.1659
MnO	0	0	0	0.0052	0.0328	0.0167	0.0253	0.0282	0.0368	0.0489	0	0.0017
MgO	0	0.0754	0.28	0	0	0	0	0	0	0.005	0	0
CaO	6.2114	6.8246	6.8455	7.0399	6.8482	6.9218	6.7257	6.9086	6.8661	6.753	8.0652	8.2393
Na2O	7.7965	7.4689	7.2899	7.4754	7.5481	7.5133	7.5644	7.4357	7.5316	7.4705	6.8566	6.7716
K2O	0.3768	0.3074	0.3015	0.3468	0.3427	0.3365	0.4039	0.3271	0.5124	0.4112	0.2689	0.2279
Total	101.4486	101.4708	101.5776	101.6466	102.4971	102.364	102.0214	101.6629	102.7262	102.3104	100.6628	101.2794
Cations	(calculated on the basis of 8 O)											
Si	2.6912	2.6496	2.6416	2.6384	2.644	2.6496	2.6576	2.6568	2.6552	2.6504	2.604	2.596
Ti	0	0	0	0	0	0	0	0	0	0	0	0
Al	1.3184	1.3544	1.3504	1.3704	1.3576	1.3496	1.3424	1.3488	1.3392	1.3456	1.4024	1.4112
Cr	0	0	0	0	0	0	0	0	0.0008	0	0	0
Fe	0.0072	0.0152	0.0304	0.0072	0.0248	0.024	0.0224	0.0104	0.0256	0.0344	0.0016	0.0064
Mn	0	0	0	0	0.0016	0.0008	0.0008	0.0008	0.0016	0.0016	0	0
Mg	0	0.0048	0.0184	0	0	0	0	0	0	0	0	0
Ca	0.292	0.3216	0.3232	0.3312	0.32	0.324	0.316	0.3248	0.3208	0.3168	0.384	0.3896
Na	0.6632	0.6368	0.6224	0.6368	0.6384	0.636	0.6424	0.6328	0.636	0.6336	0.5904	0.58
K	0.0208	0.0176	0.0168	0.0192	0.0192	0.0184	0.0224	0.0184	0.0288	0.0232	0.0152	0.0128
Total	4.9928	5.0008	5.0032	5.004	5.0064	5.0024	5.004	4.9928	5.008	5.0064	4.9984	4.9968
Mol. % end-members												
Or	3.0409357	2.6894866	2.6282854	2.9268293	2.919708	2.8117359	3.3694344	2.8255528	4.33213	3.5322777	2.5099075	2.1592443
Ab	69.430486	66.444073	65.820643	65.785124	66.611018	66.25	67.028381	66.081871	66.471572	66.666667	60.591133	59.818482
An	30.569514	33.555927	34.179357	34.214876	33.388982	33.75	32.971619	33.918129	33.528428	33.333333	39.408867	40.181518

Table B.15: Feldspar analyses (cont.)

Sample No.	NA46 03_5	NA46 03_8	NA46 03_10	NA46 03_39	NA46 03_41	NA46 03_45	NA46 03_46	NA46 03_65	NA46 03_67	NA46 03_70	NA46 03_80	NA46 02_8
Wt.%												
SiO2	58.7998	58.9886	58.74	58.664	58.5504	59.1496	58.2177	58.7167	58.9306	58.5111	59.1866	58.7636
TiO2	0	0	0	0	0	0	0	0	0	0	0	0
Al2O3	26.8979	27.0028	26.9757	26.8904	26.6692	26.6048	26.8199	27.0397	27.1363	27.0289	26.778	27.2685
Cr2O3	0	0	0	0	0	0	0	0	0	0	0	0
FeO	0.335	0.2809	0.0838	0.0903	0.0199	0.0118	0.2244	0.0349	0.058	0.0784	0.6267	0.0623
MnO	0.0006	0	0	0	0	0	0.0029	0	0	0	0	0
MgO	0	0	0	0	0	0	0.0278	0	0	0	0	0
CaO	8.2598	8.1024	8.228	8.1067	8.0288	7.8804	8.1439	8.1893	8.1248	8.1085	7.8391	8.1698
Na2O	6.7372	6.8106	6.7353	6.7688	6.9764	6.9406	6.8381	6.9132	6.7516	6.706	6.8727	6.8281
K2O	0.2369	0.284	0.3049	0.2827	0.2567	0.2782	0.2752	0.2881	0.254	0.2627	0.3778	0.2385
Total	101.2671	101.4692	101.0676	100.8028	100.5014	100.8654	100.5499	101.1818	101.2552	100.6955	101.6808	101.3307
Cations	(calculated on the basis of 8O)											
Si	2.5992	2.6008	2.5992	2.6016	2.6048	2.6184	2.5928	2.596	2.6	2.5968	2.608	2.5928
Ti	0	0	0	0	0	0	0	0	0	0	0	0
Al	1.4016	1.4032	1.4072	1.4056	1.3984	1.388	1.408	1.4096	1.4112	1.4144	1.3912	1.4184
Cr	0	0	0	0	0	0	0	0	0	0	0	0
Fe	0.012	0.0104	0.0032	0.0032	0.0008	0.0008	0.008	0.0016	0.0024	0.0032	0.0232	0.0024
Mn	0	0	0	0	0	0	0	0	0	0	0	0
Mg	0	0	0	0	0	0	0.0016	0	0	0	0	0
Ca	0.3912	0.3832	0.3904	0.3856	0.3824	0.3736	0.3888	0.388	0.384	0.3856	0.3704	0.3864
Na	0.5776	0.5824	0.5776	0.5824	0.6016	0.596	0.5904	0.5928	0.5776	0.5768	0.5872	0.584
K	0.0136	0.016	0.0176	0.016	0.0144	0.016	0.016	0.016	0.0144	0.0152	0.0216	0.0136
Total	4.996	4.996	4.9952	4.9952	5.0032	4.9936	5.0056	5.004	4.9896	4.9928	5.0024	4.9984
Mol. % end-members												
Or	2.300406	2.6737968	2.9569892	2.6737968	2.3376623	2.6143791	2.6385224	2.6281209	2.4324324	2.5675676	3.5479632	2.2757697
Ab	59.620149	60.31483	59.669421	60.165289	61.138211	61.468647	60.294118	60.440457	60.066556	59.9335	61.319967	60.181369
An	40.379851	39.68517	40.330579	39.834711	38.861789	38.531353	39.705882	39.559543	39.933444	40.0665	38.680033	39.818631

Table B.16: Feldspar analyses (cont.)

Sample No.	NA46 02_12	NA46 02_22	NA46 02_26	NA61C 02_5	NA61C 08_5	NA61C 08_2	NA61C 02_6	NA61C 08_8	NA61C 03_31	NA61C 02_24	NA61C 08_7	NA61C 04_18
Wt.%												
SiO2	57.715	58.3126	58.9259	61.9143	61.4376	60.9296	61.4767	61.9787	60.6999	60.6643	61.8674	62.5729
TiO2	0	0	0	0	0	0	0	0	0	0	0	0
Al2O3	27.3301	27.3322	27.3473	24.8252	25.1378	25.2044	25.404	25.202	25.0381	25.4494	25.1307	24.2984
Cr2O3	0	0	0	0	0	0	0	0	0	0	0	0
FeO	0.0779	0.0752	0.0683	0	0	0.0091	0	0.0134	0	0	0	0
MnO	0	0	0	0	0	0	0	0	0	0	0	0
MgO	0	0	0	0	0	0	0	0	0	0	0	0
CaO	7.9984	8.1142	8.1228	5.3838	5.4902	5.3044	5.8956	5.5787	5.6979	5.796	5.6952	4.5892
Na2O	6.8724	6.9348	6.8947	8.5382	8.329	8.6016	8.2264	8.5203	8.1924	8.1955	8.4651	9.004
K2O	0.2517	0.1912	0.2587	0.0669	0.1112	0.1167	0.1249	0.1291	0.1304	0.1304	0.1331	0.138
Total	100.2455	100.9601	101.6176	100.7283	100.5057	100.1657	101.1275	101.4221	99.7588	100.2355	101.2914	100.6024
Cations	(calculated on the basis of 8 O)											
Si	2.5768	2.584	2.5928	2.724	2.7104	2.7	2.6984	2.712	2.7008	2.688	2.7112	2.7528
Ti	0	0	0	0	0	0	0	0	0	0	0	0
Al	1.4384	1.4272	1.4184	1.2872	1.3072	1.3168	1.3144	1.3	1.3128	1.3288	1.2984	1.26
Cr	0	0	0	0	0	0	0	0	0	0	0	0
Fe	0.0032	0.0024	0.0024	0	0	0	0	0.0008	0	0	0	0
Mn	0	0	0	0	0	0	0	0	0	0	0	0
Mg	0	0	0	0	0	0	0	0	0	0	0	0
Ca	0.3824	0.3856	0.3832	0.2536	0.2592	0.252	0.2776	0.2616	0.272	0.2752	0.2672	0.216
Na	0.5952	0.596	0.588	0.7288	0.7128	0.7392	0.7	0.7232	0.7064	0.704	0.7192	0.768
K	0.0144	0.0112	0.0144	0.004	0.0064	0.0064	0.0072	0.0072	0.0072	0.0072	0.0072	0.008
Total	5.0112	5.0072	4.9992	4.9984	4.9968	5.0152	4.9984	5.0048	4.9992	5.0032	5.004	5.0048
Mol. % end-members												
Or	2.3622047	1.8445323	2.3904382	0.5458515	0.8898776	0.8583691	1.0180995	0.9857612	1.0089686	1.0123735	0.9911894	1.0309278
Ab	60.883797	60.717196	60.543657	74.185668	73.333333	74.576271	71.603928	73.436231	72.199509	71.895425	72.911598	78.04878
An	39.116203	39.282804	39.456343	25.814332	26.666667	25.423729	28.396072	26.563769	27.800491	28.104575	27.088402	21.95122

Table B.17: Feldspar analyses (cont.)

Sample No.	NA61C 08_3	NA61C 08_1	NA61C 02_25	NA61C 02_8	NA61C 03_9	NA61C 02_7	NA61C 03_1	NA61C 03_30	NA61C 02_9	NA61C 02_23	NA61C 03_8	NA61C 03_11
Wt.%												
SiO2	61.3387	60.7467	60.822	61.0605	61.4654	61.427	61.0995	60.4275	61.4278	60.6349	61.1177	61.2583
TiO2	0	0	0	0	0	0	0	0	0	0	0	0
Al2O3	25.1807	25.0281	25.3526	25.5543	25.3462	25.3294	25.3126	25.2108	25.3501	25.5611	25.357	25.5136
Cr2O3	0	0	0	0	0	0	0	0	0	0	0	0
FeO	0.0059	0	0	0.0204	0.0841	0.0086	0	0.0123	0.1043	0.021	0.0225	0.0916
MnO	0	0	0	0	0	0	0	0	0	0	0	0
MgO	0	0	0	0	0	0	0	0	0	0	0	0
CaO	5.6297	5.3687	5.6737	5.9347	5.795	5.8376	5.82	5.8738	5.9004	5.8475	6.0017	5.988
Na2O	8.4227	8.454	8.2223	8.1665	8.1828	8.0329	8.16	8.0959	8.0246	8.0464	8.2158	8.1297
K2O	0.1432	0.1501	0.1506	0.1748	0.1792	0.1821	0.1864	0.1918	0.1967	0.199	0.2092	0.2097
Total	100.7208	99.7477	100.2211	100.9111	101.0527	100.8175	100.5784	99.8122	101.0038	100.3098	100.9238	101.1908
Cations	(calculated on the basis of 8 O)											
Si	2.704	2.7032	2.6936	2.688	2.7008	2.7032	2.6976	2.6904	2.7	2.6848	2.692	2.6904
Ti	0	0	0	0	0	0	0	0	0	0	0	0
Al	1.308	1.3128	1.324	1.3264	1.3128	1.3136	1.3168	1.3232	1.3136	1.3344	1.3168	1.3208
Cr	0	0	0	0	0	0	0	0	0	0	0	0
Fe	0	0	0	0.0008	0.0032	0	0	0.0008	0.004	0.0008	0.0008	0.0032
Mn	0	0	0	0	0	0	0	0	0	0	0	0
Mg	0	0	0	0	0	0	0	0	0	0	0	0
Ca	0.2656	0.256	0.2696	0.28	0.2728	0.2752	0.2752	0.28	0.2776	0.2776	0.2832	0.2816
Na	0.72	0.7296	0.7064	0.6968	0.6968	0.6856	0.6984	0.6992	0.684	0.6912	0.7016	0.692
K	0.008	0.0088	0.0088	0.0096	0.0104	0.0104	0.0104	0.0112	0.0112	0.0112	0.012	0.012
Total	5.0064	5.0104	5.0024	5.0024	4.9976	4.988	4.9984	5.0048	4.9912	5.0008	5.0072	5.0042
Mol. % end-members												
Or	1.0989011	1.191766	1.2304251	1.3590034	1.4705882	1.4942529	1.4672686	1.5765766	1.6110472	1.594533	1.6816143	1.7045455
Ab	73.051948	74.025974	72.377049	71.334971	71.864686	71.357202	71.733772	71.405229	71.131448	71.345995	71.242892	71.076417
An	26.948052	25.974026	27.622951	28.665029	28.135314	28.642798	28.266228	28.594771	28.868552	28.654005	28.757108	28.923583

Table B.18: Feldspar analyses (cont.)

Sample No.	NA46 02_12	NA46 02_22	NA46 02_26	NA61C 02_5	NA61C 08_5	NA61C 08_2	NA61C 02_6	NA61C 08_8	NA61C 03_31	NA61C 02_24	NA61C 08_7	NA61C 04_18
Wt.%												
SiO2	57.715	58.3126	58.9259	61.9143	61.4376	60.9296	61.4767	61.9787	60.6999	60.6643	61.8674	62.5729
TiO2	0	0	0	0	0	0	0	0	0	0	0	0
Al2O3	27.3301	27.3322	27.3473	24.8252	25.1378	25.2044	25.404	25.202	25.0381	25.4494	25.1307	24.2984
Cr2O3	0	0	0	0	0	0	0	0	0	0	0	0
FeO	0.0779	0.0752	0.0683	0	0	0.0091	0	0.0134	0	0	0	0
MnO	0	0	0	0	0	0	0	0	0	0	0	0
MgO	0	0	0	0	0	0	0	0	0	0	0	0
CaO	7.9984	8.1142	8.1228	5.3838	5.4902	5.3044	5.8956	5.5787	5.6979	5.796	5.6952	4.5892
Na2O	6.8724	6.9348	6.8947	8.5382	8.329	8.6016	8.2264	8.5203	8.1924	8.1955	8.4651	9.004
K2O	0.2517	0.1912	0.2587	0.0669	0.1112	0.1167	0.1249	0.1291	0.1304	0.1304	0.1331	0.138
Total	100.2455	100.9601	101.6176	100.7283	100.5057	100.1657	101.1275	101.4221	99.7588	100.2355	101.2914	100.6024
Cations	(calculated on the basis of 8 O)											
Si	2.5768	2.584	2.5928	2.724	2.7104	2.7	2.6984	2.712	2.7008	2.688	2.7112	2.7528
Ti	0	0	0	0	0	0	0	0	0	0	0	0
Al	1.4384	1.4272	1.4184	1.2872	1.3072	1.3168	1.3144	1.3	1.3128	1.3288	1.2984	1.26
Cr	0	0	0	0	0	0	0	0	0	0	0	0
Fe	0.0032	0.0024	0.0024	0	0	0	0	0.0008	0	0	0	0
Mn	0	0	0	0	0	0	0	0	0	0	0	0
Mg	0	0	0	0	0	0	0	0	0	0	0	0
Ca	0.3824	0.3856	0.3832	0.2536	0.2592	0.252	0.2776	0.2616	0.272	0.2752	0.2672	0.216
Na	0.5952	0.596	0.588	0.7288	0.7128	0.7392	0.7	0.7232	0.7064	0.704	0.7192	0.768
K	0.0144	0.0112	0.0144	0.004	0.0064	0.0064	0.0072	0.0072	0.0072	0.0072	0.0072	0.008
Total	5.0112	5.0072	4.9992	4.9984	4.9968	5.0152	4.9984	5.0048	4.9992	5.0032	5.004	5.0048
Mol. % end-members												
Or	2.3622047	1.8445323	2.3904382	0.5458515	0.8898776	0.8583691	1.0180995	0.9857612	1.0089686	1.0123735	0.9911894	1.0309278
Ab	60.883797	60.717196	60.543657	74.185668	73.333333	74.576271	71.603928	73.436231	72.199509	71.895425	72.911598	78.04878
An	39.116203	39.282804	39.456343	25.814332	26.666667	25.423729	28.396072	26.563769	27.800491	28.104575	27.088402	21.95122

Table B.19: Feldspar analyses (cont.)

Sample No.	NA61C 08_3	NA61C 08_1	NA61C 02_25	NA61C 02_8	NA61C 03_9	NA61C 02_7	NA61C 03_1	NA61C 03_30	NA61C 02_9	NA61C 02_23	NA61C 03_8	NA61C 03_11
Wt.%												
SiO2	61.3387	60.7467	60.822	61.0605	61.4654	61.427	61.0995	60.4275	61.4278	60.6349	61.1177	61.2583
TiO2	0	0	0	0	0	0	0	0	0	0	0	0
Al2O3	25.1807	25.0281	25.3526	25.5543	25.3462	25.3294	25.3126	25.2108	25.3501	25.5611	25.357	25.5136
Cr2O3	0	0	0	0	0	0	0	0	0	0	0	0
FeO	0.0059	0	0	0.0204	0.0841	0.0086	0	0.0123	0.1043	0.021	0.0225	0.0916
MnO	0	0	0	0	0	0	0	0	0	0	0	0
MgO	0	0	0	0	0	0	0	0	0	0	0	0
CaO	5.6297	5.3687	5.6737	5.9347	5.795	5.8376	5.82	5.8738	5.9004	5.8475	6.0017	5.988
Na2O	8.4227	8.454	8.2223	8.1665	8.1828	8.0329	8.16	8.0959	8.0246	8.0464	8.2158	8.1297
K2O	0.1432	0.1501	0.1506	0.1748	0.1792	0.1821	0.1864	0.1918	0.1967	0.199	0.2092	0.2097
Total	100.7208	99.7477	100.2211	100.9111	101.0527	100.8175	100.5784	99.8122	101.0038	100.3098	100.9238	101.1908
Cations	(calculated on the basis of 8 O)											
Si	2.704	2.7032	2.6936	2.688	2.7008	2.7032	2.6976	2.6904	2.7	2.6848	2.692	2.6904
Ti	0	0	0	0	0	0	0	0	0	0	0	0
Al	1.308	1.3128	1.324	1.3264	1.3128	1.3136	1.3168	1.3232	1.3136	1.3344	1.3168	1.3208
Cr	0	0	0	0	0	0	0	0	0	0	0	0
Fe	0	0	0	0.0008	0.0032	0	0	0.0008	0.004	0.0008	0.0008	0.0032
Mn	0	0	0	0	0	0	0	0	0	0	0	0
Mg	0	0	0	0	0	0	0	0	0	0	0	0
Ca	0.2656	0.256	0.2696	0.28	0.2728	0.2752	0.2752	0.28	0.2776	0.2776	0.2832	0.2816
Na	0.72	0.7296	0.7064	0.6968	0.6968	0.6856	0.6984	0.6992	0.684	0.6912	0.7016	0.692
K	0.008	0.0088	0.0088	0.0096	0.0104	0.0104	0.0104	0.0112	0.0112	0.0112	0.012	0.012
Total	5.0064	5.0104	5.0024	5.0024	4.9976	4.988	4.9984	5.0048	4.9912	5.0008	5.0072	5
Mol. % end-members												
Or	1.0989011	1.191766	1.2304251	1.3590034	1.4705882	1.4942529	1.4672686	1.5765766	1.6110472	1.594533	1.6816143	1.7045455
Ab	73.051948	74.025974	72.377049	71.334971	71.864686	71.357202	71.733772	71.405229	71.131448	71.345995	71.242892	71.076417
An	26.948052	25.974026	27.622951	28.665029	28.135314	28.642798	28.266228	28.594771	28.868552	28.654005	28.757108	28.923583

Table B.20: Feldspar analyses (cont.)

Sample No.	NA61C 03_28	NA61C 02_30	NA61C 06_2	NA61C 03_10	NA61C 07_1	NA61C 02_33	NA61C 03_29	NA61C 02_39	NA61C 06_17	NA61C 02_28	NA61C 06_15	NA61C 07_3
Wt.%												
SiO2	59.178	61.2875	61.5466	61.6198	61.0395	61.1722	60.5907	61.574	61.1164	61.5197	60.9619	60.9841
TiO2	0	0	0	0	0	0	0	0	0	0	0	0
Al2O3	25.6251	25.3138	25.5411	25.4844	25.4583	25.1676	25.2883	25.4793	25.3536	25.2146	25.4194	25.4063
Cr2O3	0	0	0	0	0	0	0	0	0	0	0	0
FeO	1.7118	0.7345	0.7506	0.2827	0.1601	0.224	0.052	0.7109	0.2173	0.3558	0.243	0.0145
MnO	0	0	0	0	0	0	0	0	0	0	0	0
MgO	0.3545	0	0	0	0	0	0	0	0	0	0	0
CaO	3.3798	6.0393	5.9805	5.7093	6.235	6.0368	5.6692	5.9617	6.255	6.1723	5.93	6.2606
Na2O	7.6058	8.1361	8.2141	8.2395	7.9277	7.9373	8.0976	8.0868	7.9024	7.9891	7.9551	7.8401
K2O	0.2199	0.2261	0.2358	0.2581	0.2627	0.2934	0.2969	0.3025	0.3119	0.3127	0.3138	0.3203
Total	98.075	101.7372	102.2686	101.5937	101.0833	100.8312	99.9948	102.1151	101.1565	101.5641	100.8231	100.8259
Cations	(calculated on the basis of 8 O)											
Si	2.6784	2.6872	2.6848	2.6968	2.6864	2.6984	2.692	2.6888	2.6896	2.6968	2.6896	2.6896
Ti	0	0	0	0	0	0	0	0	0	0	0	0
Al	1.3672	1.308	1.3128	1.3144	1.3208	1.3088	1.324	1.3112	1.3152	1.3032	1.3216	1.3208
Cr	0	0	0	0	0	0	0	0	0	0	0	0
Fe	0.0648	0.0272	0.0272	0.0104	0.0056	0.008	0.0016	0.0256	0.008	0.0128	0.0088	0.0008
Mn	0	0	0	0	0	0	0	0	0	0	0	0
Mg	0.024	0	0	0	0	0	0	0	0	0	0	0
Ca	0.164	0.284	0.2792	0.268	0.2944	0.2856	0.2696	0.2792	0.2952	0.2896	0.28	0.296
Na	0.6672	0.692	0.6944	0.6992	0.6768	0.6792	0.6976	0.6848	0.6744	0.6792	0.6808	0.6704
K	0.0128	0.0128	0.0128	0.0144	0.0144	0.0168	0.0168	0.0168	0.0176	0.0176	0.0176	0.0184
Total	4.9784	5.012	5.012	5.0032	4.9984	4.9976	5.0016	5.0072	5.0008	4.9992	4.9992	4.9968
Mol. % end-members												
Or	1.8823529	1.816118	1.8099548	2.0179372	2.0833333	2.4137931	2.3516237	2.3945268	2.5433526	2.5258324	2.5200458	2.6713124
Ab	80.26949	70.901639	71.322925	72.29115	69.686985	70.39801	72.125724	71.037344	69.554455	70.107349	70.857619	69.370861
An	19.73051	29.098361	28.677075	27.70885	30.313015	29.60199	27.874276	28.962656	30.445545	29.892651	29.142381	30.629139

Table B.21: Feldspar analyses (cont.)

Sample No.	NA61C 06_3	NA61C 02_22	NA61E 05_17	NA61E 05_18	NA61E 05_19	NA61E 05_20	NA61E 05_21	NA61E 05_22	NA61E 05_23	NA61E 05_24	NA61E 02_5	NA61E 02_6
Wt.%												
SiO2	61.0184	60.5758	57.555	57.0312	57.2443	56.9958	57.0065	57.3608	57.9413	57.8491	56.047	56.0232
TiO2	0	0	0	0	0	0	0	0	0	0	0	0
Al2O3	25.224	25.3076	26.0544	26.4377	26.5902	26.6883	26.8537	27.0466	27.0351	27.0586	27.2193	27.0766
Cr2O3	0	0	0	0	0	0	0	0	0	0	0	0
FeO	0.2248	0.2273	0.2365	0.2319	0.3911	0.1341	0.2061	0.2623	0.1434	0.1513	0.1871	0.0773
MnO	0	0	0	0	0	0	0.0006	0	0	0	0	0
MgO	0	0	0	0	0	0	0	0	0	0	0	0
CaO	5.4194	5.1176	6.6622	7.2294	7.4164	7.7438	7.8895	7.8245	7.9053	8.0572	8.279	8.089
Na2O	7.9727	7.9129	7.4691	7.1247	6.9949	6.907	6.8519	6.872	6.7855	6.7421	6.674	6.7496
K2O	0.3807	0.6616	0.4864	0.49	0.411	0.4178	0.4143	0.3888	0.4175	0.4347	0.2473	0.33
Total	100.2399	99.8029	98.4637	98.545	99.048	98.8869	99.2226	99.7551	100.2281	100.2929	98.6538	98.3458
Cations	(calculated on the basis of 8 O)											
Si	2.7032	2.6976	2.6152	2.5928	2.5896	2.5824	2.576	2.5776	2.588	2.584	2.5496	2.5552
Ti	0	0	0	0	0	0	0	0	0	0	0	0
Al	1.3168	1.328	1.3952	1.4168	1.4184	1.4256	1.4304	1.432	1.4232	1.4248	1.4592	1.456
Cr	0	0	0	0	0	0	0	0	0	0	0	0
Fe	0.008	0.0088	0.0088	0.0088	0.0152	0.0048	0.008	0.0096	0.0056	0.0056	0.0072	0.0032
Mn	0	0	0	0	0	0	0	0	0	0	0	0
Mg	0	0	0	0	0	0	0	0	0	0	0	0
Ca	0.2576	0.244	0.324	0.352	0.3592	0.376	0.3824	0.3768	0.3784	0.3856	0.4032	0.3952
Na	0.6848	0.6832	0.6584	0.628	0.6136	0.6072	0.6008	0.5984	0.588	0.584	0.5888	0.5968
K	0.0216	0.0376	0.028	0.0288	0.024	0.024	0.024	0.0224	0.024	0.0248	0.0144	0.0192
Total	4.9928	4.9992	5.0304	5.028	5.0208	5.0208	5.0224	5.0176	5.008	5.0096	5.0224	5.0264
Mol. % end-members												
Or	3.0577576	5.2164262	4.0792541	4.3848965	3.7641154	3.8022814	3.8412292	3.6082474	3.9215686	4.0735874	2.3872679	3.1168831
Ab	72.665535	73.684211	67.019544	64.081633	63.075658	61.757526	61.106591	61.361772	60.844371	60.231023	59.354839	60.16129
An	27.334465	26.315789	32.980456	35.918367	36.924342	38.242474	38.893409	38.638228	39.155629	39.768977	40.645161	39.83871

Table B.23: Feldspar analyses (cont.)

Sample No.	NA61E 03_11	NA61E 03_14	NA61E 03_17	NA61E 04_15	NA61E 04_17	NA61E 04_20	NA61E 04_21	NA61E 04_22	NA61E 04_23	NA61E 04_24	NA61E 04_25	NA61E 04_28
Wt.%												
SiO2	55.8767	59.9353	58.019	60.7549	59.1017	58.5419	59.0353	59.0962	59.5013	58.8299	59.3744	59.1666
TiO2	0	0.0074	0	0	0	0.0129	0.0061	0.0088	0.002	0.0122	0.0142	0.0108
Al2O3	27.2552	26.1995	27.2702	25.918	26.883	27.0971	26.807	26.8789	26.6623	27.1823	26.5906	26.8542
Cr2O3	0	0	0.0246	0	0	0	0	0	0	0	0.0061	0.0111
FeO	0.2083	0.1838	0.1854	0.3217	0.2817	0.1587	0.1433	0.1268	0.2429	0.2972	0.2115	0.2193
MnO	0	0	0.0063	0.0063	0.0046	0	0	0	0	0.016	0.0126	0.0029
MgO	0	0	0	0	0	0	0	0	0	0	0	0
CaO	8.2621	6.9404	7.932	6.3321	7.8587	7.7984	7.5965	7.6762	7.3089	8.0341	7.2654	7.71
Na2O	6.6199	7.2582	6.6003	7.4996	6.8979	6.7941	6.9804	6.8596	7.0157	6.7506	7.0861	6.8272
K2O	0.3464	0.4697	0.3665	0.6778	0.3644	0.3558	0.4034	0.3943	0.414	0.3466	0.4425	0.4942
Total	98.5687	100.9942	100.4043	101.5104	101.3919	100.7589	100.972	101.0407	101.147	101.4688	101.0033	101.2962
Cations	(calculated on the basis of 8 O)											
Si	2.5456	2.6472	2.5848	2.6688	2.608	2.5976	2.6128	2.6128	2.6264	2.5952	2.6256	2.612
Ti	0	0	0	0	0	0.0008	0	0	0	0.0008	0.0008	0
Al	1.4632	1.364	1.432	1.3424	1.3984	1.4168	1.3984	1.4008	1.3872	1.4128	1.3856	1.3976
Cr	0	0	0.0008	0	0	0	0	0	0	0	0	0
Fe	0.008	0.0064	0.0072	0.012	0.0104	0.0056	0.0056	0.0048	0.0088	0.0112	0.008	0.008
Mn	0	0	0	0	0	0	0	0	0	0.0008	0.0008	0
Mg	0	0	0	0	0	0	0	0	0	0	0	0
Ca	0.4032	0.3288	0.3784	0.2984	0.3712	0.3704	0.36	0.364	0.3456	0.38	0.344	0.3648
Na	0.5848	0.6216	0.5704	0.6392	0.5904	0.5848	0.5992	0.588	0.6008	0.5776	0.6072	0.584
K	0.02	0.0264	0.0208	0.0376	0.0208	0.02	0.0224	0.0224	0.0232	0.0192	0.0248	0.028
Total	5.0248	4.9952	4.9952	4.9984	4.9992	4.996	4.9984	4.9928	4.9928	4.9976	4.9976	4.9952
Mol. % end-members												
Or	3.3068783	4.0740741	3.5182679	5.5555556	3.4031414	3.3068783	3.6036036	3.6697248	3.7179487	3.2171582	3.9240506	4.5751634
Ab	59.190283	65.40404	60.118044	68.174061	61.397671	61.222781	62.468724	61.764706	63.482671	60.31746	63.835156	61.551433
An	40.809717	34.59596	39.881956	31.825939	38.602329	38.777219	37.531276	38.235294	36.517329	39.68254	36.164844	38.448567

Table B.24: Feldspar analyses (cont.)

Sample No.	NA61E 07_18	NA61E 07_19	NA61E 07_20	NA61E 07_21	NA61E 07_22	NA61E 07_23	NA61E 07_24	NA61E 07_25	NA61E 07_26	NA61E 07_28	NA61E 07_29	NA61E 07_30
Wt.%												
SiO2	59.1564	59.1311	58.5811	59.0192	58.9309	59.4008	58.7102	58.5655	58.8457	57.9033	59.0549	58.6777
TiO2	0	0	0	0	0	0	0	0	0	0	0	0
Al2O3	26.933	26.9796	27.2841	26.9886	27.0889	26.9567	27.0055	27.4662	27.1611	25.8899	26.8741	27.1512
Cr2O3	0	0	0	0	0	0	0	0	0	0	0	0
FeO	0.1506	0.0969	0.1107	0.0559	0.1485	0.1027	0.1362	0.1277	0.0756	0.8499	0.0915	0.0814
MnO	0	0	0	0	0	0	0	0	0	0	0	0
MgO	0	0	0	0	0	0	0	0	0	0.7865	0	0
CaO	7.6812	7.7919	7.9932	7.8326	7.8041	7.5805	7.8952	8.1018	7.8831	7.3468	7.8071	7.979
Na2O	6.8955	6.8313	6.858	6.9587	6.7665	7.0127	6.8495	6.7494	6.8217	6.4616	6.8328	6.8988
K2O	0.4124	0.3619	0.3414	0.3907	0.4006	0.3715	0.3464	0.2606	0.3144	0.5007	0.3226	0.3207
Total	101.229	101.1926	101.1684	101.2457	101.1394	101.4249	100.9429	101.2711	101.1015	99.7387	100.9829	101.1087
Cations	(calculated on the basis of 8 O)											
Si	2.6112	2.6096	2.5904	2.6056	2.604	2.6152	2.6008	2.5856	2.6	2.6032	2.612	2.5952
Ti	0	0	0	0	0	0	0	0	0	0	0	0
Al	1.4016	1.404	1.4224	1.4048	1.4104	1.3992	1.4104	1.4296	1.4144	1.372	1.4008	1.4152
Cr	0	0	0	0	0	0	0	0	0	0	0	0
Fe	0.0056	0.0032	0.004	0.0024	0.0056	0.004	0.0048	0.0048	0.0024	0.032	0.0032	0.0032
Mn	0	0	0	0	0	0	0	0	0	0	0	0
Mg	0	0	0	0	0	0	0	0	0	0.0528	0	0
Ca	0.3632	0.3688	0.3784	0.3704	0.3696	0.3576	0.3744	0.3832	0.3736	0.3536	0.3696	0.3784
Na	0.5904	0.5848	0.588	0.596	0.58	0.5984	0.588	0.5776	0.5848	0.5632	0.5856	0.592
K	0.0232	0.02	0.0192	0.0224	0.0224	0.0208	0.0192	0.0144	0.0176	0.0288	0.0184	0.0184
Total	4.996	4.9904	5.0032	5.0016	4.9928	4.996	4.9976	4.9952	4.9928	5.0064	4.9904	5.0024
Mol. % end-members												
Or	3.7809648	3.3068783	3.1620553	3.622251	3.7184595	3.3591731	3.1620553	2.4324324	2.9216467	4.8648649	3.0463576	3.0144168
Ab	61.912752	61.325503	60.844371	61.672185	61.078349	62.594142	61.097257	60.11657	61.018364	61.431065	61.306533	61.005771
An	38.087248	38.674497	39.155629	38.327815	38.921651	37.405858	38.902743	39.88343	38.981636	38.568935	38.693467	38.994229

Table B.25: Feldspar analyses (cont.)

Sample No.	NA61E 09_22	NA61E 09_23	NA61E 09_24	NA61E 09_27	NA61E 09_28	NA61E 09_29	NA61E 09_30	NA61E 09_31	NA61E 09_32	NA61E 09_33	NA61E 09_34	NA61E 09_35
Wt.%												
SiO2	58.7017	59.1548	58.0664	57.9829	58.4629	57.8269	58.149	58.125	57.9087	57.9645	58.1455	58.4708
TiO2	0	0	0	0	0	0	0	0	0	0	0	0
Al2O3	26.9976	26.5873	27.3897	26.9001	26.6501	26.9144	26.5644	26.4655	26.6646	26.61	26.9658	27.1049
Cr2O3	0	0	0	0	0	0	0	0	0	0	0	0
FeO	0.2298	0.1643	0.3632	0.1558	0.1617	0.2064	0.1723	0.2484	0.225	0.2127	0.3573	0.0963
MnO	0	0	0	0	0	0	0	0	0	0	0	0.0137
MgO	0	0	0	0	0	0	0	0	0	0	0	0
CaO	7.9947	7.7648	8.4384	8.2769	8.1204	8.4482	7.9257	7.9059	8.01	8.0623	8.2113	8.1369
Na2O	6.8583	6.9367	6.6219	6.7832	6.8723	6.5836	6.8841	6.7901	6.9049	6.779	6.8238	6.796
K2O	0.3673	0.3716	0.289	0.3135	0.3217	0.4151	0.3804	0.3871	0.3357	0.3212	0.345	0.2789
Total	101.1493	100.9794	101.1685	100.4123	100.589	100.3945	100.0758	99.9221	100.0488	99.9498	100.8486	100.8974
Cations	(calculated on the basis of 8 O)											
Si	2.5976	2.6184	2.5736	2.5872	2.6016	2.5832	2.6016	2.604	2.5936	2.5968	2.5856	2.592
Ti	0	0	0	0	0	0	0	0	0	0	0	0
Al	1.408	1.3872	1.4312	1.4144	1.3984	1.4168	1.4008	1.3976	1.4072	1.4048	1.4136	1.4168
Cr	0	0	0	0	0	0	0	0	0	0	0	0
Fe	0.0088	0.0064	0.0136	0.0056	0.0064	0.008	0.0064	0.0096	0.0088	0.008	0.0136	0.0032
Mn	0	0	0	0	0	0	0	0	0	0	0	0.0008
Mg	0	0	0	0	0	0	0	0	0	0	0	0
Ca	0.3792	0.368	0.4008	0.396	0.3872	0.404	0.38	0.3792	0.384	0.3872	0.3912	0.3864
Na	0.5888	0.5952	0.5688	0.5872	0.5928	0.5704	0.5968	0.5896	0.5992	0.5888	0.588	0.584
K	0.0208	0.0208	0.016	0.0176	0.0184	0.024	0.0216	0.0224	0.0192	0.0184	0.0192	0.016
Total	5.004	4.9968	5.0048	5.008	5.0048	5.0064	5.008	5.0032	5.0128	5.0048	5.012	4.9992
Mol. % end-members												
Or	3.4120735	3.3766234	2.7359781	2.9100529	3.0104712	4.0376851	3.4928849	3.6601307	3.1047865	3.030303	3.1620553	2.6666667
Ab	60.826446	61.79402	58.663366	59.723352	60.489796	58.538588	61.097461	60.858794	60.943857	60.327869	60.04902	60.181369
An	39.173554	38.20598	41.336634	40.276648	39.510204	41.461412	38.902539	39.141206	39.056143	39.672131	39.95098	39.818631

Table B.26: Feldspar analyses (cont.)

Sample No.	NA61E 09_36	NA61E 09_37	NA61E 09_38	NA61E 12_22	NA61E 12_23	NA61E 12_24	NA61E 12_25	NA61E 12_26	NA61E 12_27	NA61E 12_28	NA61E 12_36	NA61E 12_43
Wt.%												
SiO2	58.6666	59.1896	57.7045	58.962	59.2548	59.2095	59.1081	58.8294	58.8806	58.7714	58.5606	58.9654
TiO2	0	0	0	0	0	0	0	0	0	0	0	0
Al2O3	26.3944	26.5929	25.8055	26.8027	26.7552	26.7615	26.7811	27.0028	27.0237	26.7257	26.9861	26.8156
Cr2O3	0	0	0	0	0	0	0	0	0	0	0	0
FeO	0.3994	0.0266	0.8107	0.3451	0.3643	0.1787	0.2723	0.1356	0.3845	0.1723	0.1287	0.9263
MnO	0	0.012	0	0	0	0	0	0	0	0	0	0.0017
MgO	0.186	0	0.61	0	0	0	0	0	0	0	0	0.0661
CaO	7.8245	7.6703	7.5445	7.7912	7.7125	7.6021	7.7476	7.8744	8.0365	7.7897	7.9821	7.5415
Na2O	6.8127	6.9252	6.5869	6.9277	7.0082	7.0235	6.9138	6.9124	6.8171	6.9156	6.8799	6.9374
K2O	0.3741	0.355	0.4007	0.4251	0.4184	0.4407	0.4148	0.3273	0.3258	0.3562	0.3011	0.4679
Total	100.6576	100.7716	99.4629	101.2537	101.5134	101.216	101.2376	101.0818	101.4681	100.7309	100.8384	101.7218
Cations	(calculated on the basis of 8 O)											
Si	2.6096	2.6224	2.6032	2.6072	2.6128	2.6152	2.612	2.6024	2.5984	2.6088	2.5976	2.6016
Ti	0	0	0	0	0	0	0	0	0	0	0	0
Al	1.384	1.3888	1.372	1.3968	1.3904	1.3936	1.3944	1.408	1.4056	1.3984	1.4112	1.3944
Cr	0	0	0	0	0	0	0	0	0	0	0	0
Fe	0.0152	0.0008	0.0304	0.0128	0.0136	0.0064	0.0104	0.0048	0.0144	0.0064	0.0048	0.0344
Mn	0	0.0008	0	0	0	0	0	0	0	0	0	0
Mg	0.012	0	0.0408	0	0	0	0	0	0	0	0	0.004
Ca	0.3728	0.364	0.3648	0.3688	0.364	0.36	0.3664	0.3736	0.38	0.3704	0.3792	0.3568
Na	0.588	0.5952	0.576	0.5936	0.5992	0.6016	0.592	0.5928	0.5832	0.5952	0.592	0.5936
K	0.0216	0.02	0.0232	0.024	0.0232	0.0248	0.0232	0.0184	0.0184	0.02	0.0168	0.0264
Total	5.004	4.9928	5.0104	5.004	5.004	5.0024	4.9984	5.0008	5.0008	4.9992	5.0016	5.012
Mol. % end-members												
Or	3.5433071	3.2509753	3.8718291	3.8860104	3.7275064	3.9591315	3.7711313	3.0104712	3.0585106	3.2509753	2.7595269	4.2580645
Ab	61.199001	62.05171	61.22449	61.679135	62.209302	62.562396	61.769616	61.34106	60.548173	61.640431	60.955519	62.457912
An	38.800999	37.94829	38.77551	38.320865	37.790698	37.437604	38.230384	38.65894	39.451827	38.359569	39.044481	37.542088

Table B.27: Feldspar analyses (cont.)

Sample No.	NA61E 12_49	NA61E 20_25	NA61E 20_26	NA61E 20_27	NA61E 20_28	NA61E 20_29	NA61E 20_30	NA61E 20_31	NA61E 20_45	NA61E 20_46	NA61E 20_47	NA61E 20_48
Wt.%												
SiO2	59.1078	57.9447	58.375	57.795	57.9926	57.788	58.4827	57.9726	57.8134	57.5666	58.5859	58.1269
TiO2	0	0	0	0	0	0	0	0	0	0	0	0
Al2O3	27.0606	26.6726	26.342	26.4344	26.6035	26.587	26.3176	26.1979	26.2811	26.3102	26.4891	26.4
Cr2O3	0	0	0	0	0	0	0	0	0	0	0	0
FeO	0.4424	0.0885	0.029	0.0991	0.1442	0.2127	0.059	0	0.0893	0.2672	0.0957	0.2304
MnO	0	0	0	0	0	0	0	0	0	0	0	0
MgO	0	0	0	0	0	0	0	0	0	0	0	0
CaO	7.5039	7.8902	7.4793	7.6223	7.6482	7.9034	7.4727	7.4044	7.8569	7.7822	7.8265	7.7624
Na2O	7.0394	6.8111	7.0316	6.8885	6.9341	6.7678	6.9537	6.9067	6.8251	6.9282	7.0267	6.8193
K2O	0.35	0.3374	0.3519	0.3663	0.3545	0.326	0.3698	0.3311	0.3026	0.2532	0.2674	0.3253
Total	101.504	99.7446	99.6089	99.2057	99.6772	99.585	99.6555	98.8128	99.1685	99.1077	100.2913	99.6644
Cations	(calculated on the basis of 8 O)											
Si	2.6048	2.5984	2.6176	2.6048	2.6024	2.5976	2.6208	2.6184	2.6072	2.6008	2.612	2.6088
Ti	0	0	0	0	0	0	0	0	0	0	0	0
Al	1.4056	1.4096	1.392	1.404	1.4072	1.4088	1.3904	1.3952	1.3968	1.4008	1.392	1.3968
Cr	0	0	0	0	0	0	0	0	0	0	0	0
Fe	0.016	0.0032	0.0008	0.004	0.0056	0.008	0.0024	0	0.0032	0.0104	0.0032	0.0088
Mn	0	0	0	0	0	0	0	0	0	0	0	0
Mg	0	0	0	0	0	0	0	0	0	0	0	0
Ca	0.3544	0.3792	0.3592	0.368	0.368	0.3808	0.3584	0.3584	0.38	0.3768	0.3736	0.3736
Na	0.6016	0.592	0.6112	0.6024	0.6032	0.5896	0.604	0.6048	0.5968	0.6072	0.6072	0.5936
K	0.02	0.0192	0.02	0.0208	0.02	0.0184	0.0208	0.0192	0.0176	0.0144	0.0152	0.0184
Total	5.0024	5.0024	5.0016	5.0048	5.0072	5.004	4.9976	4.9968	5.0016	5.0104	5.004	5.0008
Mol. % end-members												
Or	3.2175032	3.1413613	3.1685678	3.3376123	3.2092426	3.0263158	3.3290653	3.0769231	2.8645833	2.3166023	2.4421594	3.0065359
Ab	62.92887	60.955519	62.984336	62.077494	62.108731	60.75845	62.759767	62.790698	61.097461	61.707317	61.908646	61.373036
An	37.07113	39.044481	37.015664	37.922506	37.891269	39.24155	37.240233	37.209302	38.902539	38.292683	38.091354	38.626964

Table B.28: Feldspar analyses (cont.)

Sample No.	NA61E 20_49	NA61E 20_50	NA61E 20_51	NA61E 19_16	NA61E 19_17	NA61E 19_18	NA61E 19_19	NA61E 19_20	NA61E 19_21	NA61E 19_22	NA61E 19_23	NA61E 19_24
Wt.%												
SiO2	58.5378	58.3498	58.1534	57.7113	57.9776	58.2942	58.3843	58.491	57.7671	58.2834	58.9761	58.0161
TiO2	0	0	0	0	0	0.0061	0	0	0	0	0.0217	0
Al2O3	26.4765	26.5615	26.6463	26.6793	26.3073	26.5289	26.2689	26.5556	26.5133	26.6243	25.0602	26.6323
Cr2O3	0	0	0	0	0	0	0	0	0	0.0056	0	0
FeO	0.1865	0.2197	0.1181	0.1155	0.2989	0.1707	0.3878	0.1022	0.1588	0.2332	1.174	0.3066
MnO	0	0	0	0	0	0.0121	0.0098	0.0115	0.0069	0.0023	0.0287	0.0052
MgO	0	0	0.0005	0.0069	0	0.001	0.0076	0.0205	0.0013	0.0003	0.7205	0.0227
CaO	7.6986	7.9941	7.8924	7.9154	7.887	7.6722	7.6336	7.7667	7.9173	7.7897	6.8013	8.0137
Na2O	6.8387	6.8747	6.7993	6.884	6.8371	6.8948	6.8674	6.7469	6.7586	6.8617	6.9961	6.7147
K2O	0.373	0.3451	0.309	0.2878	0.2714	0.2976	0.3583	0.3552	0.3208	0.3368	0.4222	0.3535
Total	100.111	100.3448	99.9191	99.6003	99.5794	99.8776	99.9178	100.0496	99.4442	100.1372	100.2008	100.0648
Cations	(calculated on the basis of 8 O)											
Si	2.6136	2.6032	2.6024	2.5936	2.6064	2.6088	2.6152	2.612	2.5992	2.604	2.64	2.5968
Ti	0	0	0	0	0	0	0	0	0	0	0.0008	0
Al	1.3936	1.3968	1.4056	1.4128	1.3936	1.3992	1.3864	1.3976	1.4064	1.4024	1.3224	1.4048
Cr	0	0	0	0	0	0	0	0	0	0	0	0
Fe	0.0072	0.008	0.0048	0.004	0.0112	0.0064	0.0144	0.004	0.0056	0.0088	0.044	0.0112
Mn	0	0	0	0	0	0.0008	0	0.0008	0	0	0.0008	0
Mg	0	0	0	0.0008	0	0	0.0008	0.0016	0	0	0.048	0.0016
Ca	0.368	0.3824	0.3784	0.3808	0.38	0.368	0.3664	0.372	0.3816	0.3728	0.3264	0.384
Na	0.592	0.5944	0.5904	0.6	0.596	0.5984	0.596	0.584	0.5896	0.5944	0.6072	0.5824
K	0.0216	0.02	0.0176	0.0168	0.0152	0.0168	0.0208	0.02	0.0184	0.0192	0.024	0.02
Total	4.996	5.0048	4.9992	5.0096	5.0024	4.9984	5.0008	4.9928	5.0016	5.0024	5.0136	5.0016
Mol. % end-members												
Or	3.5202086	3.2552083	2.8947368	2.7237354	2.486911	2.7308192	3.3722438	3.3112583	3.0263158	3.1290743	3.8022814	3.3200531
Ab	61.666667	60.851761	60.941371	61.174551	61.065574	61.92053	61.928512	61.087866	60.708402	61.455749	65.03856	60.264901
An	38.333333	39.148239	39.058629	38.825449	38.934426	38.07947	38.071488	38.912134	39.291598	38.544251	34.96144	39.735099

Table B.29: Feldspar analyses (cont.)

Sample No.	NA61E 19_25	NA61E 19_26	NA61E 19_27	NA61F 08_10	NA61F 13_29	NA61F 13_25	NA61F 08_5	NA61F 08_11	NA61F 08_4	NA61F 08_6	NA61F 08_14	NA61F 03_3	NA61F 08_8
Wt.%													
SiO2	58.3299	58.221	57.9541	61.9981	63.3131	63.081	62.2007	61.0419	62.6142	61.6888	62.2679	62.1152	61.0317
TiO2	0	0	0	0	0	0.0007	0.0014	0	0	0	0.0156	0	0
Al2O3	26.4642	26.7815	26.5493	24.2971	23.9493	24.548	24.8519	24.4242	24.8308	25.1108	24.7775	24.4441	24.8806
Cr2O3	0	0	0	0	0	0	0	0	0	0	0	0	0
FeO	0.138	0.3787	0.4966	0.0748	0.431	0.6512	0.0742	0.0726	0.0246	0.3326	0.1367	0.0187	0.1047
MnO	0.0109	0.0327	0.0264	0	0	0	0	0	0	0	0.0189	0	0
MgO	0.0015	0.0057	0.0149	0	0	0	0	0	0	0	0	0	0
CaO	7.5926	7.8808	7.6232	3.7875	4.3863	4.8054	5.0664	5.0692	5.1288	5.1586	5.1847	5.2277	5.2451
Na2O	7.0249	6.9006	6.8326	8.5629	9.0166	8.8067	8.4935	8.2671	8.4656	8.1914	8.5615	8.5657	8.3825
K2O	0.3344	0.287	0.3069	0.6597	0.1997	0.1257	0.2773	0.2303	0.1999	0.4004	0.1461	0.1234	0.2766
Total	99.8964	100.4879	99.8041	99.3801	101.2959	102.0187	100.9653	99.1054	101.2638	100.8826	101.1088	100.4947	99.9212
Cations	(calculated on the basis of 8 O)												
Si	2.6104	2.5952	2.6	2.7584	2.7696	2.7448	2.7304	2.7296	2.7376	2.7152	2.7304	2.7384	2.7112
Ti	0	0	0	0	0	0	0	0	0	0	0.0008	0	0
Al	1.396	1.4072	1.404	1.2744	1.2344	1.2592	1.2856	1.2872	1.28	1.3024	1.2808	1.2704	1.3032
Cr	0	0	0	0	0	0	0	0	0	0	0	0	0
Fe	0.0048	0.0144	0.0184	0.0024	0.016	0.024	0.0024	0.0024	0.0008	0.012	0.0048	0.0008	0.004
Mn	0.0008	0.0016	0.0008	0	0	0	0	0	0	0	0.0008	0	0
Mg	0	0	0.0008	0	0	0	0	0	0	0	0	0	0
Ca	0.364	0.3768	0.3664	0.1808	0.2056	0.224	0.2384	0.2432	0.24	0.2432	0.2432	0.2472	0.2496
Na	0.6096	0.5968	0.5944	0.7384	0.7648	0.7432	0.7232	0.7168	0.7176	0.6992	0.728	0.732	0.7224
K	0.0192	0.016	0.0176	0.0376	0.0112	0.0072	0.0152	0.0128	0.0112	0.0224	0.008	0.0072	0.016
Total	5.0048	5.008	5.0024	4.9928	5.0016	5.0032	4.9952	4.9928	4.988	4.9952	4.9968	4.9968	5.0072
Mol. % end-members													
Or	3.0534351	2.6109661	2.875817	4.8453608	1.443299	0.9594883	2.0585049	1.754386	1.5367728	3.1042129	1.0869565	0.974026	2.1668472
Ab	62.612983	61.298274	61.865112	80.330722	78.812861	76.840364	75.207987	74.666667	74.937343	74.193548	74.958814	74.754902	74.320988
An	37.387017	38.701726	38.134888	19.669278	21.187139	23.159636	24.792013	25.333333	25.062657	25.806452	25.041186	25.245098	25.679012

Table B.30 Feldspar analyses (cont.)

Sample No.	NA61F 08_9	NA61F 03_8	NA61F 08_7	NA61F 03_4	NA61F 03_7	NA61F 03_5	NA61F 03_6
Wt.%							
SiO2	61.5246	60.7308	60.4954	60.6257	59.3069	58.5916	57.7053
TiO2	0	0	0	0	0	0	0
Al2O3	24.9207	24.8521	25.484	25.724	25.9438	27.2992	27.279
Cr2O3	0	0	0	0	0	0	0
FeO	0.0374	0.0443	0.2819	0.0337	0.0502	0.0876	0.2563
MnO	0	0	0	0	0	0	0
MgO	0	0	0	0	0	0	0
CaO	5.2999	5.4286	6.0165	6.3288	6.6131	7.9729	8.1984
Na2O	8.2316	8.3202	8.0121	7.763	7.7438	7.0578	6.9867
K2O	0.2808	0.1592	0.1985	0.238	0.2092	0.2059	0.1922
Total	100.2949	99.5353	100.4883	100.7132	99.8671	101.2149	100.6179
Cations	(calculated on the basis of 8 O)						
Si	2.72	2.708	2.6792	2.676	2.6472	2.5888	2.5712
Ti	0	0	0	0	0	0	0
Al	1.2984	1.3064	1.3304	1.3384	1.3648	1.4216	1.4328
Cr	0	0	0	0	0	0	0
Fe	0.0016	0.0016	0.0104	0.0016	0.0016	0.0032	0.0096
Mn	0	0	0	0	0	0	0
Mg	0	0	0	0	0	0	0
Ca	0.2512	0.2592	0.2856	0.2992	0.316	0.3776	0.3912
Na	0.7056	0.7192	0.688	0.6648	0.6704	0.6048	0.604
K	0.016	0.0088	0.0112	0.0136	0.012	0.012	0.0112
Total	4.9928	5.004	5.0048	4.9936	5.012	5.008	5.0208
Mol. % end-members							
Or	2.2172949	1.2087912	1.6018307	2.004717	1.7584994	1.9455253	1.8205462
Ab	73.745819	73.507768	70.665571	68.962656	67.964315	61.563518	60.691318
An	26.254181	26.492232	29.334429	31.037344	32.035685	38.436482	39.308682

Table B.31: Garnet analyses

Sample No.	NA23A 05_10	NA23A 05_11	NA23A 05_12	NA23A 05_13	NA23A 05_14	NA23A 05_15	NA23A 05_16	NA23A 05_17	NA23A 05_18	NA23A 05_19	NA23A 05_20	NA23A 05_21	NA23A 05_22
Wt.%													
SiO2	37.9448	37.7617	37.962	38.098	37.9001	38.1836	38.1842	38.1434	38.2116	38.2134	38.3642	38.0493	38.1795
TiO2	0.0336	0.0395	0	0.0019	0	0	0	0	0.0117	0	0	0	0
Al2O3	20.9507	21.1406	21.3821	21.2376	21.3113	21.4377	21.2733	21.3995	21.3189	21.4438	21.4893	21.1347	21.45
Cr2O3	0	0.0183	0	0	0.0012	0	0	0	0	0	0	0	0
FeO	26.8256	26.8528	26.5957	26.8763	26.2494	26.5241	26.3245	26.5148	26.0709	26.451	26.7338	26.8507	26.675
MnO	1.3224	1.279	1.2896	1.2258	1.2252	1.2647	1.2159	1.2492	1.219	1.1902	1.264	1.2803	1.2862
MgO	5.946	5.8811	6.1313	6.3256	6.4334	6.5237	6.4875	6.4317	6.3674	6.4207	6.4752	6.3174	6.1038
CaO	6.4192	6.6294	6.6649	6.5476	6.492	6.3986	6.7528	6.7207	6.923	6.7687	6.4538	6.4771	6.5596
Na2O	0.0412	0.0367	0.0454	0.057	0.0496	0.031	0.0363	0.0297	0.0247	0.0385	0.0195	0.012	0.0217
K2O	0.0197	0.0293	0.0293	0.0206	0.0119	0.0238	0.0252	0.0192	0.0261	0.0151	0.0174	0.0137	0.0238
Total	99.5033	99.6684	100.1002	100.3903	99.6741	100.3871	100.2997	100.5081	100.1732	100.5413	100.8172	100.1351	100.2996
Cations	(calculated on the basis of 12 O)												
Si	2.9892	2.9724	2.97	2.9724	2.9712	2.9724	2.976	2.9688	2.9796	2.9712	2.9748	2.9772	2.9784
Ti	0.0024	0.0024	0	0	0	0	0	0	0.0012	0	0	0	0
Al	1.9452	1.962	1.9716	1.9536	1.9692	1.9668	1.9536	1.9632	1.9596	1.9656	1.9644	1.9488	1.9716
Cr	0	0.0012	0	0	0	0	0	0	0	0	0	0	0
Fe	1.7676	1.7676	1.74	1.7544	1.7208	1.7268	1.716	1.7256	1.7004	1.7196	1.734	1.7568	1.74
Mn	0.0888	0.0852	0.0852	0.0816	0.0816	0.0828	0.0804	0.0828	0.0804	0.078	0.0828	0.0852	0.0852
Mg	0.6984	0.69	0.7152	0.7356	0.7524	0.7572	0.7536	0.7464	0.7404	0.744	0.7488	0.7368	0.7092
Ca	0.5424	0.5592	0.5592	0.5472	0.5448	0.534	0.564	0.5604	0.5784	0.564	0.5364	0.5424	0.5484
Na	0.006	0.006	0.0072	0.0084	0.0072	0.0048	0.006	0.0048	0.0036	0.006	0.0024	0.0024	0.0036
K	0.0024	0.0024	0.0024	0.0024	0.0012	0.0024	0.0024	0.0024	0.0024	0.0012	0.0012	0.0012	0.0024
Total	8.0424	8.0496	8.0508	8.0568	8.0496	8.0484	8.0532	8.0556	8.0472	8.0508	8.046	8.0508	8.0388
Mol. % end-members													
Grs	17.512592	18.027079	18.041038	17.54521	17.576461	17.221362	18.111753	17.989214	18.660472	18.160742	17.29207	17.377932	17.789023
Alm	57.070903	56.982592	56.136276	56.252405	55.516841	55.688854	55.105973	55.392912	54.858691	55.370943	55.89942	56.286044	56.442195
Prp	22.549399	22.243714	23.073945	23.585995	24.2741	24.419505	24.200385	23.959938	23.886953	23.956723	24.139265	23.606305	23.00506
Sps	2.8671058	2.7466151	2.7487418	2.6163909	2.6325978	2.6702786	2.5818882	2.6579353	2.5938831	2.511592	2.6692456	2.7297193	2.7637213

Table B.32: Garnet analyses (cont.)

Sample No.	NA23A 05_23	NA23A 05_24	NA23A 05_25	NA23A 05_26	NA23A 05_27	NA23A 05_28	NA23A 05_29	NA23A 05_73	NA23A 05_74	NA23A 05_75	NA23A 05_76	NA23A 05_77	NA23A 05_78
Wt.%													
SiO2	38.0559	38.0411	38.0858	38.1252	38.0565	38.0201	38.103	37.8059	38.2212	37.9766	38.0906	38.0179	37.9405
TiO2	0	0	0.0045	0.0265	0.0019	0	0	0.0078	0	0	0	0	0
Al2O3	21.04	21.416	21.5629	21.1952	21.1447	21.1147	20.8969	21.1064	21.0616	21.0963	21.2517	21.2782	21.276
Cr2O3	0	0	0	0.0187	0.0168	0	0.0113	0.0113	0.009	0	0.0039	0	0
FeO	26.7545	26.5262	26.4359	27.0381	27.1264	27.2298	27.1067	27.4919	27.4456	27.3725	26.991	27.0563	26.644
MnO	1.2024	1.2384	1.2878	1.2195	1.2623	1.2872	1.3376	1.2835	1.276	1.2687	1.2475	1.2206	1.1764
MgO	5.9822	6.1549	6.0278	5.9216	5.9213	5.6333	5.9327	5.6794	5.9761	6.123	6.2624	6.2043	6.157
CaO	6.7067	6.5609	6.9614	6.7924	6.688	6.7963	6.8021	6.6931	6.6118	6.6248	6.6874	6.5983	6.8405
Na2O	0.016	0.0293	0.0142	0.0169	0.0398	0.0313	0.0308	0.0323	0.0313	0.0492	0.045	0.0267	0.0262
K2O	0.016	0.0256	0.0288	0.0128	0.0224	0.0142	0.0133	0.0128	0.0137	0.0096	0.011	0.0188	0.0082
Total	99.7738	99.9925	100.409	100.3668	100.2801	100.1268	100.2344	100.1243	100.6462	100.5206	100.5904	100.421	100.0687
Cations	(calculated on the basis of 12 O)												
Si	2.988	2.9748	2.9676	2.9796	2.9784	2.9832	2.9856	2.9712	2.9832	2.9688	2.9688	2.9688	2.97
Ti	0	0	0	0.0012	0	0	0	0	0	0	0	0	0
Al	1.9476	1.974	1.9812	1.9524	1.9512	1.9524	1.9296	1.9548	1.938	1.944	1.9524	1.9584	1.9632
Cr	0	0	0	0.0012	0.0012	0	0.0012	0.0012	0	0	0	0	0
Fe	1.7568	1.7352	1.7232	1.7676	1.776	1.7868	1.776	1.8072	1.7916	1.7892	1.7592	1.7664	1.7436
Mn	0.0804	0.0816	0.0852	0.0804	0.084	0.0852	0.0888	0.0852	0.084	0.084	0.0828	0.0804	0.078
Mg	0.6996	0.7176	0.7008	0.69	0.6912	0.6588	0.6924	0.6648	0.6948	0.714	0.7272	0.7224	0.7188
Ca	0.564	0.5496	0.5808	0.5688	0.5604	0.5712	0.5712	0.564	0.5532	0.5544	0.558	0.552	0.5736
Na	0.0024	0.0048	0.0024	0.0024	0.006	0.0048	0.0048	0.0048	0.0048	0.0072	0.0072	0.0036	0.0036
K	0.0012	0.0024	0.0024	0.0012	0.0024	0.0012	0.0012	0.0012	0.0012	0.0012	0.0012	0.0024	0.0012
Total	8.04	8.04	8.0448	8.046	8.0508	8.0448	8.0508	8.0556	8.0508	8.064	8.058	8.0544	8.0532
Mol. % end-members													
Grs	18.188854	17.821012	18.796117	18.308227	18.010027	18.413926	18.258535	18.069973	17.710334	17.647059	17.843438	17.685506	18.420039
Alm	56.656347	56.264591	55.76699	56.894554	57.076745	57.601547	56.770234	57.900807	57.356896	56.951872	56.254797	56.593618	55.992293
Prp	22.56192	23.268482	22.679612	22.209347	22.213652	21.237911	22.13272	21.2995	22.243565	22.727273	23.254029	23.144944	23.082852
Sps	2.5928793	2.6459144	2.7572816	2.5878718	2.6995758	2.7466151	2.8385117	2.7297193	2.6892048	2.6737968	2.647736	2.5759323	2.504817

Table B.33: Garnet analyses (cont.)

Sample No.	NA23A 05_79	NA23A 05_80	NA23A 05_81	NA23A 05_82	NA046 03_12	NA046 03_13	NA046 03_14	NA046 03_15	NA046 03_16	NA046 03_17	NA046 03_18	NA046 03_19	NA046 03_20
Wt.%													
SiO2	38.0179	38.1257	37.9295	37.7872	37.4934	37.4441	37.7422	37.5866	37.6055	37.7719	37.6503	37.7047	37.9854
TiO2	0.0026	0.0312	0	0.0045	0.0707	0.0591	0.0676	0.0708	0.0533	0.0299	0.0747	0.0649	0.0377
Al2O3	21.1364	21.0098	21.2144	21.1199	21.1526	20.9018	21.2379	21.154	21.0801	20.9994	21.0289	20.9768	21.1749
Cr2O3	0	0	0	0	0.0268	0.048	0.0393	0.0296	0.0421	0.0564	0.055	0.03	0.0637
FeO	25.6607	25.5821	27.4493	25.9006	28.1953	27.9103	27.6449	27.4694	27.812	27.7895	27.538	28.1655	27.9828
MnO	1.1863	1.1635	1.2083	1.2241	0.9967	1.0366	0.9922	0.9766	0.968	1.014	0.9167	1.0013	0.9796
MgO	5.9718	6.2164	5.8317	6.2127	4.876	5.1559	5.2896	5.27	5.1196	4.843	5.2076	4.562	5.1638
CaO	8.1591	7.925	6.485	7.3386	6.7754	6.8272	6.8053	6.8401	6.997	7.1976	7.0195	7.1859	6.7465
Na2O	0.0278	0.0234	0.0152	0.0221	0.0338	0.036	0.025	0.0236	0.0328	0.0192	0.0191	0.0165	0.0205
K2O	0.0064	0.026	0.0252	0.0238	0.033	0.0344	0.0335	0.0257	0.022	0.0339	0.0206	0.0536	0.0239
Total	100.1689	100.1031	100.1586	99.6336	99.6538	99.4535	99.8775	99.4465	99.7324	99.7549	99.5305	99.7613	100.1787
Cations	(calculated on the basis of 12 O)												
Si	2.9712	2.9784	2.9748	2.9676	2.9688	2.97	2.9724	2.9724	2.9712	2.9844	2.9772	2.9844	2.9844
Ti	0	0.0024	0	0	0.0048	0.0036	0.0036	0.0048	0.0036	0.0012	0.0048	0.0036	0.0024
Al	1.9464	1.9344	1.9608	1.9548	1.974	1.9548	1.9716	1.9716	1.9632	1.956	1.9596	1.9572	1.9608
Cr	0	0	0	0	0.0012	0.0036	0.0024	0.0024	0.0024	0.0036	0.0036	0.0024	0.0036
Fe	1.6776	1.6716	1.8	1.7016	1.8672	1.8516	1.8204	1.8168	1.8384	1.836	1.8204	1.8648	1.8384
Mn	0.078	0.0768	0.0804	0.0816	0.0672	0.0696	0.066	0.066	0.0648	0.0684	0.0612	0.0672	0.0648
Mg	0.696	0.7236	0.6816	0.7272	0.576	0.6096	0.6216	0.6216	0.6036	0.57	0.6132	0.5388	0.6048
Ca	0.6828	0.6636	0.5448	0.618	0.5748	0.5808	0.5748	0.5796	0.5928	0.6096	0.5952	0.6096	0.5676
Na	0.0048	0.0036	0.0024	0.0036	0.0048	0.006	0.0036	0.0036	0.0048	0.0024	0.0024	0.0024	0.0036
K	0.0012	0.0024	0.0024	0.0024	0.0036	0.0036	0.0036	0.0024	0.0024	0.0036	0.0024	0.006	0.0024
Total	8.0592	8.0568	8.0484	8.058	8.0436	8.0544	8.0412	8.0412	8.0484	8.0364	8.0412	8.0364	8.0328
Mol. % end-members													
Grs	21.784074	21.163414	17.535728	19.754507	18.630883	18.665638	18.645387	18.793774	19.125048	19.766537	19.262136	19.789638	18.454936
Alm	53.522205	53.310371	57.937428	54.392021	60.521198	59.506363	59.050214	58.910506	59.310879	59.533074	58.912621	60.537593	59.773703
Prp	22.205207	23.076923	21.938973	23.245109	18.669778	19.591207	20.163488	20.155642	19.47348	18.48249	19.84466	17.491235	19.664456
Sps	2.4885145	2.449292	2.5878718	2.6083621	2.1781408	2.2367914	2.1409109	2.1400778	2.0905923	2.2178988	1.9805825	2.1815349	2.106906

Table B.34: Garnet analyses (cont.)

Sample No.	NA046 03_21	NA046 03_22	NA046 03_23	NA046 03_24	NA046 03_25	NA046 03_26	NA046 03_27	NA046 03_28	NA046 03_29	NA046 03_30	NA046 03_31	NA046 03_32	NA046 03_33
Wt.%													
SiO2	37.752	37.9324	37.8499	37.3746	37.4675	37.505	37.3293	37.4651	37.5168	37.9265	37.7343	37.8238	37.8279
TiO2	0.0481	0.0974	0.0657	0.0631	0.0585	0.052	0.0701	0.0474	0.0766	0.0566	0.0338	0.0844	0.0896
Al2O3	21.3279	21.272	21.1716	21.0077	20.9976	20.9084	20.909	21.1593	21.0604	21.204	21.0423	21.0766	21.0068
Cr2O3	0.0697	0.0416	0.0273	0.0546	0.0314	0.0674	0.094	0.0254	0.0346	0.0375	0.0647	0.0218	0.0369
FeO	27.9122	28.1438	27.4002	27.3477	27.7881	27.8995	28.1677	28.1448	28.2919	27.5956	27.6794	28.0546	28.4221
MnO	0.922	0.993	0.9264	0.9128	0.9629	1.068	1.0295	1.0185	0.9663	0.9778	0.9514	1.0255	0.958
MgO	5.1147	5.1694	5.0554	5.0759	5.2363	4.9791	4.7847	5.0858	4.7554	4.9829	5.0136	5.0687	4.4918
CaO	6.7528	6.8063	7.0973	7.1588	6.8404	7.0367	6.8834	6.6815	6.9565	7.1553	7.2073	6.9622	7.1471
Na2O	0.0287	0.0269	0.0322	0.0178	0.0219	0.0201	0.0216	0.0319	0.0215	0.0214	0.0169	0.0251	0.0166
K2O	0.0372	0.0262	0.0193	0.0344	0.0174	0.0289	0.0289	0.0275	0.0124	0.0257	0.0239	0.0266	0.0289
Total	99.9654	100.5089	99.6454	99.0475	99.4221	99.5652	99.3183	99.6873	99.6925	99.9833	99.7676	100.1692	100.0256
Cations	(calculated on the basis of 12 O)												
Si	2.9724	2.9736	2.9856	2.9712	2.97	2.9736	2.97	2.9652	2.9724	2.9844	2.9796	2.9772	2.988
Ti	0.0024	0.006	0.0036	0.0036	0.0036	0.0036	0.0036	0.0024	0.0048	0.0036	0.0024	0.0048	0.0048
Al	1.98	1.9656	1.968	1.968	1.962	1.9536	1.9608	1.974	1.9668	1.9668	1.9584	1.956	1.956
Cr	0.0048	0.0024	0.0012	0.0036	0.0024	0.0048	0.006	0.0012	0.0024	0.0024	0.0036	0.0012	0.0024
Fe	1.8384	1.8444	1.8072	1.818	1.842	1.8492	1.8744	1.8624	1.8744	1.8156	1.8276	1.8468	1.8768
Mn	0.0612	0.066	0.0624	0.0612	0.0648	0.072	0.0696	0.0684	0.0648	0.0648	0.0636	0.0684	0.0636
Mg	0.6	0.6036	0.594	0.6012	0.6192	0.588	0.5676	0.6	0.5616	0.5844	0.5904	0.5952	0.5292
Ca	0.57	0.5712	0.6	0.6096	0.5808	0.5976	0.5868	0.5664	0.5904	0.6036	0.6096	0.5868	0.6048
Na	0.0048	0.0036	0.0048	0.0024	0.0036	0.0036	0.0036	0.0048	0.0036	0.0036	0.0024	0.0036	0.0024
K	0.0036	0.0024	0.0024	0.0036	0.0012	0.0024	0.0024	0.0024	0.0012	0.0024	0.0024	0.0024	0.0024
Total	8.0388	8.0388	8.0292	8.0424	8.0508	8.0496	8.0448	8.0484	8.0424	8.0328	8.0412	8.0424	8.0316
Mol. % end-members													
Grs	18.569195	18.514197	19.584802	19.728155	18.694477	19.235226	18.938807	18.287485	19.099379	19.67149	19.720497	18.946145	19.672131
Alm	59.890539	59.782186	58.989424	58.834951	59.289301	59.521051	60.49574	60.131732	60.636646	59.170903	59.122671	59.628051	61.046058
Prp	19.546521	19.564372	19.388954	19.456311	19.930475	18.926226	18.319132	19.372336	18.167702	19.045757	19.099379	19.217358	17.213115
Sps	1.9937451	2.1392454	2.0368194	1.9805825	2.0857474	2.3174971	2.2463207	2.2084463	2.0962733	2.1118498	2.0574534	2.2084463	2.0686963

Table B.35: Garnet analyses (cont.)

Sample	NA046	NA046	NA046	NA046	NA046	NA046	NA046	NA046	NA046	NA046	NA046	NA046	NA61C
No.	03_34	03_35	03_36	02_41	02_42	02_43	02_44	02_45	02_46	02_47	02_48	02_49	03_12
Wt.%													
SiO2	37.7049	37.5761	37.5729	37.686	37.7213	37.8336	37.7788	36.693	36.4791	37.6051	37.5681	37.5754	37.48
TiO2	0.0617	0.0636	0.0565	0.0598	0.0993	0.0597	0.0468	0.0856	0.0739	0.0806	0.0676	0.0455	0
Al2O3	21.2201	20.9271	21.0781	21.1575	21.2162	21.1359	21.0799	20.6658	20.5645	20.9764	20.9348	20.9666	21.2804
Cr2O3	0.0333	0.0498	0.0369	0.0559	0.03	0.0448	0.0642	0.0534	0.0221	0.0407	0.0448	0.0438	0
FeO	28.1775	28.2879	28.3734	28.0976	28.1822	27.9315	27.7612	28.3675	28.5361	27.9304	27.9849	28.4167	32.8004
MnO	0.9258	0.9485	0.9507	0.9694	0.9788	1.0283	0.949	0.9323	0.9371	0.9802	0.951	0.9557	0.3311
MgO	4.9483	4.7744	4.8059	4.8483	4.8667	4.9857	4.9373	4.8067	4.6269	4.9901	5.042	4.4384	5.9424
CaO	7.2313	7.1737	7.0996	7.0813	6.8421	6.8189	7.1522	6.8334	6.8637	7.094	7.0381	7.3568	1.6282
Na2O	0.0365	0.0279	0.0429	0.0142	0.0242	0.0178	0.03	0.0362	0.0382	0.026	0.0328	0.0284	0.0302
K2O	0.0376	0.0206	0.0321	0.0449	0.0234	0.0399	0.0257	0.0367	0.0151	0.0243	0.0312	0.0376	0.0448
Total	100.3769	99.8497	100.0489	100.0148	99.9843	99.8962	99.8252	98.5107	98.1568	99.7479	99.6954	99.865	99.5376
Cations	(calculated on the basis of 12 O)												
Si	2.9652	2.9736	2.9676	2.9736	2.9748	2.9832	2.9808	2.952	2.9496	2.9736	2.9736	2.9772	2.9796
Ti	0.0036	0.0036	0.0036	0.0036	0.006	0.0036	0.0024	0.0048	0.0048	0.0048	0.0036	0.0024	0
Al	1.9668	1.9524	1.962	1.9668	1.9716	1.9644	1.9608	1.9596	1.9596	1.9548	1.9524	1.9584	1.9944
Cr	0.0024	0.0036	0.0024	0.0036	0.0024	0.0024	0.0036	0.0036	0.0012	0.0024	0.0024	0.0024	0
Fe	1.8528	1.872	1.8744	1.854	1.8588	1.842	1.8324	1.908	1.9296	1.8468	1.8528	1.8828	2.1804
Mn	0.0612	0.0636	0.0636	0.0648	0.0648	0.0684	0.0636	0.0636	0.0636	0.066	0.0636	0.0636	0.0228
Mg	0.5796	0.5628	0.5664	0.57	0.5724	0.5856	0.5808	0.576	0.558	0.588	0.5952	0.5244	0.7044
Ca	0.6096	0.6084	0.6012	0.5988	0.5784	0.576	0.6048	0.5892	0.5952	0.6012	0.5964	0.624	0.1392
Na	0.006	0.0048	0.006	0.0024	0.0036	0.0024	0.0048	0.006	0.006	0.0036	0.0048	0.0048	0.0048
K	0.0036	0.0024	0.0036	0.0048	0.0024	0.0036	0.0024	0.0036	0.0012	0.0024	0.0036	0.0036	0.0048
Total	8.0508	8.0484	8.0508	8.0424	8.0364	8.0328	8.0364	8.0664	8.07	8.0448	8.0484	8.0448	8.0316
Mol. % end-members													
Grs	19.644238	19.582851	19.358578	19.393704	18.813427	18.75	19.626168	18.783474	18.916857	19.381044	19.189189	20.162854	4.5687278
Alm	59.70611	60.254925	60.355487	60.046638	60.460578	59.960938	59.462617	60.82632	61.327231	59.535783	59.6139	60.837534	71.563608
Prp	18.677494	18.115102	18.238022	18.460941	18.618267	19.0625	18.847352	18.362663	17.734554	18.955513	19.150579	16.944552	23.119338
Sps	1.9721578	2.0471224	2.0479134	2.0987175	2.1077283	2.2265625	2.0638629	2.027544	2.0213577	2.1276596	2.046332	2.0550601	0.7483261

Table B.36: Garnet analyses (cont.)

Sample No.	NA61C 03_13	NA61C 03_14	NA61C 03_24	NA61C 03_25	NA61C 03_26	NA61C 03_27	NA61C 02_10	NA61C 02_11	NA61C 02_12	NA61C 02_13	NA61C 02_14	NA61C 02_19	NA61C 02_20
Wt.%													
SiO2	37.3042	37.2722	37.2919	37.1427	36.7765	37.1148	37.2411	36.9867	37.1577	37.0409	36.7437	36.8281	36.9116
TiO2	0.0365	0.0141	0.041	0	0	0.0058	0.0103	0.0269	0.0455	0.025	0.0128	0.009	0.0102
Al2O3	21.408	21.3614	21.2403	21.3178	21.1111	21.1755	21.0934	20.9154	20.7888	20.9511	20.8534	20.8339	20.7555
Cr2O3	0	0.0134	0	0.003	0	0	0	0	0	0	0	0	0
FeO	32.8964	32.8249	32.7864	32.8964	32.7367	32.5	32.3964	32.8655	32.7098	32.7564	32.6782	32.7833	32.9201
MnO	0.3183	0.349	0.3462	0.3138	0.355	0.3262	0.334	0.3483	0.3634	0.3579	0.3383	0.3344	0.3449
MgO	5.7875	5.7434	5.6285	5.8114	5.6846	5.6668	5.7299	5.7183	5.7194	5.6889	5.6787	5.755	5.6269
CaO	1.9757	2.1254	2.0797	2.1448	2.0209	2.1855	2.1938	2.1107	2.1259	2.296	2.2562	2.079	2.1422
Na2O	0.019	0.019	0.026	0.0246	0.0322	0.04	0	0.013	0.006	0.0004	0.0139	0.0149	0.0083
K2O	0.0318	0.029	0.053	0.0184	0.0433	0.0415	0.0729	0.0332	0.0277	0.0258	0.0396	0.0355	0.0415
Total	99.7775	99.7519	99.4931	99.673	98.7604	99.0562	99.0719	99.0181	98.9443	99.1425	98.6149	98.6731	98.7613
Cations	(calculated on the basis of 12 O)												
Si	2.9628	2.9628	2.9712	2.9568	2.9568	2.97	2.9772	2.9664	2.9796	2.9664	2.9604	2.9652	2.9712
Ti	0.0024	0.0012	0.0024	0	0	0	0.0012	0.0012	0.0024	0.0012	0.0012	0	0.0012
Al	2.004	2.0016	1.9956	2.0004	2.0004	1.9968	1.9872	1.9776	1.9656	1.9776	1.9812	1.9776	1.9692
Cr	0	0.0012	0	0	0	0	0	0	0	0	0	0	0
Fe	2.1852	2.1816	2.1852	2.19	2.2008	2.1744	2.166	2.2044	2.1936	2.1948	2.202	2.2068	2.2164
Mn	0.0216	0.024	0.0228	0.0216	0.024	0.0216	0.0228	0.024	0.0252	0.024	0.0228	0.0228	0.024
Mg	0.6852	0.6804	0.6684	0.69	0.6816	0.6756	0.6828	0.684	0.684	0.6792	0.6816	0.6912	0.6756
Ca	0.168	0.1812	0.1776	0.1824	0.174	0.1872	0.1884	0.1812	0.1824	0.1968	0.1944	0.1788	0.1848
Na	0.0024	0.0024	0.0036	0.0036	0.0048	0.006	0	0.0024	0.0012	0	0.0024	0.0024	0.0012
K	0.0036	0.0024	0.0048	0.0024	0.0048	0.0048	0.0072	0.0036	0.0024	0.0024	0.0036	0.0036	0.0048
Total	8.0364	8.04	8.0328	8.0484	8.0484	8.0376	8.0328	8.046	8.0376	8.0424	8.0496	8.0484	8.0496
Mol. % end-members													
Grs	5.4901961	5.9076682	5.8153242	5.9143969	5.6486171	6.1200471	6.1568627	5.8572537	5.9120965	6.3590539	6.2693498	5.7684863	5.9597523
Alm	71.411765	71.126761	71.552063	71.011673	71.445267	71.086701	70.784314	71.256788	71.100739	70.918961	71.013932	71.196283	71.478328
Prp	22.392157	22.183099	21.886051	22.373541	22.126996	22.087093	22.313725	22.110163	22.170362	21.946491	21.981424	22.299652	21.787926
Sps	0.7058824	0.7824726	0.7465619	0.7003891	0.7791196	0.7061593	0.745098	0.7757952	0.8168028	0.7754944	0.7352941	0.7355788	0.7739938

Table B.37: Garnet analyses (cont.)

Sample No.	NA61C 02_21	NA61C 04_3	NA61E 01_01	NA61E 05_1	NA61E 05_2	NA61E 05_3	NA61E 05_4	NA61E 05_5	NA61E 05_6	NA61E 05_7	NA61E 05_8	NA61E 05_9	NA61E 05_10
Wt.%													
SiO2	36.9487	37.2316	38.0883	38.1327	38.0213	37.8137	37.9492	37.7671	37.491	37.7542	37.6164	38.0077	37.8593
TiO2	0.0378	0.007	0.0706	0.041	0.0604	0.0291	0.0519	0.0629	0.0876	0.0396	0.0566	0.0324	0.066
Al2O3	20.9385	21.2181	21.3526	21.3011	21.237	21.1492	21.1249	21.1428	20.9243	21.0529	20.9459	21.2711	21.2218
Cr2O3	0	0	0.0091	0	0.0031	0.0155	0	0.0124	0.017	0.0013	0	0.0235	0
FeO	32.8222	32.8401	24.8829	22.918	23.4493	25.0441	23.9923	24.2458	23.772	24.1671	22.957	24.149	24.5723
MnO	0.3394	0.599	0.9105	0.9068	0.8661	0.9218	0.9636	0.9254	0.9069	0.9055	0.8397	0.8843	0.8449
MgO	5.6119	5.7816	7.3029	7.4282	7.8236	7.3624	8.0614	7.9922	7.7512	7.7918	7.6933	7.7415	7.9832
CaO	2.1629	1.5816	7.0864	8.3252	7.8074	6.6811	6.9181	7.0311	7.7297	7.313	8.369	7.0122	6.6968
Na2O	0.0121	0.0354	0.0352	0.0201	0.0206	0.0331	0.0055	0.0229	0.0155	0.0229	0.0227	0.0289	0.0229
K2O	0.0295	0.0332	0.026	0.0451	0.0347	0.0246	0.0306	0.0278	0.0292	0.0324	0.0274	0.0205	0.0269
Total	98.9031	99.3277	99.7645	99.1183	99.3236	99.0747	99.0976	99.2305	98.7245	99.0808	98.5281	99.1712	99.2942
Cations	(calculated on the basis of 12 O)												
Si	2.9676	2.9724	2.9652	2.9724	2.9604	2.9664	2.964	2.9508	2.9472	2.9556	2.9556	2.9664	2.9556
Ti	0.0024	0	0.0036	0.0024	0.0036	0.0012	0.0036	0.0036	0.0048	0.0024	0.0036	0.0024	0.0036
Al	1.9824	1.9968	1.9596	1.9572	1.9488	1.9548	1.944	1.9476	1.9392	1.9428	1.9392	1.9572	1.9524
Cr	0	0	0	0	0	0.0012	0	0.0012	0.0012	0	0	0.0012	0
Fe	2.2044	2.1924	1.62	1.494	1.5276	1.6428	1.5672	1.584	1.5624	1.5828	1.5084	1.5768	1.6044
Mn	0.0228	0.0408	0.06	0.06	0.0576	0.0612	0.0636	0.0612	0.06	0.06	0.0564	0.0588	0.0564
Mg	0.672	0.6876	0.8472	0.8628	0.9084	0.8604	0.9384	0.9312	0.9084	0.9096	0.9012	0.9012	0.9288
Ca	0.186	0.1356	0.5916	0.6948	0.6516	0.5616	0.5784	0.5892	0.6516	0.6132	0.7044	0.5868	0.5604
Na	0.0024	0.006	0.0048	0.0036	0.0036	0.0048	0.0012	0.0036	0.0024	0.0036	0.0036	0.0048	0.0036
K	0.0036	0.0036	0.0024	0.0048	0.0036	0.0024	0.0036	0.0024	0.0024	0.0036	0.0024	0.0024	0.0024
Total	8.0448	8.0364	8.0544	8.052	8.0652	8.058	8.0652	8.0748	8.0808	8.0748	8.0748	8.058	8.0676
Mol. % end-members													
Grs	6.0287826	4.4365921	18.968834	22.329348	20.717283	17.965451	18.375905	18.612585	20.475113	19.370735	22.218017	18.786016	17.790476
Alm	71.450797	71.731449	51.943055	48.013884	48.569248	52.552783	49.790316	50.037908	49.095023	50	47.577593	50.480215	50.933333
Prp	21.781408	22.497055	27.164294	27.7285	28.882106	27.523992	29.813191	29.416224	28.544495	28.733889	28.425435	28.851325	29.485714
Sps	0.7390121	1.3349038	1.9238169	1.9282684	1.8313621	1.9577735	2.0205871	1.9332828	1.8853695	1.8953753	1.7789553	1.8824433	1.7904762

Table B.38: Garnet analyses (cont.)

Sample No.	NA61E 05_11	NA61E 05_12	NA61E 05_13	NA61E 05_14	NA61E 05_15	NA61E 04_1	NA61E 04_2	NA61E 04_3	NA61E 04_4	NA61E 04_5	NA61E 04_6	NA61E 04_7	NA61E 04_8
Wt.%													
SiO2	38.0776	37.8455	38.0301	37.8332	37.9435	37.741	38.1605	38.1486	38.3177	38.2138	38.2684	38.0892	38.2323
TiO2	0.046	0.044	0.0602	0.044	0.0556	0.0388	0.069	0.0754	0.0306	0.0663	0.0702	0.0539	0.0149
Al2O3	20.9794	21.2645	21.0753	21.2186	21.1598	21.0648	21.1127	21.1633	21.2329	21.315	21.1194	21.1822	21.1718
Cr2O3	0.0133	0	0	0.0105	0.0137	0.0059	0.0315	0	0	0	0.0073	0.0013	0
FeO	24.235	24.3801	24.5235	24.7933	25.008	25.9166	23.5268	23.3831	23.096	23.212	23.514	23.3242	23.7786
MnO	0.9259	0.9308	0.9079	0.9142	0.9063	0.9366	0.8862	0.8971	0.8761	0.8441	0.8539	0.8958	0.9117
MgO	7.9141	7.8161	7.8728	7.6435	7.3924	6.7	7.1403	7.378	7.4978	7.3907	7.5955	7.6469	7.7491
CaO	6.6412	6.7166	6.7145	6.5676	6.7341	6.8728	8.6469	8.5641	8.5798	8.36	8.1741	8.0524	7.7793
Na2O	0.0064	0.0364	0.0234	0.0208	0.0082	0.0184	0.0207	0.0172	0.0326	0.0124	0.0073	0.0292	0.0237
K2O	0.0219	0.0247	0.0352	0.0292	0.0173	0.0561	0.0365	0.0155	0.0251	0.0242	0.0301	0.0452	0.0356
Total	98.8608	99.0588	99.243	99.075	99.2389	99.3511	99.6311	99.6424	99.6887	99.4386	99.6403	99.3204	99.6971
Cations	(calculated on the basis of 12 O)												
Si	2.9808	2.9604	2.97	2.9628	2.97	2.9664	2.97	2.9664	2.9724	2.9712	2.9724	2.9664	2.9688
Ti	0.0024	0.0024	0.0036	0.0024	0.0036	0.0024	0.0036	0.0048	0.0012	0.0036	0.0036	0.0036	0.0012
Al	1.9356	1.9608	1.9404	1.9584	1.9524	1.9512	1.9368	1.9392	1.9416	1.9536	1.9332	1.9452	1.938
Cr	0.0012	0	0	0.0012	0.0012	0	0.0024	0	0	0	0	0	0
Fe	1.5864	1.5948	1.602	1.6236	1.6368	1.704	1.5312	1.5204	1.4988	1.5096	1.5276	1.5192	1.5444
Mn	0.0612	0.0612	0.06	0.0612	0.06	0.0624	0.0588	0.0588	0.0576	0.0552	0.0564	0.0588	0.06
Mg	0.9228	0.9108	0.9168	0.8928	0.8628	0.7848	0.828	0.8556	0.8676	0.8568	0.8796	0.888	0.8976
Ca	0.5568	0.5628	0.5616	0.5508	0.5652	0.5784	0.7212	0.714	0.7128	0.696	0.6804	0.672	0.6468
Na	0.0012	0.006	0.0036	0.0036	0.0012	0.0024	0.0036	0.0024	0.0048	0.0024	0.0012	0.0048	0.0036
K	0.0024	0.0024	0.0036	0.0024	0.0012	0.006	0.0036	0.0012	0.0024	0.0024	0.0024	0.0048	0.0036
Total	8.0508	8.0628	8.0616	8.0592	8.0544	8.0592	8.0604	8.0628	8.0592	8.052	8.058	8.064	8.064
Mol. % end-members													
Grs	17.805065	17.983129	17.883072	17.606444	18.087558	18.481595	22.974006	22.675305	22.723795	22.324865	21.641221	21.414914	20.541159
Alm	50.729087	50.958589	51.01261	51.898734	52.380952	54.447853	48.776758	48.285061	47.781178	48.421863	48.587786	48.413002	49.047256
Prp	29.508826	29.102761	29.193733	28.53855	27.611367	25.076687	26.376147	27.172256	27.658761	27.482679	27.977099	28.298279	28.506098
Sps	1.9570223	1.9555215	1.9105846	1.9562716	1.9201229	1.993865	1.8730887	1.867378	1.8362663	1.7705928	1.7938931	1.873805	1.9054878

Table B.39: Garnet analyses (cont.)

Sample No.	NA61E 04_9	NA61E 04_10	NA61E 04_11	NA61E 04_12	NA61E 04_13	NA61E 04_14	NA61E 12_01	NA61E 12_2	NA61E 12_3	NA61E 12_4	NA61E 12_5	NA61E 12_6	NA61E 12_7
Wt.%													
SiO2	38.4102	38.2527	38.3658	38.237	38.2255	38.1396	38.4057	38.3614	38.3099	38.3802	38.5735	38.3378	38.6882
TiO2	0.0773	0.0208	0.0499	0.0317	0.0395	0.0427	0.0447	0.0226	0.0272	0.0181	0.0395	0.024	0.0473
Al2O3	21.369	21.5246	21.5504	21.3307	21.2403	21.3042	21.3817	21.5368	21.2521	21.6043	21.5109	21.6239	21.455
Cr2O3	0	0.0031	0.004	0	0.0123	0.016	0.0123	0	0	0.0082	0	0	0
FeO	23.4765	23.7997	24.7343	24.769	25.2478	24.9896	24.5555	24.8071	24.7561	24.8729	24.623	24.4181	24.5531
MnO	0.9158	0.9122	0.8976	0.881	0.8882	0.8779	0.9414	0.9361	0.9038	0.897	0.9301	0.9336	0.8995
MgO	7.5942	7.552	7.4883	7.451	7.3315	7.2554	8.0253	7.8382	7.698	8.0181	8.1272	7.8167	7.9286
CaO	7.7455	7.6826	6.6499	6.7755	6.6417	6.8581	6.4791	6.3922	6.5919	6.3738	6.3171	6.505	6.4432
Na2O	0.0357	0.0176	0.0317	0.0308	0.013	0.0366	0.0147	0.0386	0.0347	0.009	0.0164	0.0155	0.0216
K2O	0.0338	0.0287	0.0229	0.0269	0.0269	0.0397	0.0347	0.032	0.0484	0.0165	0.0384	0.0329	0.0453
Total	99.6581	99.7941	99.7949	99.5337	99.6668	99.5599	99.8951	99.965	99.6222	100.198	100.176	99.7076	100.0817
Cations	(calculated on the basis of 12 O)												
Si	2.9772	2.9652	2.976	2.9772	2.9784	2.9736	2.9736	2.97	2.9796	2.964	2.976	2.9712	2.9868
Ti	0.0048	0.0012	0.0024	0.0024	0.0024	0.0024	0.0024	0.0012	0.0012	0.0012	0.0024	0.0012	0.0024
Al	1.9524	1.9668	1.9704	1.9572	1.95	1.9584	1.9512	1.9656	1.9476	1.9668	1.956	1.9752	1.9524
Cr	0	0	0	0	0.0012	0.0012	0.0012	0	0	0	0	0	0
Fe	1.5216	1.5432	1.6044	1.6128	1.6452	1.6296	1.59	1.6068	1.6104	1.6068	1.5888	1.5828	1.5852
Mn	0.06	0.06	0.0588	0.0576	0.0588	0.0576	0.0612	0.0612	0.06	0.0588	0.0612	0.0612	0.0588
Mg	0.8772	0.8724	0.8664	0.8652	0.852	0.8436	0.9264	0.9048	0.8928	0.9228	0.9348	0.9036	0.912
Ca	0.6432	0.6384	0.5532	0.5652	0.5544	0.5724	0.5376	0.5304	0.5496	0.528	0.522	0.54	0.5328
Na	0.0048	0.0024	0.0048	0.0048	0.0024	0.006	0.0024	0.006	0.0048	0.0012	0.0024	0.0024	0.0036
K	0.0036	0.0024	0.0024	0.0024	0.0024	0.0036	0.0036	0.0036	0.0048	0.0012	0.0036	0.0036	0.0048
Total	8.0448	8.0532	8.04	8.046	8.0472	8.0496	8.0496	8.0508	8.0508	8.0508	8.0484	8.0424	8.0388
Mol. % end-members													
Grs	20.73501	20.500963	17.944726	18.227554	17.824074	18.445476	17.257319	17.092034	17.65613	16.942626	16.801854	17.489312	17.249417
Alm	49.052224	49.55684	52.043597	52.012384	52.893519	52.513534	51.040062	51.778809	51.734773	51.559492	51.139436	51.263117	51.320901
Prp	28.27853	28.015414	28.104321	27.902477	27.391975	27.184841	29.738059	29.156999	28.681573	29.61109	30.088837	29.265449	29.52603
Sps	1.934236	1.9267823	1.9073569	1.8575851	1.8904321	1.8561485	1.9645609	1.9721578	1.9275251	1.8867925	1.9698725	1.982122	1.9036519

Table B.40: Garnet analyses (cont.)

Sample No.	NA61E 12_8	NA61E 12_9	NA61E 12_10	NA61E 12_11	NA61E 12_12	NA61E 12_13	NA61E 12_14	NA61E 12_15	NA61E 12_16	NA61E 12_17	NA61E 12_18	NA61E 12_19	NA61E 12_20
Wt.%													
SiO2	38.2363	38.2851	38.1033	37.8007	37.9327	38.2498	38.0206	37.6945	38.2493	37.9948	38.2891	38.0958	38.3073
TiO2	0.0272	0.0531	0.0524	0.0634	0.0395	0.0628	0.0233	0.064	0.046	0.0259	0.0441	0.0389	0.055
Al2O3	21.4362	21.6695	21.6448	21.452	21.4391	21.552	21.5139	21.447	21.4459	21.6994	21.5035	21.5537	21.2747
Cr2O3	0.0022	0.0274	0	0.0107	0.0098	0	0	0	0	0.0001	0	0	0.0108
FeO	24.8299	24.7481	24.7183	25.1794	25.3401	24.6297	24.2607	25.3602	24.528	24.5588	24.5076	24.5614	24.7226
MnO	0.8942	0.9355	0.9276	0.9048	0.8891	0.8972	0.9236	0.8673	0.876	0.9033	0.9335	0.872	0.8842
MgO	7.7971	7.7942	7.462	7.5547	7.4276	7.9117	7.8644	7.0514	7.904	7.8753	7.644	7.5222	7.6511
CaO	6.5032	6.4413	6.4433	6.3512	6.4126	6.5501	6.7527	6.5805	6.3077	6.4719	6.6168	6.5317	6.5421
Na2O	0.0221	0.0358	0.0223	0.0329	0.0255	0.0223	0.0218	0.0304	0.0279	0.0388	0.024	0.0301	0.0249
K2O	0.0297	0.0242	0.0219	0.0388	0.0416	0.0256	0.0151	0.032	0.021	0.0133	0.0283	0.0261	0.0288
Total	99.7782	100.0141	99.396	99.3886	99.5577	99.9013	99.3962	99.1274	99.4059	99.5816	99.591	99.232	99.5016
Cations	(calculated on the basis of 12 O)												
Si	2.9688	2.9628	2.9676	2.9532	2.9604	2.9628	2.9592	2.9568	2.9748	2.952	2.9748	2.97	2.9808
Ti	0.0012	0.0036	0.0036	0.0036	0.0024	0.0036	0.0012	0.0036	0.0024	0.0012	0.0024	0.0024	0.0036
Al	1.962	1.9764	1.9872	1.9752	1.9716	1.968	1.974	1.9836	1.9656	1.9872	1.9692	1.9812	1.9512
Cr	0	0.0012	0	0.0012	0.0012	0	0	0	0	0	0	0	0.0012
Fe	1.6116	1.602	1.6104	1.6452	1.6536	1.596	1.5792	1.6644	1.5948	1.596	1.5924	1.602	1.6092
Mn	0.0588	0.0612	0.0612	0.06	0.0588	0.0588	0.0612	0.0576	0.0576	0.06	0.0612	0.0576	0.0588
Mg	0.9024	0.8988	0.8664	0.8796	0.864	0.9132	0.912	0.8244	0.9156	0.912	0.8856	0.8748	0.888
Ca	0.5412	0.534	0.5376	0.5316	0.5364	0.5436	0.5628	0.5532	0.5256	0.5388	0.5508	0.546	0.546
Na	0.0036	0.0048	0.0036	0.0048	0.0036	0.0036	0.0036	0.0048	0.0048	0.006	0.0036	0.0048	0.0036
K	0.0024	0.0024	0.0024	0.0036	0.0036	0.0024	0.0012	0.0036	0.0024	0.0012	0.0024	0.0024	0.0024
Total	8.0532	8.0484	8.04	8.058	8.0556	8.0532	8.0556	8.0532	8.0448	8.0556	8.0424	8.0412	8.0448
Mol. % end-members													
Grs	17.379576	17.248062	17.479516	17.058144	17.232074	17.470112	18.066256	17.847464	16.989915	17.342603	17.825243	17.724971	17.601547
Alm	51.753372	51.744186	52.360515	52.791683	53.122591	51.29194	50.693374	53.697251	51.55159	51.371186	51.533981	52.006233	51.876209
Prp	28.978805	29.031008	28.170113	28.224875	27.756361	29.348245	29.275809	26.59698	29.596587	29.354963	28.660194	28.398909	28.626692
Sps	1.8882466	1.9767442	1.9898556	1.9252984	1.8889746	1.889703	1.9645609	1.8583043	1.8619085	1.9312476	1.9805825	1.869887	1.8955513

Table B.41: Garnet analyses (cont.)

Sample No.	NA61E 12_21	NA61F 03_16	NA61F 03_17	NA61F_ 03_18	NA61F 03_19	NA61F 03_20	NA61F 03_21	NA61F 03_22	NA61F 03_23	NA61F 03_24	NA61F 02_1	NA61F 02_2	NA61F 02_3
Wt.%													
SiO2	38.2571	37.9316	37.9346	38.3852	37.9734	37.8478	37.9934	38.17	38.0463	37.865	38.1025	38.0462	38.0127
TiO2	0.0207	0.009	0.0045	0.0225	0.0611	0.0135	0.0322	0.0386	0.0367	0.0109	0.0045	0	0.0296
Al2O3	21.6329	21.4696	21.5276	21.5227	21.5342	21.4858	21.561	21.5852	21.5515	21.3375	21.5116	21.7668	21.5484
Cr2O3	0	0.0269	0.0159	0.0301	0.0378	0.0228	0	0	0.031	0.0118	0.0355	0	0.0191
FeO	24.5048	27.8281	28.1406	28.0108	28.1131	28.0722	27.8591	28.1154	27.6493	28.034	28.059	28.1749	27.8187
MnO	0.913	1.1058	1.0894	1.1025	1.0983	1.0683	1.0825	1.0439	1.1573	1.2174	1.0154	1.0917	1.0909
MgO	7.7002	7.2321	7.2252	7.2557	7.2948	7.2426	7.3351	7.3392	7.3082	6.8001	7.1403	7.2446	7.3866
CaO	6.8535	4.0769	4.1699	4.1087	4.0251	4.1878	4.1158	4.1615	4.2233	4.3181	4.0943	4.1815	4.1503
Na2O	0.0079	0.0247	0.0247	0.0287	0.0381	0.0493	0.0367	0.0135	0.0242	0.027	0.0216	0.014	0.0363
K2O	0.0302	0.033	0.0165	0.0147	0.0252	0.0312	0.0216	0.0243	0.0381	0.0174	0.0028	0.0161	0.0193
Total	99.9203	99.7378	100.1488	100.4815	100.201	100.0212	100.0373	100.4915	100.0658	99.6393	99.9875	100.5357	100.1118
Cations	(Calculated on the basis of 12 O)												
Si	2.964	2.97	2.9616	2.9808	2.9616	2.9592	2.9652	2.9664	2.9676	2.9748	2.976	2.958	2.964
Ti	0.0012	0	0	0.0012	0.0036	0.0012	0.0024	0.0024	0.0024	0.0012	0	0	0.0012
Al	1.9752	1.9812	1.9812	1.9704	1.98	1.98	1.9836	1.9776	1.9812	1.9752	1.98	1.9944	1.9812
Cr	0	0.0012	0.0012	0.0024	0.0024	0.0012	0	0	0.0024	0.0012	0.0024	0	0.0012
Fe	1.5876	1.8216	1.8372	1.8192	1.8336	1.836	1.818	1.8276	1.8036	1.842	1.8324	1.8312	1.8144
Mn	0.06	0.0732	0.072	0.072	0.072	0.0708	0.072	0.0684	0.0768	0.0816	0.0672	0.072	0.072
Mg	0.8892	0.8436	0.8412	0.84	0.8484	0.8448	0.8532	0.8508	0.8496	0.7968	0.8316	0.84	0.8592
Ca	0.5688	0.342	0.3492	0.342	0.336	0.3504	0.3444	0.3468	0.3528	0.3636	0.342	0.348	0.3468
Na	0.0012	0.0036	0.0036	0.0048	0.006	0.0072	0.006	0.0024	0.0036	0.0036	0.0036	0.0024	0.006
K	0.0024	0.0036	0.0012	0.0012	0.0024	0.0036	0.0024	0.0024	0.0036	0.0012	0	0.0012	0.0024
Total	8.0508	8.04	8.0496	8.0352	8.0472	8.0556	8.0472	8.046	8.0448	8.0424	8.0364	8.0484	8.0484
Mol. % end-members													
Grs	18.315301	11.102454	11.26597	11.128465	10.873786	11.295938	11.154295	11.21024	11.444142	11.789883	11.128465	11.257764	11.214591
Alm	51.120556	59.135177	59.272164	59.195627	59.339806	59.187621	58.880684	59.076804	58.505255	59.727626	59.625146	59.23913	58.672875
Prp	28.632148	27.386054	27.138986	27.333073	27.456311	27.234043	27.633113	27.501939	27.559362	25.836576	27.059742	27.173913	27.784245
Sps	1.9319938	2.3763148	2.3228804	2.3428348	2.3300971	2.2823985	2.3319083	2.2110163	2.4912417	2.6459144	2.1866458	2.3291925	2.3282887

Table B.42: Garnet analyses (cont.)

Sample No.	NA61F 02_4	NA61F 02_5	NA61F 02_6	NA61F 02_7	NA61F 02_8	NA61F 02_9	NA61F 02_10	NA61F 02_11	NA61F 02_12	NA61F 08_16	NA61F 08_17	NA61F 08_18	NA61F 08_19
Wt.%													
SiO2	38.101	38.0435	38.1526	38.1334	38.0585	37.9355	37.8158	37.9821	37.6255	37.917	38.0428	37.856	37.8556
TiO2	0.0103	0.0386	0.0019	0.0032	0.0206	0.0335	0.0077	0	0.0206	0.0193	0.0206	0	0.0006
Al2O3	21.6122	21.5135	21.5288	21.5224	21.6041	21.4657	21.6247	21.5495	21.7143	21.3769	21.3013	21.3972	21.2339
Cr2O3	0.0091	0.0182	0.0346	0.0588	0.0264	0.0077	0.0356	0.0374	0.0301	0.0145	0.0483	0.0314	0.0323
FeO	28.3201	27.9975	27.9602	28.0903	27.9897	28.1455	27.8618	27.9519	27.7675	28.4081	28.178	28.2834	28.2951
MnO	1.1056	1.0723	1.1158	1.0928	1.0678	1.0899	1.1008	1.1464	1.0668	1.429	1.4543	1.4769	1.4729
MgO	7.2975	7.237	7.1885	7.1662	7.2079	7.1663	7.2553	7.3042	7.2463	6.7526	6.7087	6.7496	6.7367
CaO	4.2167	4.1394	4.1489	4.1461	4.0549	4.1399	4.2075	4.1671	4.236	4.1564	4.2681	4.1406	4.1529
Na2O	0.0364	0.0224	0.0354	0.0296	0.0207	0.0265	0.0157	0.0305	0.039	0.0294	0.023	0.0284	0.0172
K2O	0.017	0.0252	0.0225	0.0294	0.0207	0.0206	0.0257	0.0115	0.0303	0.028	0.017	0.0193	0.0179
Total	100.7258	100.1075	100.1891	100.2721	100.0713	100.0311	99.9507	100.1805	99.7765	100.1311	100.062	99.9829	99.8152
Cations	(calculated on the basis of 12 O)												
Si	2.9592	2.9688	2.9736	2.9712	2.9688	2.9652	2.9556	2.9628	2.946	2.97	2.9796	2.9688	2.9748
Ti	0.0012	0.0024	0	0	0.0012	0.0024	0	0	0.0012	0.0012	0.0012	0	0
Al	1.9788	1.9788	1.9776	1.9764	1.9872	1.9776	1.992	1.9812	2.004	1.974	1.9656	1.9776	1.9668
Cr	0	0.0012	0.0024	0.0036	0.0012	0	0.0024	0.0024	0.0024	0.0012	0.0024	0.0024	0.0024
Fe	1.8396	1.8276	1.8228	1.8312	1.8264	1.8396	1.8216	1.8228	1.8192	1.8612	1.8456	1.8552	1.8588
Mn	0.0732	0.0708	0.0732	0.072	0.0708	0.072	0.0732	0.0756	0.0708	0.0948	0.096	0.0984	0.0984
Mg	0.8448	0.8412	0.8352	0.8328	0.8388	0.8352	0.846	0.8496	0.846	0.7884	0.7836	0.7896	0.7896
Ca	0.3504	0.3456	0.3468	0.3468	0.3384	0.3468	0.3528	0.348	0.3552	0.3492	0.3576	0.348	0.3492
Na	0.006	0.0036	0.0048	0.0048	0.0036	0.0036	0.0024	0.0048	0.006	0.0048	0.0036	0.0048	0.0024
K	0.0012	0.0024	0.0024	0.0024	0.0024	0.0024	0.0024	0.0012	0.0036	0.0024	0.0012	0.0024	0.0012
Total	8.0544	8.0424	8.04	8.0412	8.04	8.0448	8.0484	8.0496	8.0556	8.0484	8.0376	8.0484	8.0448
Mol. % end-members													
Grs	11.274131	11.201867	11.267057	11.249513	11.007026	11.21024	11.404189	11.24031	11.490683	11.28782	11.599844	11.257764	11.27907
Alm	59.189189	59.237651	59.220273	59.400545	59.406714	59.464701	58.882855	58.875969	58.850932	60.162917	59.867653	60.015528	60.03876
Prp	27.181467	27.265655	27.134503	27.014402	27.283372	26.997673	27.34678	27.44186	27.368012	25.484872	25.418451	25.543478	25.503876
Sps	2.3552124	2.2948269	2.3781676	2.3355391	2.3028884	2.3273856	2.3661753	2.4418605	2.2903727	3.064391	3.1140522	3.1832298	3.1782946

Table B.43: Garnet analyses (cont.)

Sample No.	NA61F 08_20	NA61F 08_21	NA61F 08_22	NA61F 08_23	NA61F 08_24	NA61F 08_25
Wt.%						
SiO2	37.7576	37.9006	37.7637	37.7397	37.8909	37.743
TiO2	0.0244	0.0064	0.0277	0.038	0.0392	0
Al2O3	21.3777	21.5763	21.46	21.4128	21.4527	21.3837
Cr2O3	0.0104	0.0496	0.0342	0.0141	0.0063	0.0068
FeO	28.6133	28.4471	27.7518	28.3554	28.3967	28.4706
MnO	1.4599	1.419	1.3816	1.3913	1.4213	1.401
MgO	6.6503	6.7228	6.4728	6.6252	6.7543	6.6607
CaO	4.3311	4.3521	4.9672	4.5089	4.2922	4.3051
Na2O	0.0114	0.014	0.0234	0.019	0.0163	0.015
K2O	0.0243	0.0312	0.0192	0.0197	0.0321	0.0252
Total	100.2604	100.5191	99.9016	100.124	100.3019	100.011
Cations	(calculated on the basis of 12 O)					
Si	2.9592	2.958	2.9628	2.9592	2.964	2.9628
Ti	0.0012	0	0.0012	0.0024	0.0024	0
Al	1.9752	1.9848	1.9848	1.9788	1.9776	1.9788
Cr	0.0012	0.0036	0.0024	0.0012	0	0
Fe	1.8756	1.8576	1.8216	1.86	1.8576	1.8696
Mn	0.0972	0.0936	0.0924	0.0924	0.0936	0.0936
Mg	0.7764	0.7824	0.7572	0.774	0.7872	0.78
Ca	0.3636	0.3636	0.4176	0.3792	0.36	0.3624
Na	0.0012	0.0024	0.0036	0.0024	0.0024	0.0024
K	0.0024	0.0036	0.0024	0.0024	0.0036	0.0024
Total	8.0544	8.0508	8.0472	8.0532	8.0496	8.0532
Mol. % end-members						
Grs	11.680802	11.739636	13.519814	12.210201	11.6189	11.669243
Alm	60.254433	59.976753	58.974359	59.891808	59.953524	60.200927
Prp	24.942174	25.261527	24.514375	24.92272	25.406662	25.11592
Sps	3.1225906	3.0220845	2.991453	2.9752705	3.020914	3.0139104

Table B.44: Ilmenite analyses

Sample	NA23A	NA23A	NA23A	NA46	NA46	NA46	NA46	NA46	NA46	NA61C	NA61C	NA61C
No.	05_39	05_47	05_58	02_16	03_49	03_50	03_56	03_66	03_73	02_31	02_37	04_20
Wt.%												
SiO2	0.0841	0.0965	0.0595	0.0728	0.0953	0.0792	0.0904	0.0652	0.0362	0.0311	0.0722	0.0649
TiO2	49.2344	45.9874	43.9513	51.401	52.2022	51.9622	52.5647	51.7117	53.2298	52.574	52.2349	52.2066
Al2O3	0.0519	0.0193	0.0647	0.0142	0.0407	0.0231	0.0083	0.0313	0.0312	0.0121	0.0483	0.0258
Cr2O3	0.2257	0.208	0.2399	0.2017	0.2209	0.1915	0.2022	0.2123	0.1842	0.1345	0.1154	0.0956
FeO	51.3584	53.1926	56.1894	49.2916	49.3174	49.2256	48.6507	49.1586	48.9653	48.8646	48.6844	48.3649
MnO	0.2903	0.3951	0.3519	0.3616	0.3623	0.3114	0.3489	0.2843	0.3153	0.1846	0.196	0.1371
MgO	0.0788	0.0643	0.0487	0.4467	0.8421	0.6612	0.5181	0.7261	0.5469	0	0.0323	0.0982
CaO	0.084	0.1507	0.1073	0.05	0.0515	0.0557	0.0974	0.0603	0.0648	0.0319	0.035	0.0189
Na2O	0	0.0118	0	0.0212	0	0	0	0.0224	0.0134	0	0.015	0
K2O	0.0621	0.0781	0.0584	0.0492	0.0568	0.0572	0.0751	0.0456	0.0535	0.0311	0.0415	0.0987
Total	101.4696	100.2037	101.0711	101.91	103.1891	102.5671	102.5557	102.3177	103.4406	101.8639	101.4749	101.1106
Cations	(calculated on the basis of 3 O)											
Si	0.0021	0.0024	0.0015	0.0018	0.0024	0.0021	0.0021	0.0015	0.0009	0.0009	0.0018	0.0015
Ti	0.9411	0.9039	0.8688	0.9663	0.966	0.9681	0.9768	0.966	0.9798	0.9852	0.9825	0.9849
Al	0.0015	0.0006	0.0021	0.0003	0.0012	0.0006	0.0003	0.0009	0.0009	0.0003	0.0015	0.0009
Cr	0.0045	0.0042	0.0051	0.0039	0.0042	0.0039	0.0039	0.0042	0.0036	0.0027	0.0024	0.0018
Fe	1.0917	1.1628	1.2351	1.0305	1.0146	1.02	1.0053	1.0212	1.0023	1.0182	1.0185	1.0146
Mn	0.0063	0.0087	0.0078	0.0078	0.0075	0.0066	0.0072	0.006	0.0066	0.0039	0.0042	0.003
Mg	0.003	0.0024	0.0018	0.0165	0.0309	0.0243	0.0192	0.027	0.0201	0	0.0012	0.0036
Ca	0.0024	0.0042	0.003	0.0012	0.0015	0.0015	0.0027	0.0015	0.0018	0.0009	0.0009	0.0006
Na	0	0.0006	0	0.0009	0	0	0	0.0012	0.0006	0	0.0006	0
K	0.0021	0.0027	0.0021	0.0015	0.0018	0.0018	0.0024	0.0015	0.0018	0.0009	0.0012	0.0033
Total	2.0547	2.0925	2.1276	2.031	2.0304	2.0289	2.0199	2.0313	2.0187	2.0133	2.0148	2.0142

Table B.45: Ilmenite analyses (cont.)

Sample No.	NA61C 06_11	NA61C 06_14	NA61C 06_8	NA61C 07_10	NA61C 07_2	NA61C 07_5	NA61F 08_27	NA61F 12_10	NA61F 12_11	NA61F 12_12	NA61F 12_13	NA61F 12_14
Wt.%												
SiO2	0.1198	0.0244	0.1126	0.0059	0.0281	0.0117	0.3417	0.129	0.0736	0.07	0.1018	0.0936
TiO2	51.4546	52.4441	51.8929	53.0185	51.5761	52.7412	48.31	48.8084	49.1472	48.814	51.829	49.0584
Al2O3	0.0099	0.0354	0.0379	0.007	0.0254	0.0295	0.6246	0.0713	0.0299	0.0239	0.0136	0.0257
Cr2O3	0.141	0.1461	0.1766	0.1275	0.15	0.1526	0.3241	0.2191	0.2395	0.2291	0.2218	0.2261
FeO	49.0581	49.2295	49.2181	48.6156	49.266	48.9137	47.9112	49.79	50.2143	50.4204	47.5853	49.9371
MnO	0.116	0.1203	0.1376	0.1264	0.1284	0.1226	0.6552	0.307	0.2709	0.2606	0.4987	0.3117
MgO	0.0221	0.0158	0.0472	0.0282	0.0226	0.0501	0.0238	0.6773	0.9169	0.9007	0.3956	0.6665
CaO	0.0585	0.0186	0.0622	0.0252	0.0751	0.0186	0.0698	0.0925	0.0727	0.0686	0.1054	0.0784
Na2O	0	0.0103	0.0129	0.0174	0.0151	0.0187	0.0064	0	0.0564	0.0216	0.0232	0.0186
K2O	0.0625	0.0497	0.0629	0.0251	0.0521	0.0386	0.0736	0.0689	0.0585	0.0565	0.0683	0.0553
Total	101.0424	102.0941	101.7608	101.9967	101.3388	102.0972	98.3405	100.1634	101.0798	100.8653	100.8426	100.4714
Cations	(calculated on the basis of 3 O)											
Si	0.003	0.0006	0.0027	0	0.0006	0.0003	0.009	0.0033	0.0018	0.0018	0.0027	0.0024
Ti	0.975	0.9816	0.9756	0.9903	0.9753	0.9855	0.9426	0.9402	0.9384	0.9354	0.9792	0.9423
Al	0.0003	0.0009	0.0012	0.0003	0.0009	0.0009	0.0192	0.0021	0.0009	0.0006	0.0003	0.0009
Cr	0.0027	0.003	0.0036	0.0024	0.003	0.003	0.0066	0.0045	0.0048	0.0045	0.0045	0.0045
Fe	1.0335	1.0248	1.029	1.0098	1.0359	1.0164	1.0395	1.0668	1.0662	1.0743	0.9996	1.0668
Mn	0.0024	0.0024	0.003	0.0027	0.0027	0.0027	0.0144	0.0066	0.0057	0.0057	0.0105	0.0066
Mg	0.0009	0.0006	0.0018	0.0009	0.0009	0.0018	0.0009	0.0258	0.0348	0.0342	0.0147	0.0255
Ca	0.0015	0.0006	0.0018	0.0006	0.0021	0.0006	0.0018	0.0024	0.0021	0.0018	0.0027	0.0021
Na	0	0.0006	0.0006	0.0009	0.0006	0.0009	0.0003	0	0.0027	0.0012	0.0012	0.0009
K	0.0021	0.0015	0.0021	0.0009	0.0018	0.0012	0.0024	0.0024	0.0018	0.0018	0.0021	0.0018
Total	2.0214	2.0166	2.0214	2.0091	2.0241	2.0136	2.037	2.0544	2.0595	2.0616	2.0178	2.0541

Table B.46: Ilmenite analyses (cont.)

Sample No.	NA61F 12_15	NA61F 12_17	NA61F 12_3	NA61F 16_1	NA61F 16_2	NA61F 16_6	NA61F 16_7	NA61F 16_8	NA61F 16_9	NA61F 17_1	NA61F 17_10	NA61F 17_5
Wt.%												
SiO2	0.1001	0.0674	0.6818	0.0912	0.1144	0.1144	0.1239	1.9824	0.0876	0.0853	0.856	0.8788
TiO2	49.251	49.1489	49.1401	47.3719	51.6304	50.1436	49.6618	49.238	49.3242	50.0041	47.3012	48.8785
Al2O3	0.052	0.0276	0.3819	0.0213	0.0344	0.012	0.0714	1.3306	0.0139	0.0175	0.4499	0.5825
Cr2O3	0.2102	0.218	0.2689	0.2614	0.2658	0.2837	0.261	0.2394	0.2792	0.2918	0.2931	0.2979
FeO	49.8204	50.3618	48.1051	51.8489	48.4966	49.6463	50.0555	46.6735	51.1644	50.385	48.3825	48.413
MnO	0.2736	0.2977	0.724	0.3527	0.4905	0.4953	0.478	0.6054	0.4217	0.4832	1.2979	0.7438
MgO	0.7966	0.8744	0.0905	0.8407	0.1214	0.4053	0.3566	0.464	0.2136	0.1366	0.3115	0.1686
CaO	0.0718	0.0822	0.1032	0.0778	0.0873	0.0891	0.1271	0.0825	0.0776	0.0726	0.0852	0.0848
Na2O	0.036	0.0084	0.0108	0	0.0052	0	0	0.0092	0	0	0.0076	0.0028
K2O	0.0521	0.0565	0.0792	0.0721	0.0735	0.0803	0.066	0.0895	0.0744	0.0664	0.061	0.0729
Total	100.6637	101.1428	99.5855	100.938	101.3195	101.27	101.2012	100.7144	101.6565	101.5424	99.046	100.1235
Cations	(calculated on the basis of 3 O)											
Si	0.0024	0.0018	0.0174	0.0024	0.003	0.003	0.003	0.0492	0.0021	0.0021	0.0222	0.0222
Ti	0.9429	0.9384	0.9441	0.915	0.9744	0.9531	0.9468	0.9177	0.9405	0.951	0.9186	0.9333
Al	0.0015	0.0009	0.0114	0.0006	0.0009	0.0003	0.0021	0.039	0.0003	0.0006	0.0138	0.0174
Cr	0.0042	0.0045	0.0054	0.0054	0.0054	0.0057	0.0051	0.0048	0.0057	0.0057	0.006	0.006
Fe	1.0605	1.0692	1.0278	1.1136	1.0176	1.0494	1.0611	0.9675	1.0851	1.0656	1.0449	1.0278
Mn	0.006	0.0063	0.0156	0.0078	0.0105	0.0105	0.0102	0.0126	0.009	0.0105	0.0285	0.0159
Mg	0.0303	0.033	0.0033	0.0321	0.0045	0.0153	0.0135	0.0171	0.0081	0.0051	0.012	0.0063
Ca	0.0021	0.0021	0.0027	0.0021	0.0024	0.0024	0.0036	0.0021	0.0021	0.0021	0.0024	0.0024
Na	0.0018	0.0003	0.0006	0	0.0003	0	0	0.0003	0	0	0.0003	0
K	0.0018	0.0018	0.0027	0.0024	0.0024	0.0027	0.0021	0.0027	0.0024	0.0021	0.0021	0.0024
Total	2.0538	2.0586	2.0313	2.0814	2.0214	2.0424	2.0478	2.0133	2.0553	2.0448	2.0511	2.0337

Table B.47: Ilmenite analyses (cont.)

Sample No.	NA61F 17_6	NA61F 17_7	NA61F 17_8
Wt.%			
SiO2	1.3149	1.4579	1.0722
TiO2	48.3896	49.0922	49.9933
Al2O3	0.8446	0.8324	0.6613
Cr2O3	0.2705	0.3073	0.2654
FeO	47.3579	47.2343	46.5035
MnO	0.7616	0.7987	0.8894
MgO	0.22	0.3342	0.1456
CaO	0.0969	0.0845	0.0694
Na2O	0.0159	0.0034	0
K2O	0.0698	0.0953	0.0697
Total	99.3418	100.2402	99.6699
Cations	(calculated on the basis of 3 O)		
Si	0.0333	0.0366	0.027
Ti	0.9255	0.9276	0.9495
Al	0.0252	0.0246	0.0198
Cr	0.0054	0.006	0.0054
Fe	1.0071	0.9924	0.9822
Mn	0.0165	0.0171	0.0189
Mg	0.0084	0.0126	0.0054
Ca	0.0027	0.0024	0.0018
Na	0.0009	0.0003	0
K	0.0024	0.003	0.0021
Total	2.0274	2.0229	2.0124

Table B.48 Orthopyroxene analyses

Sample	NA23A	NA23A	NA23A	NA23A	NA23A	NA23A	NA23A	NA46	NA46	NA46	NA46	NA46	NA61E
No.	05_42	05_35	05_36	05_37	05_48	05_56	05_32	03_11	03_51	03_48	03_75	03_55	09_5
Wt.%													
SiO2	51.7432	52.196	51.9728	52.1674	51.6772	51.9661	52.2006	52.4393	52.0134	51.6087	51.6038	52.1967	52.8845
TiO2	0.0816	0.0628	0.0583	0.0842	0.0707	0.1178	0.0382	0.0978	0.1062	0.0718	0.0699	0.0803	0.0175
Al2O3	1.6289	1.5531	1.7679	1.491	1.7133	1.8466	1.5693	1.0612	0.8449	0.9186	0.848	1.1889	1.4253
Cr2O3	0.0162	0	0.0094	0.0204	0	0	0.0034	0.0572	0.0246	0.0241	0.0357	0.037	0.0145
FeO	25.2316	25.3166	25.0508	25.429	24.0418	25.8929	25.6354	27.7837	28.1867	28.1867	28.1227	27.8164	22.7151
MnO	0.3194	0.3257	0.3307	0.3239	0.2839	0.3133	0.3328	0.28	0.3137	0.3261	0.2412	0.2964	0.28
MgO	21.4706	21.3741	21.3149	21.4786	22.1033	20.6238	21.3663	19.5533	19.408	19.2702	19.5463	19.2534	22.6608
CaO	0.3467	0.3469	0.3515	0.3542	0.3544	0.3873	0.3951	0.4203	0.4414	0.4578	0.4585	0.4864	0.2676
Na2O	0	0.0049	0.0219	0	0.0027	0.0036	0	0.02	0	0	0.0174	0.0085	0
K2O	0.0314	0.0247	0.0283	0.0354	0.0364	0.0408	0.0354	0.0306	0.0297	0.0305	0.0081	0.0292	0.0099
Total	100.8695	101.2048	100.9064	101.384	100.2836	101.1921	101.5764	101.7433	101.3685	100.8944	100.9515	101.3931	100.2751
Cations	(calculated on the basis of 6 O)												
Si	1.9368	1.9458	1.9416	1.9434	1.9356	1.9428	1.9422	1.9656	1.9632	1.959	1.9566	1.9644	1.9632
Ti	0.0024	0.0018	0.0018	0.0024	0.0018	0.0036	0.0012	0.003	0.003	0.0018	0.0018	0.0024	0.0006
Al	0.072	0.0684	0.078	0.0654	0.0756	0.0816	0.069	0.0468	0.0378	0.0408	0.0378	0.0528	0.0624
Cr	0.0006	0	0	0.0006	0	0	0	0.0018	0.0006	0.0006	0.0012	0.0012	0.0006
Fe	0.7902	0.7896	0.783	0.792	0.753	0.8094	0.798	0.8712	0.8898	0.8946	0.8916	0.8754	0.705
Mn	0.0102	0.0102	0.0102	0.0102	0.009	0.0102	0.0102	0.009	0.0102	0.0102	0.0078	0.0096	0.009
Mg	1.1982	1.188	1.1874	1.1928	1.2342	1.1496	1.185	1.0926	1.092	1.0902	1.1046	1.08	1.254
Ca	0.0138	0.0138	0.0138	0.0144	0.0144	0.0156	0.0156	0.0168	0.018	0.0186	0.0186	0.0198	0.0108
Na	0	0.0006	0.0018	0	0	0	0	0.0012	0	0	0.0012	0.0006	0
K	0.0012	0.0012	0.0012	0.0018	0.0018	0.0018	0.0018	0.0012	0.0012	0.0012	0.0006	0.0012	0.0006
Total	4.0254	4.02	4.0188	4.0236	4.0254	4.0152	4.0236	4.0098	4.0164	4.0176	4.0224	4.008	4.0068
Mol. % end-members													
En	60.259505	60.072816	60.261876	60.096735	62.107488	58.683002	59.757943	55.63703	55.101423	54.927449	55.335137	55.231666	64.012251
Fs	39.740495	39.927184	39.738124	39.903265	37.892512	41.316998	40.242057	44.36297	44.898577	45.072551	44.664863	44.768334	35.987749

Table B.49 Orthopyroxene analyses (cont.)

Sample No.	NA61E 12_32	NA61E 09_6	NA61E 20_35	NA61E 04_29	NA61E 15_2	NA61E 20_34	NA61E 09_4	NA61 20_20	NA61E 03_22	NA61E 20_21	NA61 19_4	NA61E 09_26
Wt.%												
SiO2	52.869	53.0196	52.6358	53.0566	52.2487	52.3275	52.8023	52.2564	53.5111	52.3803	52.7658	52.5247
TiO2	0.075	0.0246	0.0422	0.1039	0.0799	0.0727	0.0763	0.0216	0.1099	0.0575	0.0429	0.0607
Al2O3	1.7285	1.2829	1.0364	1.7117	1.3462	1.4034	1.8031	1.6869	1.8044	1.1547	1.4105	1.7197
Cr2O3	0.0033	0.0311	0.0307	0.0443	0.0265	0.0274	0	0.0251	0.0924	0.0598	0.0104	0
FeO	22.7049	23.0644	22.9064	21.2261	22.9666	23.2381	23.0842	23.158	20.5839	23.2905	22.4712	23.2646
MnO	0.2272	0.2844	0.3048	0.2789	0.3043	0.2681	0.2967	0.326	0.2191	0.2822	0.2453	0.3194
MgO	22.3285	22.4459	22.3285	24.0145	22.5859	22.0233	22.4772	22.2798	24.3227	22.4427	22.8947	22.126
CaO	0.3126	0.3205	0.3271	0.3358	0.3565	0.3619	0.3623	0.3679	0.3688	0.3798	0.3825	0.386
Na2O	0.0134	0.0158	0	0.0192	0.0105	0	0	0	0.0236	0	0	0.0181
K2O	0.0152	0.0134	0.0103	0.0538	0.0337	0.0229	0.0112	0.0098	0.0305	0.029	0.0081	0.0246
Total	100.2775	100.5025	99.6223	100.8447	99.9589	99.7454	100.9132	100.1314	101.0663	100.0764	100.2313	100.4437
Cations	(calculated on the basis of 6 O)											
Si	1.9614	1.9668	1.9704	1.9464	1.9524	1.9602	1.9512	1.9494	1.9506	1.9572	1.9584	1.9536
Ti	0.0018	0.0006	0.0012	0.003	0.0024	0.0018	0.0024	0.0006	0.003	0.0018	0.0012	0.0018
Al	0.0756	0.0558	0.0456	0.0738	0.0594	0.0618	0.0786	0.0744	0.0774	0.051	0.0618	0.0756
Cr	0	0.0012	0.0012	0.0012	0.0006	0.0006	0	0.0006	0.0024	0.0018	0.0006	0
Fe	0.7044	0.7158	0.717	0.651	0.7176	0.7278	0.7134	0.7224	0.6276	0.7278	0.6978	0.7236
Mn	0.0072	0.009	0.0096	0.0084	0.0096	0.0084	0.009	0.0102	0.0066	0.009	0.0078	0.0102
Mg	1.2348	1.2414	1.2462	1.3134	1.2582	1.23	1.2384	1.239	1.3218	1.2504	1.2666	1.2264
Ca	0.0126	0.0126	0.0132	0.0132	0.0144	0.0144	0.0144	0.015	0.0144	0.015	0.015	0.0156
Na	0.0012	0.0012	0	0.0012	0.0006	0	0	0	0.0018	0	0	0.0012
K	0.0006	0.0006	0.0006	0.0024	0.0018	0.0012	0.0006	0.0006	0.0012	0.0012	0.0006	0.0012
Total	3.9996	4.0056	4.005	4.0146	4.0176	4.0068	4.008	4.0128	4.0074	4.0158	4.0104	4.0098
Mol. % end-members												
En	63.675743	63.427345	63.477995	66.86011	63.680534	62.825621	63.449124	63.169165	67.805479	63.208978	64.477703	62.892308
Fs	36.324257	36.572655	36.522005	33.13989	36.319466	37.174379	36.550876	36.830835	32.194521	36.791022	35.522297	37.107692

Table B.50 Orthopyroxene analyses (cont.)

Sample No.	NA61 20_23	NA61E 07_5	NA61E 15_3	NA61E 03_21	NA61E 02_16	NA61 20_24	NA61E 07_2	NA61E 07_6	NA61E 07_7	NA61E 19_2	NA61E 02_2	NA61E 20_32
Wt.%												
SiO2	52.065	52.8161	51.6933	53.3956	51.3636	51.667	53.1419	53.0894	52.9431	51.7779	51.0089	52.3429
TiO2	0.0602	0.0855	0.1209	0.0767	0.0356	0.0832	0.1081	0.0939	0.1088	0.0507	0.0428	0.0455
Al2O3	1.5438	1.551	1.5235	1.6986	1.0756	1.5137	1.6722	1.8126	1.6889	1.5497	1.7641	1.5302
Cr2O3	0.027	0.0639	0.0715	0.0616	0	0.0251	0.0477	0.0519	0.0533	0.0215	0	0.047
FeO	23.1585	22.8206	22.8342	20.8083	22.6687	22.9794	22.8442	22.5792	22.9101	22.7607	22.7849	22.4102
MnO	0.2682	0.2616	0.323	0.2387	0.2181	0.2729	0.2611	0.2696	0.2526	0.2829	0.2322	0.2588
MgO	22.1999	22.5582	22.5277	24.0587	22.9736	22.2891	22.7922	22.609	22.5737	22.549	22.759	22.4912
CaO	0.3882	0.3986	0.4175	0.4186	0.4205	0.4221	0.4325	0.4345	0.4357	0.4398	0.4423	0.4433
Na2O	0.0044	0.02	0.0088	0.02	0.0382	0.0057	0.0037	0.0104	0.0254	0.0006	0.0382	0
K2O	0.0103	0.0399	0.0454	0.0355	0.0341	0.0201	0.0305	0.0443	0.0376	0.0157	0.0332	0.0058
Total	99.7256	100.6153	99.5658	100.8122	98.8281	99.2784	101.334	100.9948	101.0292	99.4486	99.1057	99.575
Cations	(calculated on the basis of 6 O)											
Si	1.9512	1.9566	1.941	1.9542	1.9434	1.9458	1.953	1.9554	1.953	1.9446	1.926	1.9572
Ti	0.0018	0.0024	0.0036	0.0024	0.0012	0.0024	0.003	0.0024	0.003	0.0012	0.0012	0.0012
Al	0.0684	0.0678	0.0672	0.0732	0.048	0.0672	0.0726	0.0786	0.0732	0.0684	0.0786	0.0672
Cr	0.0006	0.0018	0.0024	0.0018	0	0.0006	0.0012	0.0018	0.0018	0.0006	0	0.0012
Fe	0.726	0.7068	0.717	0.6372	0.717	0.7236	0.702	0.6954	0.7068	0.7146	0.7194	0.7008
Mn	0.0084	0.0084	0.0102	0.0072	0.0072	0.009	0.0084	0.0084	0.0078	0.009	0.0072	0.0084
Mg	1.2402	1.2456	1.2612	1.3128	1.296	1.2516	1.2486	1.2414	1.2414	1.2624	1.281	1.2534
Ca	0.0156	0.0156	0.0168	0.0162	0.0168	0.0168	0.0168	0.0174	0.0174	0.0174	0.018	0.018
Na	0.0006	0.0012	0.0006	0.0012	0.003	0.0006	0	0.0006	0.0018	0	0.003	0
K	0.0006	0.0018	0.0024	0.0018	0.0018	0.0012	0.0012	0.0018	0.0018	0.0006	0.0018	0
Total	4.0134	4.008	4.0224	4.008	4.035	4.0188	4.0074	4.0032	4.008	4.0188	4.0362	4.008
Mol. % end-members												
En	63.075984	63.798402	63.754929	67.323077	64.38152	63.365735	64.011074	64.095415	63.720357	63.854325	64.037193	64.138778
Fs	36.924016	36.201598	36.245071	32.676923	35.61848	36.634265	35.988926	35.904585	36.279643	36.145675	35.962807	35.861222

Table B.51 Orthopyroxene analyses (cont.)

Sample No.	NA61E 09_3	NA61E 03_5	NA61E 09_9	NA61E 19_1	NA61E 20_33	NA61E 19_6	NA61E 02_01	NA61E 20_18	NA61E 19_3	NA61E 07_3	NA61E 09_8	NA61E 02_3
Wt.%												
SiO2	52.6064	50.4995	52.9701	52.1931	52.2148	52.0972	51.2175	51.8612	51.6156	52.9969	52.9469	50.742
TiO2	0.0576	0.0635	0.0427	0.0617	0.0754	0.076	0.046	0.0838	0.0649	0.0972	0.0563	0.0175
Al2O3	1.6397	1.6622	1.7974	1.6085	1.7262	1.4371	1.6356	1.5624	1.646	1.6989	1.72	1.7065
Cr2O3	0.0117	0.018	0.0172	0.0057	0.0169	0.0516	0.0092	0.067	0.0247	0.045	0.0052	0.0143
FeO	22.7762	22.2081	23.0108	22.8137	22.3869	22.6647	22.5055	23.3222	22.8401	22.7136	23.2002	22.6369
MnO	0.2912	0.2221	0.3202	0.2733	0.2408	0.2424	0.2446	0.2775	0.2709	0.2981	0.2793	0.2025
MgO	22.334	23.1195	22.4856	22.5225	22.7008	22.6481	22.8423	22.0792	22.3834	22.6726	22.396	22.7826
CaO	0.4511	0.4516	0.4521	0.4526	0.4528	0.4621	0.4622	0.4632	0.4692	0.479	0.4834	0.4978
Na2O	0.0066	0.021	0.0091	0	0.0198	0.0065	0.0252	0	0	0.0428	0.0191	0.0336
K2O	0.009	0.0152	0.0148	0.0162	0.0148	0.022	0.0206	0.0164	0.0225	0.0421	0.017	0.0175
Total	100.1834	98.2808	101.1199	99.9473	99.8493	99.7078	99.0088	99.7329	99.3373	101.0861	101.1233	98.6513
Cations	(calculated on the basis of 6 O)											
Si	1.9566	1.92	1.953	1.9488	1.947	1.9494	1.9326	1.9464	1.9416	1.953	1.9536	1.9248
Ti	0.0018	0.0018	0.0012	0.0018	0.0024	0.0024	0.0012	0.0024	0.0018	0.0024	0.0018	0.0006
Al	0.072	0.0744	0.078	0.0708	0.0756	0.0636	0.0726	0.069	0.0732	0.0738	0.075	0.0762
Cr	0.0006	0.0006	0.0006	0	0.0006	0.0018	0	0.0018	0.0006	0.0012	0	0.0006
Fe	0.7086	0.7062	0.7098	0.7122	0.6984	0.7092	0.7104	0.732	0.7188	0.7002	0.7158	0.7182
Mn	0.009	0.0072	0.0102	0.0084	0.0078	0.0078	0.0078	0.009	0.0084	0.0096	0.009	0.0066
Mg	1.2384	1.3104	1.236	1.2534	1.2618	1.2636	1.2846	1.2354	1.2552	1.2456	1.2318	1.2882
Ca	0.018	0.0186	0.018	0.018	0.018	0.0186	0.0186	0.0186	0.0192	0.0192	0.0192	0.0204
Na	0.0006	0.0018	0.0006	0	0.0012	0.0006	0.0018	0	0	0.003	0.0012	0.0024
K	0.0006	0.0006	0.0006	0.0006	0.0006	0.0012	0.0012	0.0006	0.0012	0.0018	0.0006	0.0006
Total	4.0068	4.0416	4.0086	4.0146	4.014	4.0188	4.0314	4.0158	4.02	4.0098	4.008	4.0392
Mol. % end-members												
En	63.605547	64.980661	63.521431	63.766789	64.370983	64.051095	64.390977	62.793535	63.586626	64.014801	63.247073	64.204545
Fs	36.394453	35.019339	36.478569	36.233211	35.629017	35.948905	35.609023	37.206465	36.413374	35.985199	36.752927	35.795455

Table B.52 Orthopyroxene analyses (cont.)

Sample No.	NA61E 05_27	NA61E 09_10	NA61E 20_19	NA61E 09_7	NA61E 09_11	NA61E 07_4	NA61E 09_2	NA61E 02_4	NA61E 09_1	NA61E 09_12	NA61E 19_7	NA61E 15_1
Wt.%												
SiO2	52.5368	52.6852	52.0154	52.712	52.79	52.4241	52.8984	50.5707	53.0305	52.8041	51.6132	52.4107
TiO2	0.0227	0.086	0.0805	0.0485	0.0433	0.1049	0.0563	0.0609	0.0634	0.044	0.0689	0.0956
Al2O3	1.7554	1.7382	1.5906	1.694	1.7385	1.809	1.6881	1.7729	1.6615	1.7112	1.5986	1.4
Cr2O3	0	0.0278	0.014	0.0085	0	0.0852	0.0482	0.0106	0.0435	0.0431	0.0173	0.0507
FeO	21.427	23.2174	23.3113	22.8497	22.9705	22.4815	22.9834	22.5661	23.0843	22.9496	22.8282	22.6125
MnO	0.2224	0.291	0.3051	0.3102	0.2967	0.2639	0.2631	0.2405	0.3208	0.3012	0.3002	0.2662
MgO	23.6318	22.0661	22.0787	22.3601	22.0647	22.3602	22.35	22.5697	22.4787	22.1114	22.133	22.4319
CaO	0.5014	0.5082	0.5286	0.5427	0.5436	0.5453	0.546	0.5497	0.5497	0.5497	0.5557	0.5747
Na2O	0.0339	0.0233	0	0.0291	0.0204	0.0245	0.0245	0.0336	0.0216	0.0262	0.0052	0.0046
K2O	0.0202	0.0219	0.008	0.0246	0.0228	0.0345	0.0085	0.0211	0.021	0.0085	0.0207	0.0355
Total	100.1516	100.665	99.9323	100.5794	100.4905	100.133	100.8664	98.3959	101.2749	100.5489	99.1411	99.8825
Cations	(Calculated on the basis of 6 O)											
Si	1.944	1.9542	1.9482	1.9542	1.959	1.95	1.9554	1.9236	1.9536	1.9584	1.9458	1.9566
Ti	0.0006	0.0024	0.0024	0.0012	0.0012	0.003	0.0018	0.0018	0.0018	0.0012	0.0018	0.0024
Al	0.0768	0.0762	0.0702	0.0738	0.0762	0.0792	0.0738	0.0792	0.072	0.075	0.0708	0.0618
Cr	0	0.0006	0.0006	0	0	0.0024	0.0012	0.0006	0.0012	0.0012	0.0006	0.0012
Fe	0.663	0.72	0.7302	0.7086	0.7128	0.6996	0.7104	0.7176	0.711	0.7116	0.72	0.7062
Mn	0.0072	0.009	0.0096	0.0096	0.0096	0.0084	0.0084	0.0078	0.0102	0.0096	0.0096	0.0084
Mg	1.3038	1.2204	1.2324	1.236	1.2204	1.2402	1.2318	1.2798	1.2348	1.2222	1.2438	1.2486
Ca	0.0198	0.0204	0.021	0.0216	0.0216	0.0216	0.0216	0.0222	0.0216	0.0216	0.0222	0.0228
Na	0.0024	0.0018	0	0.0018	0.0012	0.0018	0.0018	0.0024	0.0018	0.0018	0.0006	0.0006
K	0.0012	0.0012	0.0006	0.0012	0.0012	0.0018	0.0006	0.0012	0.0012	0.0006	0.0012	0.0018
Total	4.0188	4.0068	4.0158	4.008	4.0032	4.008	4.0068	4.0362	4.0098	4.0038	4.0164	4.0104
Mol. % end-members												
En	66.290421	62.894249	62.794253	63.560629	63.128492	63.934426	63.422922	64.073295	63.459759	63.201986	63.336389	63.873542
Fs	33.709579	37.105751	37.205747	36.439371	36.871508	36.065574	36.577078	35.926705	36.540241	36.798014	36.663611	36.126458

Table B.53 Orthopyroxene analyses (cont.)

Sample No.	NA61E 07_01	NA61 20_17
Wt.%		
SiO2	53.0545	52.1283
TiO2	0.1308	0.1286
Al2O3	1.5905	1.5836
Cr2O3	0.0746	0.0131
FeO	22.8018	22.9039
MnO	0.2656	0.2689
MgO	22.6658	22.2714
CaO	0.5753	0.6054
Na2O	0.015	0.0087
K2O	0.0278	0.0253
Total	101.2017	99.9373
Cations	(Calculated on the basis of 6 O)	
Si	1.9536	1.9482
Ti	0.0036	0.0036
Al	0.069	0.0696
Cr	0.0024	0.0006
Fe	0.702	0.7158
Mn	0.0084	0.0084
Mg	1.2444	1.2408
Ca	0.0228	0.024
Na	0.0012	0.0006
K	0.0012	0.0012
Total	4.0092	4.0134
Mol. % end-members		
En	63.933416	63.41613
Fs	36.066584	36.58387

APPENDIX D: MICROPROBE IMAGES

Appendix D presents backscattered electron (BSE) images obtained during microprobe analysis of study samples. The number in the upper left refers to the sample number (preceding the hyphen) and images number (following the hyphen). The numbered points indicate the location of the analysis referred to by the "No." row in the Appendix C tables.

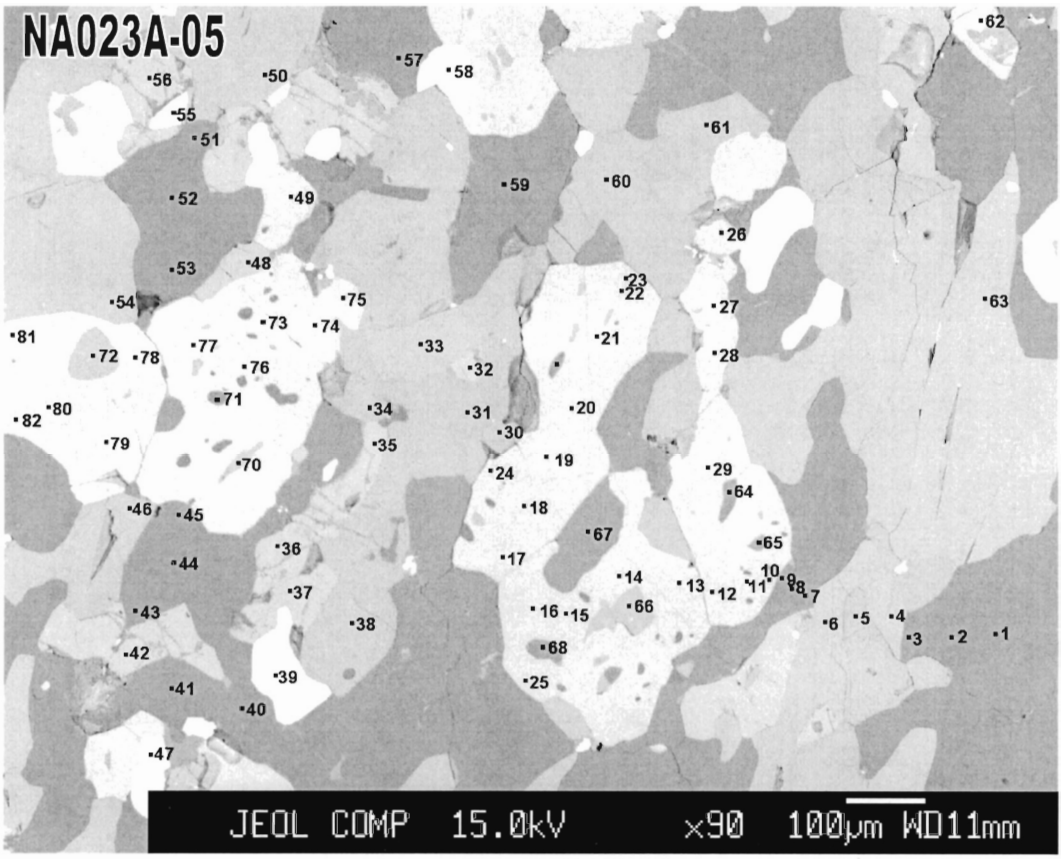

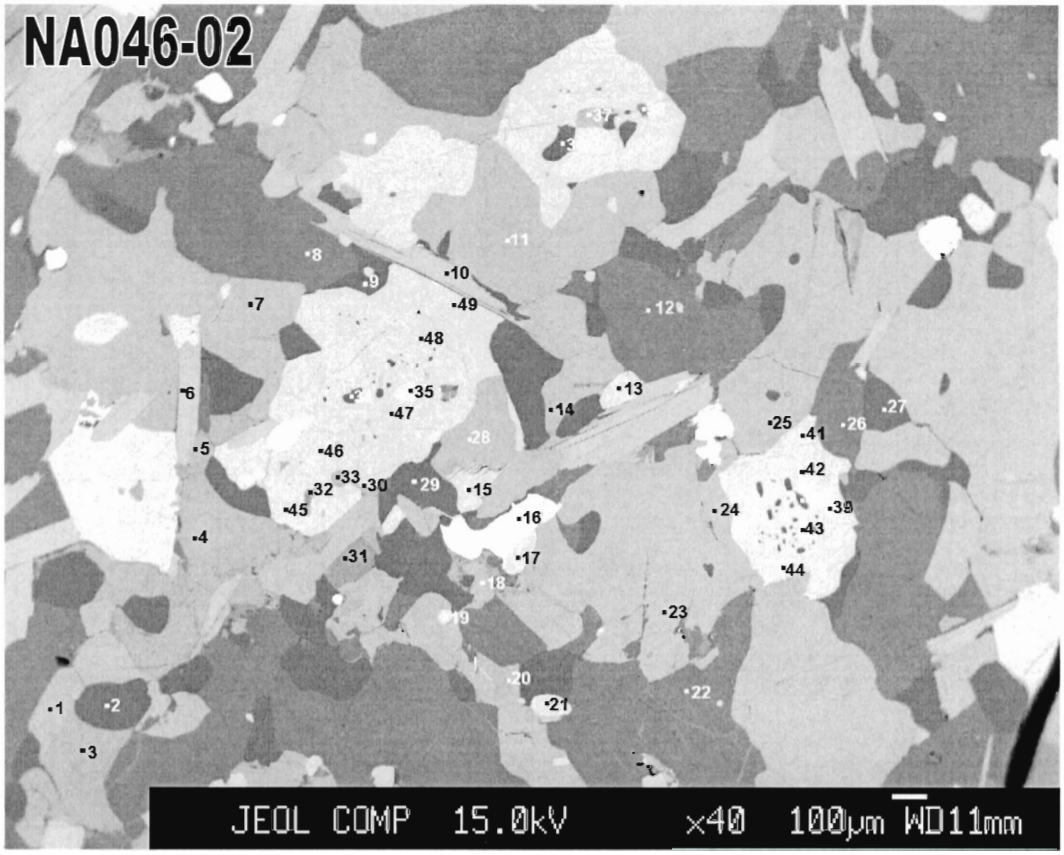
NA046-02
JEOL COMP 15.0kV ×40 100μm WD11mm

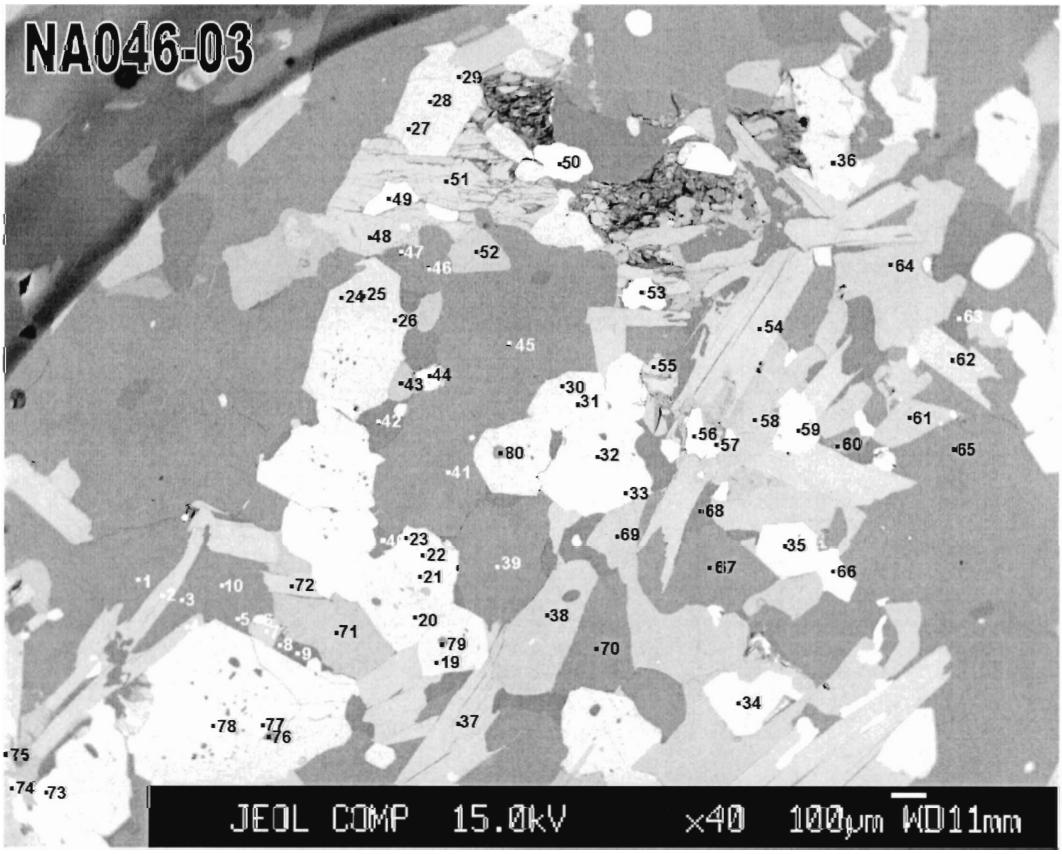
NA046-03
JEOL COMP 15.0kV ×40 100μm WD11mm

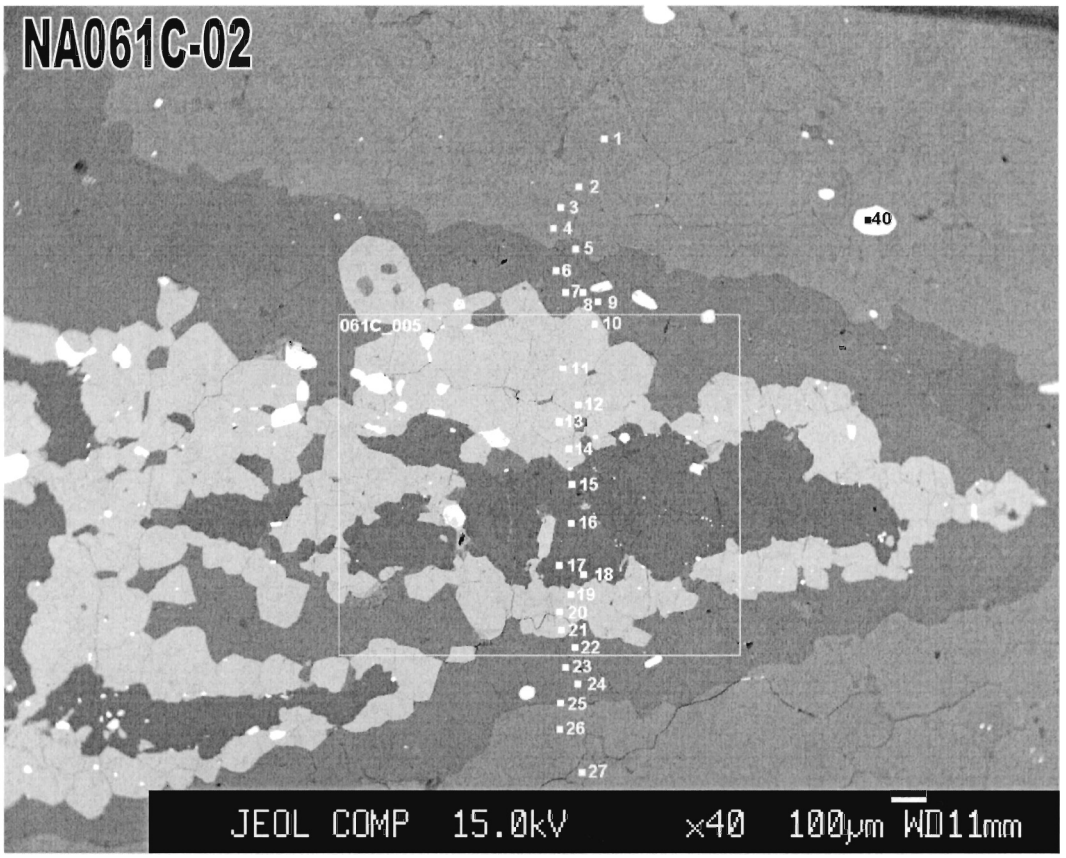
NA061C-02
061C_005
JEOL COMP 15.0kV ×40 100µm WD11mm

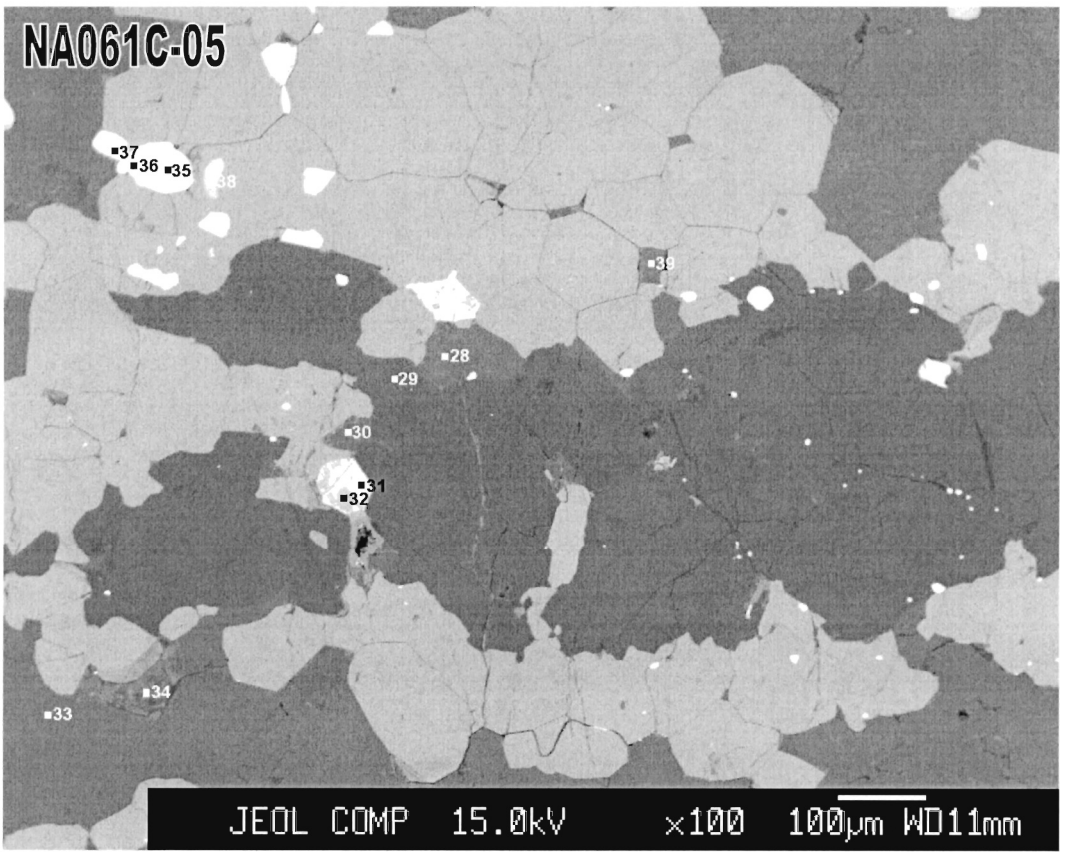
NA061C-05
JEOL COMP 15.0kV ×100 100µm WD11mm

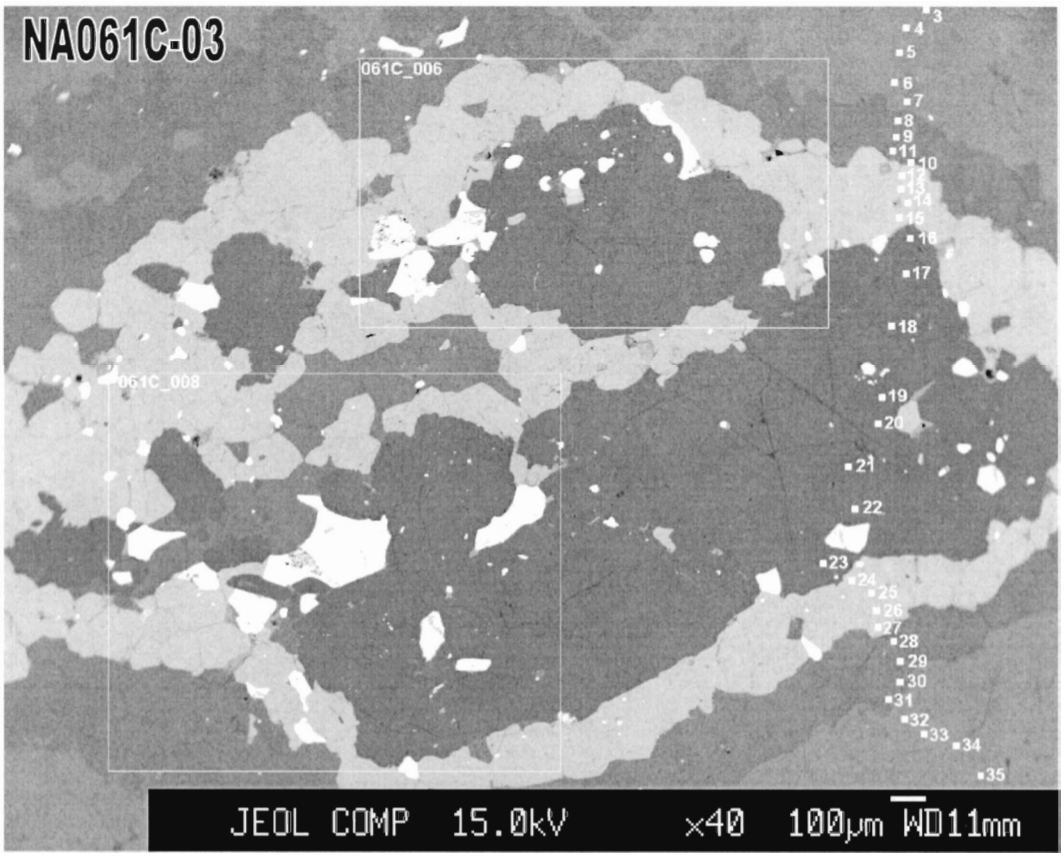
NA061C-03
061C_006
061C_008
JEOL COMP 15.0kV ×40 100µm WD11mm

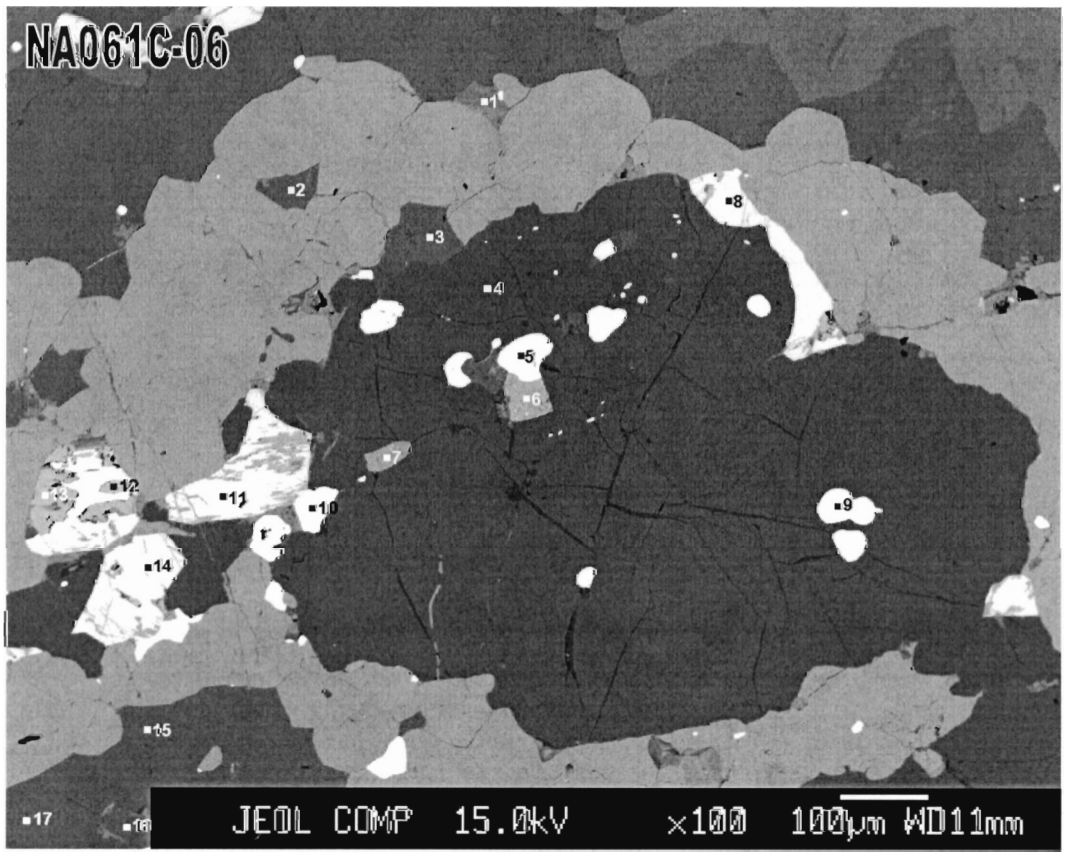
NA061C-06
JEOL COMP 15.0kV ×100 100µm WD11mm

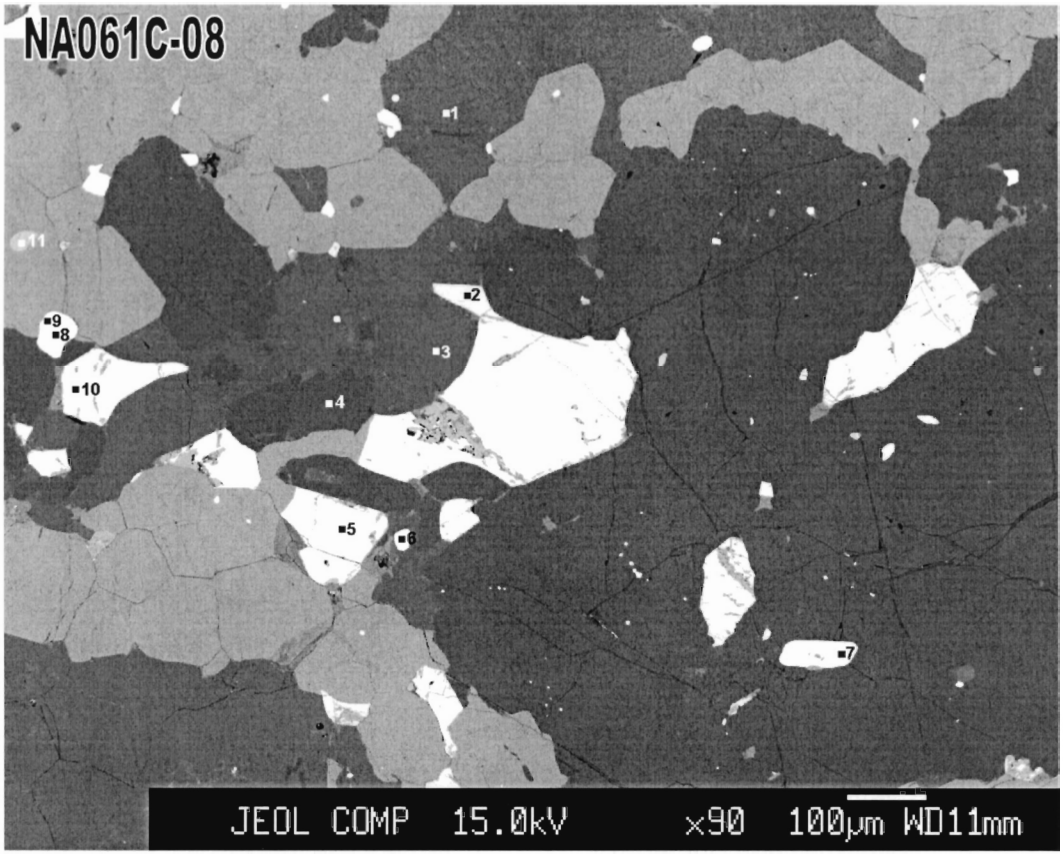
NA061C-08
1
2
3
4
5
6
7
8
9
10
11
JEOL COMP 15.0kV ×90 100µm WD11mm

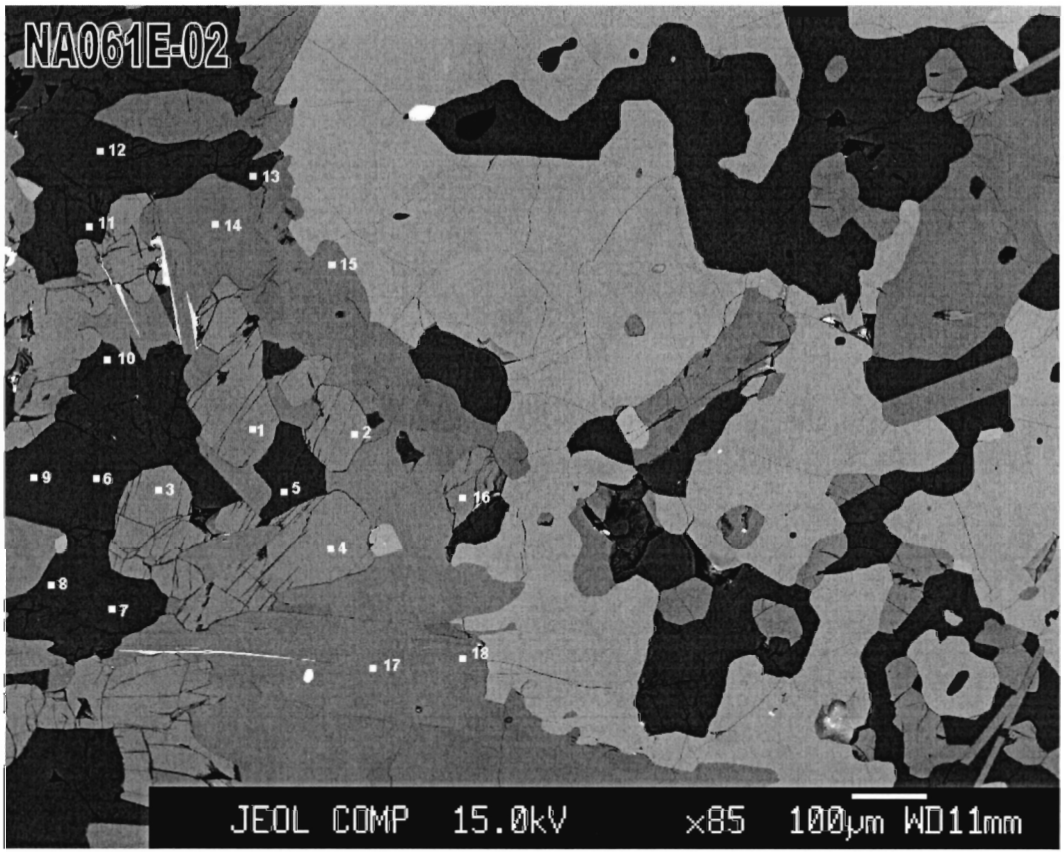
NA061E-02
1
2
3
4
5
6
7
8
9
10
11
12
13
14
15
16
17
18
JEOL COMP 15.0kV ×85 100µm WD11mm

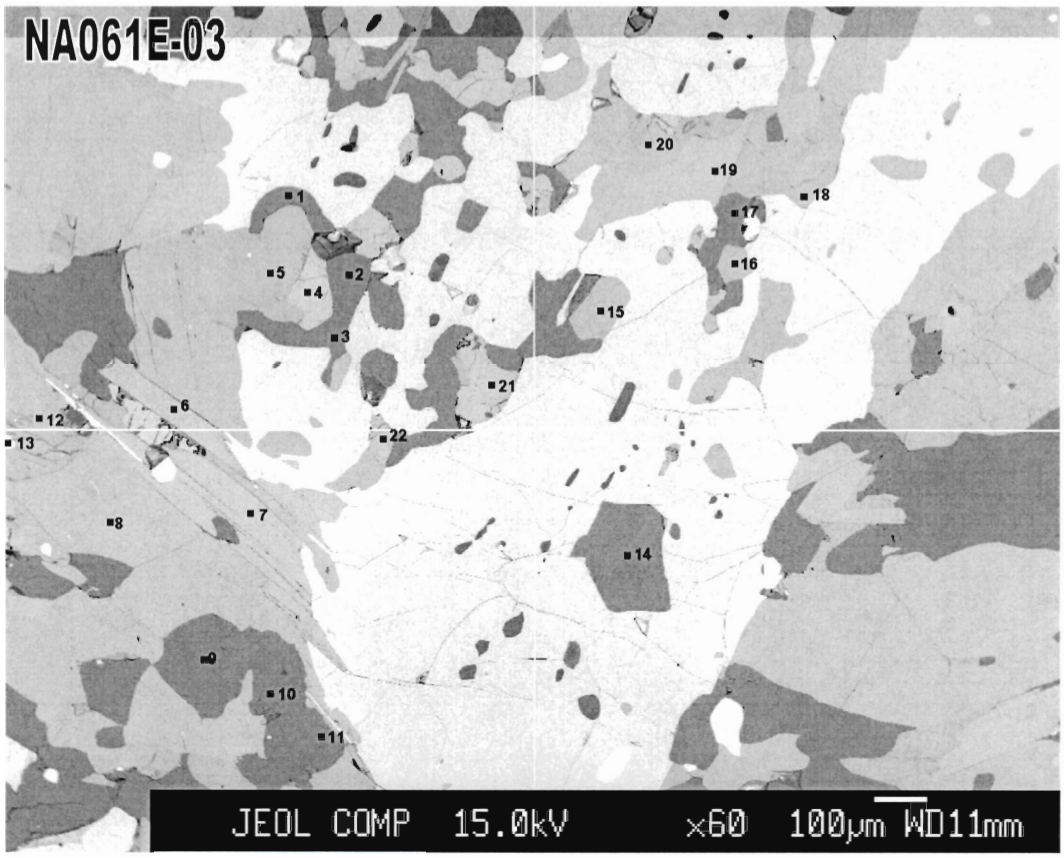
NA061E-03
JEOL COMP 15.0kV ×60 100µm WD11mm

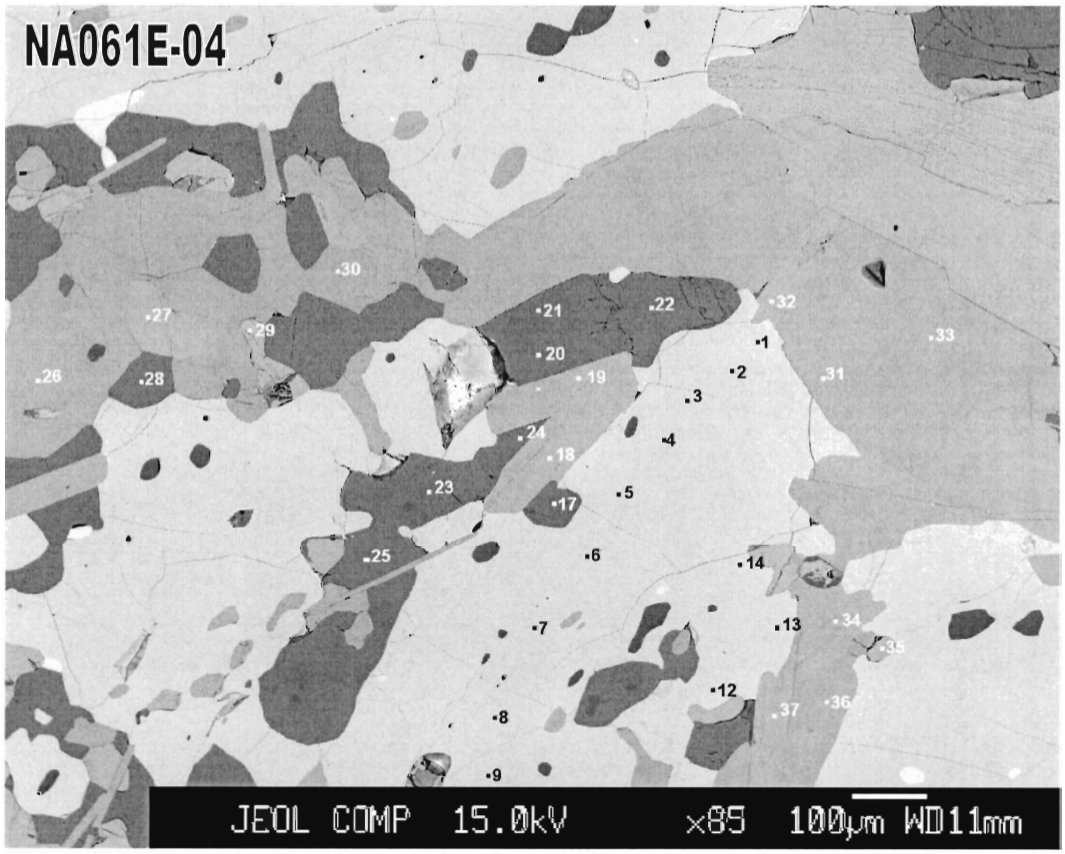
NA061E-04
JEOL COMP 15.0kV ×85 100µm WD11mm

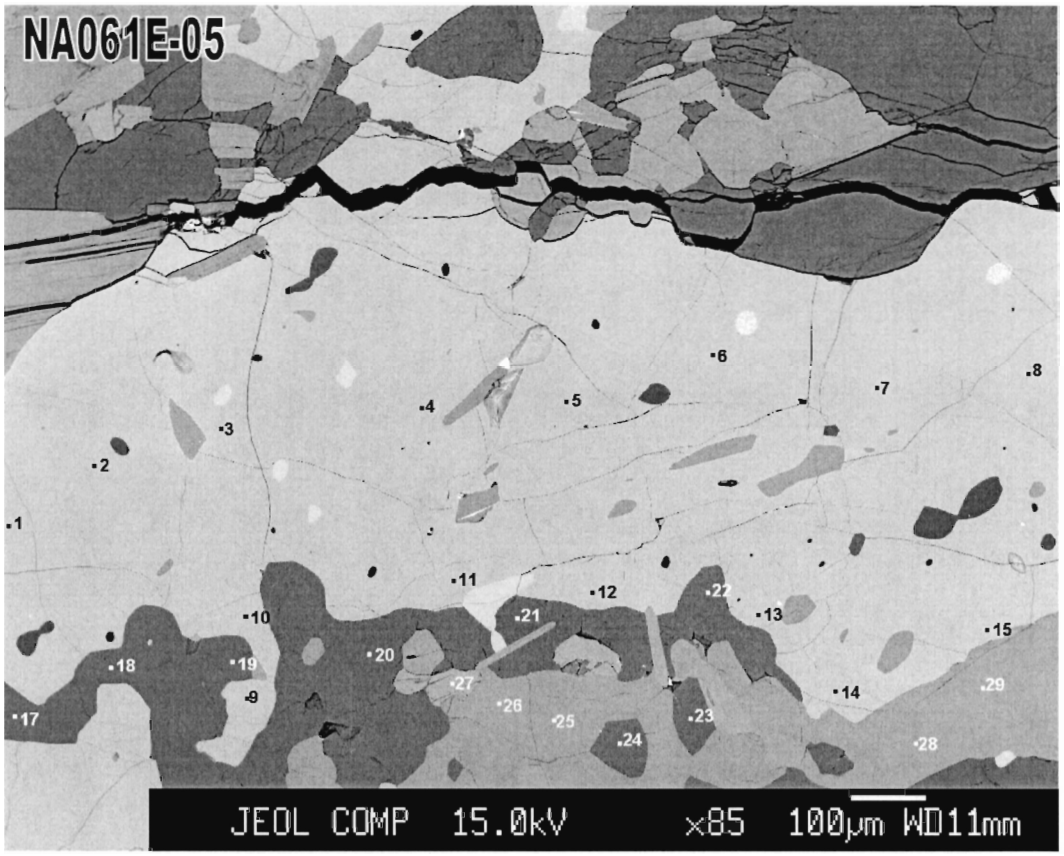
NA061E-05
JEOL COMP 15.0kV ×85 100µm WD11mm

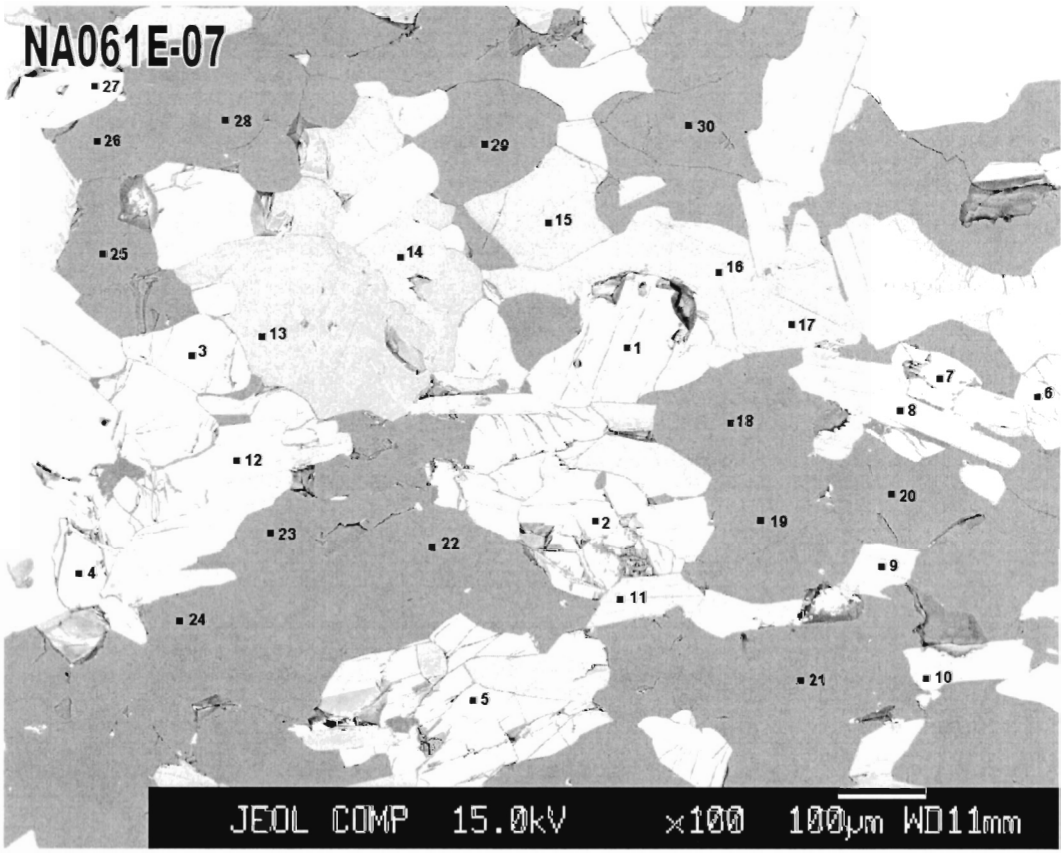
NA061E-07
JEOL COMP 15.0kV ×100 100µm WD11mm

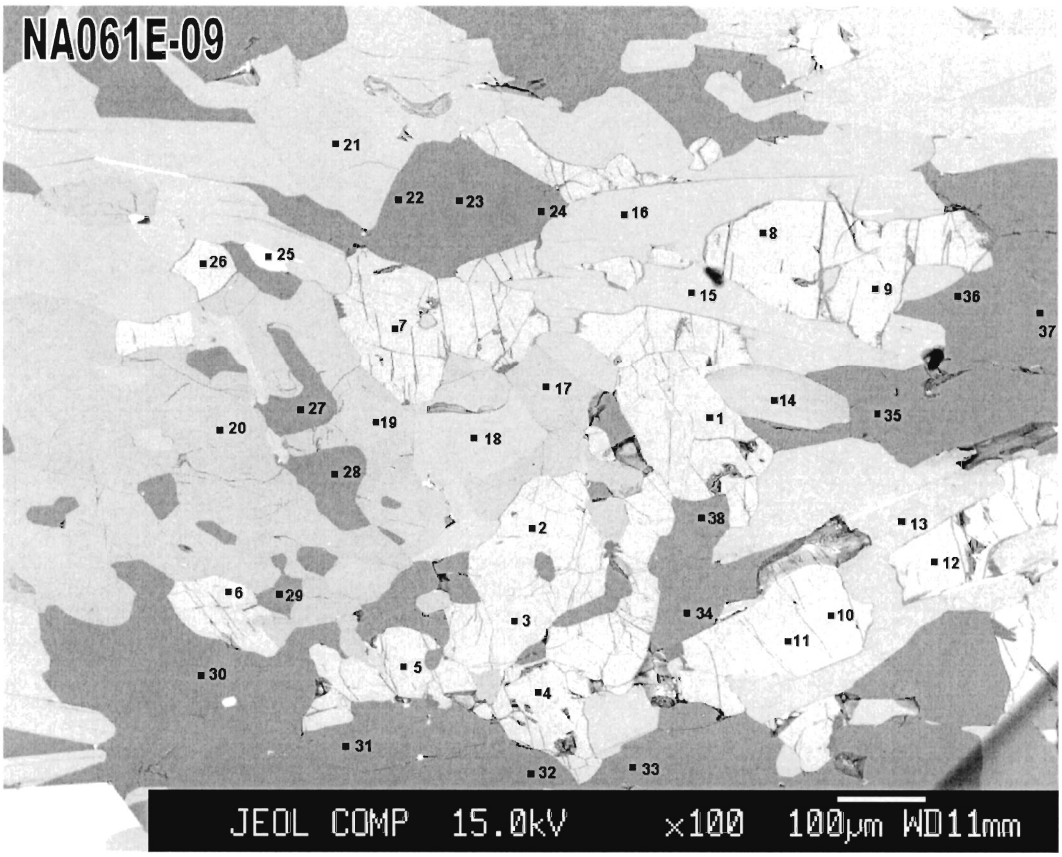
NA061E-09
JEOL COMP 15.0kV ×100 100µm WD11mm

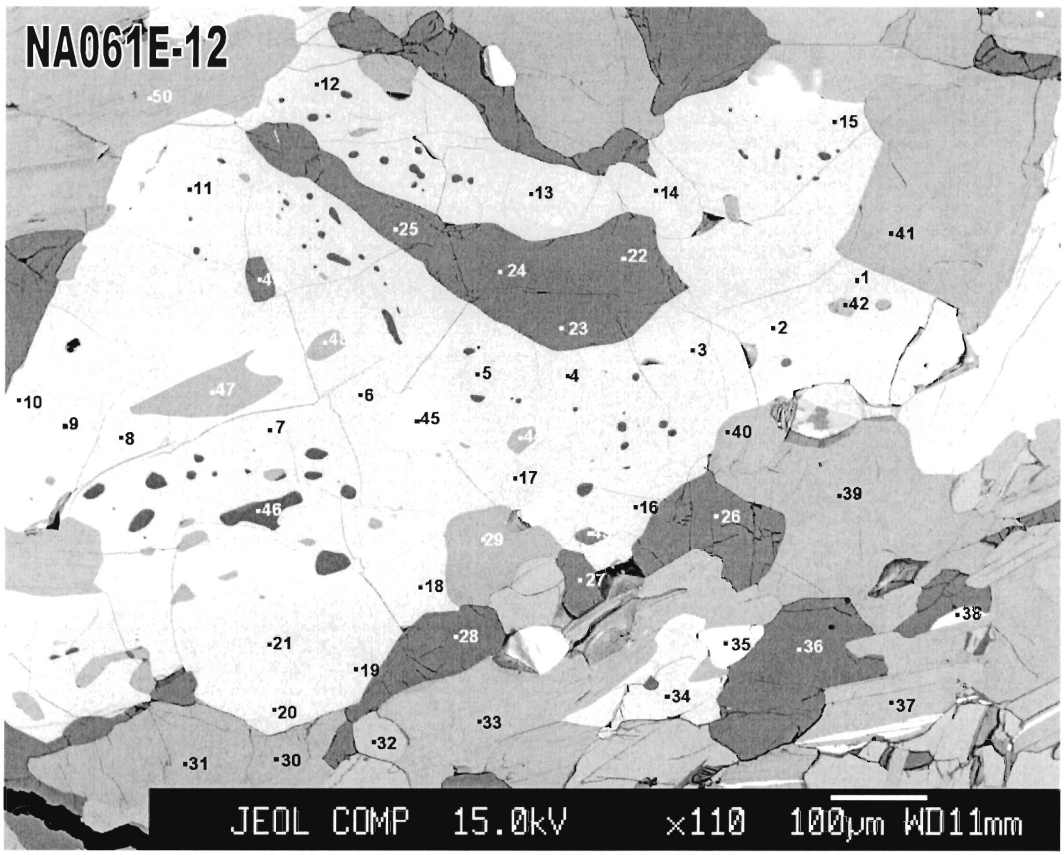
NA061E-12
JEOL COMP 15.0kV ×110 100µm WD11mm

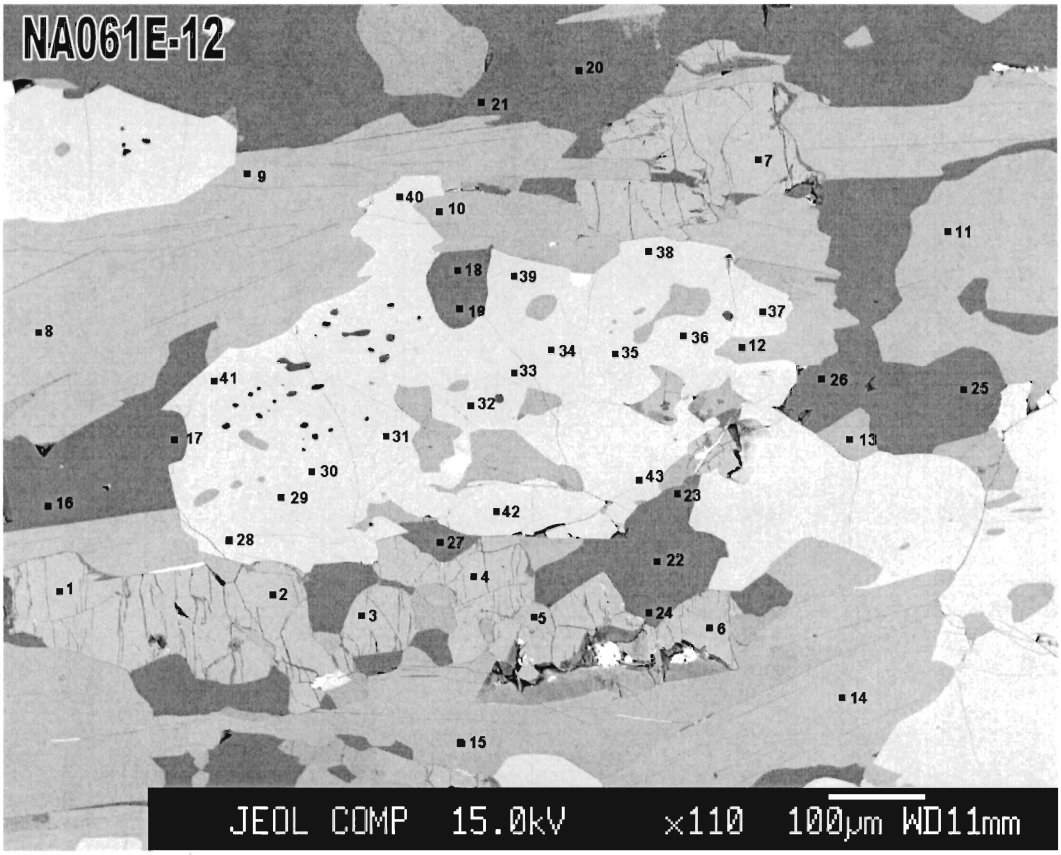
NA061E-12
JEOL COMP 15.0kV ×110 100µm WD11mm

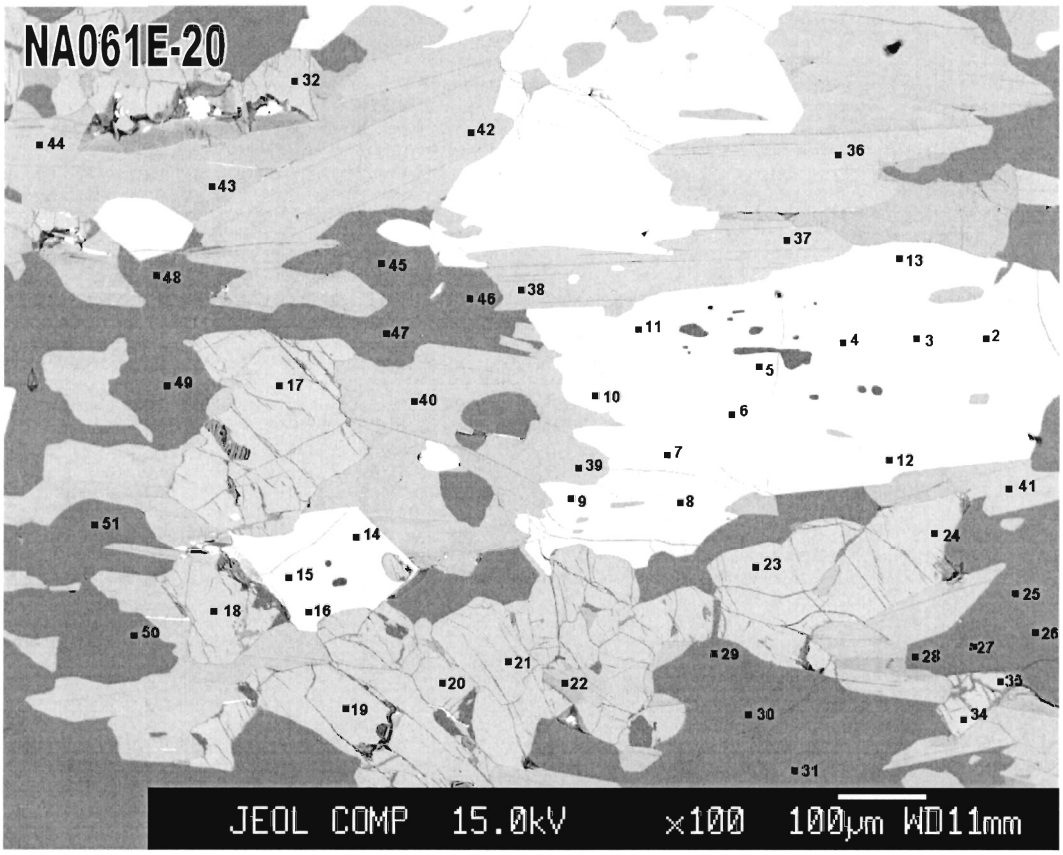
NA061E-20
JEOL COMP 15.0kV ×100 100µm WD11mm

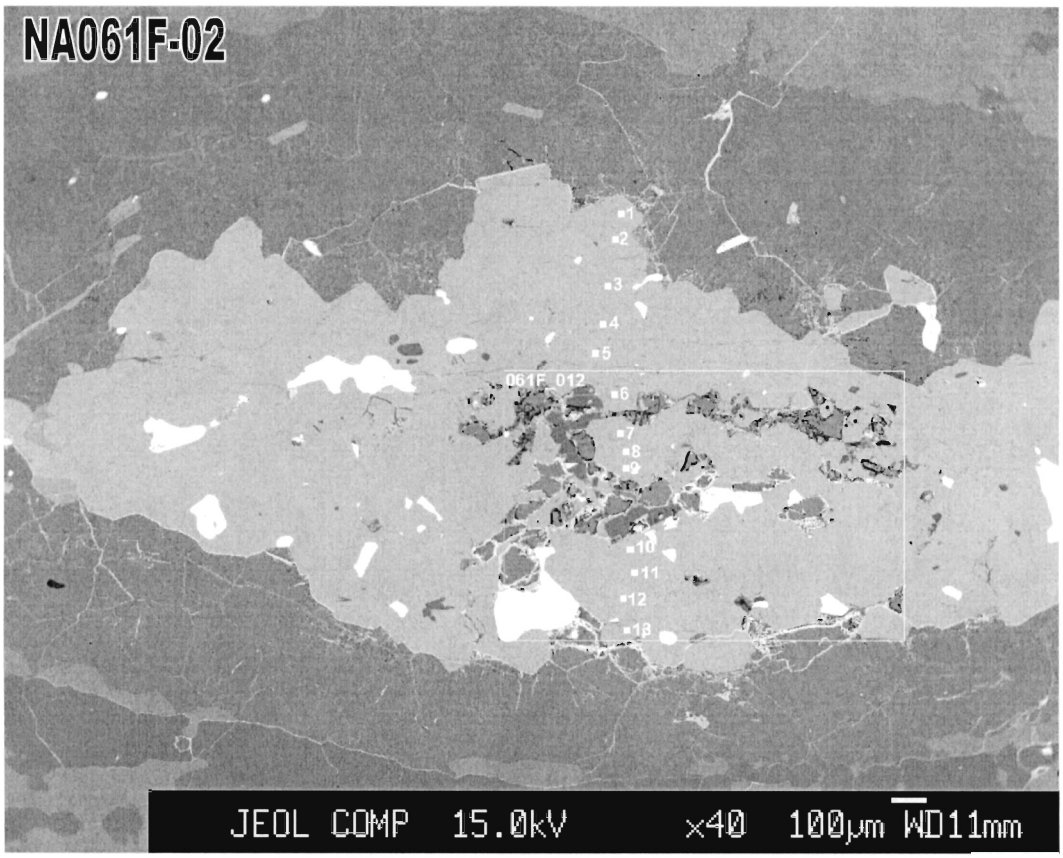
NA061F-02
061F_012
JEOL COMP 15.0kV x40 100µm WD11mm

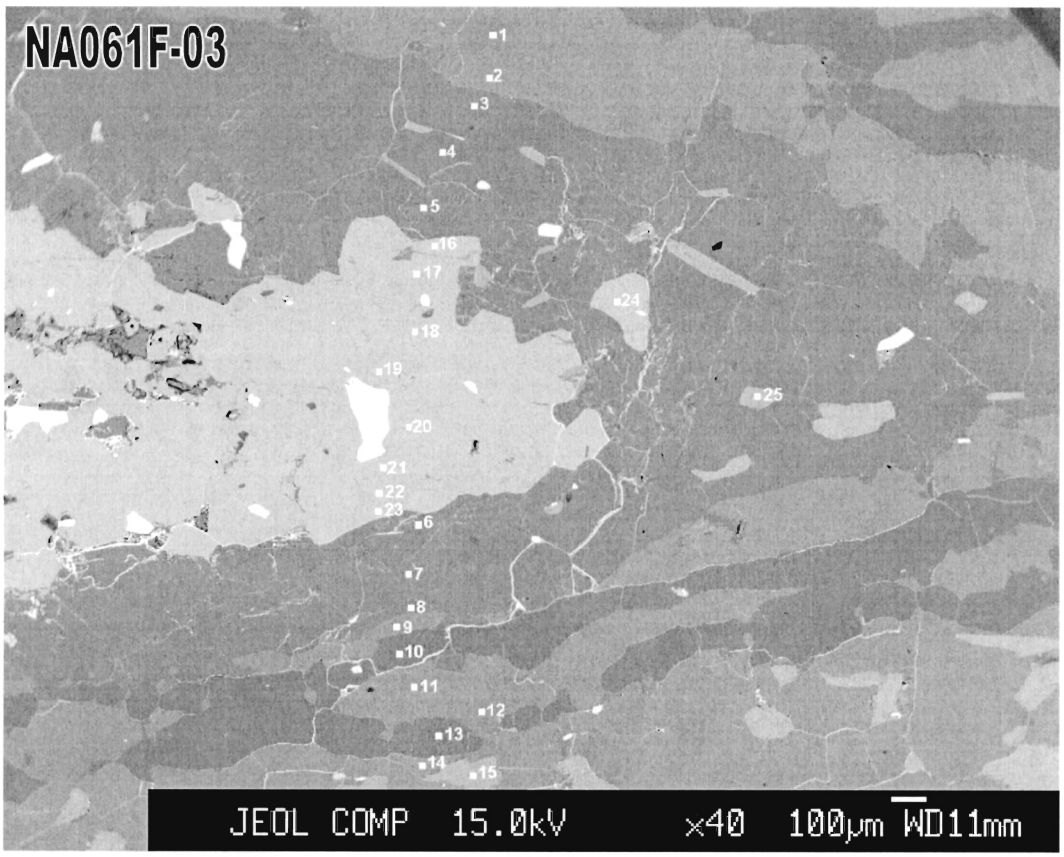
NA061F-03
JEOL COMP 15.0kV x40 100µm WD11mm

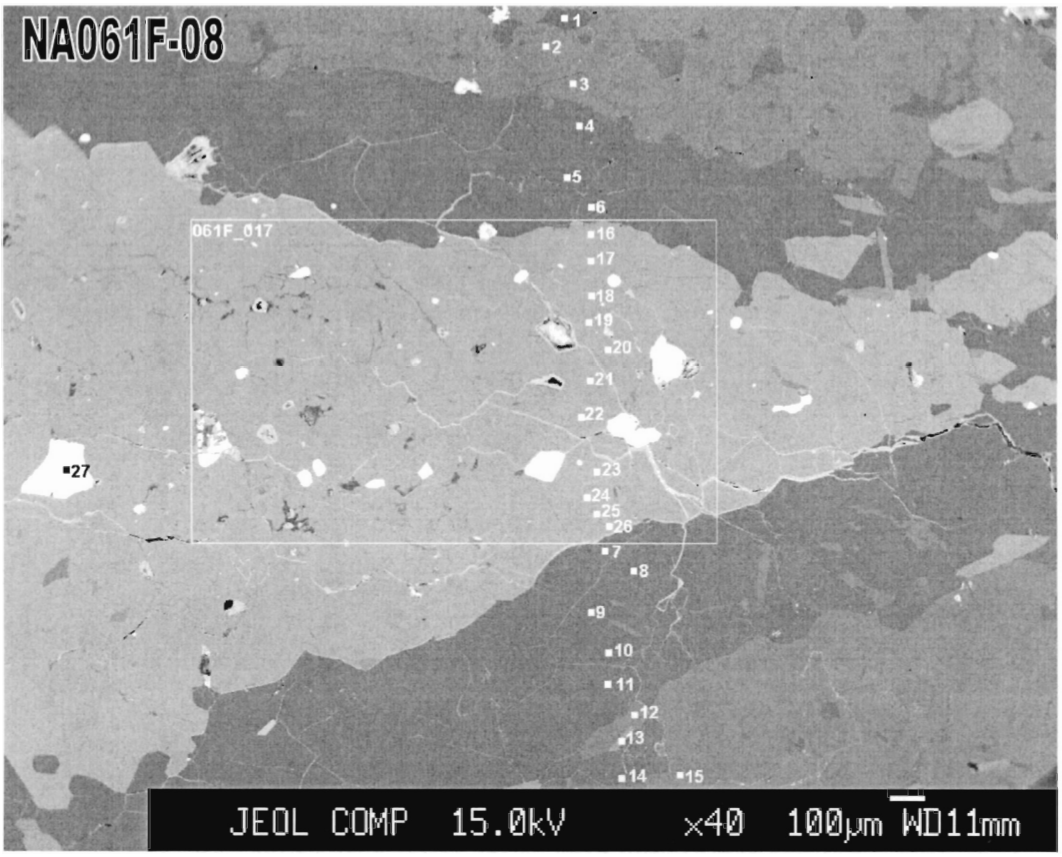
NA061F-08
061F_017
JEOL COMP 15.0kV ×40 100µm WD11mm

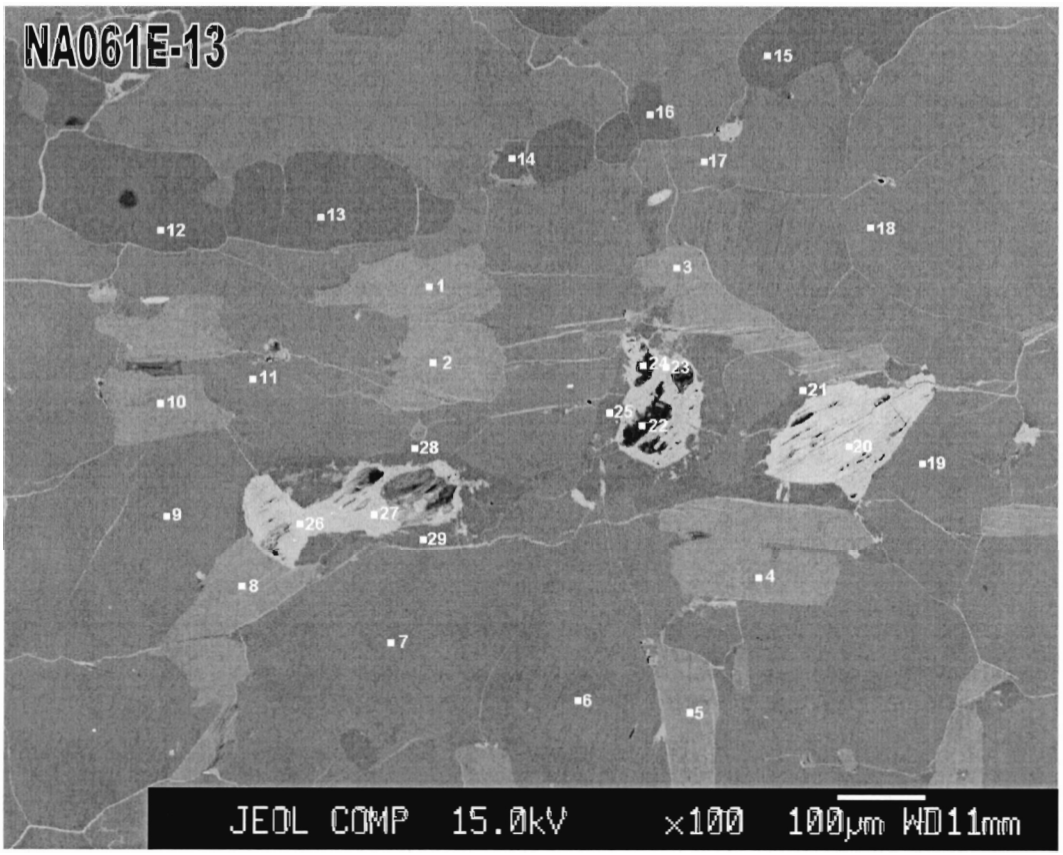
NA061E-13
JEOL COMP 15.0kV ×100 100µm WD11mm